ACS NANO

Editors' Choice

Open Access

www.acsnano.org

Targeting 100% Lithium Utilization in Lithium Metal Batteries

Seungwoo Choi,[†] Juyoung Kim,[†] Jiyeon Seo,[†] Khalil Amine, Peng Bai, Dae-Kwon Boo, Zheng Chen, Yujang Cho, Jang Wook Choi, Nam-Soon Choi, Tae Young Choi, Wootaek Choi, Yi Cui, Betar M. Gallant, Shiyu Ge, Kelsey B. Hatzell, Yushin Jang, Zhengyu Ju, Ji-Won Jung, Hee-Tak Kim, Ilgyu Kim, Min-Ho Kim, Mun Sek Kim, Patrick Joohyun Kim, Sang Cheol Kim, Yaejin Kim, Seongjae Ko, Hyegang Koo, Hochun Lee, Jiyoung Lee, Ju Li, Yuzhang Li, Ping Liu, Yijin Liu, Jeffrey Lopez, Matthew T. McDowell, Thanh Nguyen, Solomon T. Oyakhire, Sapna L. Ramesh, Mingyu Sagong, Nanyang Wang, Jamie H. Warner, Sujeong Woo, Gui-Liang Xu, Kang Xu, Yan Yao, Guihua Yu, Ji-Guang Zhang, Il-Doo Kim,* Hongkyung Lee,* and Hyun-Wook Lee*

Cite This: https://doi.org/10.1021/acsnano.6c06180

Read Online

ACCESS | Metrics & More | Article Recommendations

ABSTRACT: Anode-free lithium metal batteries (AFLMBs) represent the ultimate solution to mankind's quest for the Holy Grail of batteries, where the cell-level energy density is maximized on the assumption that lithium (Li^0) must be fully utilized with near 100% Coulombic efficiency. Although substantial progress has been made since the anode-free concept was first proposed, the challenges presented by the most powerful anode material that can be found on the periodic table still remain unresolved due to its extreme reactive nature, which not only makes it impossible to retain 100% reversibility but also induces inhomogeneity during repeated plating/stripping cycles and persistent capacity loss over a long period of time. The isolated study approaches, emphasizing either individual electrolyte components or interphasial chemistry engineering, but mostly focused on the negative-electrode current collector, hinder insight into issues arising when these components are assembled into cells and forced to interface with each other. In this review, we attempt to examine this high-dimensional topic from a panoramic perspective, with the focus placed on the liquid electrolytes. We first outline the fundamental operating principles of key individual battery components, together with practical perspectives for evaluating lithium utilization and reversibility in AFLMBs. We then discuss how these components interact when assembled into full cells, how such interactions give rise to heterogeneous electrochemical and mechanical behaviors, and how these phenomena can be characterized and regulated. It is also outlined that a hierarchical perspective on lithium behavior, spanning from the nano- to cell-scale, is essential to enable plating, stripping, and recovery in AFLMBs. Finally, we present perspectives from leading researchers actively working on the various elements that constitute AFLMBs and integrate these viewpoints to clarify the future research directions of this field. By providing a system-level framework for understanding AFLMBs, this review aims to guide future research efforts and contribute to addressing the broader challenges of sustainable energy storage.

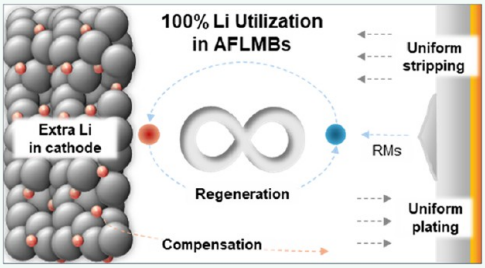

KEYWORDS: *lithium metal batteries, anode-free lithium metal batteries, lithium inventory, dead lithium, lithium recovery, perfect stripping, lithium loss, lithium compensation, current collector, self-recovering closed loop*

1. INTRODUCTION

1.1. Promises and Challenges Beyond Lithium Metal Batteries

Lithium metal has long been regarded as the ultimate anode material for high-energy storage because it provides the second highest theoretical capacity (3,860 mAh g^{-1}) and low redox potential (−3.04 V versus SHE), the combination of which renders it the indispensable component of Holy Grail

Received: April 1, 2026
Revised: June 30, 2026
Accepted: July 1, 2026

battery.[1−11] Even though the first demonstrations of rechargeable lithium metal batteries were reported in the 1970s, the use of lithium metal has been hindered by severe safety concerns and limited cycle life.[12] The root cause is the unstable lithium-electrolyte interface, which promotes uneven or sometimes dendritic growth, continuous decomposition of both electrolyte and lithium metal, and the persistently increasing cell impedances due to the overgrowth of interphase. Over the past decade, there has been a resurgence of interest in lithium metal research, motivated by the growing demand for batteries with energy density beyond what the intercalation nature of graphite anode could provide.

LMBs typically require an excess amount of lithium to compensate for lithium losses during cycling. However, due to its highly reactive nature, the use of excess lithium increases weight, cost, and even safety risks, which are attributed to the whole life of battery from manufacturing process to cycling. The concept of anode-free lithium metal batteries (AFLMBs) was demonstrated as the ultimate case of anode thinning strategies trying to maximize the energy density, as all lithium inventory will be provided by the lithiated cathode materials.[13−18] In AFLMB configurations, a bare copper current collector serves as the substrate for lithium plating during charging process, forming the lithium metal anode in situ. This design promises volumetric energy densities exceeding 1000 Wh L^{-1}, far surpassing the typical 600−800 Wh L^{-1} range of current LIBs and even the 800−900 Wh L^{-1} of LMBs with excess lithium. Such high-energy density makes AFLMBs exceptionally promising for applications where weight and space are critical, such as in electric vehicles (EVs), aerospace systems, and portable electronics.

Despite this promise of ultrahigh energy density of LMBs, the intrinsic reactivity of lithium at the nanoscale fundamentally complicates both the understanding and control of lithium electrodeposition. To overcome this long-standing challenge, research in this field has historically centered on a single guiding question: how can lithium be plated in a morphologically and chemically stable manner?[9,19−21] This question has motivated the development of diverse strategies, ranging from electrolyte optimization, artificial interphase engineering, and surface modification of current collectors to three-dimensional scaffold and advanced electrolyte salts, which together form a plating-centered paradigm that has delivered valuable insights into dendrite suppression, solid electrolyte interphase (SEI) design, and current collector engineering.[22−32]

Yet the shift toward anode-free batteries introduces a new dimension to the problem. In an anode-free configuration or reservoir-free systems, the cell is assembled without pre-existing lithium on the negative electrode. In this case, the overall inventory of lithium is finite and originates solely from the cathode, while the loss of lithium from the anode reactivity directly results in cell capacity degradation each cycle. From a practical perspective on cycle life, the key challenges of realizing an anode-free system must go beyond achieving uniform plating; they must also emphasize the complete stripping and an effective recovery pathway to address the inevitable lithium loss.

Incomplete stripping of lithium is the hidden failure mode of most lithium metal and anode-free batteries. When stripping proceeds heterogeneously, metallic fragments detach from the electronic network, or lithium particles at the tip of the wires or dendrites become trapped within the SEI. This electronically isolated fraction is often called "dead" lithium. Even if only a small fraction of plated lithium becomes inactive in each cycle, the cumulative loss rapidly depletes the lithium inventory. For instance, with an average lithium reversibility of 99%, more than half of the active lithium is lost after only 70 cycles. In anode-free batteries, where there is no excess lithium reservoir, this effect is catastrophic. The result is accelerated capacity fade, voltage instability, and premature cell death. Besides lithium inventory loss, a more serious threat from the dead lithium is their reactivity, because they are not really "dead" but remains chemically active nanosized lithium metal (Li^0), whose reactivity has been magnified by thousand-folds due to the high surface area. Thus, the central question must be reframed: the challenge is not only controlling plating but also achieving nearly perfect stripping and reactivating inactive lithium through recovery strategies. Only by fully closing this loop can AFLMBs finally realize practical lifetimes.

The historical trajectory of lithium metal research can be compared to the generational evolution. Early lithium studies (Gen 1) were observational, focusing on dendrite formation and failure signatures.[33−36] Subsequent work (Gen 2) emphasized control through additives, interphases, and mechanical pressure from an Edisonian trial-and-error approach without understanding the underneath mechanism.[30−32,37−40] With the advent of structured current collectors and advanced electrolytes, the field entered Gen 3 based on the mechanistic knowledge of dendrite formation, which emphasized engineered architectures to distribute current and suppress local hot spots.[6,26,28,41−45] Recently, data driven approaches, operando diagnostics, and modeling frameworks have led us to Gen 4, where intelligent integration of plating control is emphasized.[9,46−48] Building on this analogy, we propose a new phase, Gen 5, which is defined not by better plating, but by the capability to strip lithium completely and to recover lithium that would otherwise remain inactive. In other words, the goal is to establish a self-recovering anode-free battery that maintains a closed lithium inventory. This Gen 5 will be achieved when we fully understand and control the behavior of lithium from the nanoscale to the cell-scale.

To advance this new paradigm, it is essential to revisit the theoretical frameworks that have guided electrochemical science. Classical models such as Sand's time,[49] Marcus−Hush electron transfer theory,[50,51] the Butler−Volmer equation,[52,53] and the Newman porous electrode model[54] have been widely adopted for understanding ion transport, charge transfer, and cell-level performance. These classical theories form the foundational language of electrochemistry and continue to underpin most contemporary modeling of battery systems, including lithium metal electrodes. Rather than being obsolete, they provide the essential starting point upon which more detailed descriptions of interphase formation, multispecies reactions, and heterogeneous electrode structures are constructed in modern lithium metal and anode-free cell models.[55−57]

Nevertheless, when these frameworks are applied to AFLMBs in their simplest forms, several assumptions that are often implicit in their implementation must be carefully reconsidered. Sand-type analysis, for example, provides a useful conceptual description of transport-limited ion depletion, but the effective depletion process in anode-free lithium metal cells can be strongly influenced by SEI-mediated Li^+-ion transport, local current density heterogeneity, and continuously evolving interfacial resistance.[56,58] Marcus−Hush-type electron transfer

https://doi.org/10.1021/acsnano.6c06180
ACS Nano XXXX, XXX, XXX−XXX

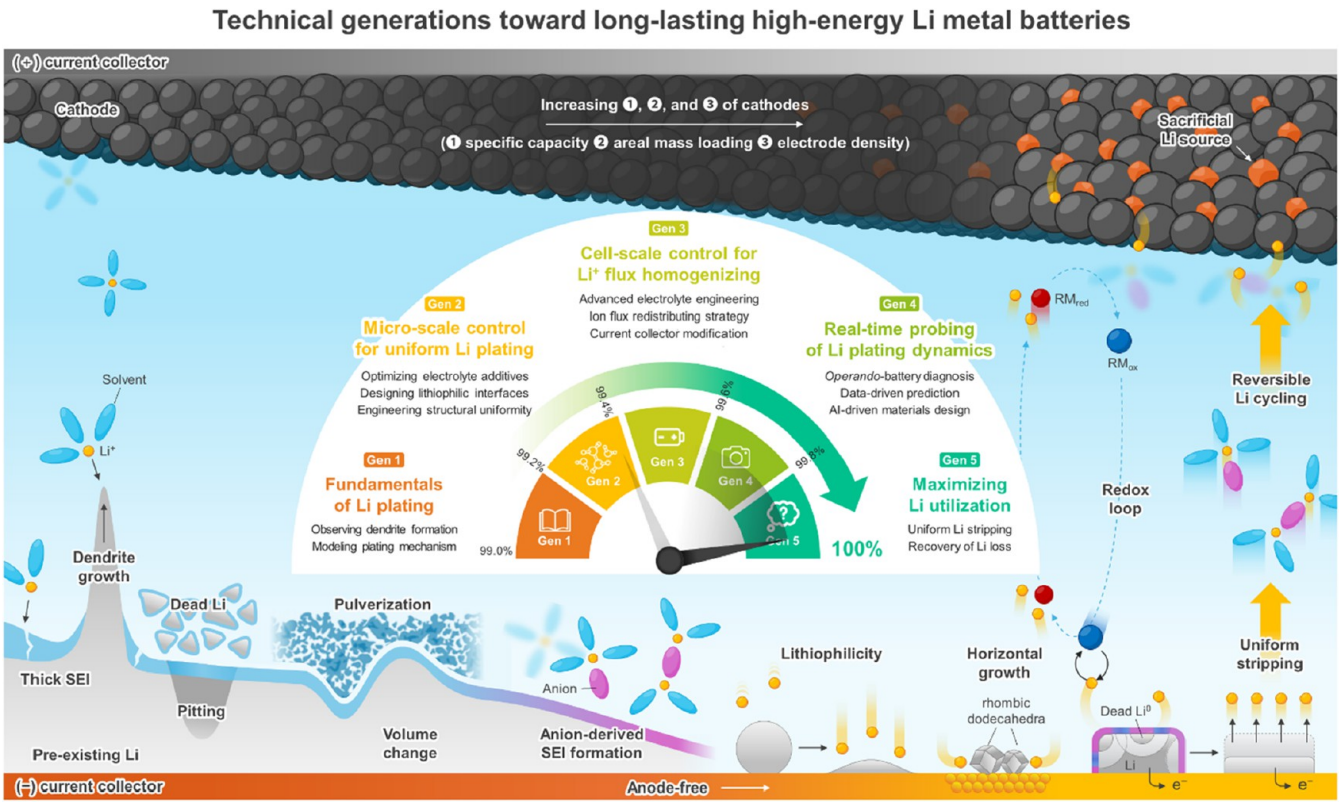

Figure 1. Technical generations of research history of high-energy density AFLMBs, starting from fundamental understanding of lithium plating behavior (Gen 1) to 100% lithium utilization in AFLMB full-cell configuration with thick cathode including sacrificial agents (Gen 5).

concepts remain valuable for describing elementary charge transfer energetics, yet lithium metal nucleation involves not only electron transfer but also desolvation, adatom migration, crystallization, and SEI-mediated structural reorganization.[59] Similarly, Butler−Volmer kinetics can serve as the charge-transfer backbone for lithium deposition and dissolution, but the exchange current density, transfer coefficient, active interfacial area, and local overpotential may evolve with SEI chemistry, deposit morphology, electrolyte concentration gradients, and mechanical contact.[55,56,60] Newman-type porous-electrode and concentrated-solution descriptions provide rigorous frameworks for macroscopic concentration and potential profiles, but practical AFLMBs require additional treatment of spatially heterogeneous current collectors, partial lithium coverage, porous SEI/dead-lithium layers, local electrolyte wetting, and the appearance or disappearance of metallic lithium domains during repeated plating and stripping.[56,57]

Therefore, rather than discarding classical theories of electrochemical kinetics and transport, anode-free batteries should be analyzed as electro-chemo-mechano dynamic systems built upon these frameworks but explicitly incorporating interphase evolution, coupled plating−stripping−recovery reactions, and multiscale reaction heterogeneity. In this context, assumptions such as time-invariant kinetic parameters, single-reaction pathways, and spatially homogeneous interfaces are often insufficient for capturing dynamic SEI growth, dead-lithium formation, and nonequilibrium interfacial conditions in AFLMBs. Recent modeling efforts exemplify this extension strategy: modified Butler−Volmer kinetics have been combined with SEI growth reactions and stress-dependent overpotentials, Newman-type porous electrode models have been extended to account for spatially heterogeneous deposition and stripping through distributed-parameter descriptions, and Marcus−Hush−Chidsey formalisms have been used to rationalize substrate-dependent charge-transfer kinetics at lithium metal interfaces.[55−57,59] These developments highlight that classical frameworks remain indispensable, but that their practical application to anode-free lithium metal batteries requires explicit treatment of evolving interphases and multiscale heterogeneity. Within this extended perspective, the plating step is coupled with SEI growth and evolution, local heat and stress fields, and interfacial molecular and electronic structure, while the stripping step is governed not only by electrochemical driving force, but also by adhesion, mechanical fracture, and the dynamic conductivity of the SEI. The recovery step further requires concepts such as redox mediators that dissolve and redeposit inactive lithium, mechanical methods that restore electronic contact, or dynamic interphases that re-establish ion-transport pathways. These processes are interdependent, as plating, stripping, and recovery dynamically reshaping the interfacial chemical, electrical, and mechanical environments that govern subsequent cell behavior. Capturing this complexity therefore requires integrated approaches that combine operando imaging, multiphysics modeling that extends classical electrochemical descriptions, and machine-learning-guided interpretation.

The implications for practical cells are profound. Complete stripping of electrodeposited lithium requires more than just a high Coulombic efficiency (CE); in addition, it also demands that nearly all plated lithium remains electronically connected

https://doi.org/10.1021/acsnano.6c06180
ACS Nano XXXX, XXX, XXX−XXX

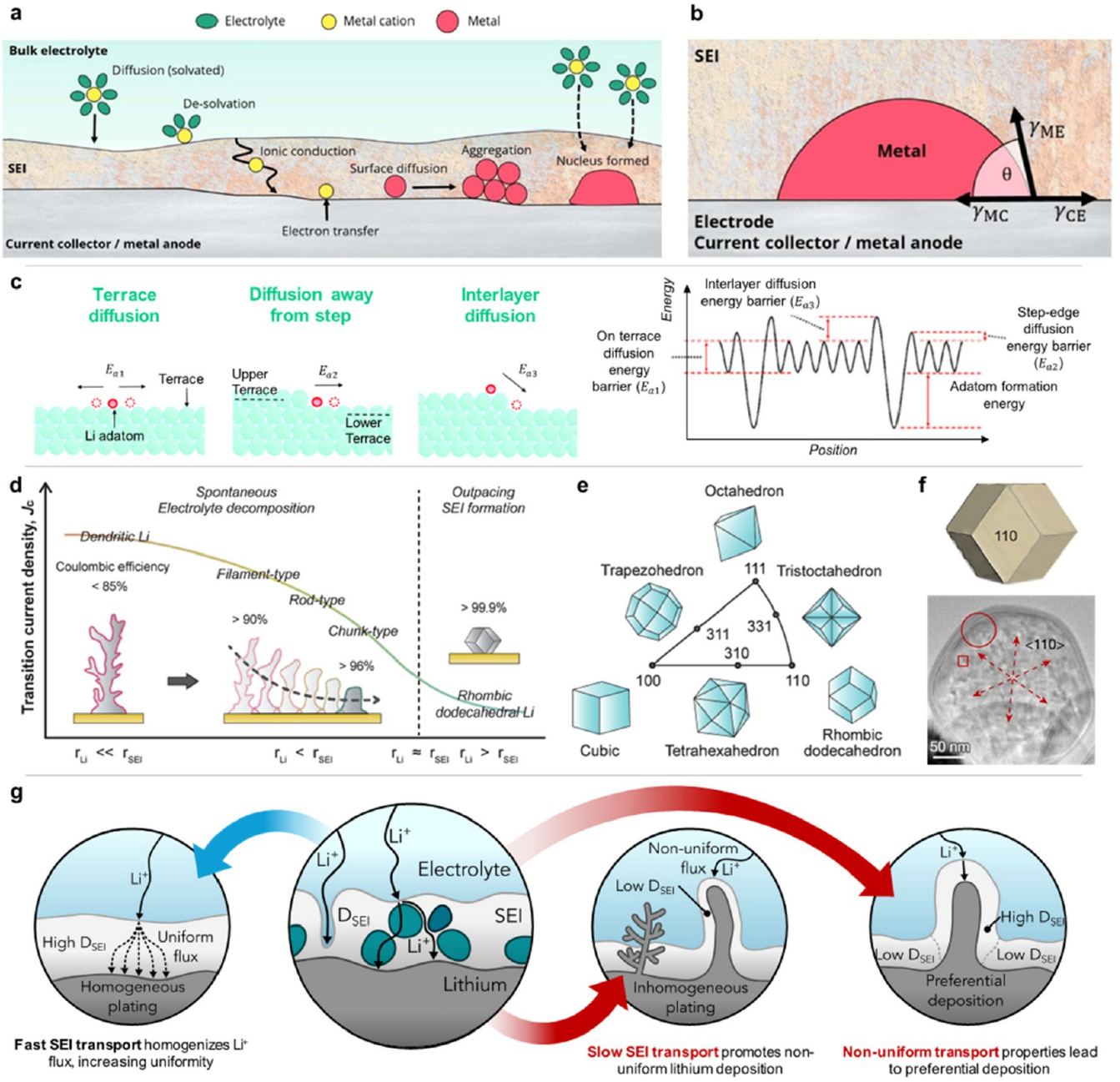

Figure 2. Mechanistic origins of lithium dendrite formation, considering thermodynamics of lithium itself and its interphase. (a) Nucleation process starting from a solvated metal cation traveling to the electrode surface. (b) Interfacial wettability at the Li-SEI-substrate interface governs heterogeneous nucleation behavior. (c) Surface diffusion kinetics of lithium adatoms regulate lateral versus vertical growth. (d) Morphology transition of lithium deposits correlated with electrolyte kinetics. r_{Li} and r_{SEI} refer to relative reaction rates of lithium and SEI during lithium deposition, respectively. (e) Various polymorphs and their morphologies exposing families of close-packed facets. (f) Scheme of rhombic-dodecahedron shape bcc crystal exposing only (110) planes on its surface (up) and electrodeposited rhombic-dodecahedron lithium under ultrafast deposition condition (down). (g) SEI transport properties regulate Li^+-ion flux uniformity and determine the stability of lithium deposition. Panels are reproduced with permission from a and b, ref 67, © 2023 Wiley-VCH GmbH; c, ref 68, © 2018 American Physical Society and ref 69, © 2020 The Royal Society of Chemistry; d and e, ref 70, © 2024 American Chemical Society; f, ref 71, © 2024 The Royal Society of Chemistry and ref 72, © 2023 Springer Nature Ltd. (the authors retain the right to reuse the figure in this work); g, ref 73, © 2023 Elsevier, CC-BY 4.0.

until every deposited lithium gets stripped away while maintaining stable and passivating interphases. The introduction of quantitative descriptors such as the stripping completion ratio and the dead lithium recovery yield will enable precise benchmarking of strategies. Recovery processes of electrically inactivated lithium, which have been relatively overlooked and underexplored, could extend the lifetime of anode-free cells by reactivating otherwise lost lithium. Chemical mediators, reconfigurable current collectors, and adaptive operating protocols are emerging as promising directions. Ultimately, the goal is to maintain a high inventory retention, meaning that the maximum of the initial lithium inventory from the cathode remains available after hundreds of cycles.

https://doi.org/10.1021/acsnano.6c06180
ACS Nano XXXX, XXX, XXX−XXX

In this review, we reposition the discussion of anode-free batteries from a plating centered paradigm to a three-step perspective: plating, stripping, and recovery (Figure 1). We first examine the current understanding of lithium plating and the advances in achieving uniform and dendrite free growth, with an emphasis on how plating morphology affects downstream stripping behavior. We then focus on the fundamental principles and design strategies for perfect stripping, highlighting approaches such as dynamic SEI layers, conductive and elastic scaffolds, and optimized current profiles. Finally, we discuss recovery strategies that aim to reactivate dead lithium, including redox shuttle additives, mechanical reinforcement, and self-healing interphases. By integrating these three elements, we outline a roadmap toward self-recovering anode-free batteries that can overcome the intrinsic irreversibility of lithium metal. Accordingly, this review also aims to illustrate how lithium behavior must be understood hierarchically, from the nano- to meso- and cell-scale, in order to enable those proposed processes. Our central belief is clear: the practical realization of anode-free batteries will be determined not by stable plating alone, but by the combined and synchronized ability to strip lithium completely and to recover lithium that has become inactive.

While all-solid-state AFLMBs represent a significant and alternative direction in this field,[61−65] this review primarily focuses on liquid electrolyte-based systems based on two reasons: (1) all existing battery chemistries on the market are operating with liquid electrolytes because of their averaged advantages when all application metrics are considered and this trend will persist for a long time in the foreseeable future even when new battery chemistries such as lithium metal become available; (2) the basic ion transport mechanism across these solid-state electrolytes remain unclear, rendering current materials engineering still Edisonian, and the rationale design and engineering of new materials and interfaces unfeasible at present.

1.2. Fundamentals of Lithium Plating/Dissolution Behavior

1.2.1. Lithium Dendrite Formation upon Charge. A fundamental step toward achieving 100% CE is to realize uniform, dense, and planar lithium electrodeposition that enables highly reversible plating and stripping with efficient lithium recovery. Accordingly, understanding the theoretical origins of lithium nucleation and propagation provides the mechanistic basis for rational strategies to regulate deposition morphology and to design electrolytes, interphases, and current collectors (or 3D hosts). Such mechanistic insight identifies the key thermodynamic, kinetic, transport, and interfacial parameters that must be controlled to achieve uniform lithium deposition and reversible stripping.

Although classical nucleation theory offers a thermodynamic framework that elucidates the competition between interfacial energy and volumetric energy terms,[66] in reality, lithium nucleation occurs within a complex and heterogeneous environment beneath or inside a mixed SEI-electrolyte region, rather than at a pristine lithium-electrolyte interface (Figure 2a and b). Decreasing the effective interfacial energy within this heterogeneous environment, specifically through the formation of lithium-compatible SEIs or solid electrolytes, thermodynamically facilitates widespread and regularly shaped nucleation. Furthermore, interfacial wettability further modulates nucleation thermodynamics; in heterogeneous systems, improved wettability effectively lowers the nucleation barrier and promotes compact, uniform lithium deposition. Consequently, lowering metal current collector interfacial energy through the use of lithiophilic current collectors is favorable to reducing the energy barrier for nucleation. From this thermodynamic perspective, minimizing effective interfacial energy and improving wettability are essential for facilitating uniform lithium nucleation and growth, which are critical for reversible lithium plating and stripping.

According to the Monroe-Newman criterion, interfacial instability arises when the mechanical shear modulus of the contacting lithium-conducting medium (e.g., SEI or solid electrolyte) is insufficient to withstand localized lithium growth.[74,75] Srinivasan's modified model further correlates dendrite initiation to the modulus ratio (G_{solid}/G_{Li}), suggesting that softer interphases favor dendritic intrusion.[76] Thus, mechanical stiffness and interfacial energy jointly dictate the morphological stability of lithium growth. Accordingly, SEI emerges as a critical interfacial layer governing mechanical constraint. Its elastic modulus, largely determined by electrolyte chemistry, governs both interfacial ion transport and mechanical integrity. Although solid electrolytes or rigid coatings with high shear moduli can theoretically suppress dendrite penetration, most liquid-derived SEIs lack sufficient mechanical strength in practice.[77] Enriching SEIs with inorganic components (e.g., LiF or Li_2O) has been shown to enhance both mechanical stability and interfacial ion homogeneity.[78] Moreover, the chemical and structural heterogeneity of SEI often leads to nonuniform Li^+-ion conduction and uneven nucleation sites as lithium deposition preferentially occurs along low-resistance spots. Once volumetric expansion exceeds the elastic limit of the SEI, interfacial cracking exposes fresh lithium, triggering continuous electrolyte decomposition and ultimately leading to uncontrolled dendritic propagation. Therefore, rational SEI engineering with enhanced mechanical robustness and homogeneous Li^+-ion transport is critical for suppressing dendritic lithium growth.

In addition to thermodynamics, lithium deposition morphology is also governed by interfacial kinetics and ion transport in the electrolyte. As depicted in Figure 2c, lithium deposition morphology can be governed by surface diffusion of lithium adatoms, which can migrate across terraces and step edges via Arrhenius-type hopping. A high activation barrier restricts lateral redistribution and favors vertically extended growth, whereas lithiophilic substrates or alloy seeds lower the diffusion barrier, enhance adatom mobility, and promote dense lithium deposits.

When the true local current density exceeds the system-specific limiting current, this surface-level kinetic control can also be governed by bulk ion transport processes aside from the surface diffusion of lithium adatoms, including Li^+-ion electro-diffusion through the electrolyte, interfacial desolvation, and transport through the SEI prior to reduction at the substrate. At current densities exceeding the critical current density, the surface Li^+-ion concentration becomes depleted, leading to a sharp increase in overpotential magnitude. This triggers the formation of a space-charge region and initiates tip growth.[79,80] Within the Chazalviel model, the onset of such dendritic growth is described by Sand's time (τ_s), which increases with square of decreasing current density (J) and with increasing salt concentration (c_0), ion diffusivity (D), and cation transference number (t_+).

https://doi.org/10.1021/acsnano.6c06180
ACS Nano XXXX, XXX, XXX−XXX

$$\tau_s \propto \frac{Dc_0^2}{J^2(1-t_+)^2}$$

Although Sand's time is not strictly applicable to practical lithium metal systems, it provides a useful conceptual framework for understanding transport-limited dendrite growth under conditions such as high current density, low temperature, or hindered ion transport through porous layers developed by accumulated SEI.[80−83] To address this practical limitation, Bai and co-workers introduced the concept of Sand capacity ($C_s = J\tau_s$), which represents the maximum charge that can be passed before ion depletion occurs at the electrode surface.[80] Cycling beyond this capacity induces a transition from reaction-limited mossy lithium growth to transport-limited dendritic growth (Figure 2d), highlighting Sand capacity as a useful design descriptor for evaluating the onset of transport-limited lithium deposition.[80]

However, in practical AFLMBs, Sand's time and Sand capacity should be regarded as conceptual upper bounds rather than quantitatively predictive criteria. Their classical forms assume a planar metal interface, homogeneous liquid electrolyte transport with constant properties, and a spatially uniform current distribution, which are often violated when lithium deposition occurs beneath or within a dynamically evolving mixed SEI/electrolyte interphase. Because the SEI thickness, composition, porosity, and ionic conductivity can vary in both space and time, the actual Li^+-ion concentration field no longer follows a simple one-dimensional depletion profile, and the effective depletion time can deviate strongly from the classical Sand's time and instead follow a modified Sand-type behavior governed by SEI-mediated transport as well as bulk electrolyte diffusion.[82,84,85]

In this context, the interfacial properties of the SEI become particularly important because they regulate Li^+-ion transport across the interface and influence the effective cation transference number. Accordingly, forming a thin, highly Li^+-ion conducting SEI can delay ion depletion at the interface and mitigate the onset of transport-induced dendritic growth.[86] In practical AFLMBs, however, dendrite initiation is not governed solely by the area-averaged current density or bulk electrolyte depletion. Local electric field concentration at surface protrusions, SEI defects, cracks, or low resistance pathways can amplify the true local current density, inducing severe Li^+-ion depletion in confined regions even when the nominal current remains below the classical limiting value. This localized depletion generates strongly nonuniform overpotentials and promotes tip-driven lithium growth, indicating that Sand-type analyses are best regarded as conceptual guides rather than quantitatively predictive models for dendrite onset in practical anode-free cells.

More realistic descriptions therefore require multiphysics modeling frameworks, such as phase-field or moving-boundary models, that couple ion transport, electric potential, SEI-mediated interfacial transport, charge-transfer kinetics, mechanical stress, and evolving lithium morphology. By capturing feedback among concentration gradients, electric field focusing, SEI heterogeneity, and morphological instability, these models provide a more appropriate framework for describing localized dendrite formation under realistic AFLMB operating conditions.

Taken together, the SEI plays a central role in governing lithium deposition behavior by simultaneously influencing thermodynamics, interfacial kinetics, and ion transport. As a notable breakthrough in understanding lithium deposition behavior, applying ultrafast current densities (1,000 mA cm^{-2}) allows lithium deposition to outpace SEI formation, yielding discrete rhombic dodecahedral deposits consistently across different electrolytes and current collectors (Figure 2d−f).[72] This morphology contrasts sharply with the irregular and ill-defined deposits typically observed under practical conditions, highlighting the dominant role of SEI structure, chemistry, and substrate surface properties in dictating lithium growth behavior. As illustrated in Figure 2g, SEI heterogeneity can locally focus current and bias the Li^+-ion flux, promoting nonuniform and filamentary growth even below the classical diffusion limit. Effective stabilization therefore requires coordinated control of interfacial kinetics and ion transport so that ionic flux remains spatially uniform and lithium plating and stripping proceed reversibly over extended cycling.

High-aspect-ratio lithium growth arises from the coupled effects of interfacial thermodynamics, ion-transport kinetics, and mechanical instability, rendering complete suppression fundamentally difficult. While various stabilization strategies, ranging from modified current collectors to engineered SEIs, have improved the morphological control of lithium deposition, these approaches must be re-evaluated in the context of anode-free systems where lithium inventory is intrinsically limited. In such configurations, the critical challenge extends beyond dendrite suppression to ensuring full reversibility of the plating/stripping cycle. Notably, even when uniform lithium plating is achieved, incomplete stripping can result in the isolation of metallic lithium from the conductive matrix, forming electronically disconnected dead lithium. Therefore, understanding the fundamental mechanisms of lithium deactivation during stripping is essential for closing the lithium inventory loop, which we address in the next section.

1.2.2. Lithium Deactivation upon Discharge. The practical reversibility of lithium metal in batteries relies on uniform, complete stripping during discharge. Any local inhomogeneity or inefficiency may convert active lithium into inactive lithium, depletes the finite lithium inventory, and depresses CE and cycle life.[87,88] These effects are particularly pronounced in anode-free configurations,[14] where a transient lithium layer is removed directly from the current collector without an excess-lithium buffer.[89,90] While much effort has focused on uniform plating, the ceiling of reversibility and stability is set by discharge-stage deactivation, void formation, SEI breakdown, and pitting, as well as the electronic isolation of lithium, which collectively accumulates dead lithium, raises impedance, and accelerates capacity fading and safety risks.[35] Thus, despite lithium metal's high theoretical capacity, dead lithium formation during stripping remains a decisive failure pathway, underscoring the need to prioritize homogeneous stripping and interphase integrity alongside plating control.

Dead lithium arises primarily from nonuniform and incomplete dissolution of deposited lithium during discharge process, governed by the coupled evolution of heterogeneous mechanics and morphology of lithium deposit and SEI on it. As lithium is stripped, the SEI stretches, cracks, and collapses, severing electronic pathways and mechanically isolating lithium fragments from the current collector. The resulting chemical and structural heterogeneity amplify local dissolution asymmetry and promotes the accumulation of dead lithium. Quantification and diagnosis, e.g., operando ^{7}Li-Nuclear Magnetic Resonance (NMR),[91,92] mass-spectrometry titra-

https://doi.org/10.1021/acsnano.6c06180
ACS Nano XXXX, XXX, XXX−XXX

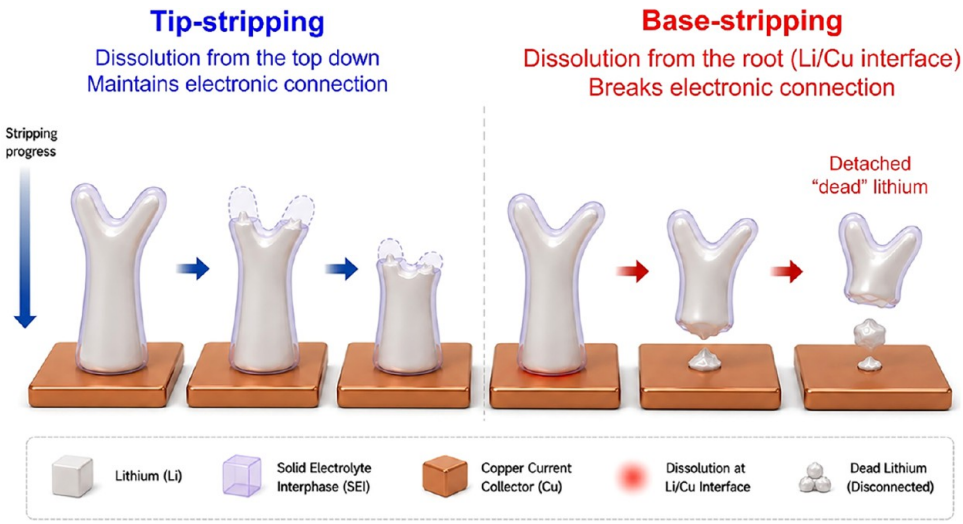

Figure 3. Schematic comparison of tip-stripping and base-stripping in AFLMBs, illustrating the morphological evolution of Li dendrites during delithiation and the formation of electrochemically inactive dead lithium through dissolution-induced detachment.

tion,[93,94] and cryogenic electron microscopy,[95,96] consistently reveal the progressive buildup of inactive lithium under discharge-biased conditions.

Consistent with prior studies, dendrite shrinkage follows three limiting modes: (i) uniform, isotropic dissolution when the SEI is ultrathin or absent (minimal dead lithium), (ii) asymmetric dissolution when SEI coverage is one-sided (residual fragments persist), and (iii) crack-mediated detachment when island-like SEI defects cause piecewise break-off (dead lithium maximal).[97] Together, these behaviors identify SEI integrity and dendrite geometry as principal determinants of dead lithium yield.

To complement the above morphology/SEI perspective, Jiang et al. classified stripping by the dominant dissolution site.[87] (1) Tip-stripping (top-down thinning) proceeds from the outer surface while maintaining electronic contact at the base; this preserves percolation, slows void coalescence, and minimizes dead lithium formation. (2) Base-stripping (root-first detachment) initiates at the Li/substrate interface, leading to early contact loss and detachment of overhanging segments that become electrically isolated. (3) Mixed tip/base stripping involves both directions of dissolution; biasing the process toward tip-dominated stripping, by developing robust Li-collector adhesion, high SEI Li^+-ion conductivity, and moderated end-of-discharge overpotential extends the beneath-SEI regime and mitigates pit formation.

Thermodynamically, base-stripping becomes favorable when weak lithium−collector adhesion lowers the energetic cost of root detachment, particularly under a thick, rigid, swollen, or mechanically mismatched SEI that stores interfacial stress. Under such conditions, dissolution near the lithium−current collector contact region can relieve accumulated stress, but it prematurely disrupts electronic percolation and leaves the upper lithium segment isolated as dead lithium. Kinetically, a resistive or heterogeneous SEI generates nonuniform potential drops and concentrates the stripping driving force at defect-rich or low resistance regions near the base. In contrast, strong lithium−collector adhesion, homogeneous SEI lithium-ion transport, and moderated end-of-discharge overpotential preserve electronic connectivity and favor progressive tip-dominated stripping until the final stage of discharge. Together, these thermodynamic and kinetic factors provide actionable design criteria, adhesion enhancement, SEI homogenization, and overpotential control, to steer the stripping pathway toward tip-dominated dissolution and minimize dead lithium accumulation. Overall lithium stripping phenomena are illustrated in Figure 3.

The formation of dead lithium is a multifactor phenomenon affected by multiple interdependent factors, ranging from electrolyte properties to operational conditions. Most intimately, it is strongly regulated by the SEI. Additives such as fluoroethylene carbonate (FEC) and designs that promote LiF-rich interphases can suppress corrosion, improve stripping efficiency, and extend cycle life. Lithium carbonate phases, promoted by CO_2 additive, are a second example supporting decreased dead lithium, specifically by supporting higher SEI ion conductivity.[98] Interface properties at the current collector, e.g., surface-chemistry modification of copper or conformal polymer coatings, govern ionic/electronic transport and stabilize the lithium/electrolyte contact, thereby reducing dead lithium yield. Deposit morphology is equally decisive: high-aspect-ratio structures (dendrites, mossy lithium) coupled with chemically and spatially heterogeneous SEI induce uneven stripping and electronic isolation of fragments.

The continuous formation and accumulation of dead lithium have profound, compounding effects on long-term performance and safety. With cycling, dead lithium progressively carpets the current collector and electrode surfaces, blocking active sites for deposition/stripping and effectively shrinking the electrochemically available area. SEI encapsulation of such isolated deposits also effectively becomes electrically disconnected, contributing to inactive material accumulation. More critically, the growing, electronically isolated layer interrupts electron pathways and raises internal resistance. The net result is a sharp reduction in reversible lithium inventory, degrading capacity and CE and shortening practical lifetime.[99] In parallel, dead lithium/SEI debris and unstable SEI amplify safety risks by fostering local hot spots, dendritic shorting pathways, and thermal instability. Consequently, understanding and mitigating the formation of dead material is essential to realize the full potential and commercial viability of lithium−metal batteries.[100]

Achieving high lithium reversibility is critical to unlocking the full energy potential of AFLMBs. One effective strategy to

https://doi.org/10.1021/acsnano.6c06180
ACS Nano XXXX, XXX, XXX−XXX

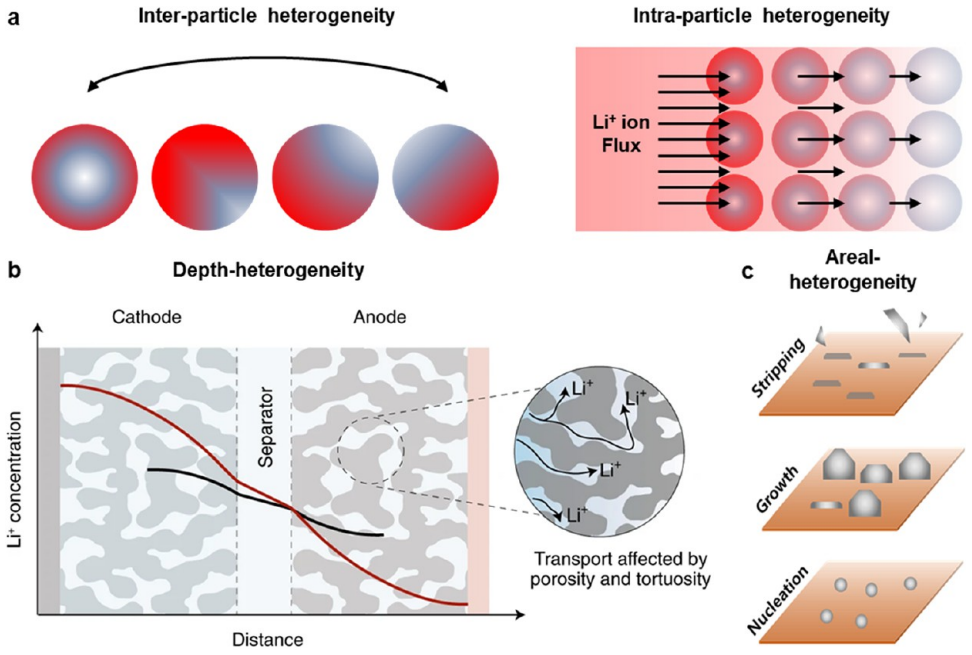

Figure 4. Schematic illustration of reaction heterogeneity phenomena occurring in the anode-free full-cell: (a) inter and intraparticle heterogeneity of cathode active materials, (b) concentration gradient of Li^+-ion long depth of cathode and anode of AFLMBs leading to electrode depth heterogeneity, and (c) areal heterogeneity on copper substrate during the cell operation. Panel b is reproduced with permission from ref 105, © 2019, Springer Nature. The authors retain the right to reuse the figure in this work.

minimize dead lithium formation is the careful optimization of cycling protocols, such as employing asymmetric cycling profiles—slow charging to promote uniform lithium deposition and fast discharge to induce uniform dissolution. Specifically, the formation of transient high-concentration layers during fast stripping can induce more uniform lithium dissolution. Complementarily, the reactivation of dead lithium through rejuvenating additives has emerged as a promising avenue. These additives facilitate the dissolution of electrically isolated lithium and transfer back to cathode, effectively recycling otherwise lost lithium contents. Together, these strategies not only suppress the generation of dead lithium but also recover it, thereby maximizing lithium utilization and pushing the reversibility of AFLMBs toward its theoretical limits. The following sections (Section 5.1, Cycling Protocols for Precise Evaluation, and Section 3.3.3, Electrolyte Additives, respectively) will provide a more detailed discussion of these approaches and their implications for advancing AFLMB technology.

1.2.3. Heterogeneous Reactions over Anode and Cathode. In AFLMBs, cathode and anode have different working mechanisms, such as intercalation/deintercalation and plating/stripping. It leads to different tendencies for reaction heterogeneity over the electrode in both horizontal and vertical directions, which can be understood as areal- and depth-heterogeneity, respectively. A combination of two electrodes with different reaction kinetics makes it more difficult to understand the overall phenomenon of cells, such as electrode-pulverization. Understanding the reactions occurring at the two different electrodes individually, as well as the evolution that occurs when they are combined into a single cell, is essential to enhancing the stability of AFLMBs.

For intercalation materials, there has been much research about heterogeneity with consideration of figuring out the rate-determining step for the charging/discharging process. There are controversies about the role of solid diffusion vs charge transfer, and which step suffers from intra-inter particle heterogeneity between charging and discharging process (Figure 4a).[101−104] These are affected by various factors such as active materials, particle sizes, surface diffusion kinetics, grain properties, current density, or even electrode thickness (or mass loading). Phenomena of intercalation materials itself is still complicated so that it is not clearly understood yet. Such reaction heterogeneity leads to the lower utilization of active materials, resulting in poor cell performance.

For the high-energy density AFLMBs, a highly loaded cathode (>4 mAh cm^{-2}) is required. When we apply thick electrodes to the battery, there can be more severe reaction heterogeneity leading to a distribution of current through the depth of electrode. Unlike conventional electrodes with moderate thickness, more parameters such as tortuosity and electrical connections should be considered to control the uniform Li^+-ion flux over the whole depth and area of the electrode (Figure 4b).[106−110] In this point, reaction heterogeneity of thick electrode can also be changed, leading to the unpredictable deterioration of cell performance.

On the anode side of AFLMBs, it is different from cathode, which is based on the reaction of active materials. It has been regarded that plating morphology is critical for both LMBs and AFLMBs, but it is also important how the Li deposits are distributed across the substrate. Because the lithium plating occurs on the bare copper substrate, its plating heterogeneity has been observed over the electrode area coming from various factors, which leads to the dendritic plating when the current is localized (Figure 4c).[80,83,111] It results in the loss of ability to complete stripping for full lithiation of the cathode during the discharge step, leading to continuous capacity degradation. Therefore, it is necessary to understand the reaction heterogeneity in both vertical and horizontal directions to prevent loss of active lithium sources in AFLMBs.

https://doi.org/10.1021/acsnano.6c06180
ACS Nano XXXX, XXX, XXX−XXX

Taken together, these observations underscore that tortuosity in thick cathodes inevitably generates local heterogeneity in Li^+-ion transport, which subsequently shapes the spatial distribution of Li^+-ion flux at the anode during cycling. Such interconnected effects highlight the importance of integrating cathode and anode perspectives into a unified framework of reaction heterogeneity. While achieving overall balance between cathode loading and anode reversibility is essential for high-energy density AFLMBs, it is equally critical to regulate local balance—controlling heterogeneity at the scale of pores, interfaces, and ion pathways. Only by managing both global and local environments of Li^+-ion can AFLMBs be operated stably, ensuring reliable lithium utilization and long-term performance.

1.3. New Roles in Anode, Cathode, and Electrolytes for AFLMBs

1.3.1. Anode: A Complete Receiver for Higher Reversibility. From the perspective of Sand's theory, dendritic growth of lithium is largely influenced by diffusion limitations from the bulk electrolyte to electrode surface. Traditional understandings of lithium plating assume that reduced lithium is deposited directly onto the current collector upon reduction. However, by homogenizing the Li^+-ion flux the dynamics of lithium deposition can shift from vertical lithium transport and deposition to a more horizontal lithiation process across the electrode surface. Various novel approaches have been explored, such as applying artificial SEI layer,[112−115] electrolyte engineering,[116−124] and introducing lithiophilic materials. Lithiophilic agents such as lithium alloying materials have shown success in guiding smoother lithium deposition by facilitating chemical binding-driven deposition which can minimize vertical interactions between electrodes and electrolytes. For example, Ag-coated layer can promote the uniform and nondendritic lithium deposition. In addition to Ag, other lithium-alloying materials such as Au, Zn, Sn, Si, and Mg are generally considered as the Li^+-ion flux distributor at the interface between electrolyte and current collector.[41,43,44,125−132]

Although these approaches effectively reduce dendritic lithium growth, an important question remains: is nondendritic plating sufficient?[17,133,134] Maximum lithium utilization of AFLMBs is not solely dependent on the uniform plating. Still, many root causes of active lithium loss are not well-considered, such as the formation of electronically disconnected dead lithium during the stripping step and continuous chemical corrosion during the cell's lifespan. It is now time to consider not only uniform electrodeposition but also uniform stripping and storage for 100% utilization of lithium in AFLMBs. Although approaches employing mechanically robust SEI layers, such as LiF-rich SEI, demonstrated its effectiveness to lithium utilization, the fundamental working principle is still under debate.[114,135−138] Addressing this issue requires the development of all cell components—cathode, anode, and electrolyte—to meet the new demands of stability of AFLMBs. Commercialization of AFLMBs can be closer when the current collector becomes a 'complete receiver' where lithium deposition and dissolution are perfectly reversible.

1.3.2. Cathode: Storage of Extra Lithium Source. Even if we found the way to perfectly control the plating/stripping behavior of lithium, there is still unavoidable loss of lithium source during continuous cycling attributed to the high reactivity of lithium. This lithium depletion stems from a variety of factors including the irreversible consumption of lithium during the formation of the SEI on the anode and ongoing side reactions over time. To achieve higher CE and longer calendar life, it is essential to introduce additional lithium sources somewhere in the cell structure. In AFLMB systems, continuous lithium supply can be integrated into the positive electrode by using prelithiation agents and a thick cathode.

Cathode prelithiation agents are compounds that are specifically used to release lithium ions into the electrolyte during cell operation. The key advantage of these materials lies in their ability to provide extra amounts of lithium within the cathode, compensating for the lithium loss at the anode over time. Since this is achieved without introducing additional lithium source at the anode, it has been considered as a critical strategy for maintaining the AFLMB configuration. The design of these materials needs to follow certain criteria within the defined voltage window: they must release lithium at voltages lower than the upper cutoff, and at the same time, they should not take up lithium again at voltages higher than the lower cutoff. When these conditions are fulfilled, prelithiation agents can act as an extra lithium source during charging, helping to offset the lithium loss that occurs on the anode.

From a capacity maximization perspective, the integration of thick cathodes is essential for AFLMBs and must be considered in conjunction with overall cell design. Beyond simply increasing specific capacity, thick cathodes provide the necessary physical space to accommodate prelithiation agents. However, considering the extension to Ah-scale practical applications, kinetic limitations associated with ion transport can induce multidimensional heterogeneity in lithium distribution across the electrode. Under such conditions, achieving uniform and efficient operation requires the development of prelithiation agents, cathode active materials, and electrode architectures that can operate reliably without kinetic constraints, while simultaneously addressing wetting issues under lean electrolyte conditions. Only through such integrated approaches can the cathode in AFLMBs effectively serve as a reservoir for an extra lithium source.

1.3.3. Electrolytes: Lithium Transporter and Reactivator. While the anodes in AFLMBs act as a "complete receiver" and the cathodes must store an "extra lithium source", the electrolyte medium plays more complex roles in ionic transport, (de)solvation, and SEI chemistry. The electrolyte governs how fast Li^+-ions pass from the bulk to the interface, how they are (de)solvated and reduced, and what interphase chemistry is formed throughout the whole life cycle of the battery. Beyond high-power performance, fast ion transport in AFLMBs is theoretically crucial for lithium dendrite suppression, as it avoids Li^+-ion depletion and electric field focusing, thereby mitigating localized and unstable lithium nucleation.[80,139] Moreover, because AFLMBs operate with a strictly limited lithium inventory, electrolyte-driven corrosion directly translates into irreversible lithium loss and rapid capacity fading.[140−142] Therefore, electrolyte engineering is not only a supportive approach but can be a central requirement to achieve near-100% lithium utilization in AFLMBs.

From the perspective of attaining near-100% lithium utilization, the key challenge lies in minimizing the net loss of cyclable lithium per cycle. While such losses could, in principle, be eliminated if electrode operating potentials resided entirely within the electrochemically stable window of the electrolyte, as in $LiFePO_4||Li_4Ti_5O_{12}$ redox couple,

https://doi.org/10.1021/acsnano.6c06180
ACS Nano XXXX, XXX, XXX−XXX

lithium metal electrodes inevitably induce SEI formation owing to their extremely low reduction potential and remains highly reactive toward most electrolyte components.[58,143] Thus, this necessitates an electrolyte that forms an ideal SEI, which should be electronically insulating, Li^+-ion conducting, and mechanically resilient against swelling,[144] fracture,[73] and dissolution,[145] such that the lithium metal is completely passivated without further parasitic reactions between lithium and the electrolyte.

Moving away from additive-guided SEI engineering, modern electrolyte design has increasingly emphasized solvation chemistry to steer reductive pathways toward anion-derived, inorganic-rich interphases. At the same time, spatially uniform SEI across the anodes is also crucial, because chemical robustness alone can be undermined by the spatial heterogeneity of interphase morphology that induces localized ion transport, current focusing, and persistent parasitic reactions.

Crucially, practical-level AFLMBs also demand addressing lithium losses associated with stripping, where interphase contraction and loss of electronic contact generate dead lithium. During the stripping process, metallic Li^0 is oxidized to form Li^+-ions that will desorb from the surface, traverse across the SEI layer, and then become solvated by anions and solvent molecules present at the top of the SEI.[56,58,146,147] The desorption of Li^+-ions is governed by the overpotential and exchange current density which are related to the thermodynamic and kinetics of species interactions in the electrolyte as well as SEI compositions.[56,87] A more ordered Li^+-ion diffusion through the SEI promotes a more uniform lithium stripping which reduces the amount of dead lithium. The solvation step after stripping is crucial because it determines the plating environment of lithium during the next charging.[148] Therefore, understanding the thermodynamics and kinetics of each elementary step provides insights in electrolyte engineering toward achieving complete lithium stripping.

In addition, additive engineering is evolving beyond SEI engineering toward a complementary function: rejuvenation of dead lithium.[149] Redox mediators and related "Li^+-ion regenerators" can chemically reactivate the inactive lithium and reincorporate it into the electrochemical system, providing a pathway to mitigate cumulative lithium inventory loss that cannot be fully eliminated by SEI stabilization alone. Although such additives must be designed to avoid detrimental shuttling, cathode-side penalties, and unwanted chemical reactivity toward lithium metal, their ability to couple favorable SEI formation with dead lithium recovery highlights why electrolyte engineering is indispensable for approaching near-100% lithium utilization in practical AFLMB systems.

2. POSTULATED STANDARD IN LITHIUM-INVENTORY ASSESSMENT

CE is the most widely used metric for evaluating lithium reversibility, but it is insufficient by itself to describe the cumulative depletion of lithium inventory in AFLMBs. As AFLMB research progresses beyond simple lithium plating behavior toward Gen 5 concepts that additionally consider stripping, dead-lithium accumulation, and lithium recovery, it becomes increasingly necessary to adopt evaluation metrics that more comprehensively reflect the overall lithium-utilization behavior of the full cell. In this regard, we introduce this section before the discussion of cell design to provide readers with a practical framework for interpreting the design strategies discussed throughout this review. In a strict anode-free configuration, no pre-existing lithium metal is supplied on the negative electrode, and the capacity-defining lithium inventory is provided by the lithiated cathode. Therefore, even a small irreversible lithium loss per cycle can accumulate into rapid capacity decay. To complement CE, we suggest the Lithium Inventory Retention Index (LIRI) as a cumulative descriptor of how much of the initial electrochemically accessible lithium inventory remains after repeated cycling.

For a strict anode-free full cell, the initial accessible lithium inventory is defined as the reversible lithium capacity supplied by the cathode:

$$Q_{\mathrm{LI},0} = Q_{\mathrm{cathode},0} = x_0$$

where x_0 is the initially designed cell capacity. Equivalently,

$$Q_{\mathrm{LI},0} = \Lambda x_0$$

where Λ is the initial lithium-inventory factor normalized to the designed cell capacity. For a strict and ideal anode-free cell,

$$\Lambda = 1,\ N/P_{\mathrm{Li}} = 0$$

In practice, however, Λ can deviate from unity due to initial irreversible lithium losses arising from factors such as cathode prelithiation inefficiency, thick-electrode transport limitations, incomplete cathode utilization under practical cutoff voltages, electrolyte wetting heterogeneity, temperature-dependent kinetic constraints, and interfacial side reactions during formation. Accordingly, Λ should be experimentally determined from the practically reversible discharge capacity after formation or few initial cycles rather than from the theoretical cathode capacity only. The detailed origins of these initial irreversible-capacity losses and their impact on the reduction of Λ under practical AFLMB conditions will be discussed in the following sections.

Here, N/P_{Li} denotes the ratio of pre-existing negative-electrode lithium capacity to positive-electrode capacity. Importantly, we have clarified that the lithium contained in conventional supporting electrolyte salts, such as $LiPF_6$, LiFSI, or LiTFSI, is not counted as an independent capacity-defining lithium reservoir in $Q_{\mathrm{LI},0}$. Although electrolyte lithium ions participate in transport, solvation/desolvation, and interfacial reactions, the net cyclable lithium inventory in a true anode-free full cell is supplied by the cathode. Including ordinary salt-derived lithium as part of the accessible inventory would artificially favor cells with excessive electrolyte or higher salt concentration. Instead, lithium consumption associated with electrolyte decomposition, SEI growth, corrosion, or dead-SEI formation should be included as a loss term.

For the i-th cycle, lithium inventory loss can be expressed as the sum of four primary contributions:

$$\Delta Q_{\mathrm{LI},i} = \Delta Q_{c,i} + \Delta Q_{a,i} + \Delta Q_{\mathrm{deadLi},i} + \Delta Q_{\mathrm{deadSEI},i}$$

where $\Delta Q_{c,i}$ represents cathode-side irreversible lithium loss, $\Delta Q_{a,i}$ represents anode-side lithium plating/stripping inefficiency, $\Delta Q_{\mathrm{deadLi},i}$ represents physically isolated dead lithium, and $\Delta Q_{\mathrm{deadSEI},i}$ represents lithium consumed into electrochemically inactive SEI/corrosion products.

These terms are expressed as

https://doi.org/10.1021/acsnano.6c06180
ACS Nano XXXX, XXX, XXX−XXX

$$\Delta Q_{c,i} = x_i(1 - \mathrm{CE}_{c,i})$$

$$\Delta Q_{a,i} = x_i(1 - \mathrm{CE}_{a,i})$$

$$\Delta Q_{\mathrm{deadLi},i} = \delta_i x_i$$

$$\Delta Q_{\mathrm{deadSEI},i} = \gamma_i x_i$$

where x_i is the capacity cycled during the i-th cycle, $\mathrm{CE}_{c,i}$ is the cathode-side Coulombic efficiency, $\mathrm{CE}_{a,i}$ is the anode-side lithium plating/stripping Coulombic efficiency, δ_i is the fraction of cycled lithium that becomes physically isolated as dead lithium, and γ_i is the fraction of cycled capacity consumed by additional chemical reactions such as SEI growth, lithium corrosion, electrolyte decomposition, or dead SEI formation. The γ_i term should be defined to avoid double-counting lithium already included in the physically isolated dead-lithium term.

Accordingly, the base form of LIRI after N cycles is

$$\mathrm{LIRI}_N^{\mathrm{base}} = 1 - \frac{\sum_{i=1}^{N} x_i[(1 - \mathrm{CE}_{c,i}) + (1 - \mathrm{CE}_{a,i}) + \delta_i + \gamma_i]}{\Lambda x_0}$$

For a strict anode-free cell, where $\Lambda = 1$, this becomes

$$\mathrm{LIRI}_N^{\mathrm{base}} = 1 - \frac{\sum_{i=1}^{N} x_i[(1 - \mathrm{CE}_{c,i}) + (1 - \mathrm{CE}_{a,i}) + \delta_i + \gamma_i]}{x_0}$$

This expression emphasizes that LIRI is not a single-cycle CE value, but a cumulative lithium-inventory balance normalized by the finite initial lithium inventory.

The same framework can be extended to recovery-enabled AFLMBs. If redox mediators, adaptive cycling protocols, or electronically reconnecting interphases reactivate a fraction ρ_i of dead lithium during the i-th cycle or subsequent recovery step, the recovery-corrected LIRI can be written as

$$\mathrm{LIRI}_N^{\mathrm{rec}} = 1 - \frac{\sum_{i=1}^{N} x_i[(1 - \mathrm{CE}_{c,i}) + (1 - \mathrm{CE}_{a,i}) + \delta_i(1 - \rho_i) + \gamma_i]}{\Lambda x_0}$$

where ρ_i is the dead-lithium recovery yield, which may be experimentally quantified using dead-lithium characterization techniques discussed in Section 3.3.3, such as NMR, Titration gas chromatography (TGC), and Morphological surface texture (MST) analysis.

When cathode prelithiation agents, sacrificial lithium sources, preloaded lithium, or intentionally designed electrolyte-based lithium donors are introduced, the cell should be distinguished from a strict zero-excess lithium inventory system. In this case, the effective initial lithium inventory becomes

$$Q_{\mathrm{LI},0}^{\mathrm{pre}} = x_0 + \eta_{\mathrm{pre}} Q_{\mathrm{pre}}$$

and

$$\Lambda_{\mathrm{pre}} = 1 + \frac{\eta_{\mathrm{pre}} Q_{\mathrm{pre}}}{x_0}$$

where Q_{pre} is the theoretical lithium capacity supplied by the prelithiation source and η_{pre} is its practical lithium-release efficiency. Thus, strict anode-free cells have $\Lambda = 1$, whereas prelithiated or lithium-reservoir-containing AFLMBs have $\Lambda_{\mathrm{pre}} > 1$.

In addition to defining lithium-inventory-based metrics, meaningful comparison of AFLMB studies requires standardized reporting of cell-design and testing parameters. Because AFLMB performance is strongly affected by cell format, cathode loading, electrolyte amount, stack pressure, formation protocol, and CE calculation method, these conditions should be explicitly reported rather than treated as incidental experimental details.

At minimum, future AFLMB studies should report the following parameters: cell format, cathode chemistry, cathode areal capacity, N/P_{Li}, Λ, electrolyte-to-capacity ratio (E/C, g Ah^{-1}), total electrolyte amount, stack pressure, pressure measurement method, pressure uniformity, testing temperature, formation protocol, current density or C-rate, voltage window, CE calculation method, and capacity-retention criterion.

As suggested benchmark conditions for strict anode-free full cells, we recommend:

$$N/P_{\mathrm{Li}} = 0$$

$$E/C \leq 2.0\ \mathrm{g\,Ah^{-1}}$$

$$\text{Cathode areal capacity} \geq 4.0\ \mathrm{mAh\,cm^{-2}}$$

These conditions are intended to distinguish practical zero-excess lithium inventory cells from cells stabilized by hidden lithium reservoirs, excess electrolyte, or low-loading cathodes.

Stack pressure should also be treated as a controlled cell-design variable rather than an incidental assembly condition, because it strongly affects lithium morphology, interfacial contact, stripping behavior, SEI evolution, and dead-lithium formation. We suggest reporting both low-pressure and moderate-pressure conditions, such as 0.1 and 1.0 MPa, unless a different pressure range is required by the target cell format. For coin cells, crimping-induced pressure should be experimentally quantified rather than assumed. For pouch cells, externally applied pressure and spatial pressure uniformity over the electrode area should be reported.

Together, these suggested metrics and benchmark conditions are not intended to restrict the diversity of AFLMB research, but to provide a transparent basis for comparing different strategies. By reporting LIRI together with N/P_{Li}, Λ, E/C ratio, cathode areal capacity, and controlled stack pressure, future studies can more clearly distinguish intrinsic improvements in lithium utilization from performance gains arising from excess lithium, excess electrolyte, or favorable testing conditions. Based on these standardized perspectives, the following sections discuss how individual materials and cell-level design factors collectively influence lithium utilization, heterogeneity evolution, and long-term stability in AFLMBs.

3. HOLISTIC MATERIAL DESIGNS FOR LONG-LASTING ZERO-EXCESS LITHIUM METAL BATTERIES

3.1. Anodes

In the case of AFLMBs, the anode, or more precisely, the anode current collector, experiences direct interaction with lithium metal during the plating/stripping cycles. During this

https://doi.org/10.1021/acsnano.6c06180
ACS Nano XXXX, XXX, XXX−XXX

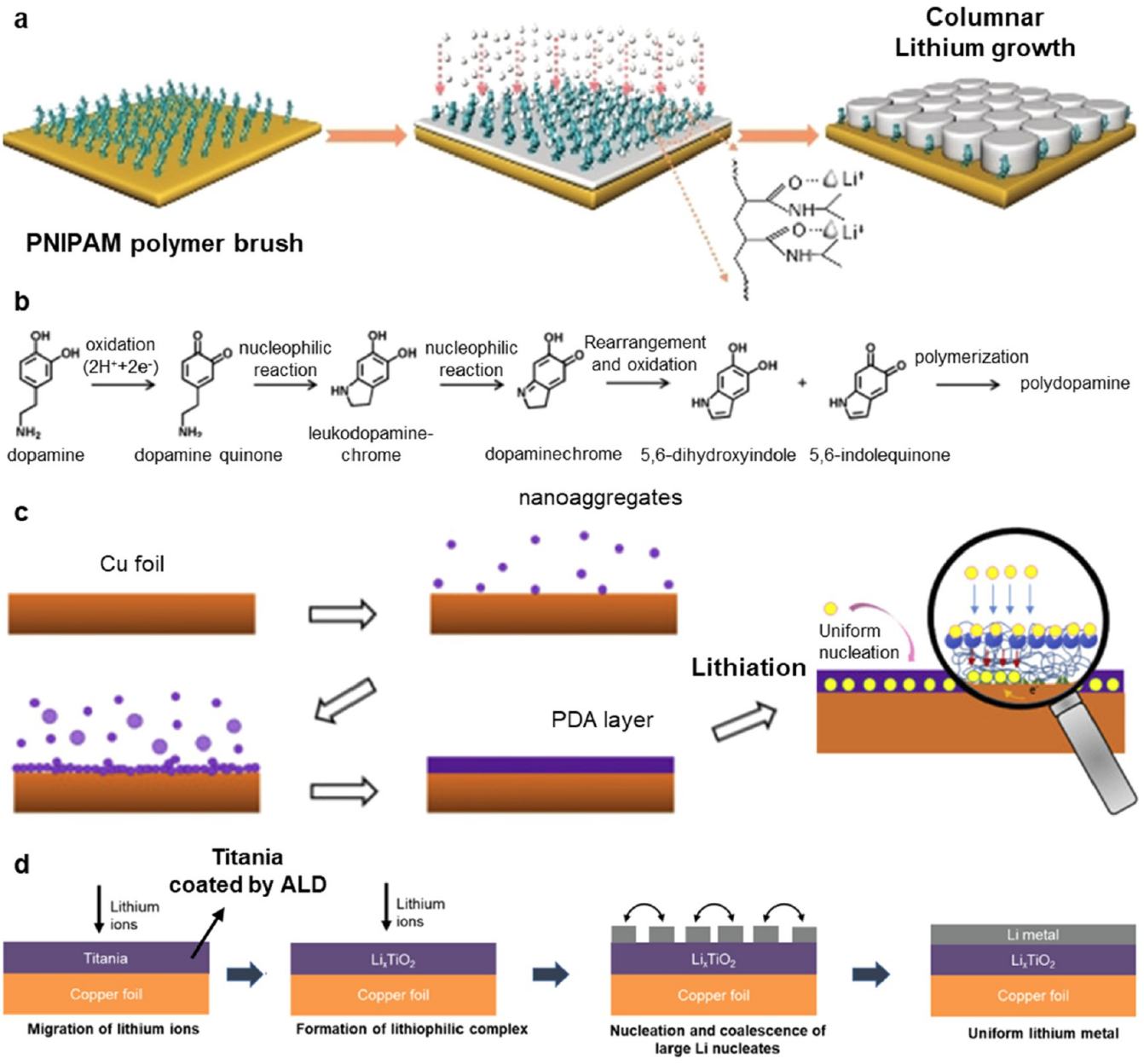

Figure 5. (a) Comparison of Li nucleation behavior on the bare Cu foil and PNIPAM-grafted Cu substrates. (b) Reaction mechanism of a self-initiated PDA interfacial layer. (c) Conceptual illustrations depicting how a high-dielectric-constant artificial SEI mitigates Li^+-ion depletion and surface concentration difference, thereby suppressing concentration polarization compared to unprotected systems. (d) Schematic of Li deposition mechanisms on pristine Cu compared to TiO_2-functionalized surfaces. Panels are reproduced with permissions from a, ref 155, © 2019 Wiley-VCH Verlag GmbH, Weinheim; b–c, ref 156, © 2019 Elsevier; d, ref 159, © 2020 Wiley-VCH GmbH.

time, the surface is initially in direct contact with the electrolyte, undergoes electron transfer reactions, and participates directly in the reaction, leading to electrolyte decomposition and increased internal cell resistance.[150,151] Heterogeneous and random nucleation of lithium can also induce the formation of lithium dendrites and dead lithium.[152−154] For these reasons, the primary cause of cell degradation in AFLMBs is often the anode. To overcome this challenge, it is crucial to adjust the structure, surface properties, and composition of the current collector to maintain stable lithium plating/stripping cycles over long periods of time. From this perspective, this chapter introduces structural and compositional modification, surface treatment strategies, the influence of surface crystallographic texture, and fundamentals of lithium corrosion during storage period. Through these strategies, we will summarize the breakthrough for physically and chemically controlling the continuous volume change of anode and examine the parameters to consider for inducing uniform plating/stripping cycles.

3.1.1. Surface Modification. Even if research on the current collector itself continues, it will ultimately lead to finding optimal conditions within limited choice of materials and structures. Considering cell manufacturing processes and cost, it is inevitable to develop a current collector that delivers optimal performance within these limitations. The fundamental limitations of the material itself and its surface properties will finally need to be overcome through surface modification methods. Typically, these surface treatment methods are

https://doi.org/10.1021/acsnano.6c06180
ACS Nano XXXX, XXX, XXX−XXX

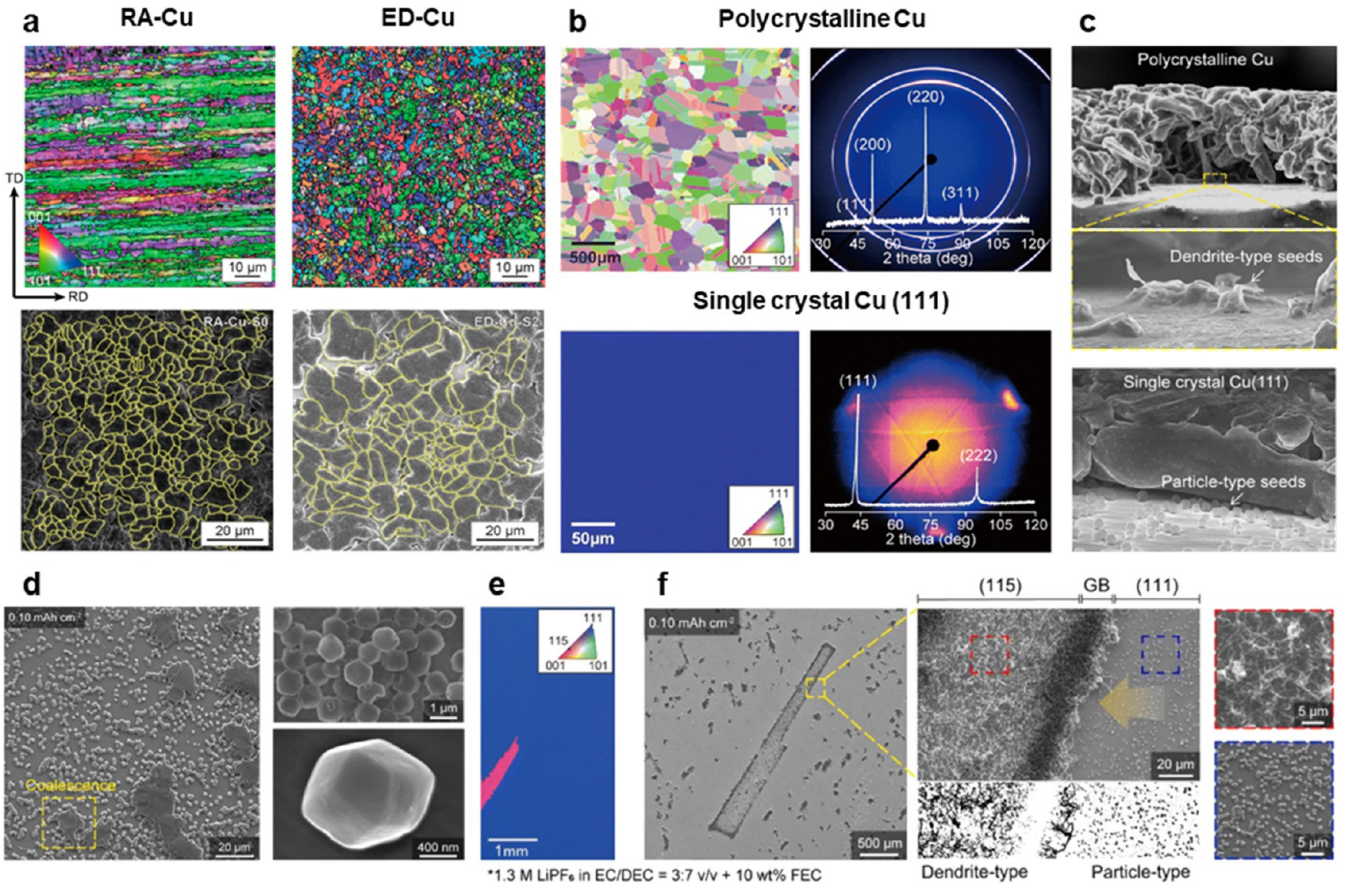

Figure 6. Influence of surface texture of copper substrates on lithium plating. (a) EBSD IPF maps (up) of rolled-annealed copper (RA-Cu) and electrodeposited copper (ED-Cu) and their lithium plating morphologies, (b) EBSD inverse pole figure (IPF) map (left) and their corresponding XRD 2θ and WAXS results (right) of polycrystalline and (111)-single crystalline copper, respectively, (c) Cross-section images of plated lithium on polycrystalline and single crystalline copper, (d) Electroplated lithium particles with rhombic dodecahedron shape on (110)-single crystalline copper substrate. (e) EBSD IPF map of (111)-single crystalline copper with high-index defect of (115)-plane and (f) their different lithium nucleation behaviors at plating capacity of 0.1 mAh cm^{-2}. Panels are reproduced with permissions from a, ref 165, © 2023 American Chemical Society; b–f, ref 71, © 2024 The Royal Society of Chemistry. (the authors retain the right to reuse the figure in this work).

suggested to facilitate electrolyte wettability and Li^+-ion adsorption properties between the surface of the current collector and the electrolyte, thereby promoting better transport of Li^+-ions from bulk electrolyte to electrode surface. In addition, artificially treated interphase layer can act in a more predictable and intended way rather than ion transport behavior of randomly formed SEI of pristine electrode. We introduce the polymer and inorganic coating methods, which have been recently proposed as representative approaches.

Functional polymer coatings not only reduce dendritic formation but also help in regulating Li^+-ion transport. Unique properties of the polymer matrix or their imbedded nanoparticles successfully facilitate the lithium transport on the surface of current collectors, leading to stable plating/stripping cycles. Li et al. applied poly(*N*-isopropylacrylamide) (PNIPAM) polymer brushes to Cu substrates to achieve uniform lithium deposition for dendrite-free lithium metal anodes.[155] The self-initiated polymerized coating layer of PNIPAM has its unique brush-shaped structure improved electrolyte wettability, ion transfer and lithium nucleation, leading to a columnar lithium layer with a flat surface (Figure 5a). A self-polymerized polydopamine (PDA) coating onto Cu current collectors, introduced by He et al., demonstrated improved uniformity of lithium plating.[156] The PDA layer promotes uniform nucleation by forming Li-complexing carbonyl groups, acting as uniformly distributed nucleation spots, and achieved extended cycle life of AFLMBs (Figure 5b and c). Strategies to evenly disperse functional nanoparticles in a stable and uniform polymer matrix have also been proposed. Tamwattana et al. tuned the dielectric properties of the surface of current collector with polymer coating.[157] A coating layer made of polyvinylidene fluoride (PVDF) matrix containing LiF nanoparticles, which has highly dielectric properties, successfully modulate the plating/stripping environment over current collector by promoting efficient Li^+-ion transport at the interphase. Considering the diversity of polymers and the functional materials that can be incorporated into the matrix, as well as the importance of coating uniformity, polymer coating represents a widely applicable approach for surface treatment.[158]

Surface modification of current collectors with inorganic materials is typically achieved through atomic layer deposition (ALD) to regulate Li^+-ion flux and deposition. Unlike traditional surface treatments, ALD allows for the precise deposition of inorganic materials, such as SnO_2 and TiO_2, which enhance the lithiophilicity of current collectors. The ALD-derived inorganic layers can serve as a lithiophilic platform for uniform lithium deposition, leading to more

https://doi.org/10.1021/acsnano.6c06180
ACS Nano XXXX, XXX, XXX–XXX

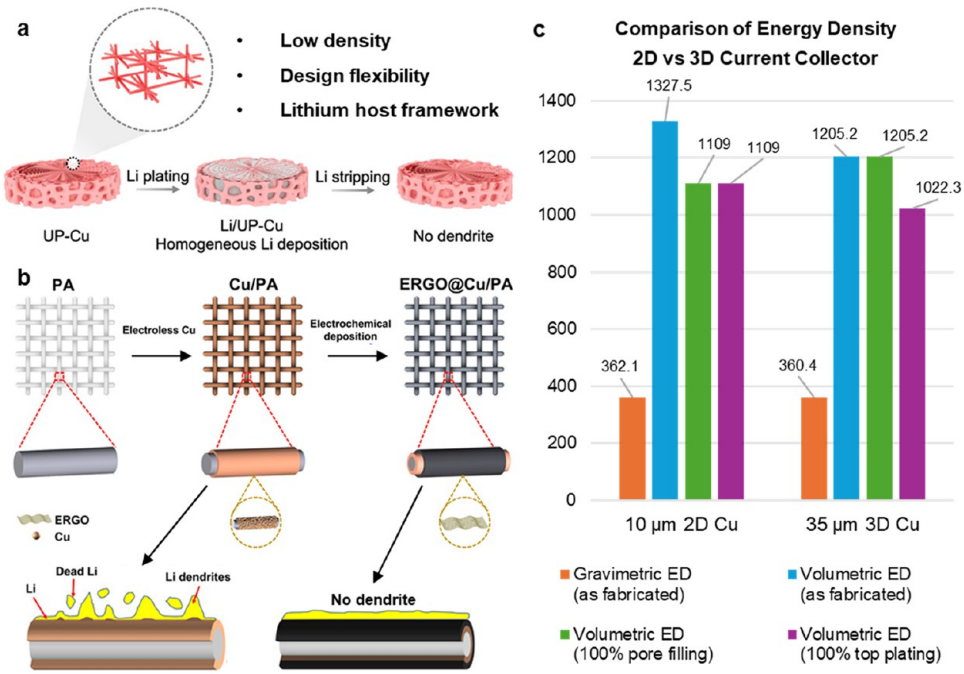

Figure 7. Lithium hosting and dendrite suppressing abilities of 3D current collectors based on porous copper framework. (a) Li plating/stripping dynamics on an ultralight porous copper (UP-Cu) 3D framework, demonstrating stable lithium hosting. (b) Nucleation and deposition mechanisms contrasted between pristine Cu/PA and ERGO@Cu/PA mesh electrodes. (c) Comparison of gravimetric and volumetric energy densities of 2D and 3D copper current collectors. Numerical comparison was made between cases where lithium plating occurred with complete pore filling and cases where it occurred with complete top plating when cells were fabricated using each current collector, assuming 2.55 Ah-class anode-free pouch-cell configuration with a cathode areal capacity of 5 mAh cm^{-2}. Panels are reproduced with permissions from a, ref 167, © 2022 American Chemical Society; b, ref 168, © 2023 American Chemical Society.

uniform deposition and reducing dendritic lithium formation. Kim et al. improved the electrochemical performance of anode-free lithium metal batteries by applying an ultrathin lithiophilic layer (ULL) to copper current collectors via an ALD process.[160] The SnO_2-based ULL reduces the nucleation overpotential, thereby promoting uniform lithium deposition on the SnO_2 layer. A smoother, dendrite-free lithium layer forms on the ULL, which guides the subsequent deposition of uniform, thick lithium layers. These sequential steps in lithium deposition contribute to the more stable operation of LMBs. Oyakhire et al. developed a method to control deposition morphology using ALD of TiO_2 on copper current collectors.[159] The TiO_2 layer, applied at the Cu−Li interface, acts as an underlayer, reducing nucleation overpotential and promoting the formation of uniform lithium particles. This approach minimizes dendrite formation and improves the electrochemical reversibility of lithium deposition. As a result, the Cu foil coated with a 5 nm TiO_2 layer demonstrated excellent cycling performance and high CE (Figure 5d).

Various approaches utilizing surface coating have been proposed to promote uniform lithium plating. However, further development must consider actual battery cycles, including not only the lithium plating but also stripping and storage. Advanced coating technologies must be multifunctional that can maintain its stable structure over long periods of cycling, induce uniform lithium plating/stripping, and prevent lithium corrosion during storage.

3.1.2. Crystallographic Approaches. The process of lithium plating on the current collector is complex, involving multiple steps such as mass transport in the electrolyte, desolvation of Li^+-ions, charge transfer, electro-adsorption, surface migration, nucleation, and growth. From a crystallographic perspective, the surface features of current collectors, such as crystallographic facets and grain boundaries, play a critical role in lithium plating and stripping process. Understanding the relationship between the surface texture of current collectors and lithium plating behavior could provide us with new insights for improving AFLMBs.[161−164] However, the exact mechanism by which these crystallographic properties influence the nucleation and growth remains poorly understood.

In the case of polycrystalline Cu foil, lithium plating behavior has been statistically studied across large areas consisting of numerous grains and grain boundaries (Figure 6a). Wang et al. demonstrated a correlation between grain size, the spatial distribution of deposited lithium, and the density of coincidence site lattice (CSL) type grain boundaries on the surface of polycrystalline copper foil by utilizing EBSD.[165] They found that controlling the fraction of low $\sum$ CSL grain boundaries can lower the surface energy of Cu, increase nucleation overpotential, and result in fewer but larger lithium particles. Ideally, introducing single-crystalline Cu foil is suggested to minimize surface energy and promote the preferential growth of larger particles.

Recently, Kim et al. reported that single crystalline Cu (111) foil, obtained from Contact-free annealing (CFA),[166] outperforms conventional polycrystalline Cu foil due to its higher lithium affinity and lower migration barrier (Figure 6b and c).[71] Among various crystallographic facets of Cu, Cu (111) plane has the lowest surface migration barrier (0.01 eV) for Li^0 adatoms, promoting the horizontal migration of growth of lithium nuclei. Due to the relatively weak interaction between Li^0 adatom and Cu (111), rhombic-dodecahedron lithium seeds are created during the early stage of plating instead of the

https://doi.org/10.1021/acsnano.6c06180
ACS Nano XXXX, XXX, XXX−XXX

dendritic seeds observed in the case of conventional polycrystalline Cu foil. These uniquely shaped seeds, which are thermodynamically the most stable,[72] indicate that the Cu (111) surface did not interrupt the reduction-migration-nucleation process of lithium (Figure 6d–f). This work successfully highlights the relationship between the surface texture of the substrate and lithium plating behavior.

Although the role of surface texture of current collectors on lithium plating is not yet fully understood, it is obvious that the crystallographic features of current collectors significantly impact the process of lithium deposition. We propose that the whole process of lithium plating in AFLMBs should be re-examined, considering the surface texture of current collectors, alongside the effects of the electrolyte, SEI layer, and other surface oxide impurities.

3.1.3. Designing 3D Current Collectors. Despite significant advancements in 2D current collectors through surface coatings and crystallographic texturing, they still face limitations, particularly in accommodating the volume changes that occur during plating and stripping. For instance, the theoretical volumetric change in an anode-free cell, comprising a cathode with an areal capacity of 5 mAh cm^{-2} coupled with a 2D current collector, is calculated to be approximately 20–30% during charge–discharge cycling. During the continuous volume change in AFLMB cycles, uncontrollable mechanical stress can accumulate throughout the entire cell, leading to deformation of contacts and increased internal resistance. Unable to withstand such extreme volume changes, the SEI often forms defects or cracks, which are a major cause of cell degradation. To address this issue, a 3D current collector strategy has been proposed, offering free space for lithium accommodation from the outset. These 3D current collectors have been studied for their design flexibility compared to conventional 2D designs and for their ability to reduce cell resistance by providing a larger surface area that can be used for lithium plating (Figure 7a).[167]

3D current collectors, such as porous metal foams and carbon scaffolds, significantly reduce local current density and promote a more uniform distribution of Li^+-ions. This uniformity helps suppress dendritic formation, alleviates mechanical stress on the SEI layer, and ultimately enhances battery stability and cycle life.[153,154] Moreover, the porous architecture of 3D collectors accommodates volume fluctuations during cycling, preventing the SEI degradation commonly observed in 2D current collectors. However, the apparent benefit of 3D current collectors should be evaluated together with their cell-level energy-density penalty, because high porosity inevitably introduces inactive pore volume and additional scaffold thickness. Further improvements can be achieved by modifying the surface of 3D collectors with lithiophilic materials, which reduces nucleation overpotential and further suppress dendritic lithium growth. The interconnected porous network of 3D structures also provides improved pathways for electrolyte infiltration, ensuring more efficient Li^+-ion transport. This not only enhances ion mobility but also promotes more uniform lithium deposition.[169,170] Zhang et al. demonstrated lithiophilic reducing graphene oxide (ERGO) covered copper/nylon mesh as a porous current collector for AFLMB fabrication.[168] It was confirmed that its lithiophilic surface coating plays a key role in uniform distribution of Li^+-ion flux, while also acting as a flexible and stable lithium host materials (Figure 7b). The low density resulting from the porous structure and low-density polymer substrate also leads to an increase in energy density. These properties are particularly advantageous in AFLMBs, since this 3D framework can serve as a stable host structure from the initial state. These developments, including metal-based, carbon-based, and hybrid 3D collectors, address the limitations of 2D structures by offering favorable advantages such as increased surface area, uniform lithium deposition, and enhanced electrochemical stability.

Ironically, from the perspective of side reactions, the large surface area of 3D current collectors can also represent a critical drawback. While the expanded surface facilitates uniform lithium nucleation, it simultaneously increases the interfacial area susceptible to parasitic reactions, such as electrolyte decomposition and corrosion, which can be particularly problematic under lean electrolyte conditions. To prevent this, as in the previous example, it may be necessary to design an interphase layer that can function stably even in long-term cycles. In addition, although the porous architecture provides additional free volume for lithium accommodation and can enhance gravimetric energy density, it inevitably compromises volumetric energy density (Wh L^{-1}). It should also be noted that there may be a limit to the capacity that can maintain the advantages of the 3D current collectors. Unlike planar 2D current collectors, which are not intrinsically limited in capacity, 3D current collectors may impose an upper bound on lithium storage defined by the initially available pore volume under zero-volume-change conditions.

To quantitatively evaluate this trade-off, we considered a representative 2.55 Ah-class anode-free pouch-cell configuration with a cathode areal capacity of 5 mAh cm^{-2}. The total cell capacity used in this calculation was 2.55 Ah, obtained from an electrode area of 51.03 cm^2 and ten cathode-coated sides. Assuming dense lithium deposition, 5 mAh cm^{-2} corresponds to approximately 24.3 μm of lithium thickness, based on the theoretical capacity and density of lithium metal. Therefore, a 3D current collector with 70% porosity requires a minimum thickness of approximately 35 μm to fully accommodate this amount of plated lithium within its internal pore volume under an ideal single-side-equivalent pore-filling assumption.

Using this condition, we compared a conventional 10 μm 2D Cu current collector with a 35 μm-thick 3D Cu current collector with 70% porosity (Figure 7c). In the as-fabricated state, replacing 10 μm 2D Cu with 35 μm 3D Cu slightly decreases the gravimetric energy density from 362.1 to 360.4 Wh kg^{-1}, because the Cu-equivalent solid thickness of the 3D scaffold is 10.5 μm. More significantly, the volumetric energy density decreases from 1327.5 to 1205.2 Wh L^{-1}, corresponding to an approximately 9.2% volumetric penalty caused by the larger initial thickness of the 3D scaffold.

However, when the fully charged state is considered, the conclusion changes depending on the lithium deposition mode. In the 2D Cu case, dense lithium plating occurs on top of the current collector, increasing the cell thickness and decreasing the charged-state volumetric energy density to approximately 1109.0 Wh L^{-1}. In contrast, if lithium is completely accommodated inside the pores of the 35 μm 3D Cu current collector, the volumetric energy density remains approximately 1205.2 Wh L^{-1} even in the charged state. This indicates that 3D current collectors can become volumetrically advantageous when the charged-state cell volume, rather than only the as-fabricated volume, is considered. Under this ideal pore-filling condition, the 3D current collector provides

https://doi.org/10.1021/acsnano.6c06180
ACS Nano XXXX, XXX, XXX–XXX

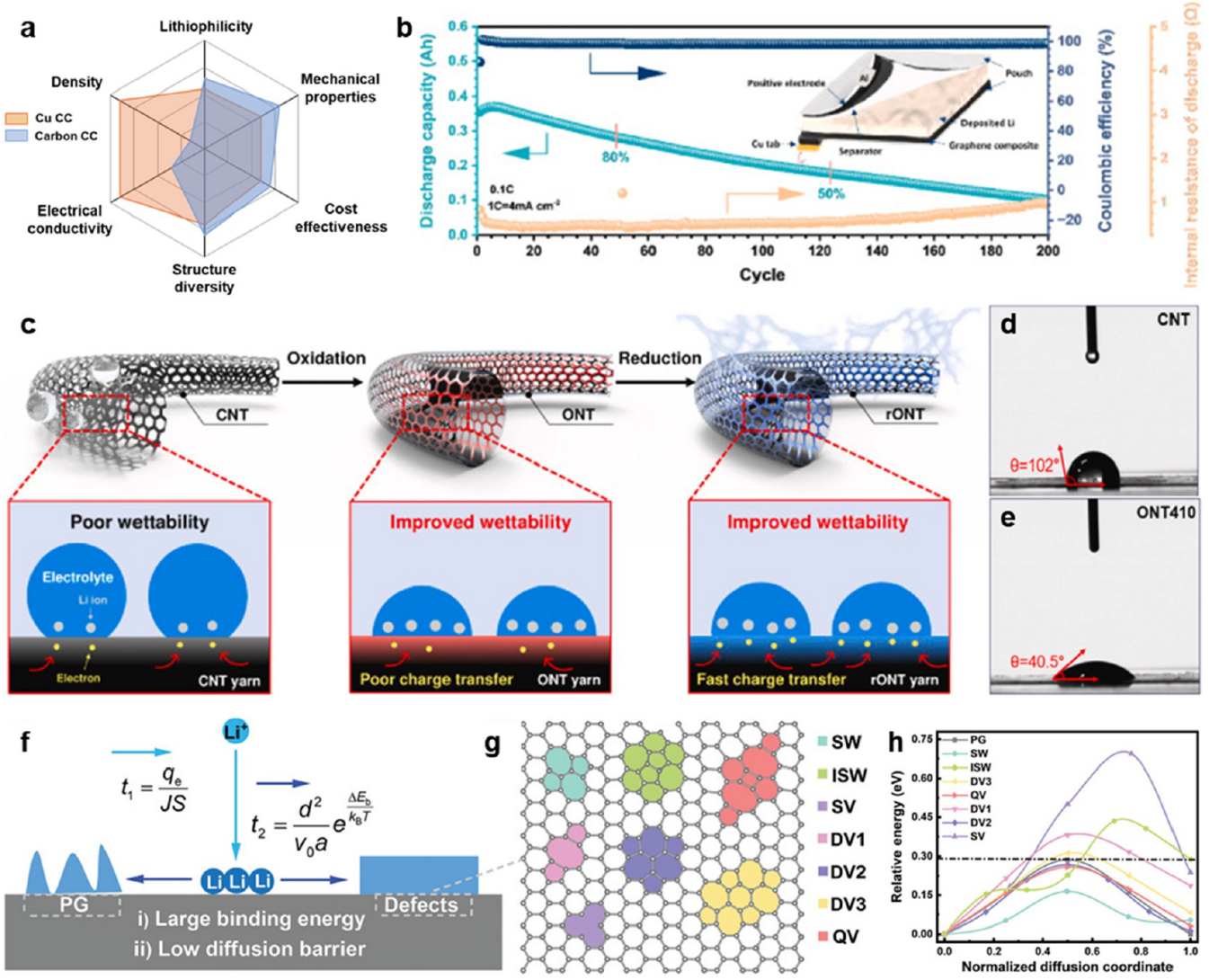

Figure 8. (a) Comparative analysis between Cu and carbon-based current collectors. (b) Cycling stability enhancement in AFLMBs using graphene-integrated composite electrodes. (c) Surface-dependent Li deposition: Schematic detailing how CNT, ONT, and rONT surface characteristics influence lithium plating. (d–e) Contact angle measurements of polar solvents on various current collector surfaces. (f–g) Modeling and visualization of lithium interactions with graphene defects: SW, ISW, SV, DV1, DV2, DV3, and QV. The abbreviations for each defect are as followed: Stone–Wales (SW), inversion Stone–Wales (ISW), single vacancies (SV), double vacancies (DV), and quadra vacancies (QV). (h) Calculated lithium diffusion barriers on pristine versus defect-rich graphene surfaces. Panels are reproduced with permissions from a, ref 176, © 2020 Elsevier; b, ref 179, © 2020 Elsevier; c–e, ref 180, © 2024 Elsevier; f–h, ref 181, © 2021 Wiley-VCH GmbH.

approximately 8.7% higher charged-state volumetric energy density than the 2D current collector.

Nevertheless, this advantage is not guaranteed. If lithium deposition occurs predominantly on top of the 3D scaffold without utilizing the internal pores, the 3D current collector suffers from both scaffold-thickness and lithium-plating-thickness penalties. In this worst-case scenario, the charged-state volumetric energy density decreases to approximately 1022.3 Wh L^{-1}, which is even lower than that of the 2D Cu case. This result highlights that the energy-density advantage of a 3D current collector is realized only when the plated lithium is effectively accommodated within the internal pore volume.

It should also be noted that the above calculation represents an idealized single-side-equivalent pore-filling case. In practical double-sided pouch-cell architectures, the required 3D scaffold thickness may need to be increased if both sides of a single current collector must accommodate plated lithium simultaneously. Therefore, the design of 3D current collectors for practical anode-free pouch cells must consider not only porosity and mass loading but also pore accessibility, wettability, lithiophilicity, and the directionality of lithium deposition. In this regard, 3D current collectors should be evaluated by their charged-state energy density and lithium-hosting efficiency, rather than by their as-fabricated cell geometry alone.

Even considering these trade-offs, from a cell design perspective, 3D current collectors offer an additional degree of freedom by enabling alternative electrode architectures that can be tailored to specific performance requirements. Their practical viability therefore depends on the development of effective interfacial stabilization strategies, such as conformal coatings to suppress parasitic reactions, as well as the identification of application scenarios where their advantages,

https://doi.org/10.1021/acsnano.6c06180
ACS Nano XXXX, XXX, XXX–XXX

particularly in terms of structural accommodation and gravimetric performance, outweigh the associated drawbacks.

3.1.4. Carbon-based Current Collectors. The selection of materials for 3D structure current collectors in AFLMBs is essential, leveraging the intrinsic properties of each material, such as electrical conductivity, lithiophilicity, mechanical properties, cost-effectiveness, and density, etc. These days, to fulfill these properties, copper-based[167,171] and carbon-based current collectors[168,172] are predominantly utilized for AFLMBs. These two materials for the current collector present distinct properties as shown in Figure 8a. Although copper exhibits high electrical conductivity (1.68×10^{-8} Ω m) owing to its delocalized 4s orbital structure,[173] intrinsically high density (~8.9 g cm^{-3}) limits the energy density of the AFLMBs.[174] In contrast, carbon-based current collector, especially in the case of carbon fiber current collector, showed inferior intrinsic electrical conductivity (8×10^{-4} Ω m),[175,176] making their use in the pristine state challenging. This limitation can be overcome by additional pretreatments such as annealing,[177] Joule heating,[178] etc. Because carbon-based current collectors are intrinsically low-density materials (0.44 g cm^{-3})[175] and can offer design flexibility (0D to 3D), research on them is an option that can be sufficiently considered from the perspective of long-term cell performance.[176]

To utilize advantages and maximize the performance of carbon-based current collectors, the mechanical properties of carbon current collectors are considered. From a practical perspective, the first issue to consider is the high melting point of carbon materials. Unlike metal-based current collectors, which are relatively easy to weld, carbon materials have a high melting point, making it difficult to achieve reliable tab welding when used in their untreated form. To overcome this issue, strategies such as using a composite substrate composed of a material suitable for tab welding and carbon materials are often suggested. One example reported by Guo et al. demonstrated a Cu/Graphene composite current collector to address the welding problem of carbon materials.[179] Etched Cu substrate improves welding performance, while the graphene layer covering it can successfully function as a carbon-based current collector (Figure 8b). However, this strategy ultimately compromises energy density because it relies on a relatively high-density metal substrate. This case implies the need to consider how to minimize this trade-off when developing carbon-based current collectors.

Another issue of carbon-based current collectors arises from their poor wettability toward the electrolyte. When considering carbon current collectors capable of 3D design, such as carbon nanotubes (CNTs), poor contact between the electrolyte and carbon negates all the advantages of this current collector system. Rather it can induce local currents, which can lead to dendrite growth and further side-reactions. Therefore, some treatment is needed to address carbon's poor intrinsic wettability. Lee et al. demonstrated that the wettability of CNT surfaces, influenced by pretreatment, could significantly impact the electrochemical performance of lithium metal batteries (Figure 8c–e).[180] A method of forming various types of defects on the surface of CNTs through heat treatment has been proposed. These defects facilitate interaction between lithium and carbon and act as hot spots of electrochemical reaction of lithium by reducing the interfacial energy and solvation barrier (Figure 8f–h).[181]

Consequently, replacing a current collector material from Cu to carbon involves inherent trade-offs as shown in Figure 8a. Careful consideration of various factors is necessary to optimize performances, including material properties, structure, operating mechanism, wettability, and surface modifications, etc. Particularly for carbon-based current collectors, surface modifications such as surface coating or defect engineering are crucial to mitigate challenges associated with their intrinsic low electrical conductivity. In case of carbon-based 3D current collectors, surface modification techniques such as defect engineering, introduction of functional groups, and surface coating can be promising approaches for enabling high-performance AFLMBs.

3.1.5. Mitigating Lithium Corrosion. Uniform lithium plating and stripping are widely regarded as essential for the operation of AFLMBs. However, in practical cells, storage periods are unavoidable and can be as long as, or longer than, the actual cycling time. Despite this, the impact of storage on lithium metal stability has received comparatively limited attention. In this context, battery reliability cannot be evaluated solely based on cycling performance but should consider the strategies for stable lithium metal storage. Early studies often assumed that lithium metal reaches a chemically stable state after the formation of the initial SEI during the first few cycles. Recent experimental observations challenge this assumption.[182,183] Lithium metal has been shown to undergo continuous chemical and morphological evolution even under open-circuit storage conditions. These results indicate that degradation processes persist in the absence of applied current, highlighting calendar stability as an independent degradation mode in AFLMBs.

Among the degradation pathways active during storage, galvanic corrosion of lithium metal is particularly relevant.[184] When the cell is stored at a low state of charge, partial lithium stripping can locally expose the current collector to the electrolyte. This configuration enables the formation of a galvanic couple between lithium and the more noble current collector, which can thermodynamically drive spontaneous lithium corrosion facilitated by Li^+-ion leakage through the SEI and additional SEI formation on the nearby Cu. Such corrosion, often described as a Kirkendall-type process, results in irreversible lithium loss and promotes highly nonuniform lithium redistribution during subsequent cycling.

In parallel, the SEI layer itself exhibits pronounced dynamic behavior during storage. Multiple studies have reported continued SEI growth under open-circuit conditions, particularly but not exclusively in carbonate electrolytes, whereas others have demonstrated that partial SEI dissolution can electrically reconnect previously isolated, or "dead," lithium upon further cycling.[185−187] More recently, electrolyte additives have been shown to trigger SEI reconstruction during storage, leading to LiF-rich passivation layers with enhanced mechanical integrity and chemical stability.[185]

Taken together, these observations suggest that mitigating lithium corrosion while preserving high plating/stripping reversibility requires carefully engineered interfacial layers, whether artificial or natively formed SEI. Such layers must effectively passivate lithium metal, block direct electrolyte access to the current collector, and simultaneously support fast Li^+-ion transport with limited electrolyte permeability.[48,91,142,188−190] Addressing these interfacial requirements under realistic storage conditions is therefore critical for the development of long-life AFLMBs suitable for practical applications. As SEI formation is largely governed by

https://doi.org/10.1021/acsnano.6c06180
ACS Nano XXXX, XXX, XXX−XXX

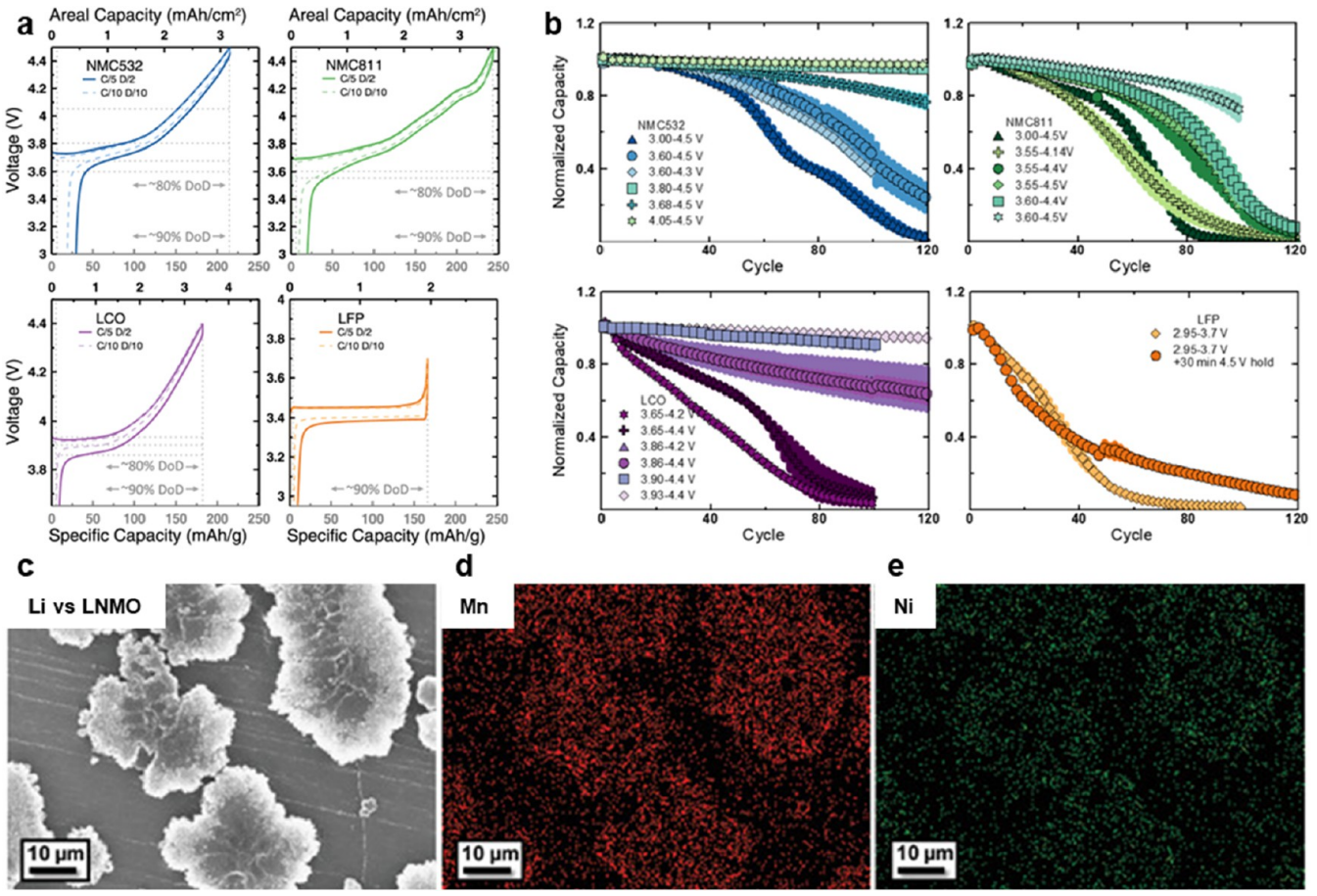

Figure 9. Effects of cathode active materials on the performance of AFLMBs. (a) First-cycle voltage profiles of AFLMBs using four representative cathode chemistries: NMC532, NMC811, LCO, and LFP. (b) Corresponding cycling performances under different cutoff voltages highlighting the strong dependence of capacity retention on cathode type and operating voltage range. (c-e) Crosstalk between LNMO cathode and lithium anode, showing plated lithium morphology (left) and EDS maps of Mn (red) and Ni (green). The detected transition metals confirm their dissolution from LNMO and redeposition on lithium, showing a degradation pathway that impacts interfacial stability and cycling. Panels are reproduced with permissions from a and b, ref 191, © 2022 IOP Publishing/ECS, CC-BY 4.0; c–e, ref 192, © 2019 Wiley-VCH GmbH.

electrolyte chemistry and has been extensively studied, further discussion is reserved for Section 3.3 (Electrolyte).

3.2. Cathodes

In anode-free lithium metal batteries, the absence of excess lithium fundamentally changes the factors governing cell performance and lifetime. Because irreversible lithium loss cannot be offset during cycling, overall capacity retention becomes highly dependent on how efficiently lithium is utilized throughout repeated charge–discharge processes. Under these conditions, the cathode plays a more critical role than in conventional battery systems, as its chemistry, operating voltage, and interfacial reactivity can strongly influence lithium consumption and long-term stability. Nevertheless, much of the existing research on anode-free configurations has focused on controlling lithium deposition behavior at the anode side or on optimizing electrolyte compositions. Comparatively less attention has been paid to how different cathode materials behave in anode-free cells and how they contribute to degradation mechanisms. To address this imbalance, this section reviews studies that specifically investigate cathode materials in anode-free architecture, with the goal of clarifying cathode design considerations and performance characteristics unique to these systems.

3.2.1. Selection of Active Materials.

In an anode-free full-cell system, technically where the cathode serves as the sole lithium source, both the specific and volumetric energy density as well as capacity retention, are strongly dependent on the cathode active material, reflecting its distinct electrochemical and structural characteristics.[191,192] During the early cycles, lithium ions delivered from the cathode form a lithium reservoir on the copper surface, which can be divided into reversible lithium and reservoir lithium distinctive to dead lithium. This excess amount of lithium deposited on the anode, similar to the first plating step of the Aurbach method (Section 5.1, Cycling Protocols for Precise Evaluation), can compensate for some of the capacity loss in subsequent cycles. The reservoir effect can be regulated by various cell conditions, including cutoff voltage, C-rate, electrolyte composition, and external pressure.[193] If this reservoir is maintained throughout cycling, the anode-free full-cell can preserve its capacity.

Dahn's group demonstrated that four representative cathode active materials show different cycle performances with various cutoff voltage ranges in AFLMBs (Figure 9a and b).[191] Different cathode materials affect the phenomena occurring on the anode side. Cathode active materials, such as lithium cobalt oxide (LCO), lithium nickel–cobalt-manganese oxide (NCM), and lithium iron phosphate (LFP), and even lithium-rich

https://doi.org/10.1021/acsnano.6c06180
ACS Nano XXXX, XXX, XXX–XXX

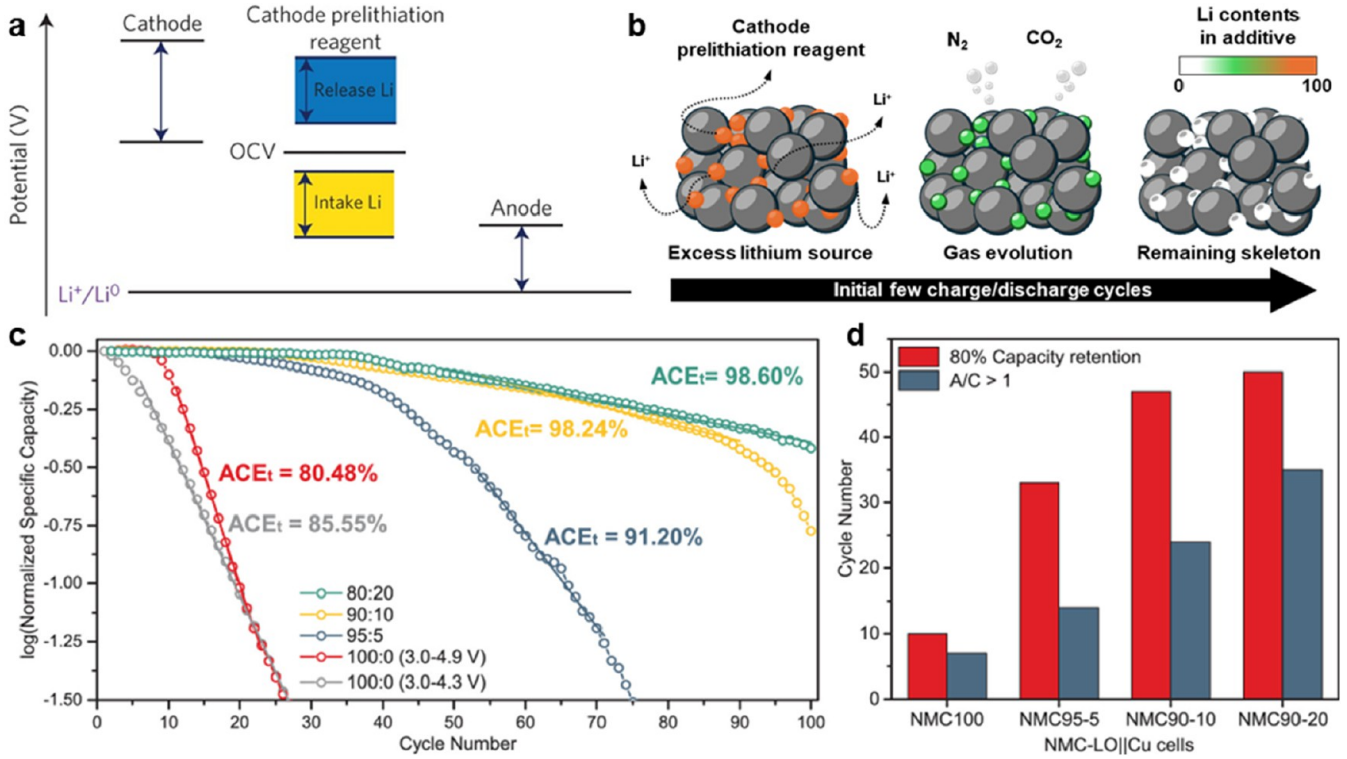

Figure 10. (a) Potential requirement for effective cathode prelithiation agents: complete delithiation below the upper cutoff of the cathodes and lithiation below its lower cutoff voltage. (b) Schematic illustration of two potential issues that can occur when cathode prelithiation reagents react: gas evolution and increased resistance due to the remaining skeleton. (c) Cycling performance of AFLMBs with different NMC-LO ratios, showing enhanced average CE and prolonged capacity retention with increasing additive contents. (d) Cycle numbers to 80% capacity retention and A/C ratios for the corresponding cells, demonstrating the beneficial role of prelithiation agents. Panels are reproduced with permissions from a, ref 215, © 2016, Springer Nature Ltd. (the authors retain the right to reuse the figure in this work); c and d, ref 216, © 2022 American Chemical Society.

layered oxide (LLO) for higher capacity, which is not mentioned in this work, have different redox kinetics.[194−198] Also, the difference of their operating voltage ranges varies the electric field environments inside the cell, which can influence the transport phenomena of ionic species.

Additionally, the crosstalk of transition metals from the cathode can influence lithium plating behavior at the anode.[192] Even if electrochemically stable cathode materials are employed, Mn and Ni dissolution can occur due to atomic-scale degradation that occurs during long-term cycling or high-voltage operation, and this leads directly to crosstalk (Figure 9c−e). This crosstalk can alter lithium plating morphology and increase overpotential depending on the type of transition metal, implying that understanding the working principle of AFLMBs should not be focused solely on anode.

Apart from conventional oxide- or polyanion-based frameworks, sulfur represents a highly promising cathode chemistry that plays a crucial role in the landscape of high-energy lithium metal batteries. When utilizing a sulfur cathode, addressing the interfacial crosstalk driven by the shuttle effect is paramount. Lithium polysulfides (LiPSs) are soluble intermediates inevitably generated during the chemical conversion between sulfur and lithium during cycling. Unfortunately, LiPSs readily dissolve into standard organic electrolytes and exhibit severe chemical reactivity toward the lithium metal anode. Consequently, these species migrate back and forth between the electrodes during cell operation, giving rise to the detrimental shuttle effect. This parasitic reactivity between LiPSs and the highly active lithium metal fundamentally accelerates cell degradation through cross-contamination, inducing severe anode corrosion, active material isolation, and severe self-discharge. To mitigate these issues, extensive research focuses on suppressing either the dissolution of LiPSs or their direct chemical reaction with lithium. Promising strategies include engineering the electrolyte solvation structure to restrict polysulfide solubility or deploying functional host materials within the sulfur cathode architecture to strongly anchor LiPSs via chemisorption or physical confinement.[199−205] For a more comprehensive evaluation of Li−S specific degradation pathways and engineering solutions, readers are directed to the dedicated literature cited herein.[206−209]

Overall, it is still not fully understood whether these results are due to differences in kinetics depending on the type of cathode materials, compatibility with the electrolyte, differences in electrode morphology, or other reasons.[195,197,210−214] Nevertheless, this indicates that the optimization of energy density of anode-free batteries involves adequate selection of cathode material with consideration of the phenomena in the full-cell system.

3.2.2. Electrode Additives (Extra Lithium Supply). As discussed in Section 1.3.2, anode-free batteries often suffer from low CE due to the consumption of Li^+-ions during the formation of the SEI. To realistically achieve full lithium utilization while maintaining the anode-free configuration, it is necessary to establish a system in which prelithiation materials supplement the lithium sources that will inevitably be consumed during the activation step. The SEI formed by this sacrificial lithium helps to establish chemical equilibrium at the

https://doi.org/10.1021/acsnano.6c06180
ACS Nano XXXX, XXX, XXX−XXX

interface, ultimately preventing further lithium consumption in subsequent cycles. These cathode prelithiation materials are typically designed to be completely delithiated below the upper cutoff voltage of cathodes and lithiated below their lower cutoff of discharge voltage. This specially designed working potential range of those materials effectively supplies the extra lithium for lithium reservoir plating and SEI formation in the first cycle, while preventing its subsequent consumption (Figure 10a and b).

Various compounds have been reported as effective prelithiation agents, including lithium phosphide (Li_3P), lithium nitride (Li_3N), and lithium oxide (Li_2O).[217−228] Du et al. employed lithium oxalate ($Li_2C_2O_4$, LO) as a prelithiation agent in NCM cathodes. LO was utilized under a higher voltage during the first cycle to extract lithium ions and successfully compensated the lithium loss in the first cycle (Figure 10c and d).[223] Meanwhile, Sun et al. utilized nanoscale composites composed of a transition metal and a lithium oxide mixture, relying on a conversion reaction between metal oxide and lithium.[215] They investigated various transition metals, such as cobalt, nickel, and iron, demonstrating that these mixtures exhibit a high capacity and can serve as efficient prelithiation agents.

However, selecting appropriate prelithiation agents remains challenging. When these sacrificial materials release active lithium via decomposition, they often produce electrochemically inactive byproducts that can increase internal cell resistance. Because the decomposition of these compounds is irreversible, the remaining skeletons typically persist as resistive particles that adversely affect battery performance. Furthermore, the decomposition of certain additives can lead to gas evolution, such as the generation of nitrogen gas when utilizing lithium nitride (Li_3N) as a prelithiation agent.[226] Gas accumulation within the cell obviously poses several risks, including increased internal pressure, which can lead to mechanical degradation. Critically, these degradation pathways are severely exacerbated at the cell level when transitioning to thick-electrode architectures, where the absolute amount of prelithiation agent can increase (4.1 Thick Cathodes with Functional Additives).

Cathode prelithiation agents also introduce an intrinsic energy-density penalty that must be considered at the cell level. Because these sacrificial additives are incorporated into the cathode composite, they often replace a fraction of the electrochemically active cathode material rather than simply adding usable cell energy.[227] In this case, the penalty originates primarily from the loss of reversible cathode capacity. For example, a first-order pouch-cell estimation based on an NMC622 cathode shows that replacing 5 or 10 wt % of the cathode active material with Li_3N decreases the modeled gravimetric energy density from 366.6 Wh kg^{-1} to approximately 348 and 330 Wh kg^{-1}, respectively. The volumetric energy density is also reduced because the sacrificial additive dilutes the host cathode capacity and changes the cathode volume. Although Li_3N can theoretically provide a substantial amount of compensating lithium, this lithium reservoir is obtained at the direct expense of energy-storing cathode material.[228] It should be emphasized that this estimation is based on a simple, first-order cell-level model that assumes uniform electrode utilization and does not account for irreversible lithium losses, gas evolution, or long-term degradation.

This trade-off becomes clearer when cathode prelithiation is compared with the direct addition of an equivalent lithium inventory as a thin lithium−metal reservoir on the negative-electrode side. Direct lithium addition is generally more mass-efficient for supplying the same amount of lithium because lithium metal has an extremely high specific capacity. However, this approach sacrifices the strict anode-free configuration and introduces pre-existing reactive lithium at the negative electrode. In contrast, cathode prelithiation preserves the anode-free architecture by storing the compensating lithium source in the positive electrode, but it does so at the cost of active-material dilution, inactive residues, possible gas evolution, and impedance growth.[225,228−230] Therefore, cathode prelithiation agents should be evaluated not only by their lithium-release capacity and activation voltage, but also by whether the lifetime gain from lithium compensation outweighs the loss in cell-level energy density and byproduct-induced degradation.[219,227]

Despite the promise of cathode prelithiation strategies, further optimization is required to balance lithium-inventory compensation with practical cell-level penalties. If the goal is to compensate mainly for the initial lithium loss during SEI formation, the sacrificial additive should release a controlled amount of lithium during early formation while minimizing active-material displacement.[215,228,231] If the goal is to compensate for continuous lithium loss during long-term cycling or storage, a different design may be required in which the additive is not fully consumed during the first cycle. In either case, the decomposition products of these agents must be carefully considered because they can introduce inactive mass, resistive residues, gaseous species, and interfacial contamination.[228−230,232] These factors may offset the benefit of lithium compensation by increasing polarization, disturbing electrode/electrolyte contact, and lowering practical cell-level energy density. In contrast to the conservative estimates from simple cell-level models, recent work on lattice-engineered Co−Li_2CO_3 sacrificial additives has shown that incorporating around 5 wt % sacrificial material into high-Ni cathodes can still yield pouch cells with high specific energy and excellent capacity retention over 1000 cycles, suggesting that carefully optimized prelithiation can provide a net gain in cycle-retained energy density despite a modest cathode-level penalty.[225] Therefore, the optimal cathode prelithiation agent should provide a precisely controlled amount of lithium with minimal energy density penalty, chemically benign residues, negligible gas evolution, and compatibility with high-loading cathodes under lean-electrolyte conditions.

3.3. Electrolytes

In AFLMBs, the electrolyte plays a multifaceted role that goes far beyond enabling Li^+-ion transport. While high ionic conductivity and uniform ion flux are essential prerequisites for reversible lithium plating and stripping, they do not, by themselves, determine interfacial stability or lithium utilization in AFLMBs. Instead, the chemical nature of the electrolyte critically governs lithium solvation and desolvation at the electrode interface, thereby dictating the nucleation behavior of lithium and the subsequent formation of interfacial layers. In this context, the composition and evolution of the SEI on plated lithium, as well as the cathode electrolyte interphase (CEI), are strongly dependent on electrolyte formulation. Equally important, the homogeneity and mechanical integrity of these interphases during repeated cycling and storage are

https://doi.org/10.1021/acsnano.6c06180
ACS Nano XXXX, XXX, XXX−XXX

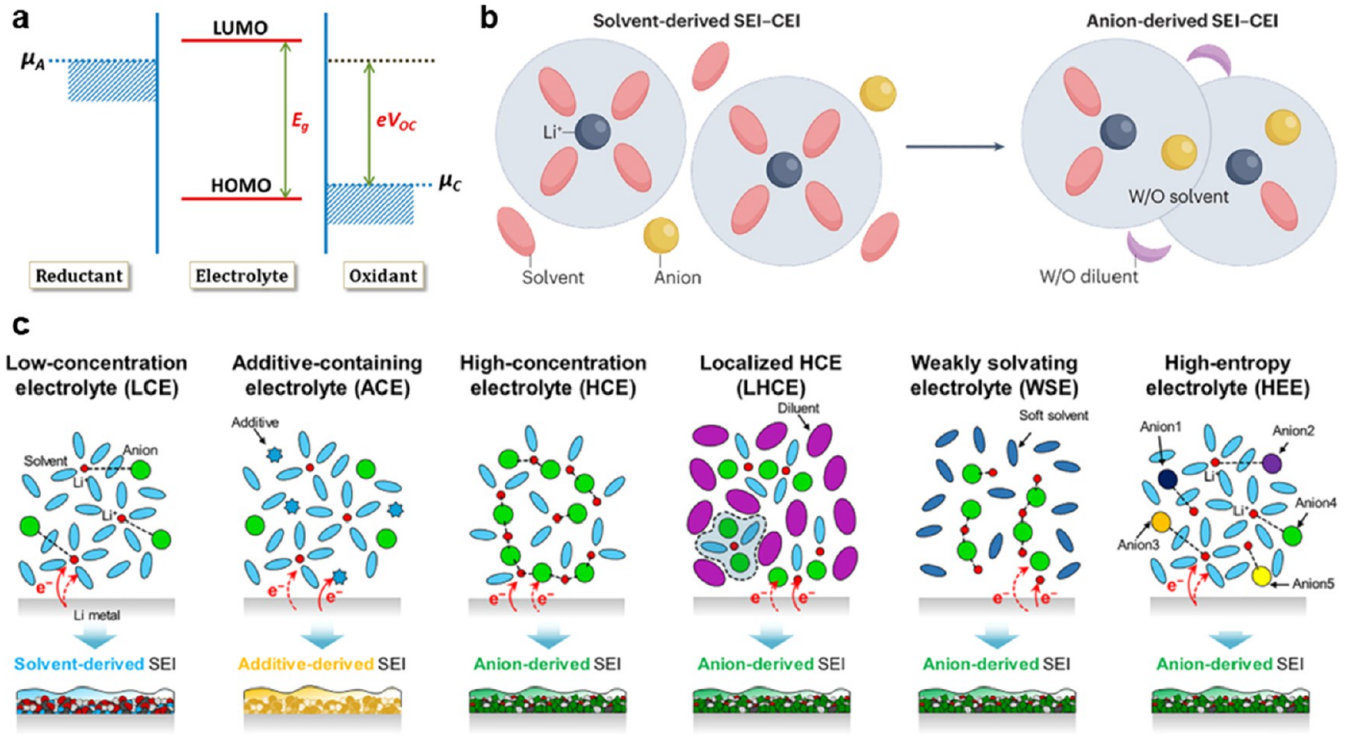

Figure 11. (a) Schematic illustration of electrolyte working mechanisms containing voltage window, where E_g is energy gap between LUMO and HOMO, V_{OC} is open-circuit voltage, and μ_A and μ_C are chemical potentials of anode and cathode, respectively. (b) Comparison of solvation structure which composing dominated by solvent or anion in the solvation shell. (c) Schematic of electrolytes regulating the solvation structures within the Li^+-ion microenvironment to create a stable interphase on lithium metal batteries. Panels are reproduced with permission from a, ref 235, © 2013 American Chemical Society; b, ref 236, © 2024 Springer Nature Ltd.; c, ref 237, © 2024 Wiley-VCH GmbH.

closely linked to electrolyte-derived reaction pathways. Beyond interphase regulation, emerging studies have demonstrated that specific electrolyte systems can promote the electrochemical reactivation of dead lithium via redox-mediated processes, offering an additional strategy to enhance lithium reversibility. Although electrolyte additives designed to introduce excess lithium have been reported,[233] such approaches primarily address lithium inventory compensation and are not considered here. Accordingly, this section focuses on electrolyte properties associated with lithium solvation behavior, SEI/CEI chemistry, interphase uniformity, and dead-lithium reactivation, highlighting how rational electrolyte design can enable stable interfaces and improved cycling reversibility in AFLMBs.

3.3.1. Solvation and SEI/CEI Chemistry. Although lithium dendrites can be suppressed, pure lithium metal remains highly reactive; chemical corrosion and electrochemical side reactions inevitably proceed instantly upon exposure to electrolyte, resulting in rapid and permanent active lithium loss. From the perspective of full-utilization of lithium, the formation of a robust and flexible SEI is indispensable, serving as a passivating layer that protects the lithium surface while allowing Li^+-ion conduction. Electrolyte components, including salts, solvents, and their specific compositions, play a decisive role in governing the structure and properties of SEI. Accordingly, extensive efforts have been devoted to establishing electrolyte design principles tailored for lithium−metal anodes. Traditionally, strategies to control SEI formation have focused on tuning the lowest unoccupied molecular orbital (LUMO) energy levels of electrolyte components, thereby dictating the sequence of reductive decomposition (Figure 11a). It is worth mentioning that the concept of highest occupied molecular orbital (HOMO) and LUMO of single electrolyte species cannot precisely represent actual values in an electrolyte environment where there is active interaction among ions and molecules. A detailed discussion is beyond the scope of this review; interested readers are referred to the cited reference for further information.[234]

More recently, however, it has become evident that tuning the Li^+-ion solvation structure can be a more promising approach by controlling which chemical species coordinate with Li^+-ions (Figure 11b). Most solvation engineering aims to incorporate anion-derived, inorganic-rich SEI components, as these reinforce the mechanical properties of the SEI film, thereby suppressing solvent-derived SEI swelling, chemical corrosion, and electrolyte dry-out. Early research demonstrated that electrolyte stability improves as salt concentration increases, leading to an intensive focus on high-concentration electrolytes (HCEs).[238] HCEs promote the formation of an anion-based SEI through strong interactions between Li^+-ions and anions, achieving a remarkably high CE of approximately 99%. Nevertheless, HCEs suffer from high viscosity, resulting in low ionic conductivity. To address this limitation, localized high-concentration electrolytes (LHCEs) containing diluent molecules have been adopted as an advanced solvation engineering strategy.[239−243] Recently, weakly solvating electrolytes (WSEs) have also been investigated, which preferentially form contact ion pairs (CIPs) and aggregates (AGGs) rather than solvent-separated ion pairs (SSIPs) without requiring any diluent.[244−249] In parallel, high-entropy electrolytes (HEEs),

https://doi.org/10.1021/acsnano.6c06180
ACS Nano XXXX, XXX, XXX−XXX

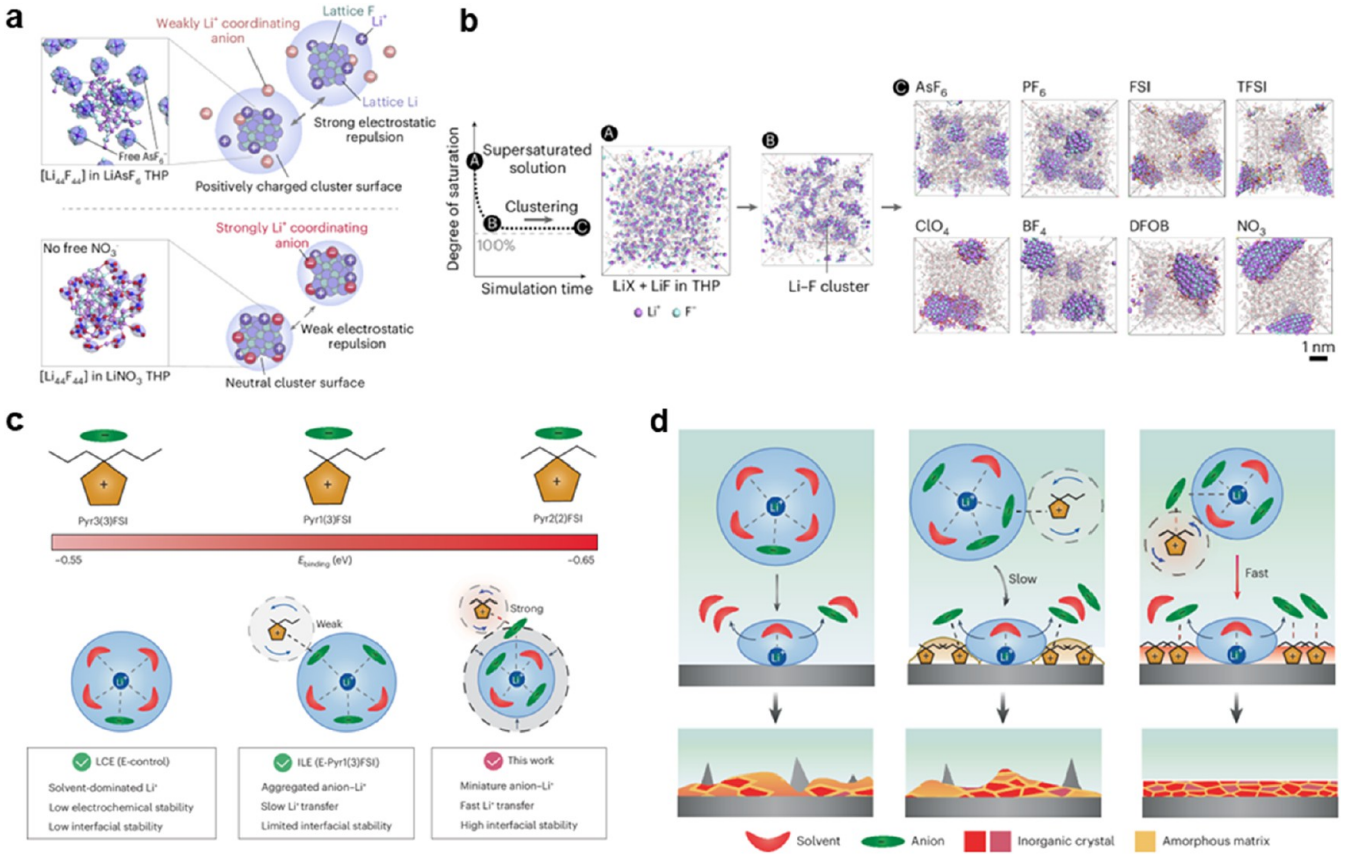

Figure 12. (a) Representative snapshots of $[Li_{44}F_{44}]$ clusters within $LiAsF_6$ THP and $LiNO_3$ THP, along with a schematic illustrating the association of Li^+-ion, weakly Li^+-coordinating and strongly Li^+-coordinating anions around LiF cluster and their interactions. (b) Snapshots of the simulation cell of supersaturated LiF in pyran-based electrolytes, depicting the structural evolution from the initial state to 5 ns of equilibration. (c) Comparative models of Li^+-ion solvation structures in diverse electrolyte environments. ILE, ionic-liquid-based electrolyte; LCE, low-concentration electrolyte. (d) Schematic of SEI formation by E-control, E-Pyr1(3) FSI and E-Pyr2(2) FSI. The close ion-pair packing in $Pyr2(2)^+$ facilitates a compact stationary layer and refined solvation structure, promoting a uniform, inorganic-rich SEI compared to the heterogeneous layers formed in other systems. Panels are reproduced with permission from a–b, ref 269, © 2025 Springer Nature Ltd.; c–d, ref 270, © 2025 Springer Nature Ltd. (for both references, the authors retain the right to reuse the figures in this work).

comprising multiple cationic, anionic, and solvent species, provide an alternative approach to tuning solvation chemistry and improving ionic conductivity without sacrificing electrochemical stability.[116,123,250−253]

In addition to solvation tuning, additive engineering has been widely employed to regulate SEI composition. Additive molecules typically possess higher reduction potentials than other solvent molecules, meaning they decompose preferentially to form a desired SEI layer. Common additives include fluoroethylene carbonate (FEC),[254] lithium nitrate ($LiNO_3$),[255] vinylene carbonate (VC),[256] vinyl ethylene carbonate (VEC),[257] and tris(2,2,2-trifluoroethyl) borate (TTFEB).[258] Their reductive decomposition increases the content of inorganic components, such as lithium fluoride (LiF), lithium nitride (Li_3N), lithium carbonate (Li_2CO_3), lithium oxide (Li_2O), and lithium hydroxide (LiOH), strengthening the SEI and improving CE.

The SEI can exist in various structural forms, but is generally understood to adopt a mosaic structure in which inorganic species are embedded within an organic matrix.[73] As discussed in Section 1.2, increasing attention has been paid to the mechanical stability of the SEI as a critical factor for achieving stable cycling, leading to extensive studies on the role of inorganic components. Among them, LiF has been one of the most intensively investigated species due to its excellent chemical and mechanical stability when considered as a bulk material, and many studies have attributed improved LMB performance to the presence of LiF-rich interphases.[137,259−261] More recently, significant attention has also been directed toward Li_2O, another major SEI component, which similarly exhibits favorable chemical and mechanical stability. Several studies have further suggested that Li_2O located near the anode surface can influence the local Li^+-ion solvation environment and homogenize ionic flux during deposition.[262−265] However, SEI components, such as LiF and Li_2O, do not exist as isolated bulk particles, but rather function as constituents within the complex SEI architecture. Although some studies have attempted to understand their roles in composite forms rather than at the individual particle level, the correlation between these SEI components and overall cell-level performance, particularly in conjunction with the electrolyte and cathode, remains insufficiently understood. This limitation highlights that electrolyte design cannot rely solely on targeting specific SEI compositions but must instead consider the broader solvation−interphase relationship that governs interfacial stability.

Despite significant progress in electrolyte design, fundamental limitations remain, including an incomplete understanding of solvation−SEI correlations and the lack of universal design principles for simultaneously optimizing ion

https://doi.org/10.1021/acsnano.6c06180
ACS Nano XXXX, XXX, XXX−XXX

transport and interphase stability. Critical questions remain regarding how to mitigate the trade-off between anion-solvating strategies and ionic conductivity, as well as whether high-entropy electrolytes are intrinsically electrochemically stable. In addition, the fundamental role of the SEI layer has not yet been fully clarified. While machine learning (ML) and artificial intelligence (AI) have accelerated electrolyte discovery,[47,266−268] current models still fall short of accurately representing realistic electrolyte environments, particularly when complex ionic interactions and dynamically evolving interphases are involved. Direct operando characterization of SEI composition and morphology across various electrolytes would therefore provide critical insights yet remains challenging due to the intrinsic instability of the interphase. Further discussion on SEI characterization is presented in Section 5.3 (Hierarchical Heterogeneity Analysis). The overall scheme of current electrolyte design is illustrated in Figure 11c.

3.3.2. Homogeneous SEI Formation. Spatial inhomogeneity or structural instability within the SEI is an equally important factor as the composition of SEI. Even though reinforcing anion-derived SEI formation effectively enhances interfacial stability, its effect might be limited locally in such a heterogeneous SEI morphology across the electrode area. If the decomposed products anions are unevenly distributed or lead to the coarsening of LiF-rich domains, heterogeneous ion transport and localized current density may arise. Such morphological evolution not only limits uniform Li^+-ion flux but also fails to suppress SEI swelling, eventually triggering continuous side reactions and irreversible electrolyte consumption during cycling.

Recent developments have introduced novel electrolyte design approaches focusing not only on anion-derived SEI formation but also on uniform SEI formation. Pyran-based electrolytes incorporating tetrahydropyran (THP) and FEC have been developed,[269] with particular attention to electrolyte designs leveraging the weak Li^+-ion coordination characteristics of AsF_6^- anions (Figure 12a). The AsF_6^- anion increases the solvent-separated Li^+-ion (SSL) ratio up to 94% and generates strong positive charges on LiF cluster surfaces, inducing electrostatic repulsion between clusters to uniformly distribute LiF crystals across the SEI with minimized crystallite size of 2.9 nm (Figure 12b). Additionally, the introduction of a symmetric organic salt, 1,1-diethylpyrrolidinium bis-(fluorosulfonyl)imide (Pyr2(2)FSI),[270] induces strong ion-pair association between cations and anions, preventing excessive anion clustering of solvated Li^+-ion and realizing miniature anion−Li^+-ion solvation characterized by high ionic conductivity and low desolvation barriers (Figure 12c). This solvation structure design enables the compact stationary layer of symmetric cations to uniformly distribute anions across the electrode, stabilizing the SEI with uniform inorganic components (Figure 12d).

During lithium stripping process, SEI undergoes contraction and collapse, while electron conduction pathways can be lost due to lithium deposits becoming delaminated from the current collector.[97] Heterogeneous SEI layers and structurally unstable lithium are highly susceptible to electronic and structural disconnection, resulting in increased formation of dead lithium. Additionally, swelling of the SEI, caused by electrolyte penetration into its porous organic components,[271] increasing complexity to the system. SEI swollen in electrolyte exhibits significantly lower elastic modulus, which increases their susceptibility to fracture upon electrode volume changes during electrochemical cycling process.[144] Notably, such issues are not fully resolved even in cells employing LHCE or HEE electrolytes. Even with anion-derived SEI homogenization markedly improving interphase uniformity, eliminating local current-density fluctuations arising from mechanical defects at the interface and heterogeneities in ion transport within the SEI is exceedingly challenging. Moreover, in contrast to the anion-derived SEI formation upon lithium plating, lithium stripping can expose fresh lithium underneath the SEI, but electrochemical reduction of electrolyte may not occur. Instead, chemical decomposition of the electrolyte possibly occurs in contact with fresh, nonpassivated lithium, detrimentally leading to lithium-consuming side reactions and thus imposing constraints on achieving 100% lithium utilization.

Although there is a high correlation between inorganic-rich SEI and high-CE electrolytes, the organic components in SEI also play an important role in stabilizing the passivation layer during cycle.[265] As discussed in the Section 1.2, fracture of SEI caused by its poor mechanical properties during repeated cycles is pointed out as one of the degradation modes. Organic matrix typically offers mechanical elasticity to SEI layer, which is crucial for maintaining its structure during the continuous cycles. For example, in the case of carbonate-based electrolytes, the effects of cyclic and linear carbonate solvents have been compared on the SEI growth on Cu. Ethylene carbonate (EC)-based electrolyte with higher CE (∼90%) results in a more compact lithium morphology under an organic-rich SEI layer dominated by lithium ethylene decarbonate (LEDC) with very small amount of Li_2CO_3. Meanwhile, the ethyl methyl carbonate (EMC)-based electrolyte with much lower CE (<15%) produces a more porous lithium morphology covered by a thick inorganic-dominated SEI layer, most of which is LiF and Li_2O.[272] It was also reported that LiF can drift away from the SEI layer during the stripping process, suggesting that a stable SEI requires a supporting organic matrix to maintain the mechanical stability of the SEI during prolonged cycles.[273] In addition, the energy barrier of Li^+-ion diffusion across the continuous organic medium is lower than that in the rigid, discontinuous inorganic phase, which helps facilitate a more uniform Li^+-ion flux across the SEI.[264,272,274]

As seen in the previous examples, SEI research must move beyond the narrow perspective of merely implementing specific components. Next-generation electrolyte design must extend beyond simply controlling SEI composition, moving toward strategies that spatially homogenize its components while preserving structural integrity during continuous plating/stripping cycles.

3.3.3. Electrolyte Additives (Li^+-ion Regenerator). Beyond the purpose of introducing additives for SEI engineering, a new role of additives has been proposed to reactivate electrically isolated dead lithium. Accordingly, a complementary strategy has been proposed to maximize lithium utilization by reactivating dead lithium back into electrochemically active species. Redox mediators (RMs), which perform reversible oxidation−reduction reactions (i.e., redox shuttling) as electrolyte additives, have evolved to fulfill several key functions. Initially, they were utilized for overcharge protection in lithium-ion batteries, in which RMs with oxidation potentials below the cathode cutoff voltage are preferentially oxidized to prevent cell voltage from exceeding hazardous ranges. Building upon this principle of mediating electron transfer, the role of RMs has evolved beyond mere overcharge protection to catalytically facilitating core electro-

https://doi.org/10.1021/acsnano.6c06180
ACS Nano XXXX, XXX, XXX−XXX

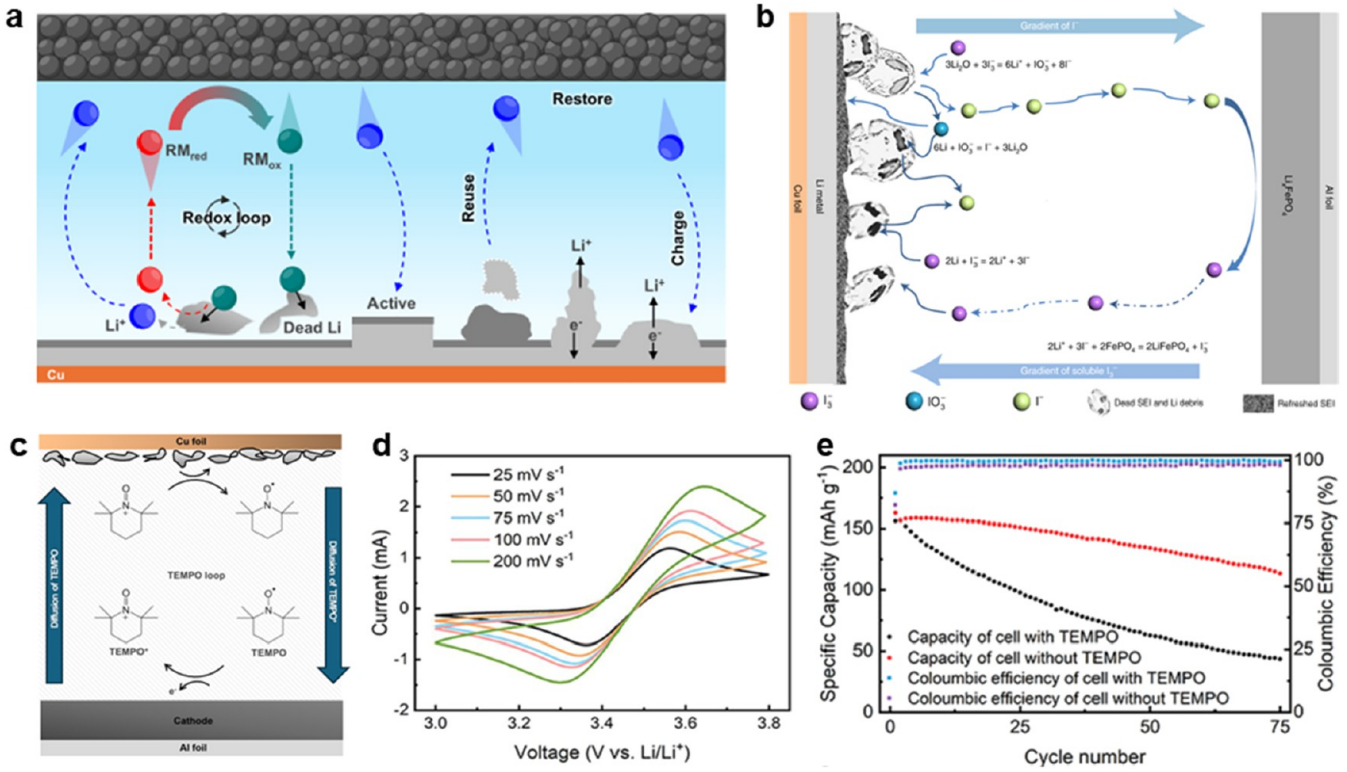

Figure 13. (a) Schematic of the chemical restoration pathway utilizing redox shuttling to recover inactive lithium. (b) Illustration of the simultaneous suppression of Li dendrites and the chemical reactivation of isolated dead lithium via iodide-based redox reactions. (c) Conceptual diagram of the catalytic cycle involving TEMPO for the electrochemical recovery of detached lithium segments. (d) CV profiles at varying scan rates, characterizing the redox behavior of the TEMPO-integrated electrolyte. (e) Cycling performance of Cu\|\|Li $LiNi_{0.5}Co_{0.2}Mn_{0.3}O_2$ (NCM) anode-free systems with and without the addition of TEMPO. Panels are reproduced with permission from b, ref 277, © 2021 Springer Nature Ltd.; c–e, ref 278, © 2023 Wiley-VCH GmbH.

chemical reactions.[275] Notably, in lithium–oxygen ($Li–O_2$) batteries, RMs function as "liquid catalysts" to mitigate the accumulation of insulating Li_2O_2 on the cathode surface during discharge. During charging, RMs are first electrochemically oxidized to RM^+ at conductive sites on the cathode surface, after which the oxidized RM^+ diffuses through the electrolyte and chemically oxidizes Li_2O_2, decomposing the discharge product while regenerating the original RMs. This redox shuttling mechanism effectively bypasses the electron-transport bottleneck imposed by insulating Li_2O_2, enabling Li_2O_2 oxidation at significantly reduced overpotentials and thereby substantially improving the energy efficiency and cycling stability of $Li–O_2$ batteries.[276]

Recently, RMs have been applied to anode-free batteries to address the accumulation of dead lithium over repeated cycles. In this context, the soluble mediator chemically reacts with inactive metallic lithium deposits, redissolving them and reincorporating lithium into the plating/stripping process (Figure 13a). This rejuvenation strategy goes beyond SEI stabilization by focusing on recovering inactive lithium, which is crucial for anode-free batteries due to their lack of excess lithium to compensate for losses during cycling. By reactivating dead lithium, these novel additives not only enhance battery performance but also significantly extend operational lifespan, offering a promising solution to maintain efficiency over extended cycles.

For example, the lithium iodide (LiI) redox shuttle has been shown to greatly improve the cycling stability of anode-free batteries.[277−280] The iodine in LiI undergoes a shuttle mechanism, cycling between I^- and I_3^- where it reacts with dead lithium and lithium dendrites to dissolve them back into active lithium ions (Figure 13b). Initially, upon the introduction of iodine into the electrolyte, the subsequently generated triiodide (I_3^-) attacks the Li_2O present in the dead SEI on the lithium metal surface and the electrically isolated dead lithium, as described by eqs 1 and 2. As a decomposition product of Li_2O, IO_3^- is present in the electrolyte and reacts with lithium to form a new SEI on the lithium metal anode surface (eq 3). During this interfacial reaction, I^- formed at the anode is transferred to the cathode, where it undergoes oxidation to regenerate I_3^- (eq 4).

$$3Li_2O + 3I_3^- \rightarrow 6Li^+ + IO_3^- + 8I^- \quad (1)$$

$$2Li + I_3^- \rightarrow 2Li^+ + 3I^- \quad (2)$$

$$6Li + IO_3^- \rightarrow I^- + 3Li_2O \quad (3)$$

$$2Li^+ + 3I^- + 2FePO_4 \rightarrow 2LiFePO_4 + I_3^- \quad (4)$$

$$8Li + 3I_3^- + 2FePO_4 \rightarrow 6Li^+ + 9I^- + 2LiFePO_4 \text{ (Overall)}$$

Similarly, 2,2,6,6-tetramethylpiperidine-1-oxyl (TEMPO) serves as another effective additive for rejuvenating dead lithium.[278] During charging, TEMPO is oxidized at the cathode and subsequently reacts with dead lithium in the electrolyte, converting it back into active lithium ions (Figure 13c). This reaction continuously proceeds within the redox potential range of TEMPO, which is approximately 3.4 V (Figure 13d). This reversible redox cycle enhances lithium

https://doi.org/10.1021/acsnano.6c06180
ACS Nano XXXX, XXX, XXX–XXX

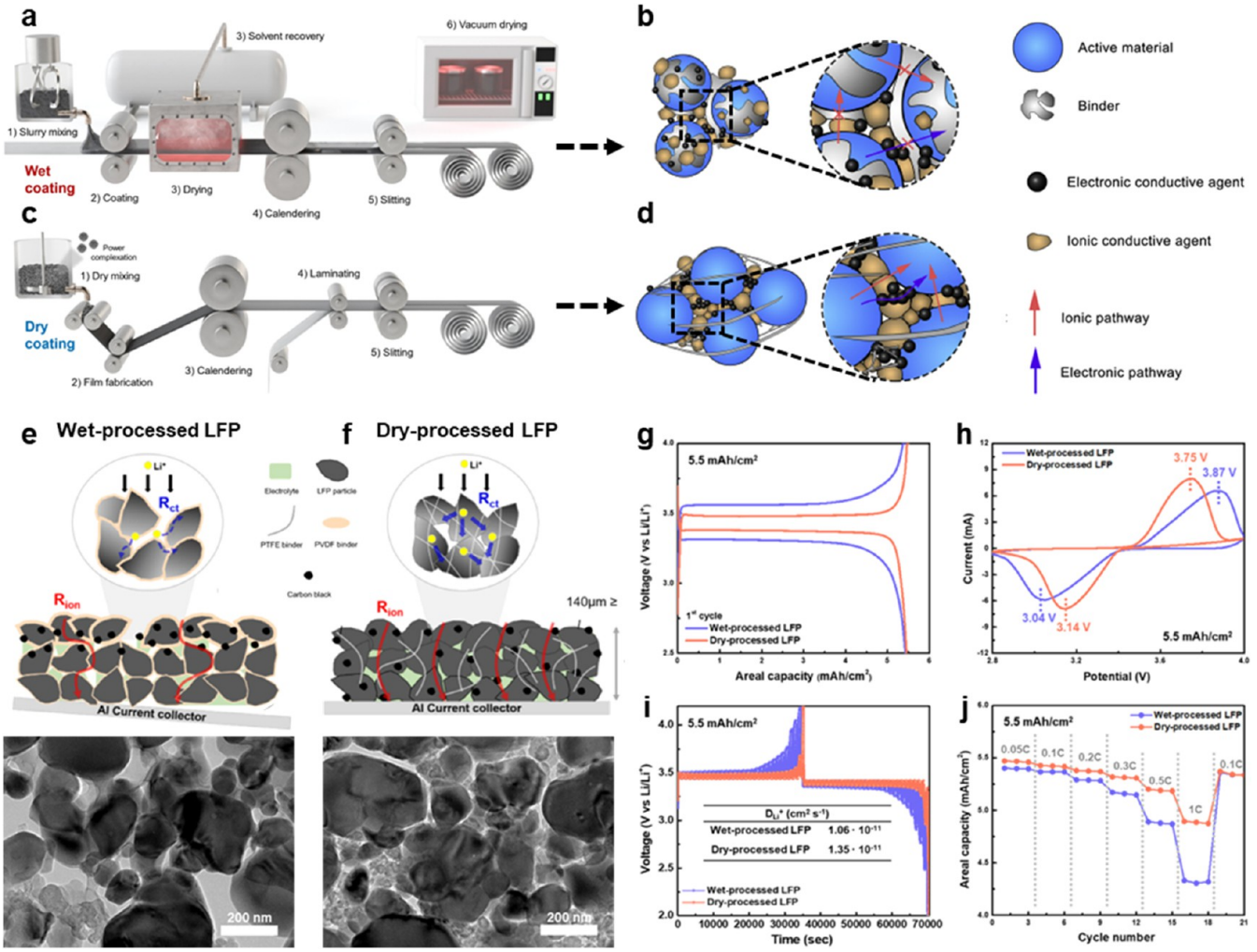

Figure 14. Comparison of wet- and dry-processing for electrode fabrications. (a, c) Schematic illustrations of conventional slurry-based wet coating and solvent-free dry coating, respectively. (b, d) Conceptual diagrams of particle-level connections in the two processes, showing differences in electronic and ionic pathways. (e, f) Cross-sectional and microstructural images of dry-processed LFP electrodes, demonstrating compact architecture and efficient ion transport networks. (g–j) Electrochemical characterization of wet- and dry-processed LFP electrodes with high areal mass loading of 5.5 mAh cm^{-2}, including first cycle voltage profiles (g), Cyclic voltammetry profile showing lower cell overpotential of dry-processed LFP electrode (h), Li$^+$-ion diffusion coefficient from GITT (i), and superior rate performance. Panels are reproduced with permissions from a and c, ref 291, © 2024 Wiley-VCH GmbH, CC-BY 4.0; b and d, ref 292, © 2022 Elsevier; e–j, ref 293, © 2024 Wiley-VCH GmbH, CC-BY 4.0.

utilization and prolongs battery life by maintaining higher CE. Anode-free batteries using TEMPO have demonstrated significantly better performance, with CE exceeding 99%, compared to approximately 97% in cells without the additive (Figure 13e).

Employing redox mediators in AFLMBs can also be important from a perspective of safety. In conventional LIBs using graphite anode, lithium plating is one of the main failure modes caused by the accumulation of charge on the anode surface during the charging process. The dead lithium formed at this time initially affects capacity reduction, and over time, causes the accumulation of resistance and heat generation, which in severe cases can become the starting point of thermal runaway. Incorporating RMs, such as TEMPO, offers a robust chemical strategy to mitigate these risks by reactivating electrically isolated metallic lithium. This process can fundamentally alter the thermal runaway profile in three key aspects: Increasing self-heating onset temperature (T_{onset}), delaying the triggering temperature of thermal ramp (T_{trig}), and decreasing total heat release (THR).[281−283] Consequently, RM-assisted lithium recovery of AFLMBs can help maintain lithium inventory for a long time while also helping to ensure safety.

The efficiency of redox mediators must be carefully optimized, because excessively slow kinetics may fail to effectively suppress dead lithium accumulation, whereas overly fast reactions can induce unwanted self-discharge. Therefore, quantitatively evaluating the kinetics of redox mediators is essential. Broadly, such analysis can be categorized into two main approaches: (1) morphology-based and (2) electrochemistry-based analysis. Morphology-based quantification focuses on post-mortem analysis of the anode to evaluate parameters such as surface roughness using Morphological Surface Texture (MST) and porosity analysis through Focused Ion Beam (FIB)-based cross-sectional imaging.[96,284] These approaches can visualize morphological evolution in lithium deposits induced by redox mediator operation and provide indirect evidence for the extent of dead lithium recovery. In

https://doi.org/10.1021/acsnano.6c06180
ACS Nano XXXX, XXX, XXX−XXX

contrast, electrochemistry-based analysis cannot directly visualize the morphological evolution of lithium but enable more quantitative evaluation of recovery behavior. Representative examples include ex-situ NMR and TGC, which can estimate the amount of electrically isolated dead lithium.[91,92,285] As discussed in Section 1.2, lithium morphology itself strongly influences local current distribution, stripping behavior, and long-term dead lithium accumulation. Therefore, future development of redox mediators should incorporate both morphology-based and electrochemistry-based analysis to comprehensively validate their effectiveness. By combining these complementary techniques, future studies may be able to more rigorously determine how effectively redox mediators contribute to LIRI discussed in Section 2.

While TEMPO and LiI have shown significant potential in reactivating dead lithium and improving anode-free battery performance, further research is needed to optimize their concentrations and fully understand the underlying mechanisms. Indeed, redox mediators are promising for lithium rejuvenation, but they inherently entail risks, such as unwanted lithium loss due to self-discharge and the complexity of reaction pathways at the anode. As a prime example, it has been reported that an I_3^-/I^- redox couple can cause self-discharge by chemically reacting with the deposited lithium on the negative electrode during LMB's rest period at charged state.[279] Therefore, to develop next-generation redox mediators, it is crucial to elucidate precise material design principles by thoroughly understanding the detailed electrochemical and chemical reaction mechanisms within the electrolyte. It is necessary to select an RM molecule that satisfies conditions such as an appropriate shuttling speed to prevent dead lithium accumulation, an appropriate potential window to prevent self-discharge in the operating potential range, and chemical stability to prevent chemical side-reaction that may occur when resting in a charged state. Ultimately, these design principles must be validated through comprehensive experimental and computational studies.[286−289] Continued innovation in additive design and electrolyte formulation will drive the advancement of anode-free batteries toward broader commercial use.

4. REDESIGN OF CELL STRUCTURES

4.1. Thick Cathodes with Functional Additives

To achieve the maximum energy density goals of AFLMBs, increasing cathode thickness or mass loading is essential; however, this necessitates the strategic use of functional additives to ensure both lithium inventory stability and high electrical conductivity. Since the primary focus of AFLMBs development is maximizing energy density, the use of thicker cathodes directly contributes to this goal by boosting energy at the cell-level while reducing the fraction of inactive components such as separators, current collectors, and casings. Thick cathodes also provide an additional benefit by providing a physically larger space to accommodate prelithiation additives. Since all lithium source in AFLMBs originates from the cathode, unstripped lithium remaining on the anode during early cycles can act as a substrate for subsequent plating and stripping cycles.[290] Although this residual lithium causes slight capacity loss initially, the surplus lithium from a thick cathode compensates for it, leading to more stable cycling over time. Thus, increasing cathode thickness is necessary in AFLMBs from two main perspectives: enhancing energy density and capacity retention.

Despite these advantages, traditional wet-processes face several issues when coating electrodes exceeding a certain thickness (typically thicker than 100 μm). Challenges such as binder migration, particle agglomeration, and uncontrollable slurry viscosity can occur, which hinder the uniform coating of thick cathode films. Additionally, the wet-process is neither eco-friendly nor cost-effective. During the process, the toxic solvent *N*-methyl-2-pyrrolidone (NMP) must be removed by a highly energy-consuming drying step (Figure 14a). These limitations have driven attention toward dry electrode processing as a more practical solution.

In dry electrode fabrication, all electrode components are mixed in powder form, technically ensuring a homogeneous mixture and creating well-connected ions and electron transfer channels are key for producing high-performance electrodes.[294−298] To satisfy these conditions, carbon nanotubes (CNTs) and polytetrafluoroethylene (PTFE) are typically introduced as conducting materials and polymeric binders, respectively. PTFE can be fiberized under the shear force during the dry process, bridging the active materials particles altogether (Figure 14c and d). CNTs, with their high electrical conductivity and aspect ratio, can serve dual functions as both conductive agents and structural binders, making binder-free electrodes feasible in some cases.[292,299,300]

Although PTFE is widely used as a fibrillating binder in solvent-free dry electrode processing, its electrochemical stability is highly potential-dependent. This issue has been most clearly demonstrated in graphite-based dry anodes, where PTFE with a low LUMO level can be reductively decomposed during initial lithiation, producing LiF and carbonaceous species; this parasitic reaction lowers the initial Coulombic efficiency, weakens binder integrity, and accelerates long-term performance degradation.[301,302] In contrast, the cathode systems discussed in this section operate within a positive-electrode potential window, where PTFE is generally considered sufficiently stable to provide mechanical fibrillation and particle-bridging functions in high-loading dry cathodes. Nevertheless, PTFE should not be regarded as completely electrochemically inert. Recent studies on PTFE-based dry-processed NMC cathodes showed that LiF can be detected even in $LiClO_4$-based electrolytes, where other fluorine sources are largely excluded, indicating that PTFE may contribute to cathode−electrolyte interphase (CEI) formation through limited side reactions.[303] In related solvent-free NMC composite cathodes, the physicochemical state of PTFE, including its crystallinity, has also been shown to influence particle−particle contact, interfacial resistance, and interphase evolution.[304] Therefore, while PTFE remains a highly practical binder for high-loading dry cathodes, its possible contribution to CEI chemistry and long-term interfacial evolution should be considered in future cathode and electrolyte designs for AFLMBs.

For example, in the case of LFP based cathode, Kwon et al. demonstrated a dry electrode fabrication method that overcomes the energy density limit of LFP (Figure 14e−j).[293] The powder mixture composed of LFP particles, carbon black (Super P), and PTFE binder in a ratio of 97:1:2, was dry processed into thick film and laminated onto a 20 μm thick Al current collector. The resulting 175 μm thick electrode contained a high fraction of active material, delivered an areal capacity of 7.8 mAh cm^{-2}, and maintained excellent cycle

https://doi.org/10.1021/acsnano.6c06180
ACS Nano XXXX, XXX, XXX−XXX

stability over 300 cycles in full-cell operation. This work illustrates how dry-processed thick electrodes enable the fabrication of thick cathodes that overcome energy density limitation of wet-processed electrodes.

Dry-processing has also been applied to Ni-rich layered oxide electrodes. Choi et al. demonstrated a Li-$Ni_{0.88}Co_{0.06}Mn_{0.03}Al_{0.03}O_2$ (NCMA) cathode fabricated by a dry process in which PTFE and carbon black were combined into a composite using surface treatments with cationic (cetrimonium bromide, CTAB) and anionic (ribonucleic acid, RNA) surfactants.[305] The electrode contained 98% active NCMA and achieved a high electrode density of 3.8 g cm^{-3} and volumetric capacity of 760 mAh cm^{-3}, along with improved discharge rate capability and cycle stability. These superior performances of dry-processed NCMA cathode were attributed to the uniform distribution of inactive components, even in the thick cathode structure.

While many studies have demonstrated that thick cathodes can effectively improve the cell-level energy density, their role in fully addressing the lithium loss challenge in AFLMBs remains unresolved. In fact, even if a thick cathode can supply additional lithium to compensate for lithium lost during cycling, there are still questions as to whether this characteristic can be maintained continuously over long-term cycling. Moreover, the interplay between thick cathodes, lithium utilization efficiency, and appropriate cycling protocols to utilize them is more complex and has not yet been studied. To fully apply the thick cathode in AFLMB systems and supply the maximum amount of lithium over extended cycling, detailed optimization of material composition, electrode structure, and operating conditions are required.

4.2. Li^+-ion Flux Distributors

In Li-metal based battery systems, the regulation of Li^+-ion flux has garnered significant attention as a factor that directly influences Li nucleation and dendrite growth.[306,307] The separator, through which Li^+-ions directly permeate, is a critical component closely associated with Li^+-ion flux. However, the widely commercialized polyolefin-based separators have limitations in effectively controlling Li^+-ion flux due to their electrically insulating properties, low ionic conductivity, and uneven pore distribution. In response, continuous research has been conducted to enhance the performance of Li-metal based battery systems by controlling Li^+-ion flux through separator modification. Modifying the surface of the separator with functional materials is one of the most straightforward approaches because of its simple processes, making it a promising candidate for large-scale application and commercialization. In general, the principles for these coating approaches can be defined in two ways: (1) mechanical ion distribution, and (2) electrostatic ion regulation (Figure 15). It is important to ensure that the separator operates in a way that uniformly distributes Li^+-ion flux or increases the transference number of Li^+-ion, including the methods to be organized in this chapter.

4.2.1. Mechanical Ion Distribution. From the mechanical perspective, engineering of pores has been considered for separator research. The size and uniformity of pores are directly related to the ion flux distributing ability of the separators. Several porous materials with macro- or microscopic pores are commonly adopted as separator modification materials in LMBs due to their ability to homogenize Li^+-ion flux. Li^+-ion flux regulated by porous materials mitigates locally

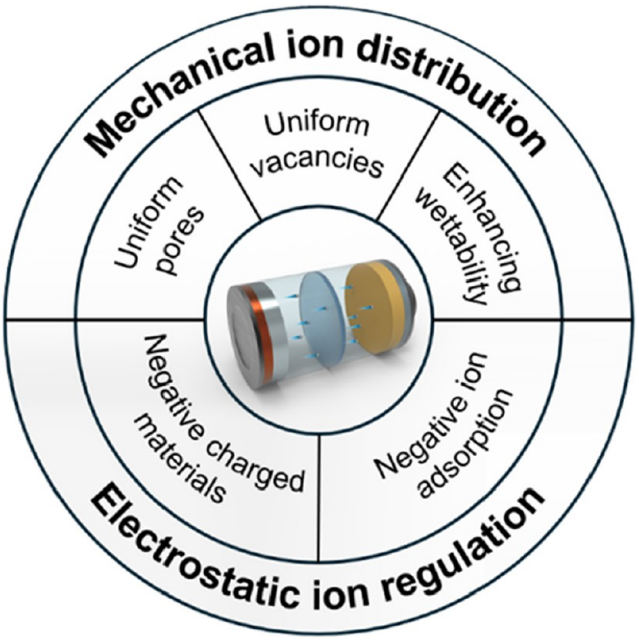

Figure 15. Diagram of the classification of principles for controlling Li^+-ion flux by coating functional materials on the separator.

accumulated ion concentrations within the electrolyte, promoting uniform lithium deposition/dissolution at the electrode.

Ren et al. effectively demonstrated the control of Li^+-ion flux by applying dendritic mesoporous silica (DMS) with various pore structures to PP separators (Figure 16a).[308] The internally connected 3D ion channels constructed by the DMS-coating on separator evenly distributed Li^+-ion and suppressed dendrite penetration through the separator, leading to the most stable cell voltage among other materials. This directly demonstrates that a separator coating material with a uniform pore distribution effectively controls Li^+-ion flux. The effectiveness of coating materials with a uniform pore distribution on separators has also been validated by the study conducted by Liu et al.[309] Inert hexagonal boron nitride (BN) was coated onto polypropylene using the widely adopted tape casting method. Consistent with previous studies, the uniform pores formed between the layered structure of BN serve as pathways for redistributing Li^+-ion, thereby ensuring a more uniform Li^+-ion flux. X-ray computed tomography (X-CT) and SEM analyses conducted on the Li anodes of cycled symmetric Li−Li and Li-LFP cells with BN@PP demonstrated that the Li^+-ion flux induced by the uniform pores resulted in a more compact lithium anode surface and internal structure.

Research on using nanoscale atomic vacancies, such as the nonstoichiometric oxygen vacancies of metal oxides, referred to as an 'ion-sieve' to control Li^+-ion flux have also been conducted (Figure 16b). Compared to previous materials with microscopic pores, materials with 'nanoscopic' pores (referred to as vacancies) can selectively interact with ions in the electrolyte due to the similarity in size between the vacancies and the ions. Li^+-ions, with their small size of 0.76 Å, can pass through the vacancies, while larger anions are either filtered by the 'ion-sieve' or become intercalated within the vacancies. Lei et al. designed separators modified with LiAl layered double hydroxide (LiAl LDH@PP) by applying $[LiAl_2(OH)_6]Cl$

https://doi.org/10.1021/acsnano.6c06180
ACS Nano XXXX, XXX, XXX−XXX

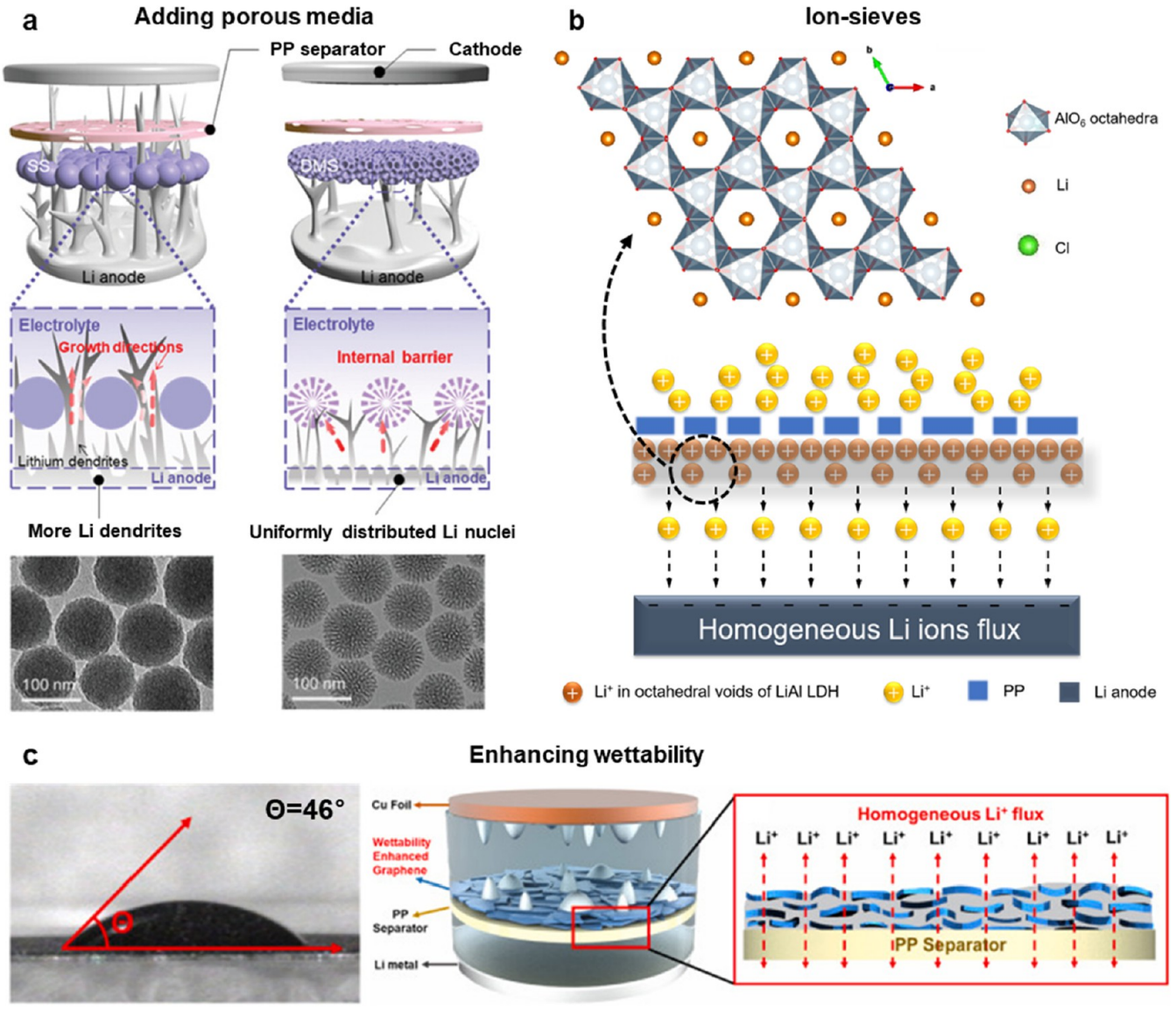

Figure 16. (a) Schematic illustration and TEM images of lithium dendrite growth in cells coated with mesoporous silica of various pore structures. (b) Schematic diagram and TEM images of LiAl-LDH with vacancies capable of functioning as an ion-sieve. (c) Contact angle images of graphene coated separator and wettability-enhanced graphene coated separator, along with a schematic illustration of the Li^+-ion flux. Panels are reproduced with permissions from a, ref 308, © 2023 Wiley-VCH GmbH; b, ref 310, © 2020 Elsevier; c, ref 311, © 2024 Elsevier.

nanoflakes onto PP separators through a simple coating process.[310] The nanoscale octahedral vacancies and interlayer distances in LiAl LDH provide abundant 3D Li^+-ion channels, leading to excellent Li^+-ion conductivity. Additionally, $TFSI^-$ and NO_3^- anions are intercalated into the interlayer structure of LiAl LDH, which enhances the interfacial stability between the separator and the electrolyte.[312] Meanwhile, Xiong et al. fabricated a separator coated with $Ti_{0.87}O_2$ containing Ti vacancies using the vacuum filtration method.[313] The octahedral Ti vacancies are sufficiently small to permit the passage and redistribution of Li^+-ions, while larger anions are effectively blocked. Due to the selective flux control effect on Li^+-ions through the nanoscale vacancy engineering in both cases, cycled lithium showed extremely smooth surface, indicating the well-dispersed Li^+-ion flux.

While increasing the number or uniformity of pores is important, electrolyte wettability of the separator also significantly impacts the ion flux. As wettability increases and more pores become available for ion migration, the dispersion of Li^+-ions trapped in small separator pores is reduced, leading to less roughened lithium deposition on the anode (Figure 16c). Choi et al. proposed two types of separators to overcome the poor electrolyte affinity of graphene-coated separators: one coated with MnO_x and the other with polydopamine, using an additional solution coating method.[311] MnO_x and polydopamine, as representative hydrophilic materials, significantly reduced the contact angle with polar solvents (e.g., DI water) on the separators. The improved wettability of these separators resulted in lower internal cell resistance and IR drop. Considering that similar effects have been achieved using other hydrophilic materials such as $Mg(OH)_2$, coating the separator with hydrophilic particles can dramatically enhance their wettability and further promote a more uniform ion flux.[314]

https://doi.org/10.1021/acsnano.6c06180
ACS Nano XXXX, XXX, XXX−XXX

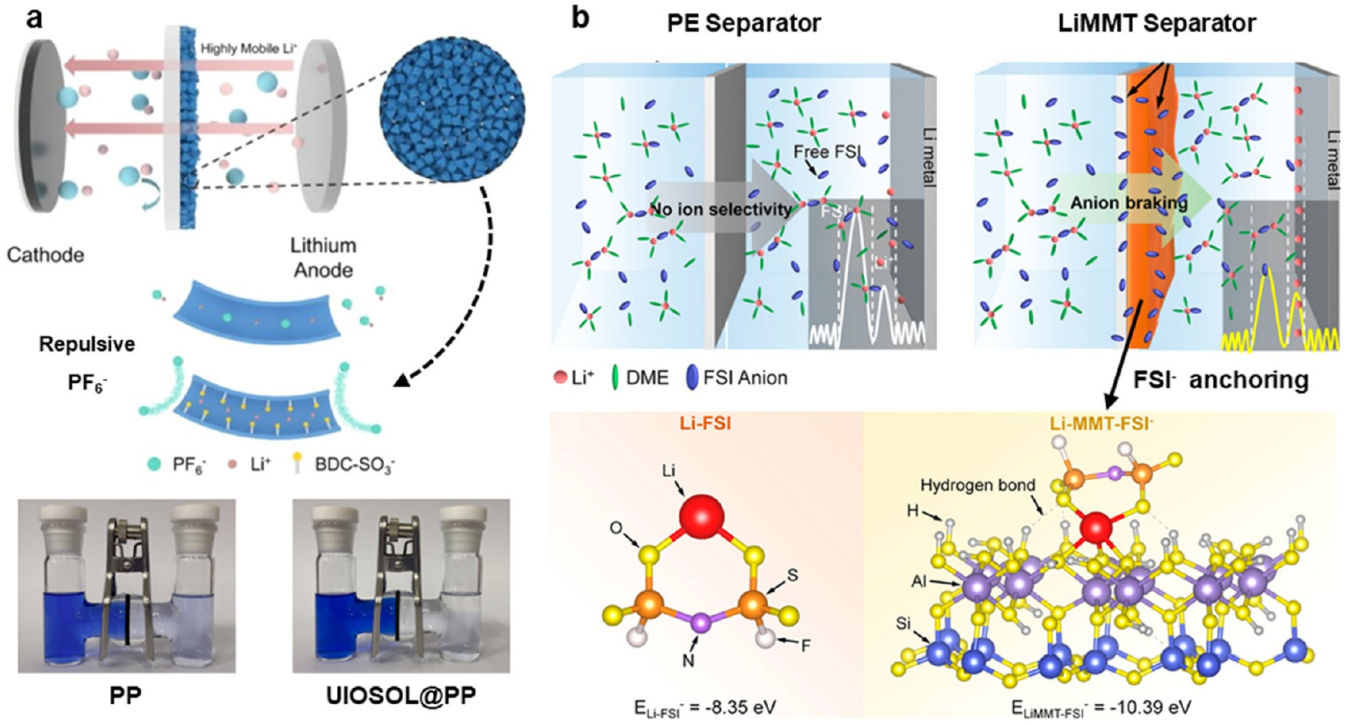

Figure 17. (a) Schematic illustration of the anion repulsion mechanism of UISOL@PP and photo images of the penetration test. (b) Schematic illustration of the principle of the anion-anchoring separator, along with the adsorption structure and adsorption energy for negative and positive ions. Panels are reproduced with permissions from a, ref 316, © 2022 Elsevier; b, ref 317, © 2024 American Chemical Society.

4.2.2. Electrostatic Ion Regulation. With respect to the anions in Li-metal based battery systems, a negatively charged separator can interact with anions in the electrolyte, thereby functioning as a regulator for Li^+-ion flux. Excessively accumulated anions cause concentration polarization around the Li anode, leading to the formation of the local electric field. This ultimately results in an uneven Li^+-ion flux, which promotes the growth of lithium dendrites. To inhibit anion diffusion, many studies have widely explored separators with functional materials featuring charged groups. Similar to the principle of Donnan exclusion, this approach induces electrostatic interactions between anions in the electrolyte and charged species fixed in separator pore, thereby suppressing their diffusion. It has been confirmed that when materials with a uniform distribution of positive or negative charges are used to cause this electrostatic effect, it can have a positive effect on the performance of AFLMBs.

In the case of using electrostatic attraction with anions, organic frameworks (OFs) that can provide abundant anionic species are typically adopted. Wang et al. demonstrated separators coated with covalent organic frameworks (COFs) designed for LMBs. The PP separator was modified with TpPa-2SO_3H COF nanosheets through a vacuum-assisted self-assembly method.[315] These functionalized COF nanosheets are acquired from the interfacial polymerization of 1,3,5-Triformylphloroglucinol (TP) in octanoic acid and 2,5-diaminobenzene-1,4-disulfonic acid (Pa-2SO_3H). Due to the negatively charged characteristics of the COF, the designed separator suppressed anion diffusion within the cell and facilitated Li^+-ion transport, thereby enhancing electrochemical performance of LMBs. Li et al. proposed an anionic metal organic framework (MOF) with the chemical formula $Zr_6O_4(OH)_4BDC_3[BDC\text{-}NaSO_3]_3$ and the MOF was further modified through ion exchange (denoted as UIOSOL) (Figure 17a).[316] This MOF was then coated onto PP separators using a spray method. Cells with this separator exhibited lower anion transference number (t_{anion}) and higher Li^+ transference number (t_{Li^+}), indicating a more uniform Li^+-ion flux. All these characteristics contributed to the excellent cycle life performance observed in the symmetric Li−Li and Li-LFP cells using the modified separator.

In contrast to materials with negative charges, investigating the modification of separators with materials that can adsorb negative charged ions from the electrolyte have been studied to control Li^+-ion flux. When anions in the electrolyte are adsorbed onto the separator, t_{anion} around the anode surface is reduced. According to the Sand equation, reduced t_{anion} delays the growth of lithium dendrites which could inhibit electrolyte decomposition and enhance interfacial stability. Zhang et al. fabricated a separator coated with two-dimensional lithiated-montmorillonite (LiMMT) onto PE separator using a blade coating method (Figure 17b).[317] The abundant −OH groups present in LiMMT can selectively adsorb FSI^- ions in the electrolyte as Lewis acid sites and electron acceptors. As previously mentioned, this induces a decrease in t_{anion} and an increase in t_{Li^+}, leading to uniform Li^+-ion flux and, as a result, more uniform lithium plating/stripping.

4.3. External Stimuli Engineering

Despite the provision of an ample lithium source, such as thick lithium metal layers, the lifespan of AFLMBs remains limited due to severe interfacial evolution at the anode side, including dendrite formation, evolution of porous SEI layer, and dead lithium formation. While these issues have been addressed through the design of active materials, current collectors, and electrolytes, commercialization requires strategies capable of

https://doi.org/10.1021/acsnano.6c06180
ACS Nano XXXX, XXX, XXX−XXX

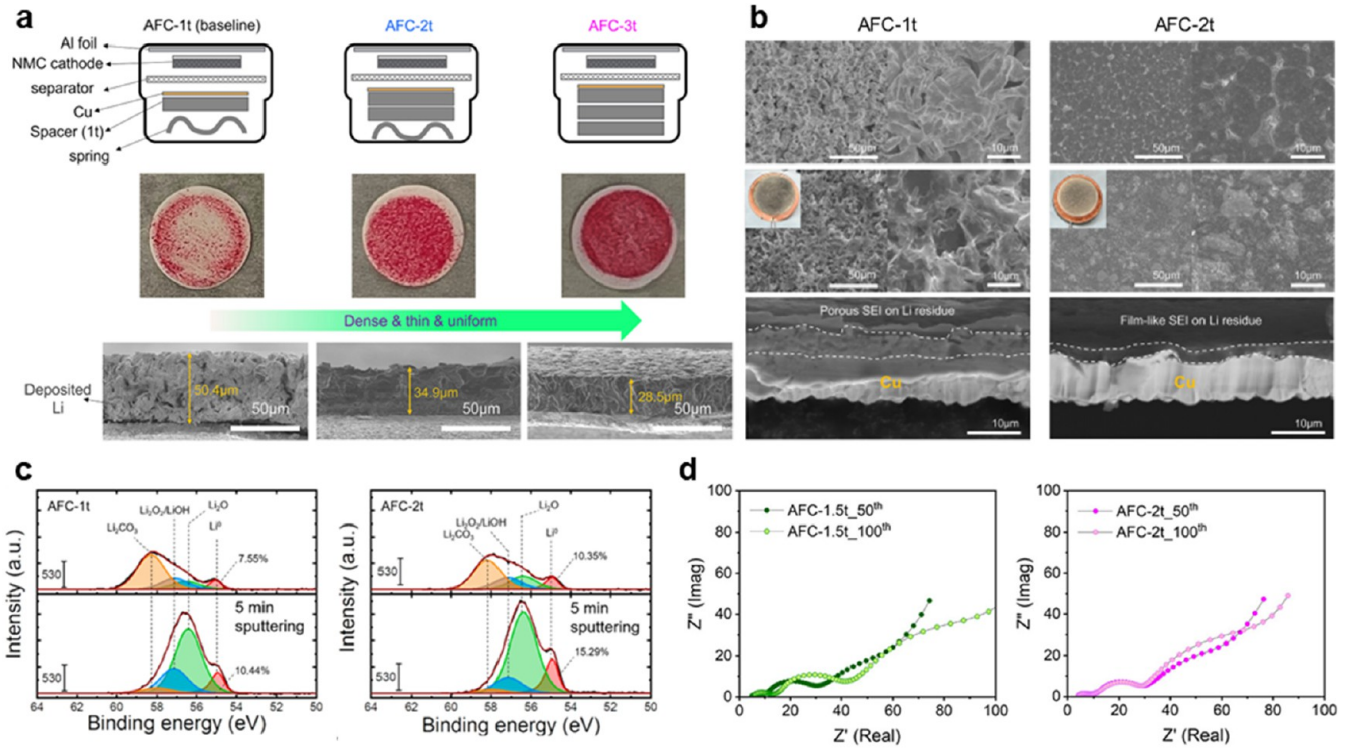

Figure 18. (a) Cross-sectional SEM of initial lithium deposits in anode-free coin cells assembled with 1t, 2t, or 3t stainless-steel spacers (no wave spring in 3t) after the first charge (C/10 to 4.5 V). (b) Top-view SEMs of lithium on Cu current collectors from Cu||NMC811 cells after the first charge (C/10 to 4.5 V) and the first discharge (to 3.5 V); left, AFC-1t; right, AFC-2t. (c) Fitted XPS Li 1s spectra characterizing the solid electrolyte interphase layers formed on lithium deposits under distinct pressure conditions. (d) Nyquist plots illustrating the changes in EIS signatures during extended cycling of Cu||NMC811 (AFC-1.5t, AFC-2t) after formation cycles. Panel a-d are reproduced with permission from ref 320, © 2023 American Chemical Society.

controlling cell-level behavior across multiple cells via the external cycling environment. External stimuli provide additional routes to regulate lithium behavior within the cell. For example, magnetic fields have been reported to modulate Li^+-ion flux during cycling, either by directly influencing ion transport through Lorentz force or by employing magnetically responsive nanosheets to promote a more uniform ion flux under an applied field.[318,319] These approaches demonstrate that lithium migration and deposition behavior can be regulated through externally applied forces, even after cell assembly. In this section, the effects of external stimuli, including pressure, temperature, ultrasound, and scaling up on Li^+-ion flux and dendrite suppression (or removal) are discussed.

4.3.1. Pressure. Since AFLMB in its initial state does not include a soft anode (e.g., lithium metal) that can absorb and distribute stack pressure, which is different from conventional LMBs or LIBs, pressure can be uneven across the cell, strongly influencing the deposited lithium morphology and exacerbating SEI growth. Vice versa, heterogeneous lithium deposition and SEI growth can also induce local pressure evolution. These conditions accelerate interfacial evolution and deplete reversible lithium, compromising SEI integrity and cell performance. Optimizing internal pressure in AFLMBs is therefore essential, as appropriately managed pressure can enhance cycling stability and extend cell life.

Recent studies (e.g., Zhang et al.) show that both the magnitude and uniformity of pressure govern SEI quality and lithium morphology.[320] Uneven pressure promotes porous, dendritic deposits with continuously growing SEI, leading to electrolyte depletion, low CE, and short cycle life. In contrast, uniform pressure compacts the deposit and stabilizes the SEI. For instance, adding stainless-steel (SS) spacers and springs can homogenize pressure in coin-type AFLMBs (AFCs). Increasing spacer count flattens the pressure field and yields denser lithium adhering to Cu (Figure 18). A "2t" spacer configuration outperformed "1t," lowering overpotential and raising average CE (≈99.6%; Figure 18a). However, excessive pressure (e.g., "3t") may risk separator deformation and soft shorts, decreasing CE and capacity. Microscopy and XPS indicate that moderate-uniform pressure forms thinner, more inorganic-rich, and mechanically robust SEI (Figure 18b and c) and sustains lower impedance/overpotential over long-term cycling (Figure 18d). Thus, AFLMBs benefit most from moderate, spatially uniform pressure that stabilizes the SEI and suppresses morphological instabilities without mechanically compromising the cell.

These observations further imply that operational pressure should be considered not only as a parameter governing lithium plating morphology, but also as a dynamic regulator of SEI structure, density, mechanical properties, and stripping efficiency.[39] Systematic studies over the MPa pressure range have shown that external pressure can substantially modulate both lithium deposit morphology and SEI chemistry. Under relatively low or spatially nonuniform pressure, lithium deposits tend to become porous, heterogeneous, or filament-like, and the resulting SEI is often more organic-rich, less compact, and mechanically fragile.[321] By contrast, increasing the pressure within an appropriate range can compact electrodeposited lithium and promote the formation of a

https://doi.org/10.1021/acsnano.6c06180
ACS Nano XXXX, XXX, XXX−XXX

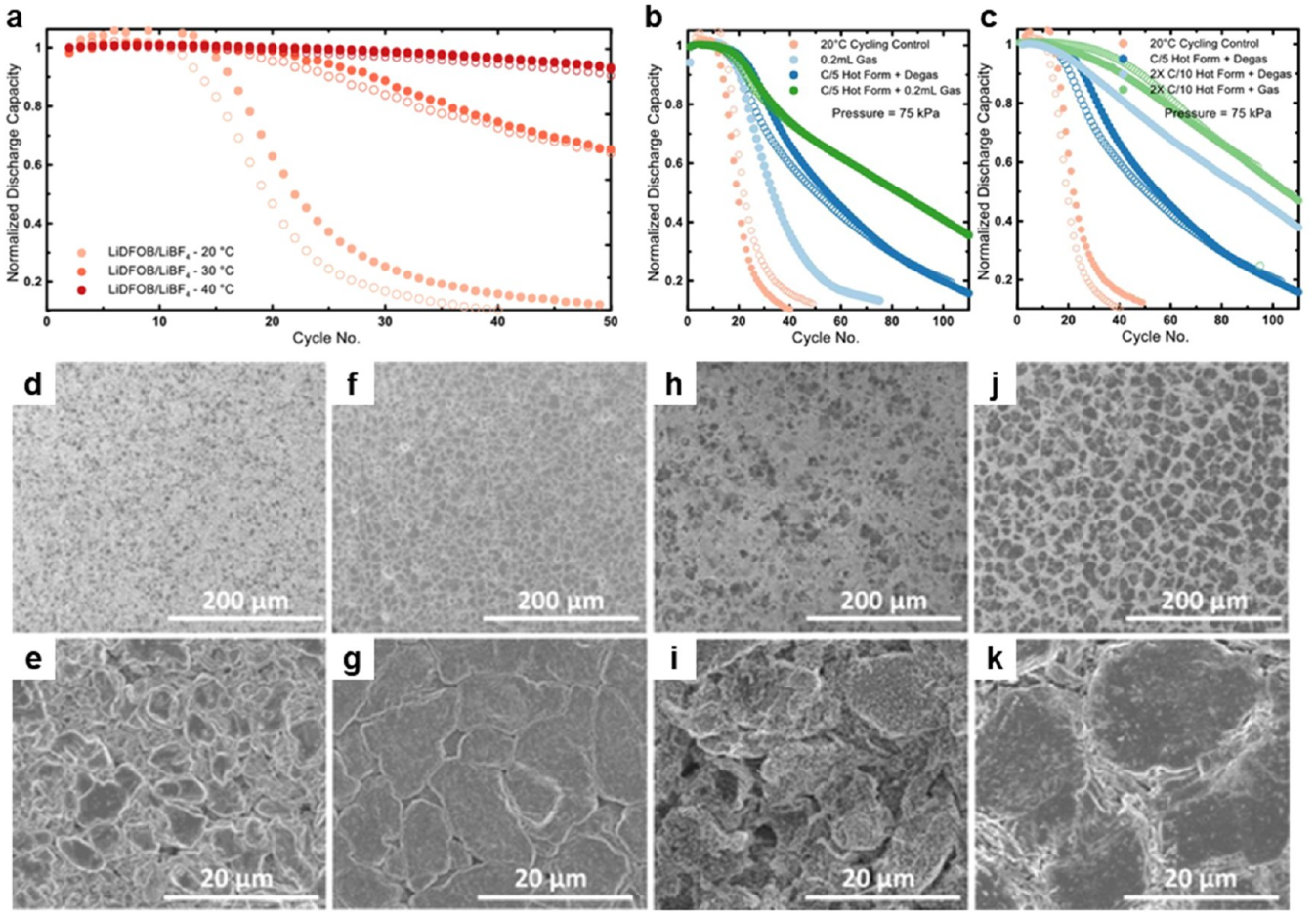

Figure 19. (a) Temperature-dependent cycling stability: Normalized discharge capacity of Cu|NMC532 anode-free cells utilizing a dual-salt LiDFOB/$LiBF_4$ electrolyte across a range of operating temperatures (20 to 40 °C). (b, c) Impact of formation protocols on capacity retention: Comparison of anode-free cell performance at 20 °C, evaluating the synergistic effects of hot formation cycles and initial gas volume control under low-pressure (75 kPa) conditions. (d–k) Morphological evolution of Li anodes: Low- and high-magnification SEM characterization of lithium plating morphologies on Cu current collectors. The images contrast the structural integrity of the Li deposits between standard cycling at 20 °C and specialized hot formation protocols at 40 °C, both at 2 cycles and 20 cycles. Panel a–k are reproduced with permission from ref 331, © 2019 IOP Publishing/ECS, CC-BY 4.0.

thinner, denser, and more inorganic/F-rich SEI, thereby improving mechanical robustness and interfacial contact.[321,322] Molecular-level simulations further suggest that pressure-induced SEI densification can increase elastic stiffness and interfacial adhesion, although excessive compression may alter lithium-ion diffusion pathways and increase transport resistance. Therefore, operational pressure should be regarded not simply as a mechanical constraint for suppressing dendritic growth, but as a cell-level variable that simultaneously regulates SEI density, stiffness, adhesion, fracture resistance, and lithium-ion transport.[321−323]

In practical anode-free cells, the local pressure at the current collector/SEI/lithium interface is not static but evolves dynamically during repeated plating and stripping.[39,324] During plating, the volumetric expansion of electrodeposited lithium increases local mechanical constraint and can compress the lithium/SEI composite, promoting in situ densification of the interphase. During stripping, the reverse volume change reduces local pressure and may induce SEI relaxation, cracking, or partial delamination, particularly when the SEI is too rigid or mechanically mismatched with lithium and the current collector. This cyclic pressure variation creates a chemo-mechanical feedback loop: dense lithium plating under moderate and spatially uniform pressure can stabilize the SEI, preserve electronic contact, and favor tip-dominated stripping, thereby reducing dead-lithium accumulation.[39,325] In contrast, excessive or highly localized pressure can increase impedance, deform cell components, and generate interfacial stress; during subsequent volume contraction, these effects may facilitate interfacial delamination or base-stripping-like detachment of lithium from the current collector.[322,324,325] Thus, future anode-free cell designs should incorporate dynamic pressure management strategies that balance lithium/SEI densification during plating with sufficient interfacial compliance during stripping.

However, pressure-based strategies should not be interpreted as a simple monotonic solution for improving lithium reversibility. The optimal pressure window is highly system-dependent and can be narrow, as evidenced by studies showing that both insufficient and excessive stack pressure can accelerate interfacial degradation and short-circuiting in lithium metal cells. More broadly, recent analyses of pressure−electrochemistry coupling in lithium metal batteries have emphasized that the reported "optimal" pressure range varies substantially across cell designs and pressure-control setups, highlighting the need for standardized pressure control

https://doi.org/10.1021/acsnano.6c06180
ACS Nano XXXX, XXX, XXX−XXX

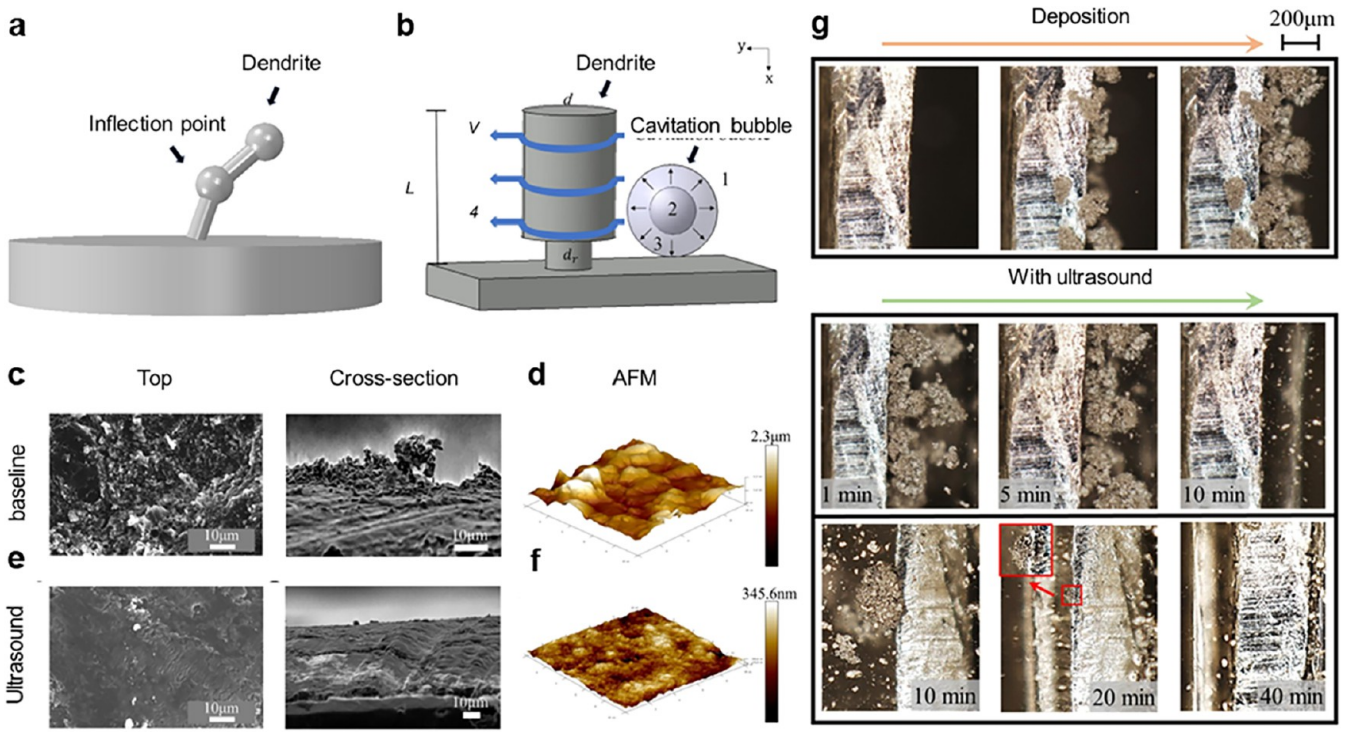

Figure 20. (a) Schematic representation of the dendritic morphology proposed by Yamaki, highlighting the characteristic inflection point in growth kinetics. (b) Schematic illustration of the dynamic interaction between acoustic cavitation bubbles and lithium dendrites, depicting the physical suppression of dendritic growth. (c) SEM images of Bare Li electrodes at current density of 2 mA cm^{-2} after 200 cycles. (d) AFM image of Li plate of Bare Li. (e) SEM images of Li electrodes with ultrasound at current density of 2 mA cm^{-2} after 200 cycles. (f) AFM image of Li plate treated by ultrasound. (g) Visualization of dendrite suppression at 2 mA cm^{-2}, illustrating the structural transformation of the Li electrode after 1, 5, 10, 20, and 40 min of continuous ultrasonic application. Panel a-g are reproduced with permission from ref 332, © 2024 Elsevier.

and reporting. In practical AFLMBs with liquid electrolytes, pressure management becomes even more complex because lithium plating/stripping, gas evolution, electrode swelling, and separator deformation can dynamically change the internal pressure distribution over cycling. Therefore, pressure is one of the more scalable external stimuli, but only if its magnitude and spatial uniformity can be maintained across large-area and multilayer cell formats through appropriate mechanical and module-level design.[326−328]

4.3.2. Temperature. Electrochemical reactions, including the lithium plating, stripping, and regeneration, are fundamentally governed by kinetic processes and are therefore strongly influenced by temperature. It has been reported that during cell operation, self-heating induced by high current densities can locally increase the temperature, thereby accelerating surface diffusion of lithium and in some cases, mitigating dendritic growth.[329] Extending this consideration of temperature to the choice of electrolyte further opens the possibility of exploring diverse combinations of electrolyte chemistries and operating temperatures under which a stable SEI can be formed.[330] Accordingly, identifying appropriate temperature conditions during cycling is essential for suppressing dendrite formation, promoting higher cycling efficiency, and faster regeneration.

Recently, Genovese et al. investigated the impact of temperature on the performance of anode-free pouch cells.[331] To elucidate the performance enhancements of anode-free cells attributable to temperature, they conducted cycling tests under low (20 °C) and high (40 °C) temperature conditions. Additionally, to assess the effects of pressure, they included low (75 kPa) and high (1200 kPa) pressure conditions. As shown in Figure 19a, it is evident that the cycling temperature affects the electrochemical performance of Cu||NMC532 pouch cells using a lithium difluoro(oxalato)-borate/lithium tetrafluoroborate ($LiDFOB/LiBF_4$) dual salt electrolyte. At 40 °C, anode-free cells exhibited minimal capacity fade after 50 cycles, still maintaining over 80% capacity retention. However, when the temperature was lowered to 30 °C, these cells dropped below 80% capacity retention shortly after 30 cycles. Further decreasing the temperature to 20 °C accelerated the fade even more, achieving only 18 cycles to 80% retention and nearly complete depletion after just 50 cycles. This is because the physical properties of lithium become softer at higher temperatures due to changes in yield stress and creep stress, making deformation easier. Furthermore, CO_2 gas generation increases during the hot formation process, acting as a beneficial additive. As shown in Figure 19b and c, the presence of CO_2 enhances the cycling performance of anode-free cells, and this positive improvement is maintained even after degassing.

The effect of this hot formation protocol could be confirmed once again through morphological studies. The difference can be clearly seen when examining the morphology of deposited lithium after formation and cycling at 20 or 40 °C, respectively. Deposited lithium formed at 20 °C exhibits a porous and dispersed structure, whereas lithium formed at 40 °C shows denser morphology with larger particles (Figure 19d−g). This phenomenon is also observed when comparing lithium morphology after 20 cycles under each condition (Figure 19h−k). The benefits established during the two high-

https://doi.org/10.1021/acsnano.6c06180
ACS Nano XXXX, XXX, XXX−XXX

temperature formation cycles have a significant impact on the quality of lithium plated in subsequent cycles, ultimately affecting the cycling stability of anode-free cells. In other words, operation at high temperature has a significant impact on the quality of initially plated lithium and consequently plays a substantial role in the overall cycling stability of anode-free cells.

Despite these benefits, temperature control should be distinguished from a broadly scalable operating strategy. Genovese et al. demonstrated that "hot formation" at 40 °C can improve lithium morphology and cycling stability in anode-free lithium metal pouch cells, indicating that thermal history strongly influences interfacial evolution and low-temperature performance.[331] However, maintaining elevated or finely tuned temperatures during long-term cycling would require active thermal management at the pack level, which introduces additional energy consumption, hardware, and control complexity. Moreover, large-format and multilayer cells can develop thermal gradients because of nonuniform heat generation and heat dissipation, leading to spatially heterogeneous reaction kinetics, SEI evolution, lithium deposition, and aging. Thus, temperature control is highly valuable for mechanistic studies and formation-protocol optimization, but its practical use as an operating strategy should be evaluated together with thermal uniformity, energy efficiency, pack-level integration, and safety margins.

4.3.3. Ultrasound. One method for mitigating lithium dendrite growth and the interfacial evolution of lithium metal, which lead to a reduction in reversible lithium capacity without damaging the structure of the battery, is the application of ultrasound. Depending on the way to apply this external power, ultrasound induces both cavitation effects and acoustic streaming-driven fluid motion in liquid electrolytes, analogous to its use in lithotripsy (a medical procedure for breaking kidney stones) and ultrasound cleaning.[332−334] Given that lithium dendrites possess mechanical strength properties similar to calcified deposits, ultrasound has been employed to target and address dendrite growth. Upon reaching the cavitation threshold, the ultrasound energy directly acts on the dendrites, facilitating their exfoliation, while the acoustic streaming wave (ASW) enhances electrolyte convection and promotes a more homogeneous Li^+-ion flux near the electrode surface. Although ASW can also influence the ion transport and deposition behavior, this review primarily focuses on cavitation-driven mechanisms, as they play a more direct role in the mechanical removal of lithium dendrites.

Ultrasound-induced cavitation typically arises from both microjets and shock waves. When ultrasound is applied, cavitation bubbles form in the liquid phase and collapse, releasing mechanical energy that contributes to material fracture, particularly for lithium dendrites. As shown in Figure 20a, during dendritic growth on the lithium metal surface, mechanical stress develops between the lithium and the SEI, causing the dendrites to bend along with its direction of growth. Continued growth of dendrites leads to the SEI ruptures due to the accumulation of mechanical stress, typically at the inflection point of the bend, which corresponds to a defect site within the crystal structure. This inflection point thickens over time, while the dendrite below remains relatively thin and narrow, making it prone to stress concentration.

Upon the application of ultrasound, the following process occurs: (1) cavitation bubbles encounter the dendrite below the inflection point, (2) the bubbles collapse, (3) the bubbles then rebound and expand, and (4) the formation of a flow velocity field perpendicular to the dendrite causes stress concentration at its base, (Figure 20b). Since the yield strength of lithium dendrite is reported to be approximately 0.9 MPa, which is less than the mechanical stress value of 1.54 MPa formed by cavitation bubbles, lithium dendrite can be effectively removed using ultrasound. Zhao et al. demonstrated the feasibility of using ultrasound treatment through morphological studies (Figure 20c−f). After the cavitation cleaning, lithium dendrites are clearly removed, and when quantitatively analyzed from the perspective of roughness, R_a and R_q values showed reduction of 77 and 75%, respectively. Operando optical study also revealed that lithium dendrite can mostly be exfoliated in 40 min of exposure to ultrasound (Figure 20g).

Completely mitigating the formation of lithium dendrite remains challenging from a practical standpoint since its failure strength has recently been reported as 150 MPa.[335] Nevertheless, methods such as the ultrasound treatment shown in the example here, which apply external forces during the cell operation, to artificially remove the dendrites, can be effective. However, it is also worth noting that the effect of ultrasound is not fully optimized now as it has been reported that ultrasound treatment may degrade the LMBs due to dead lithium accumulation under ultrasound.[336] Beyond developing internal components of the battery, such as electrode materials and electrolyte, it is necessary to find out how to effectively increase the lithium utilization through external forces even after cell operation begins.

Ultrasound faces even greater barriers to scalable implementation. Although ultrasonic fields can induce acoustic streaming, enhance local electrolyte convection, and mechanically disrupt dendritic lithium under controlled laboratory conditions, their continuous use in practical cells would require additional components such as ultrasonic generators, transducers, coupling structures, and potentially cooling systems. These components increase system complexity and may reduce effective cell- or pack-level energy density. Moreover, acoustic-field distribution is highly sensitive to cell geometry, transducer position, electrolyte distribution, and stack configuration, making uniform application across large-area or multilayer pouch cells difficult. Importantly, recent work has reported that real-time ultrasound can accelerate dead-lithium accumulation on the anode, increase overpotential, lower Coulombic efficiency, and promote faster capacity fading compared to nonultrasound-treated cells in both symmetric and full-cell configurations.[336] Therefore, ultrasound should currently be regarded primarily as a mechanistic research tool for probing and transiently modifying lithium morphology, rather than as a near-term scalable operating strategy for practical AFLMBs.

Overall, these examples show that external stimuli should be evaluated not only by their ability to improve lithium morphology under laboratory conditions, but also by their scalability, energy cost, integration complexity, and spatial uniformity. Consequently, future AFLMB development should prioritize intrinsic materials and interfacial designs, such as optimized current collectors, stable electrolytes, and functional separators, which enable uniform lithium plating and stripping without requiring continuous external intervention.

4.4. Practical-level Cells with Lean Electrolyte

Despite promising performance demonstrated in coin cells, scaling up from coin to commercial level remains a great

https://doi.org/10.1021/acsnano.6c06180
ACS Nano XXXX, XXX, XXX−XXX

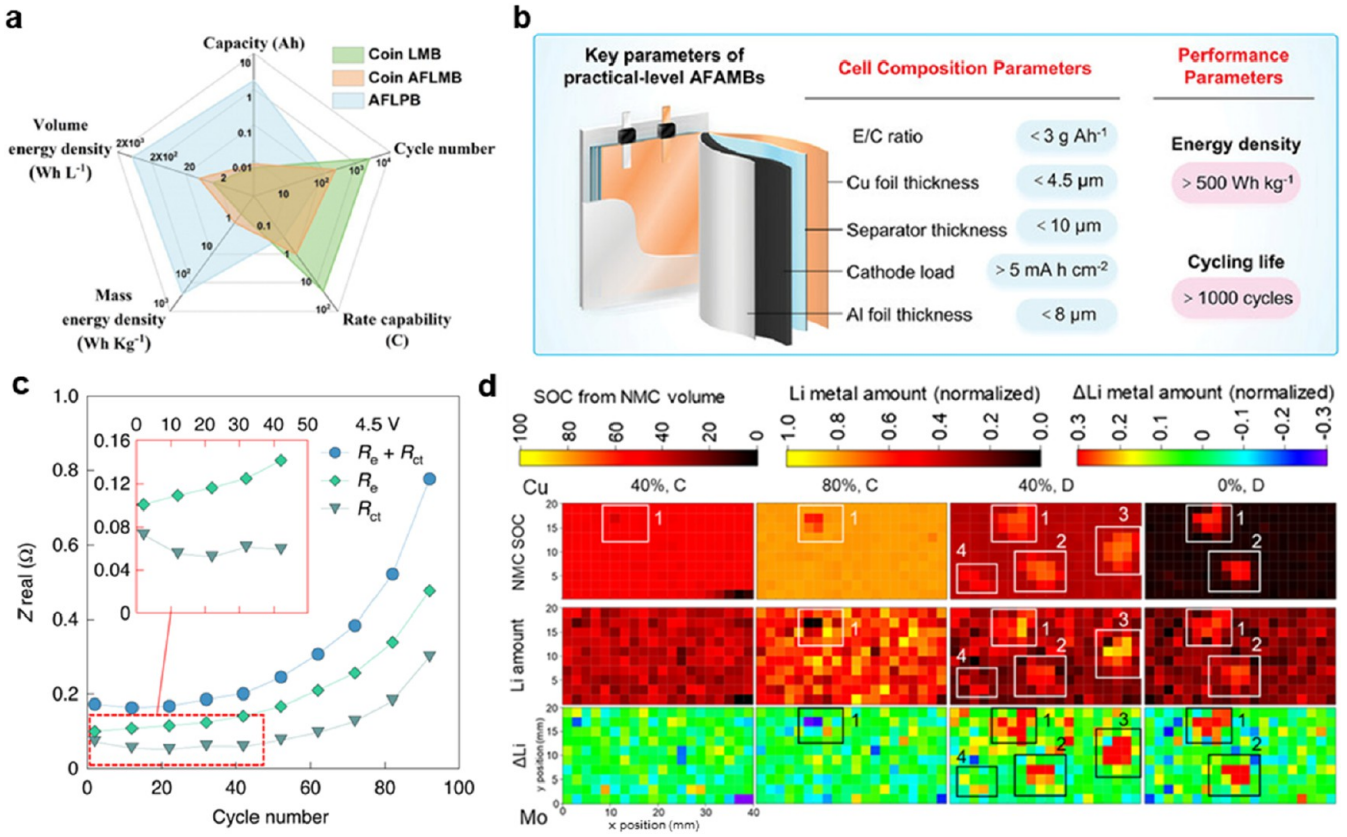

Figure 21. Required parameters for commercial-level AFLMBs and their limitations under lean electrolyte conditions. (a) Quantitative comparison of coin LMB, coin AFLMB, and AFLPBs in five parameters of cell performance: capacity, volume energy density, mass energy density, rate capability, and cycle number. (b) Requirements of practical-level anode-free alkali metal batteries (AFAMBs). (c) Increase of electrolyte resistance (real component of impedance) as a function of cycling number for the lean electrolyte cells. (d) Spatially resolved maps showing distribution of NMC SOCs, normalized lithium content and the deviation of amount of lithium from the mean (ΔLi) in the Cu/NMC cell, evaluated at different resting steps throughout cycling. Panels are reproduced with permissions from a, ref 15, © 2023 The Royal Society of Chemistry; b, ref 337, © 2024 Wiley-VCH GmbH; c, ref 140, © 2020 Springer Nature Ltd.; d, ref 338, © 2022 IOP Publishing/ECS.

challenge. Coin cells commonly apply excess electrolyte and low-loading cathodes to ensure good wetting and long cycle life, while anode-free lithium pouch batteries (AFLPBs) must operate under lean electrolyte and high-loading cathode conditions for practical applications. The electrolyte to cathode capacity ratio (E/C ratio) often exceeds 10 g Ah^{-1} in coin cells while it is below 3 g Ah^{-1} in pouch cells.[15] Under such conditions, a large performance gap exists between laboratory coin cells and AFLPBs (Figure 21a and b). Inferior performance in such practical conditions is fundamentally due to an insufficient quantity of electrolyte. As discussed in Section 3.3 Electrolyte, electrolytes in LMBs suffer from continuous decomposition during the entire life span of the cell either by electrochemical reaction or chemical corrosion. Lean electrolyte conditions significantly amplify the electrolyte depletion effect, resulting in a faster increase in electrolyte resistance (Figure 21c).[140]

Rapid depletion of electrolytes induces heterogeneous electrolyte distribution across the electrode. For porous electrodes, such as cathodes in AFLMBs, the absolute quantity of electrolyte may not be sufficient in terms of uniform wetting to entire electrode. Incomplete wetting of electrode due to electrolyte deficiency becomes more severe when considering the decomposition during the prolonged cycles or the thick cathode strategy considered earlier (Section 4.1). Khalifah et al. observed the spatially distributed state-of-charge (SOC) and lithium distribution in NCM cathode from operando synchrotron X-ray diffraction.[338] The cathode remained relatively uniform SOC at the midpoint and near the end of the first charge, but significant deviations appeared in the middle of the subsequent discharge step (Figure 21d). This severe heterogeneity, which is mainly from nonuniform electrolyte distribution, induces locally focused current and hinders the full utilization of lithium.

In addition to the case of porous electrodes, anode side, which can actually be considered as planar electrodes, are also not free from the wetting problem. Assuming the use of a 2D current collector without any scaffold, it may be appropriate to identify as a planar electrode in the initial state. However, after several plating/stripping cycles, in an environment where dead lithium and SEI have accumulated on current collector surface, the anode also possesses a porous structure. Electrode wetting occurs due to capillary action within the porous layer, and through this, ion transfer takes place. Under lean electrolyte conditions, insufficient and heterogeneous wetting of the porous anode structure induces progressively uneven lithium plating/stripping, thereby accelerating cell failure.[339,340] Detailed discussion of this porous structure formed on the surface of anode will be continued in Section 5.2. For the commercialization of AFLMBs, research must go beyond all

https://doi.org/10.1021/acsnano.6c06180
ACS Nano XXXX, XXX, XXX−XXX

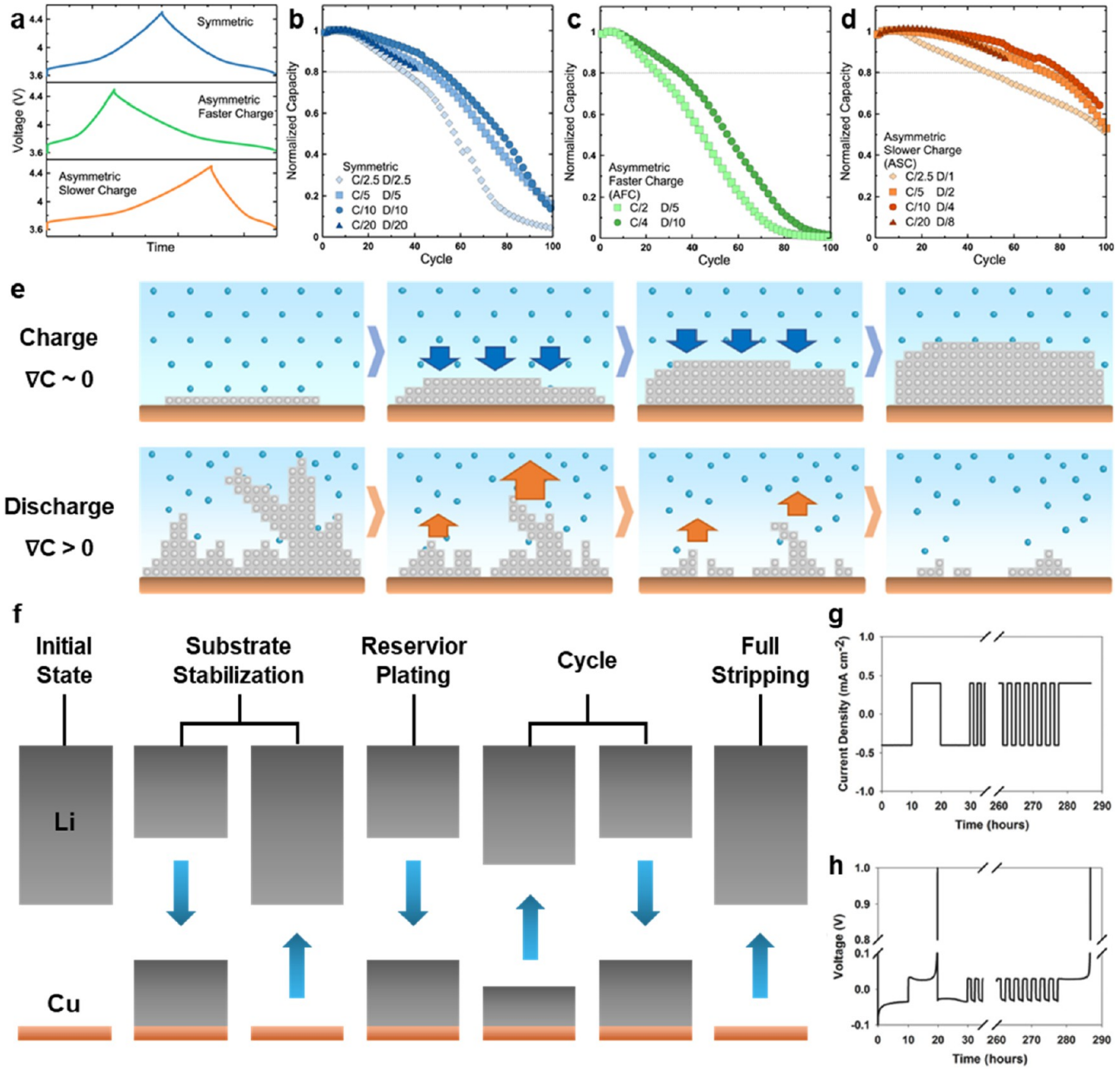

Figure 22. Cycling protocols and CE measurement strategies for AFLMBs. (a–d) Comparison of symmetric cycling and two asymmetric cycling protocols, where adjusting charge/discharge asymmetry changes cell capacity retention. (e, f) Schematic illustration of Li plating/stripping behavior, showing that asymmetric slower charge cycling promotes more uniform deposition and stripping and successfully mitigates capacity loss. (g) Proposed cycling protocol incorporating substrate stabilization to enable accurate CE evaluation in AFLMBs and its corresponding current profile and expected voltage response, respectively. Panels are reproduced with permissions from a–e, ref 341, © 2021 IOP Publishing/ECS, CC-BY 4.0; f–h, ref 344, © 2017 Wiley-VCH GmbH.

aspects discussed in the previous section, from the material-level to electrode-level and cell-level developments, Ah-grade cell design applicable in real-world application must be considered.

5. DIAGNOSTICS FOR AFLMBS: UNVEILING FAILURE AND REVERSIBILITY

5.1. Cycling Protocols for Precise Evaluation

Almost all battery-related research involves operating cells and demonstrating the improving impact of their research on cell performance. However, there are no consistent standards for operating conditions. Furthermore, researchers share results obtained by operating cells in intentionally more harsh or stable environments to emphasize their research findings. Therefore, direct comparisons between research results are often difficult and lack significant meaning. Of course, battery operating environments are bound to vary, and standardizing them based on a single standard is impractical for both research and industry. Nevertheless, it is crucial to understand how operating conditions affect cell performance, and based on this understanding, it is necessary to establish a "most common operating condition" for cross-reference across studies. Establishing these standard protocols is the first step toward

https://doi.org/10.1021/acsnano.6c06180
ACS Nano XXXX, XXX, XXX–XXX

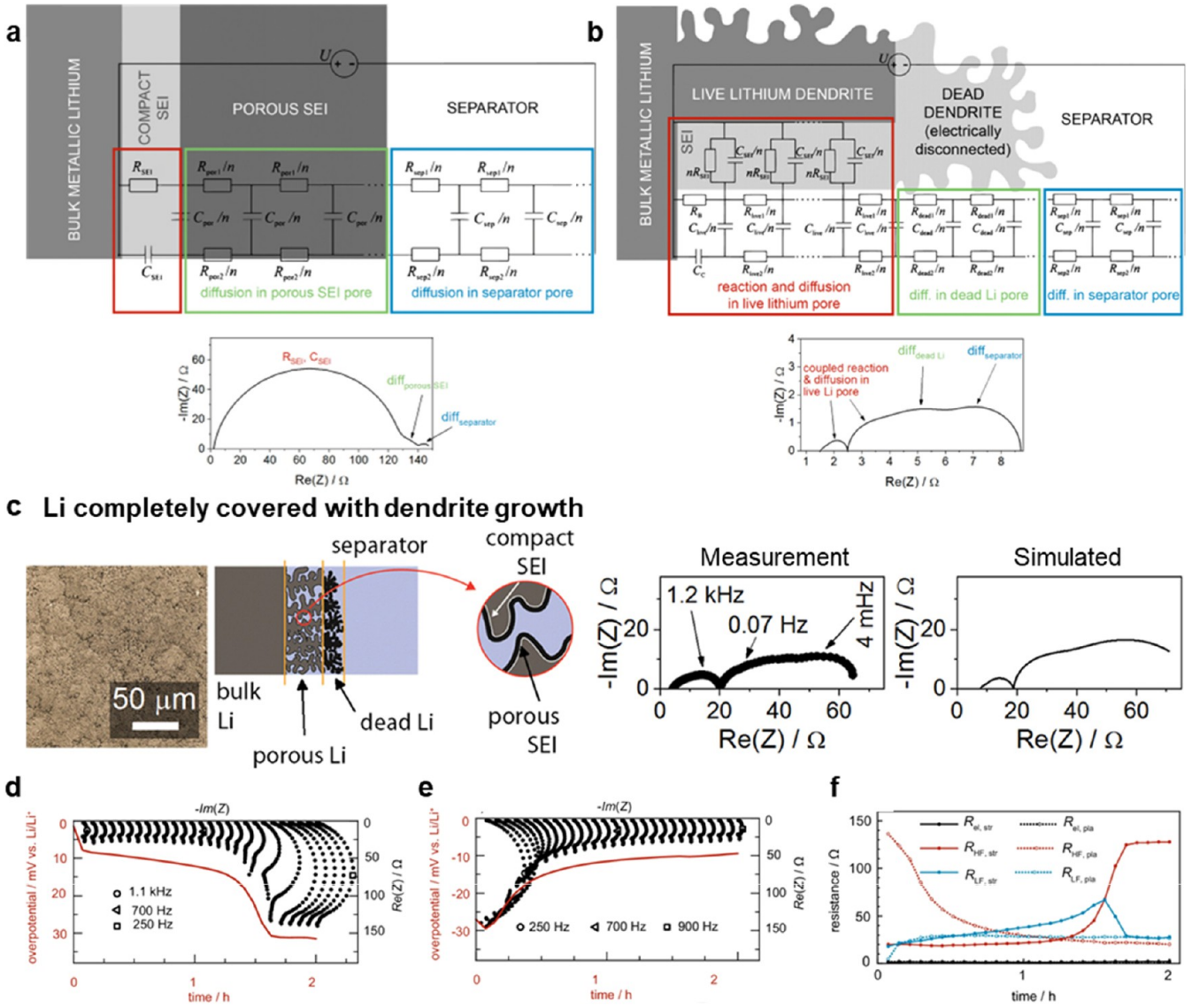

Figure 23. Proposed transmission line model (TLM) to analyze electrochemical impedance in lithium metal batteries. (a-b) Schematic TLM circuits representing pristine Li with compact SEI and cycled Li with porous SEI and dendritic lithium live lithium layer, illustrating how morphological changes can affect the EIS elements. (c) Comparison of Li plating morphology and measured and simulated EIS spectra based on TLM, showing the morphology-impedance correlation. (d-f) Operando EIS of Li symmetric cells, showing time-dependent impedance evolution and asymmetric evolution of overpotential of plating and stripping electrodes, evidencing asymmetric interfacial Li dynamics. Panels are reproduced under permissions from a–c, ref 355, © 2019 American Chemical Society, CC-BY 4.0; d–f, ref 356, © 2025 Springer Nature Ltd.

accurate diagnostics, as it ensures that the observed degradation is a result of intrinsic material behavior rather than inconsistent testing environments. This chapter briefly proposes criteria for testing cells, particularly for AFLMBs.

Two of the most critical parameters for evaluating LMBs and AFLMBs are cycle life and CE, both of which are highly sensitive to the testing protocols. Contrary to conventional wisdom, works from multiple research groups demonstrated that employing an asymmetric charge/discharge protocol with a slow charge and a fast discharge significantly extends cell lifespan and improve capacity retention.[341−343] For example, a work from Dahn's group discovered this asymmetric slower charge (ASC) protocol is believed to be optimal because slow plating encourages the formation of a dense, compact lithium morphology with minimal surface area (Figure 22a–d).[341] Subsequently, faster stripping preferentially removes nonuniform, porous lithium deposits from the tips of protrusions, effectively 'healing' the electrode surface for the next cycle. This illustrates that the relative rates of plating and stripping, not just their absolute values, are a determining factor in battery degradation (Figure 22e).

The CE is also profoundly affected by the conditions of the initial cycles, specifically whether a residual layer of lithium is left on the current collector. The formation and stability of the SEI are critical, as noted in studies by Zhang's group and in methods developed by Aurbach et al.[344−346] Initial cycles often exhibit lower CE as the SEI forms and stabilizes on the fresh electrode surface. Research shows that performing a high-capacity conditioning cycle at the beginning can passivate the substrate and establish a more stable foundation for subsequent cycling, leading to more accurate and higher average CE measurements. Similarly, limiting the depth of

https://doi.org/10.1021/acsnano.6c06180
ACS Nano XXXX, XXX, XXX−XXX

discharge in AFLMBs is a strategy to intentionally create an *in situ* lithium reservoir from the very first charge. This reservoir then serves as a stable host for subsequent plating and compensates for lithium inventory loss, thereby extending cycle life. Using Aurbach method, the CE of AFLMBs can be more accurately determined while minimizing errors due to those side reactions (Figure 22f–h).

As mentioned in earlier sections of this review, the situation can become more complicated when constructing a cell that undergoes full stripping to create a completely anode-free LMB while adding residual lithium to the anode. Since the Aurbach method does not assume full stripping of lithium in each cycle, it cannot evaluate the accurate lithium utilization efficiency. In addition, if lithium loss at the anode continues to be compensated, changes in CE, capacity retention, and cycle life may manifest differently than expected. Given these considerations, it may be worthwhile to explore more accurate CE evaluation methods that overcome the limitations of the Aurbach protocol and better reflect the true utilization of AFLMBs as discussed in Section 2.

ASC can also be regarded as a potential obstacle to the commercialization of AFLMBs. Since batteries generally require stable high-rate charging, and controlling the discharge rate in electronic devices is practically impossible, such a cycling protocol may remain confined to laboratory-scale demonstration rather than being viable for industrial applications. To overcome this limitation, research must continue to elucidate the fundamental mechanisms of the lithium plating/stripping cycle and enable its control. In an increasingly complex operating environment, the careful preparation of a standardized battery-testing checklist is important for enabling meaningful comparisons across research outcomes.[347,348]

5.2. Electrochemical Diagnostics of Interphase

Electrochemical Impedance Spectroscopy (EIS) is one of the most powerful methods to evaluate various electrochemical properties of LMBs. Simply by fitting the experimental results with the calculated results that came out from the Randles circuit, one can quantitatively analyze electrochemical properties of cells such as electrolyte resistance (R), resistance of SEI (R_{SEI}), charge-transfer resistance (R_{ct}), and other diffusion-related values.[30,31,116,117,349−351] However, conventional analysis using a Randles circuit for impedance measurements often oversimplifies the complex electrochemical system of a battery, which can lead to significant misinterpretations. Specifically, traditional EIS analysis has two main limitations: (1) Misunderstandings from oversimplified model and (2) absence of information from operating condition since EIS in current state is restricted to small perturbations around equilibrium. This idealized model fundamentally struggles to capture crucial degradation mechanisms from structural evolution of electrode, such as changes in electrode porosity or the formation of dead lithium. Relying on fitting experimental data to such a simplified equivalent circuit risks obscuring the battery's actual physical state and providing a misleading assessment of its status. Consequently, this approach can hinder the accurate diagnosis and prediction of battery performance and lifetime, highlighting the need for more physically representative models.

It should be noted that, in the case of AFLMBs in their initial state, EIS analysis applying ideal conditions may be effective because only a flat copper substrate exists on the anode side. However, as cycle proceeds, the accumulation of residual species such as intact active lithium, SEI, and dead lithium (inactive) adds complexity to the electrode, leading to mismatch between the initial electrode model and the experimental results from the later cycles. Even if the cell is not in operation, significant changes in impedance may occur over time due to the chemical reaction between electrolyte and lithium. To overcome the above-mentioned limitations of current EIS analysis, a new model that can describe porous characteristics of anode under operating conditions is necessary.

The transmission line model (TLM) approach has been introduced in the field of LMB analysis to address these issues. The TLM provides a framework to describe systems where resistive and capacitive properties are distributed over space, rather than lumped into a single interface.[352−354] Originally developed for signal propagation in electrical engineering, the concept can also be adopted into electrochemistry to analyze porous electrodes, SEI, and composite interfaces. In this context, the electrode−electrolyte can be divided into repeating elements consisting of ionic resistance and parallel interfacial capacitance or charge-transfer pathways. TLM can capture how alternating current penetrates to different depths depending on frequencies. High frequency regions mainly probe surface processes, whereas low frequencies reveal deeper diffusion, porosity effects, and long-range ionic transport (Figure 23a and b). This distributed approach is particularly powerful for lithium metal electrodes and even for cycled AFLMBs, where evolving SEI layers and dendritic structures make the interfacial response inherently heterogeneous.

Clear demonstrations of using TLM in the LMB field were delivered by Gaberščček's group. In their studies, multisection TLM was applied to analyze the impedance response of lithium metal electrodes during cycling.[355] By discretizing each section into hundreds of slices, the model captured the overlapping impedance arcs that arise when multiple distributed processes act simultaneously. For example, the growth of dendrites was reflected as increased effective thickness and surface area, leading to changes in both migration resistance and chemical capacitance. Reproduced impedance results from sequential domains, including compact SEI, porous SEI, live dendrites, dead lithium dendrites, and electrolyte soaked in separator, showed excellent matching with the experimental results without using any constant-phase elements (CPEs) that might distort the physical meaning of electrochemical properties (Figure 23c). Importantly, this framework allowed observed EIS features to be linked to real morphological changes seen in SEM images, such as the doubling of live and dead dendrite contribution with cycling.

Building on these foundations, a more recent study from the same group further advanced this methodology by introducing operando EIS in a three-electrode configuration.[356] This design enabled separate monitoring of plating and stripping electrodes, directly decoupling their asymmetric contribution to impedance evolution.[357] By measuring impedance in real-time during cell operation, this study successfully captured dynamic interfacial evolutions that would be missed in ex-situ experiments, such as the continuous evolution of SEI resistance, the growth of dendritic lithium, and the accumulation of electronically isolated dead lithium dendrites (Figure 23d–f). Importantly, the impedance spectra were analyzed through a TLM rather than conventional Randles circuits, allowing the impedance response to be interpreted in

https://doi.org/10.1021/acsnano.6c06180
ACS Nano XXXX, XXX, XXX−XXX

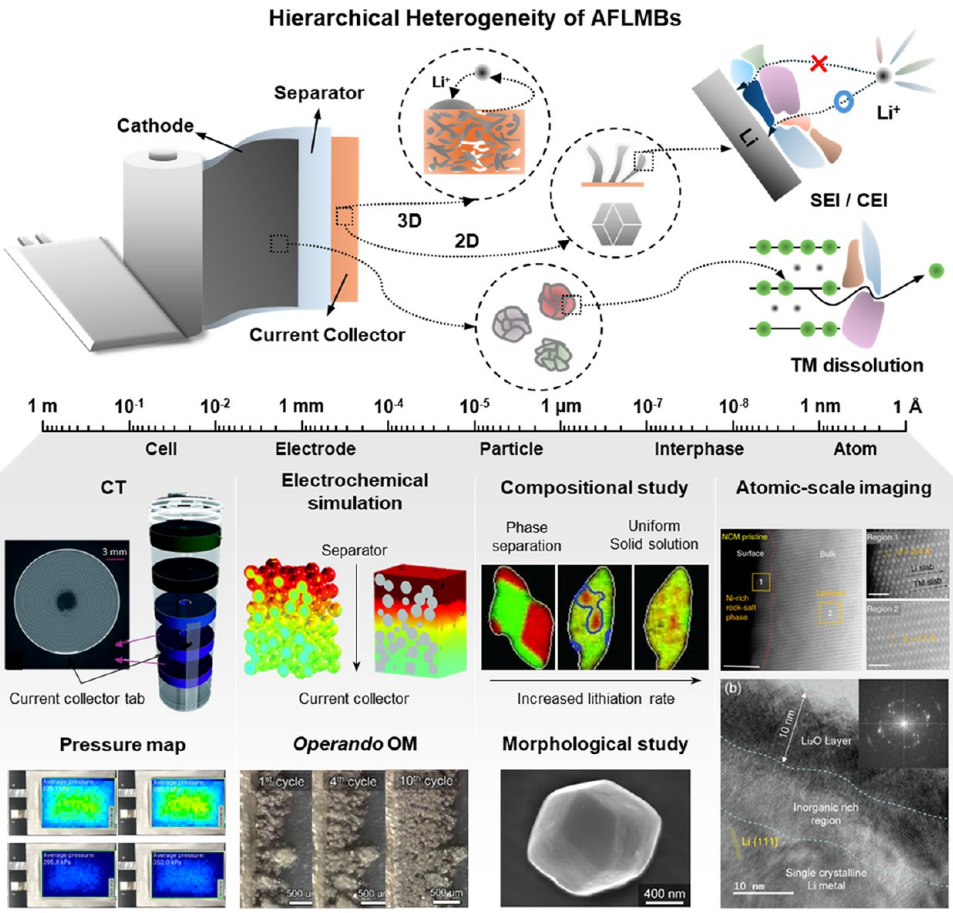

Figure 24. Schematic diagram of hierarchical heterogeneity characterization in AFLMBs. Figures above and below the arrows are illustrations of possible heterogeneity from atomic to cell-level and results from previous studies, respectively. Results of previous studies include (from top-left to bottom-right): Cell degradation in cell-level revealed by CT imaging; Heterogeneous lithiation in electrode-level; intraparticle heterogeneity of single LFP particle revealed by STXM; Irreversible phase transition of NCM particle observed in TEM; Pressure evolution of LMB after cycle revealed by operando pressure mapping technique; Li dendrite growth observed by operando optical microscopy; Rhombic-dodecahedron Li particles plated on copper (111) surface; SEI layer of Li-metal revealed by cryo-TEM. Panels are reproduced with permissions from (from top-left to bottom-right): ref 377, © 2019 The Royal Society of Chemistry, CC-BY 3.0; ref 378, © 2021 The Royal Society of Chemistry, CC-BY 3.0; ref 379, © 2016 The American Association for the Advancement of Science; ref 380, © 2020 Springer Nature Ltd., CC-BY 4.0; ref 327, © 2024 Springer Nature Ltd.; ref 381, © 2023 The Royal Society of Chemistry; ref 71, © 2024 The Royal Society of Chemistry, (the authors retain the right to reuse the figure in this work); ref 371, © 2023 American Chemical Society, (the authors retain the right to reuse the figure in this work).

terms of distributed structural domains with more clear physical meaning. This operando-TLM framework thus provides a powerful tool for linking electrochemical signatures to evolving electrode morphology and points to future opportunities for stabilizing interfaces in AFLMBs. Through this, it becomes possible to quantify the interfacial characteristics of SEI that vary by electrolyte and provide clues for electrolyte development.

Even when the measurement system and equivalent circuit model are carefully constructed, EIS data inherently represent a convolution of multiple lithium kinetic processes occurring within the cell in the frequency domain. Because the impedance response integrates the entire kinetic landscape, meaningful interpretation ultimately requires the separation of individual contributions. In this context, the distribution of relaxation times (DRT) method has emerged as a powerful analytical approach, grounded in the principle that each lithium kinetic process is associated with a characteristic time scale. By transforming impedance components that overlap in the frequency domain into the time domain, DRT enables their deconvolution without relying solely on predefined equivalent circuit assumptions. When combined with three-electrode configurations and operando analysis, DRT provides a robust framework for rapidly and precisely tracking kinetic evolutions within AFLMBs. A more comprehensive discussion of DRT methodology and its practical implementation can be found in the references cited herein.[358−363]

5.3. Hierarchical Heterogeneity Analysis

Characterizing AFLMB systems is inherently difficult due to the high reactivity of lithium itself. The continuous morphological evolution of plated lithium deposits also adds more complexity. These changes enlarge the effective surface area, promote parasitic reactions, and generate a SEI layer with complicated composition and structures. This reactive nature of lithium also makes it more difficult to prepare samples in their native state, because even minor deviations during sampling or transfer can induce structural or chemical defects. Therefore, specialized methods are required to preserve the initial form.

https://doi.org/10.1021/acsnano.6c06180
ACS Nano XXXX, XXX, XXX−XXX

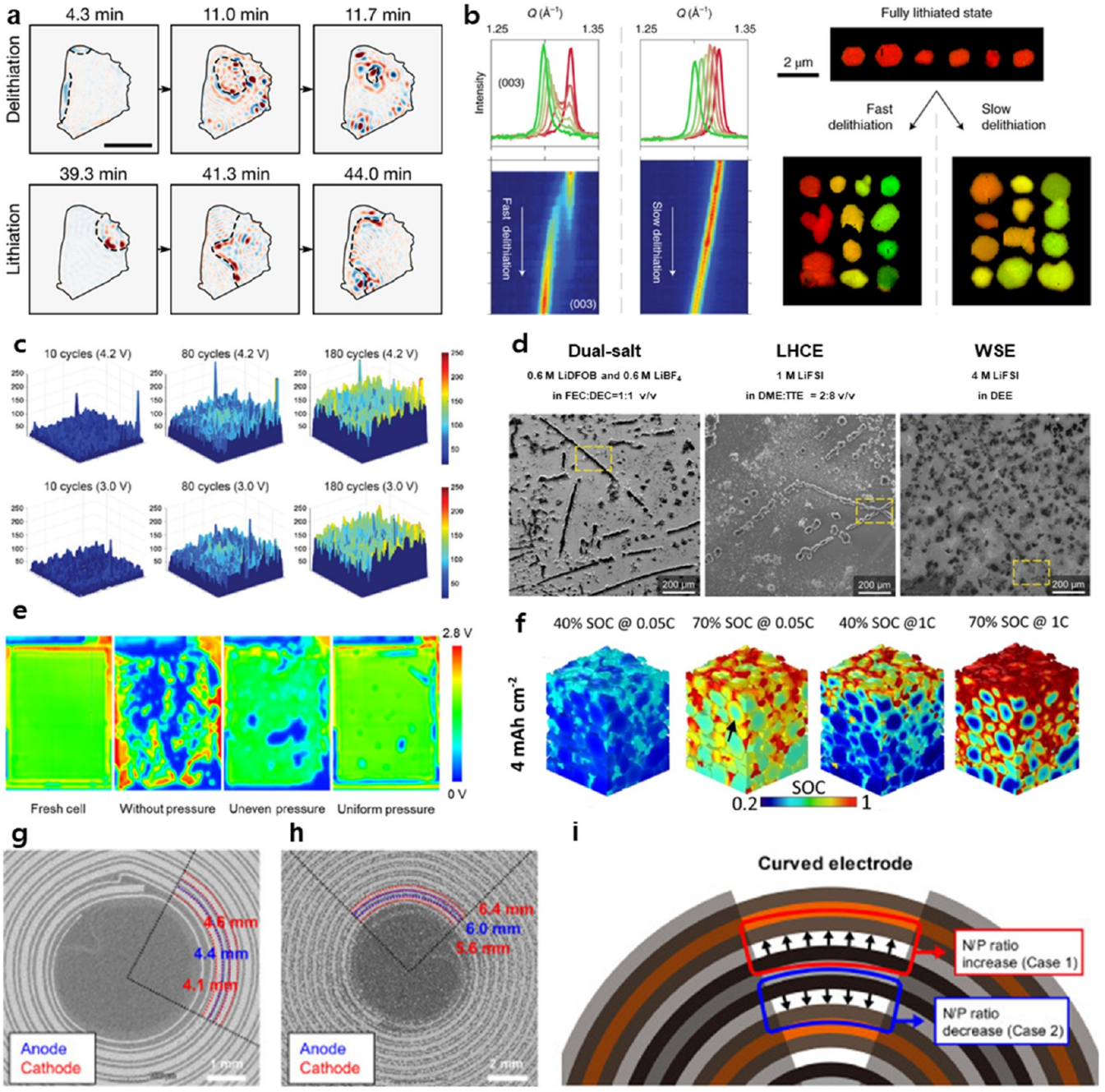

Figure 25. Multiscale heterogeneity of Li behavior expected in AFLMBs. Li distribution can become heterogeneous across multiple length scales and operational conditions. (a) intraparticle heterogeneity within individual cathode particles, (b) interparticle heterogeneity between particles during delithiation. (c–e) Areal heterogeneity that can be followed by continuous plating/stripping cycle, electrolyte chemistry, and local pressure distribution, respectively. LHCE and WSE of d stand for localized high concentration electrolyte and weakly solvating electrolyte. (f) Li^+-ion concentration gradients arise in thick electrode along electrode depth. (g–i) N/P variations induced by the electrode curvature in cylindrical cells, further amplifying spatial heterogeneity in cell-level. These examples highlight how particle-level, electrode-level, and cell-level factors cooperatively govern heterogeneous Li transport and deposition/dissolution. Panels are reproduced with permissions from a, ref 382, © 2021 Springer Nature Ltd.; b, ref 101, © 2021 Springer Nature Ltd.; c, ref 383, © 2023 Wiley-VCH GmbH, CC-BY 4.0; d, ref 71, © 2024 The Royal Society of Chemistry, (the authors retain the right to reuse the figure in this work); e, ref 384, © 2024 American Chemical Society; f, ref 385, © 2023 Springer Nature Ltd., CC-BY 4.0; g–i, ref 386, © 2025 Elsevier.

Despite the inherent challenges in analyzing these complex systems, a wide range of methods have been developed to study their behavior across multiple scales, from atomic-level to electrode-level. For morphology characterization, techniques such as cryogenic transmission electron microscopy (cryo-TEM), scanning electron microscopy (SEM), and optical microscopy (OM) are representative for imaging lithium metal plating.[22,364−368] Multiscale imaging studies have shown that lithium morphology changes in response to various factors, including electrolyte composition, current density, external pressure, and electrode pretreatment. Furthermore, SEI composition and structure can be analyzed by techniques such as cryo-TEM, energy-dispersive X-ray spectroscopy (EDX), electron energy loss spectroscopy (EELS), Time-of-

https://doi.org/10.1021/acsnano.6c06180
ACS Nano XXXX, XXX, XXX−XXX

flight secondary ion mass spectroscopy (TOF-SIMS) and X-ray photoelectron spectroscopy (XPS).[144,369−372] These studies suggest various SEI structures and ongoing efforts continue to refine these analytical processes to better account for the system's complexity.

Although various analytical methods have been developed to probe fragile SEI structures, significant limitations remain. In particular, the SEI may undergo structural deformation due to temperature fluctuations between cryogenic conditions and room temperature. In addition, contamination during sample preparation cannot be ruled out. For example, cryo-TEM observations suggest that the SEI can exist in a swollen state in the presence of electrolyte, implying its susceptibility to damage during solvent washing.[144] Similarly, XPS studies have reported the possibility of SEI degradation induced by the washing process.[372,373] More than three decades after the initial definition of the SEI,[374−376] its composition and structure are still discussed based on fragmented and often indirect evidence, largely reflecting persistent limitations in accurately characterizing such highly sensitive systems. This continued reliance on partial observations highlights the fundamental challenge that a comprehensive and unified understanding of the SEI remains unveiled.

Conventional characterization techniques often yield only localized or averaged information, limiting their ability to resolve the electrode-level heterogeneity. This shortcoming is even more critical for anode-free batteries, where both lithium plating on copper and substrate-induced interfacial reactions must be considered as additional factors. Moreover, heterogeneity is not confined to the anode side. In anode-free full-cells, cathode active materials exhibit nonuniform reactions and kinetic-driven phase separation, further complicating the reaction dynamics. Thus, simultaneous characterization of both electrodes in various scales is essential to accurately describe electrochemical processes in these systems. As illustrated in Figure 24, multiscale approaches ranging from atomic to cell-level characterization are required.

5.3.1. Depth-Heterogeneity. Reaction heterogeneity manifests at multiple scales and is often first recognized at the level of individual particles during battery operation, which is often called intraparticle heterogeneity. Classical descriptions such as the shrinking-core and intercalation-wave models illustrate how solid-state diffusion, surface charge-transfer kinetics, and local current density dictate the spatial distribution of phases inside active materials. Figure 25a presents intraparticle heterogeneity observed in a LCO particle showing lithiation and delithiation having different phase separation models. Interestingly, even materials typically regarded as solid-solution electrodes, which are not expected to undergo phase separation, have displayed heterogeneous behavior under certain conditions.[382] These findings emphasize that intraparticle heterogeneity is not confined to a specific class of materials but instead reflects the complex interplay of intrinsic and extrinsic factors during operation.

In addition to intraparticle heterogeneity, interparticle heterogeneity is also significant and should be carefully distinguished from intraparticle effects. For instance, Park et al. demonstrated that neighboring NCM particles within the same electrode can exhibit markedly different lithiation states, sometimes leading to misinterpretation of cell behavior (Figure 25b).[101] This interparticle phase separation is driven by the autocatalytic effect, where regions with a higher state of charge (SOC) react more quickly due to charge transfer limitations rather than solid diffusion, particularly under fast charging (delithiation) conditions.[387] The degree of heterogeneity varies across different materials due to their unique kinetic properties.[105]

Whether due to charge transfer or diffusion limitations, heterogeneity along the depth of the electrode is inevitable. In porous electrodes, lithium ions must traverse tortuous pathways within the electrolyte-filled pores, leading to concentration gradients along the electrode depth during battery operation.[378] These gradients are directly related to the uneven local current densities, with particles near the separator experiencing higher currents compared to those located deeper in the electrode. Lu et al. highlighted that particle-scale heterogeneity differs between the upper and lower regions of the electrode, emphasizing the presence of reaction heterogeneity throughout the depth (Figure 25f).[385,388] Such nonuniformity becomes more pronounced at higher rates, reflecting the limitations imposed by Li^+-ion mass transfer. This can lead to the degradation of cathode materials, ultimately impairing cell performance. Consequently, heterogeneity cannot be viewed solely as a particle-level issue but must also be considered as a property of the porous electrode as a whole.

Similarly, depth heterogeneity must be considered for three-dimensional (3D) anode current collectors, which are often introduced to improve lithium deposition. While 3D frameworks provide additional surface area and help regulate local current density, their complex geometry can also create uneven transport fields.[389−392] Tortuosity, pore size distribution, and conductivity gradients across the structure influence how uniformly lithium is deposited. Optimizing these architectural parameters through controlled pore design, conductive additives, or integrated binding agents has been shown to alleviate depth heterogeneity while maintaining mechanical robustness.[153,393−394]

Overall, heterogeneity is a defining characteristic of electrochemical processes in AFLMBs, spanning from intra-particle to electrode-level heterogeneity. While most studies have focused on local-scale mechanisms, practical devices demand a comprehensive understanding that links microscopic phenomena with macroscopic behavior. Depth-dependent heterogeneity in both thick cathodes and 3D anodes represent a critical obstacle to stable cycling but also an opportunity for innovation through materials and structural design.

5.3.2. Areal-Heterogeneity. Areal heterogeneity can arise from the surface properties of electrodes and strongly influence lithium metal plating and stripping. In particular, the characteristics of the substrate play a decisive role in determining plating behavior. For example, on graphite anodes, it has been reported that lithium nucleation preferentially occurs at sites with the lowest impedance, often leading to dendrite growth.[395] This effect is further intensified under harsh conditions such as higher C-rates or higher electrode mass loading. In AFLMBs, spatial variations in plating are also observed with contributing factors including pressure distribution and crystal orientation, both of which lead to areal reaction heterogeneity.

Pressure is one key source of areal variation across the substrate and can both result from and reinforce nonuniform plating. Park et al. showed that pressure heterogeneity, originating from inconsistent plating thickness and morphology, evolves with state of charge (SOC), electrolyte composition, and cycle number (Figure 25c). They further

https://doi.org/10.1021/acsnano.6c06180
ACS Nano XXXX, XXX, XXX−XXX

demonstrated that greater deviations in pressure distribution accelerate capacity fading, directly linking areal heterogeneity to the cell degradation.[383] In addition, pressure strongly affects the morphology of plated lithium and subsequently influences the stripping process.[396] Yang et al. reported that in multilayer ampere-hour-level AFLMBs, stacking pressure plays a decisive role in plating behavior (Figure 25e). Their findings demonstrated that stack pressure needs to be well-distributed across the copper substrate to ensure uniform lithium deposition, indicating the impact of areal heterogeneity.[384]

Crystal orientation is another source of areal plating and stripping heterogeneity, as Li^+-ion interactions vary across different crystallographic surfaces (Figure 25d).[71] Substrates with stronger affinity for Li^+-ions tend to promote preferential adsorption at lithiophilic sites, triggering nucleation in these regions. Consequently, plating often occurs at high-index grains or along grain boundaries, which facilitates dendritic growth. These observations indicate that substrate properties should be considered carefully when addressing areal heterogeneity. This suggests that substrate properties must be carefully considered to address areal heterogeneity, rather than simply applying lithiophilic materials to reduce nucleation overpotential.

Although the possibility of areal heterogeneity in electrochemical plating and stripping is widely recognized, its detailed behavior in AFLMBs remains insufficiently understood. Most existing studies have concentrated on localized morphologies captured by conventional analysis techniques. However, improving practical performance requires a more macroscopic perspective, since large-scale spatial nonuniformity can dominate long-term cycling behavior. A major challenge lies in the difficulty of directly observing and quantifying spatial heterogeneity with current characterization tools, which limits progress toward fully resolving this issue in AFLMBs.

5.3.3. Curvature of Current Collectors. Battery cells are manufactured in diverse form factors, including prismatic, cylindrical, and pouch designs, and each configuration influences reaction dynamics and degradation pathways. It is well established that cell geometry plays a major role in defining the conditions under which electrochemical reactions occur and how deterioration progresses over cycling. In particular, prismatic and cylindrical formats, especially those assembled with a jelly roll, introduce intrinsic curvature into the electrode, which directly affects thermal distribution, internal pressure, electrolyte distribution, and current distribution across the electrode surface.[397−405]

Previous studies have shown that this curvature can exacerbate cell degradation, especially in the bent regions of the electrodes. For example, it has been revealed that the imbalance of N/P ratio can occur due to the electrode curvature (Figure 25g−i).[386] This suggests that in curved electrode geometries, especially in anode-free configurations, lithium plating and stripping behaviors can differ from those seen in flat cells, leading to more pronounced spatial heterogeneity. The resulting heterogeneity in plating and stripping from uneven current densities can further accelerate the degradation process in localized areas of the cell.

Heterogeneity caused by cell curvature tends to be greater when the cell is operated for a longer time in harsher environments, such as high C-rate cycling and conditions of nonambient temperature. Under these stresses, the concentration gradient of Li^+-ions and mechanical stress caused by curvature can be more pronounced, which adversely affects the capacity fading and overall cycle life. In fact, as the AFLMB is a kind of next-generation battery, the precise impact of the form factor on such a large scale has not yet been defined. Nevertheless, considering the eventual commercialization of AFLMBs, research into internal and external components within the cell that can minimize the impact of form factors is necessary.

6. CONCLUSION

6.1. Overall Summary

Research on AFLMBs is now entering a new phase. Since the conception of the anode-free system, a wide range of studies have been conducted to realize this Holy Grail battery system, spanning from material design to external devices and cycling protocols. Strategies have been employed to achieve uniform lithium deposition that successfully improved cell performance over prolonged cycles. However, most studies to date have been carried out using coin cells or low-capacity pouch cells short of meeting the standards for practical real-life application scenarios. Moving forward, research must address this gap. Lithium plating alone cannot serve as an effective descriptor; but instead, uniform stripping and regeneration of dead lithium must be systematically investigated in large-scale cell formats to move beyond LIB-level cycle life and CE.

Heterogeneity occurring on multiple length-scale and in multiple dimensions is one of the first aspects to be understood for the realization of AFLMBs. Even slight heterogeneities generated during the first cycle can accumulate in the prolonged cycles and accelerate cell degradation. Therefore, it is necessary to understand and prevent heterogeneity that can occur at various scales, from particle to cell, throughout the entire cell manufacturing and operation process. Inter- and intraparticle heterogeneity of cathode active materials lead to uneven local stress and potential Li^+-ion concentration gradient, which can result in nonuniform plating and stripping of lithium on the anode side. Areal heterogeneity of anode current collector can induce localized depletion or accumulation of lithium which in the long term leads to increased cell resistance and decreased CE. In the case of depth heterogeneity, which can be seen in cathodes or porous lithium plated on anodes, it causes nonuniformity in the utilization of active materials according to depth, making it impossible to deliver the desired capacity. At a larger scale, cell-level heterogeneity, such as mechanical stress and thermal gradients, may occur, which is another challenge to overcome for practical use of AFLMBs.

Developing innovative strategies to maintain cell capacity is just as important as understanding how cells work. This review introduces two representative approaches: cathode prelithiation and addition of a lithium regenerator to the electrolyte. Each method has the disadvantages of potentially reducing the energy density of the cell and causing self-discharge, respectively. Additionally, from the perspective of a thick cathode, the phenomenon of depth-heterogeneity may become more severe. Nevertheless, to achieve high-energy density and long-term cycle stability, it is necessary to develop efficient internal lithium source replenishment methods, in addition to the approaches mentioned above to overcome these trade-offs. Taken together, these considerations highlight that the realization of practical AFLMBs cannot rely on a single strategy, but instead requires a balanced integration of lithium management, interfacial stability, and structural uniformity

https://doi.org/10.1021/acsnano.6c06180
ACS Nano XXXX, XXX, XXX−XXX

across multiple length scales. Ultimately, advancing AFLMBs toward real-world applications will depend on the ability to simultaneously address these interconnected challenges within a unified cell-level design framework.

6.2. Prospects for Future AFLMB Research

It is a fact that many scientific and engineering challenges remain before AFLMBs can be incorporated into practical applications. Although the research community has begun to consider the Gen 5 paradigm, the theoretical models currently available still deviate significantly from reality. As a simple example, even if an AFLMB with a CE of 99% is assumed, practical experience shows that neither the lifespan nor the capacity retention follows the expected trend. Even within a single coin cell, performance can vary depending on spatial location and time, and these discrepancies often become more pronounced when scaling up to commercially relevant formats. In fact, this occurs because assuming CE to be 99% is already far from reality. The CE itself is strongly affected by multiple factors, including electrolyte composition, cycling hysteresis, lithium plating/stripping morphology, and cycling protocol, making it difficult to maintain a constant value as assumed. Under such constraints, it is increasingly evident that conventional approaches alone may not be sufficient to establish a complete mechanistic model. Furthermore, when lithium replenishment strategies are incorporated, as discussed in this review, the system becomes even more complex, potentially exceeding the limits of human intuition and predictability. In this context, data-driven approaches based on machine learning (ML) and artificial intelligence (AI) offer a promising alternative by enabling the extraction of hidden correlations from high-dimensional data sets and providing predictive capabilities beyond conventional intuition.

As research transitions toward system-level integration, it is essential to recognize that individual components cannot be considered independently, but rather as strongly interrelated factors. For example, the solvation structure of the electrolyte and the composition and structure of the SEI/CEI are inherently coupled, which may further lead to phenomena such as spatial pressure heterogeneity during cell operation. As discussed in previous sections, additional complexities may arise when incorporating prelithiation agents, thick cathodes, or different types of cathode materials, many of which have not yet been systematically investigated. It must be acknowledged that the governing principles of such complex systems are difficult to fully capture using human intuition alone. Instead, AI-based predictions and simulations trained on large data sets can reveal correlations that are not accessible through existing physical models, thereby offering new insights that can support the advancement of these models. Indeed, data-driven approaches have already demonstrated their capability in predicting complex systems more efficiently than conventional methods, including protein structure prediction, fluid dynamics modeling, electrolyte design, module-level thermal behavior, and early stage lifetime forecasting based on initial cycling conditions. These examples highlight the potential of AI to accelerate discovery by identifying the most probable outcomes within vast design spaces.

For AI to deliver reliable predictions, both the quantity and quality of data are critical. In many cases, experimental conditions are intentionally selected to emphasize specific results, which may limit the general applicability of the data. While such approaches are effective for demonstrating individual findings, it is important to consider whether these data sets are suitable for training robust AI models. Therefore, the adoption and sharing of standardized testing protocols are essential. For instance, conditions commonly used in lithium-ion battery studies, such as 1C charge/discharge profiles, may serve as a useful baseline for generating comparable data sets. The accumulation of large-scale, high-quality data under unified conditions will significantly enhance the predictive power of AI-driven approaches.

It is also important to recognize that AI provides probabilistic predictions rather than definitive answers. Regardless of the sophistication of AI models, experimental validation remains indispensable for confirming their relevance and establishing physically meaningful interpretations. Through this iterative process of prediction and validation, fundamental principles can be progressively uncovered, ultimately enabling the development of models that accurately describe real battery systems. Such validated models may eventually be extended into digital twin frameworks capable of simulating battery behavior without the need for extensive experimentation.

In parallel, advances in analytical techniques have enabled increasingly multidimensional and real-time characterization approaches. For example, dendrite growth mechanisms, initially inferred from post-mortem morphology analysis, can now be observed in real time or simulated using phase-field models. However, many of these techniques still rely on modified conditions, such as specially designed cells for operando X-ray analysis or cryogenic environments for TEM studies, which may not fully represent actual operating conditions. While these methods have significantly advanced our understanding, questions remain regarding their ability to capture true cell behavior. Therefore, it is crucial to carefully evaluate how closely such analyses reflect realistic operating environments, as only such insights can contribute to a deeper physical understanding of battery systems.

From a commercialization perspective of such Ah-cell-level or GWh-module-level, cost and productivity remain major concerns. Although various strategies, such as electrolyte optimization, electrode engineering, and external control methods, have demonstrated improvements in lithium utilization, many of these approaches deviate from established LIB manufacturing processes and may introduce challenges related to cost or scalability. This naturally raises questions regarding the practicality of such technologies. Nevertheless, from the standpoint of energy density, AFLMBs represent one of the most promising ultimate battery configurations. Historical precedents in battery development suggest that early stage technologies often face skepticism due to high cost and low efficiency, but these limitations are progressively mitigated through industrial scaling and process optimization. Therefore, while economic considerations are important, current research should prioritize establishing a clear understanding of operating principles and demonstrating practical feasibility. Once these foundations are secured, industrial adoption and cost reduction are likely to follow.

Despite the remaining challenges, it is important to recognize the progress achieved within a relatively short time. Less than a decade after the introduction of the AFLMB concept, the field has already advanced toward a multidimensional and system-level understanding of battery behavior. Rather than focusing solely on individual components, current research increasingly considers the dynamic interactions

https://doi.org/10.1021/acsnano.6c06180
ACS Nano XXXX, XXX, XXX−XXX

among materials, interfaces, and cell architectures.[406] It is also a positive aspect that researchers have started considering overall stability of full-cells rather than focusing solely on maximizing energy density.[407] Continued efforts along this direction may ultimately enable the realization of AFLMBs with near-complete lithium utilization.

We conclude this review by introducing the perspectives of leading researchers who are actively advancing the AFLMB field. We hope that this work provides a meaningful roadmap toward the eventual commercialization of AFLMBs.

6.3. Authors' Personal Perspectives

Hyun-Wook Lee: Conventional descriptions of Li^+-ion reduction typically assume one-dimensional ion transport and localized charge-transfer reactions at the electrode surface. However, this simplified picture becomes insufficient when Li^+-ion concentrations in the electrolyte are high and strong electric fields are applied. Under such conditions, ion migration in the electrolyte can become highly nonuniform and even turbulent-like rather than smoothly directed. In these regimes, Li^+-ions do not simply migrate perpendicularly from the cathode to the anode and stop immediately after reduction. Instead, newly formed lithium adatoms arriving at the current collector remain dynamically active. They continue to vibrate, diffuse along the surface, and aggregate with neighboring adatoms until a critical nucleus size is reached. As a result, lithium transport and growth are intrinsically multidirectional, involving not only vertical ion flux but also lateral surface migration and interfacial reorganization. This implies that the electrolyte−current-collector interface hosts far richer dynamics than those captured by classical electrochemical reduction models. I believe that the frequently observed lithium dodecahedral morphology provides an important structural clue to these underlying growth mechanisms, reflecting the balance between ion transport, surface diffusion, and crystallographic energetics. While many innovative strategies are currently being developed to overcome the formidable challenges associated with fully reversible lithium redox reactions, I am optimistic that the key technical barriers will be resolved in the near future. That said, achieving simultaneous safety, long cycle life, and reliable performance over wide temperature ranges remains a more distant but essential goal for practical anode-free lithium metal batteries.

Hongkyung Lee: From the perspectives of materials cost, manufacturing simplicity, and system-level energy density, there is arguably no other approach that can more straightforwardly outperform the anode-free concept. However, achieving near-100% lithium utilization remains challenging even at the laboratory scale and becomes more unrealistic under extended cycling and large-area cell conditions. In this sense, the central challenge of AFLMBs shifts from 'how efficiently lithium can be plated' to "how lithium is inevitably lost," and "how such losses can be managed or partially recovered over time". Electrolytes play a particularly critical role in AFLMBs. SEI formation is inseparable from lithium loss. Yet, paradoxically, a "good SEI" remains essential for stable cycling of AFLMBs. Then, what defines a "good SEI"? Even with a general understanding of its desirable properties, the SEI inevitably evolves in composition, thickness, and uniformity over cycling. Research efforts should therefore focus on developing control strategies that sustain the desired SEI and minimize continuous side reactions during repeated cycling. In this context, SEIs that exhibit shape-recovery capability, resist swelling by liquid solvents, and effectively block solvent penetration are likely to be essential for long-term stability. At the same time, uniformity of lithium plating in the early stages can be decisive for maintaining cell homogeneity over extended cycling. Lithium pulverization, which inevitably produces electrically isolated dead lithium and residual inactive SEI, does not always grow indefinitely. If this layer can evolve into a more conformal or structurally stabilized morphology, it may even contribute to improved long-term stability. Thus, the problem is not pulverization itself, but the absence of strategies to control it. From this perspective, early cycle lithium loss should be viewed as an unavoidable cost, while introducing lithium reservoirs, such as sacrificial cathode materials, is an essential design option in anode-free systems. To manage and recover lithium inventory loss, rejuvenation strategies based on redox mediation offer a promising route by reactivating inactive lithium. However, redox shuttling can negatively impact cell performance and must be carefully controlled. Beyond materials design, responsive strategies that use heat, stress, or external fields could enable partial lithium recovery when combined with tailored cycling protocols. These approaches highlight the need for holistic, cell-level control rather than isolated materials optimization.

Il-Doo Kim: In AFLMBs, controlling interfacial overpotential during lithium plating and stripping, particularly when using artificial SEIs (a-SEI) in pouch-type, large-area, multistacked cells, remains an underexplored yet decisive bottleneck under limited lithium inventory. While prior efforts have emphasized electrolyte and current collector design, I believe that engineering ultrathin a-SEIs, especially organic−inorganic hybrids, offers a more direct route to regulate interfacial energetics from the earliest stages of lithium nucleation. Rather than acting as passive barriers, such a-SEIs should minimize local overpotential and ensure spatial uniformity of overpotential while maintaining uniform Li^+ flux, thereby suppressing spatial heterogeneity and the onset of dead lithium formation. This shifts the design target from static protection toward dynamic interfacial energy regulation. Critically, the practical impact of a-SEIs will depend on their realization through scalable, large-area processes. Achieving conformal, ultrathin coatings without introducing additional resistance or process complexity remains a key challenge, particularly when transitioning from coin-cell demonstrations to pouch-cell formats. Moving forward, bridging interfacial energetics with manufacturing-compatible deposition strategies will be essential. In this context, ultrathin hybrid a-SEIs, designed to operate under low-overpotential conditions and implemented via scalable processes, could provide a realistic pathway toward durable, high-energy-density AFLMBs.

Ji-Guang Zhang: Although significant progress on AFLMBs has been achieved in the past decade, their practical applications are still limited by many barriers as discussed in this work. The main limitations in this field include: 1. Most approaches used in this field often focus on improving one aspect of the performance of AFLMBs in a given condition. However, optimization of one parameter may be detrimental to other parameters. Therefore, more comprehensive characterization methods need to be used to evaluate the merit of different approaches. 2. Some of approaches are very sensitive to operation conditions. For example, improvement in CE is strongly limited by operating parameters, especially Li deposition (battery charge) rate. High rate can change the

https://doi.org/10.1021/acsnano.6c06180
ACS Nano XXXX, XXX, XXX−XXX

distribution of Li ion concentration profiles, disabling the fundamental mechanism which enabled high CE of Li cycling in high concentration or localized high concentration electrolyte (LHCE). 3. Another limitation in this field is that some of approaches, such as coating of protective layers can only be effective for limited cycles. Although these protection layers can smooth Cu substrate and enhance the uniformity of Li deposition/stripping, Li will predominately deposit on the top of these protection layers after a few cycles, so the effect of these protection layers will be dimmish with increasing cycle number. The same is true for some of additives, their effect will be dimmish with increasing cycle numbers. Therefore, a long-lasting solution needs to be identified in Li protection. A few examples of the fundamental approaches to addressing the challenges in AFLMBs include: 1. Increase the initial CE in AFLMBs by prepassivating Cu substrate before the cell assembly to minimize the consumption of Li during the formation process of AFLMBs. 2. Develop a protection layer which favors the Li deposition below the protection layer instead of the top of protection layer. In this case, most of SEI layers will form on the top of the protection layer. These SEI layers will endure much less volume changes, therefore they will be much more stable. Very minimal SEI can form on Li particles deposited below the protection layer. Therefore, the loss of Li can be minimized. Although there are many approaches that can be explored in the development of AFLMBs, priority should be put on the approaches that will have a high impact on the performance of AFLMBs. These approaches include: 1. Have high impact (instead of incremental improvement) on several key performance matrixes (such as CE, cycle life, and safety) simultaneously. 2. Have a long last effect of the cell performance. 3. Less sensitive to the operating parameters (such as charge/discharge rate etc.) 4. AFLMBs can be tailored to operate in two different applications. One is for high charge rate but low discharge rate applications (such as electrical vehicle applications). Another is for high discharge rate but low charge rate applications (such as drone applications). These two applications need to be optimized separately to have an optimized balance on their specific applications. Finally, new approaches and knowledge obtained in the development of AFLMBs can also be used in the development of LMBs to accelerate their broader market penetration.

Guihua Yu: Research thrusts in AFLMBs that move beyond material development toward a deeper scientific understanding of interfacial evolution are highly desirable. Despite significant advances achieved in improving Coulombic efficiency, the formation and dynamic evolution of SEI remain insufficiently understood. Advanced operando and time-resolved techniques are essential to elucidate how SEI chemistry and structural heterogeneity govern lithium nucleation and interfacial stability. From a practical point of view, the future use of AFLMBs requires scalable, reliable, and affordable technologies holistically solving the challenges facing high-areal-capacity cathodes and anodes. Direct and facile strategies that are compatible with existing battery manufacturing infrastructures are particularly appealing. The emerging integration of machine learning techniques into battery research, such as material discovery and protocol optimization, is also expected to open new opportunities along this direction and accelerate progress towards practical implementation.

Yan Yao: I only want to add one observation: in anode-free cells, CE does not always correlate directly to cycle life as we typically expect. I have seen many cells hitting 99% CE that still manage to push past 300 cycles. The fundamental reason for this is not fully understood yet, but it is an interesting deviation from standard models.

Kang Xu: As the Holy Grail of all batteries, AFLMB represents both ultimate level of energy densities that a battery could ever achieved and unparallel challenges stemming from the extreme reactivity of lithium metal with essentially every known electrolyte system. To ensure 100% reversibility of lithium metal chemistry, one must consider every factor that could affect the electrodeposition of lithium metal in the dynamic cell environment. The significant knowledge accumulated in the past decade has enabled us to evolve from the individual efforts on designing a better electrolyte alone or engineering lithium electrode interface alone to more integrated efforts that view the cycling lithium metal cells as a dynamic and closely interwoven ecosystem where every intimately interact with each other. This new optimization strategy would involve numerous parameters that dictate the eventual cell performances from a very high dimension space. Aside from traditional approaches, artificial intelligence (AI) and machine learning (ML) techniques should be employed, as these tools are best at recognizing patterns in relationships that often escape the human sensing. Before we can establish first-principles understanding of the complicated chemical and physical processes and mechanisms, data-driven AI/ML models serve as the most appropriate options, whose success requires the availability of the large-scale and high-quality datasets. Such a synchronized effort must be made by battery scientists around the globe.

Gui-Liang Xu: AFLMBs represent the ultimate pathway to achieve both high energy density and improved safety while calling for a nearly 100% lithium utilization during electrochemical process. From my perspective, stack pressure not only plays a critical role in the reversibility of lithium plating/stripping via mechanical constraint, but also greatly determines the microstructures of deposited lithium and the consequent electrochemical/chemical reactivity. Despite significant progress via interface engineering and electrolyte optimization, when translated to low stack pressure operation, the existing AFLMBs show disappointingly lower specific energy and shorter cycle life. Moving forward, it is essential for the battery community to benchmark the cell testing conditions for the ongoing AFLMBs development, which represents a critical step to unify the learning across different groups. Developing operando/in situ characterization techniques to track lithium plating/stripping under practically relevant conditions particularly zero/low stack pressure is critical to understand the distinct lithium loss mechanism. Specifically, leveraging multiscale in situ imaging techniques spanning from optical to electron, X-ray, neutron and magnetism can allow direct visualization of lithium growth/dissolution process and the associated chemomechanical behaviors.

Jamie H. Warner: A central challenge in realizing practical anode-free lithium metal batteries is the fundamental requirement of near-perfect lithium utilization. In contrast to conventional lithium metal cells that contain an excess lithium reservoir, anode-free systems operate with a strictly limited lithium inventory supplied entirely by the cathode. Under these conditions, even minute irreversible losses per cycle accumulate rapidly and ultimately limit the achievable lifetime of the cell. While substantial progress has been made in controlling lithium plating morphology and suppressing

https://doi.org/10.1021/acsnano.6c06180
ACS Nano XXXX, XXX, XXX−XXX

dendrite formation, it is increasingly clear that smooth deposition alone is insufficient to guarantee long-term reversibility. Instead, the decisive issue becomes whether lithium can remain electronically connected and fully recoverable throughout repeated plating−stripping cycles. From this perspective, the ultimate objective of anode-free battery design should be the realization of a closed-loop lithium cycle, in which lithium continuously shuttles between electrodes without permanent loss to parasitic reactions or electronic isolation. Achieving such a closed loop requires addressing several interconnected processes simultaneously. First, electrolyte chemistry and interphase design must minimize parasitic lithium consumption by forming mechanically robust and ionically conductive solid electrolyte interphases that suppress continuous electrolyte decomposition. Second, lithium deposition must occur uniformly across the current collector in order to avoid the formation of high-aspect-ratio structures that are prone to electronic disconnection during stripping. Third, the stripping process itself must be engineered to preserve electronic connectivity until lithium is completely removed, which requires strong adhesion between lithium deposits and the substrate together with interphases capable of accommodating repeated mechanical deformation. Finally, because some degree of inactive lithium formation may be unavoidable, strategies capable of reactivating dead lithium, such as redox mediators or dynamic interphases, may ultimately become essential components of practical anode-free systems. To guide progress toward this goal, it may also be necessary for the field to reconsider how lithium utilization is quantified. Coulombic efficiency, although widely used, reflects only cycle-to-cycle reversibility and does not directly measure the cumulative retention of the original lithium inventory. A complementary metric, here referred to as the Lithium Inventory Retention Index (LIRI), could instead track the fraction of the initial lithium inventory that remains electrochemically accessible after extended cycling. Such a metric would directly capture lithium losses arising from dead lithium formation, interfacial side reactions, and structural degradation, providing a more meaningful benchmark for evaluating strategies aimed at approaching complete lithium utilization. Equally important will be the development of diagnostic techniques capable of resolving how lithium becomes inactive at the nanoscale. Many of the critical processes governing lithium reversibility, including SEI fracture, deposit detachment, and the formation of electronically isolated lithium, occur at length scales that remain difficult to observe using conventional characterization approaches. Advanced cryogenic electron microscopy, combined with focused ion beam sample preparation and correlative multimodal imaging, is beginning to provide unprecedented insight into these processes by preserving the native structure of lithium and its interphases. Such approaches will be essential for directly visualizing the structural pathways through which active lithium becomes electronically disconnected and for validating emerging strategies designed to maintain a closed lithium cycle. Looking forward, the realization of near-100% lithium utilization will likely require coordinated advances across materials, interfaces, and cell architectures. Rather than treating plating, stripping, and recovery as independent phenomena, future research must address them as interconnected processes within a dynamic electro-chemo-mechanical system. If these challenges can be addressed simultaneously, anode-free lithium metal batteries may evolve from systems limited by irreversible lithium loss into self-recovering electrochemical architectures capable of sustaining a nearly closed lithium inventory over long cycling lifetimes.

Nanyang Wang: Recent efforts including electrolyte engineering, artificial interphase construction, advanced current collector design, and cathode optimization have improved lithium plating reversibility and suppressed dendrite growth to some extent. However, from a mechanistic standpoint, completely eliminating dead lithium formation may remain intrinsically challenging. Rather than treating inactive lithium solely as an irreversible degradation product, it may be more insightful to consider it as a dynamic component within an evolving interfacial system. From this perspective, future research could shift partially from suppressing inactive lithium toward enabling its reactivation. Reactivating dead lithium or dormant dendritic structures may restore isolated lithium into the electrochemical cycle, sustain lithium inventory, and mitigate CE decay, highlighting the importance of adaptive interfacial chemistries capable of dynamically reconstructing ion and electron transport pathways. Among various strategies, electrolyte engineering represents a particularly powerful platform because it can simultaneously regulate cation solvation structures, influence SEI formation, and modulate nanoscale interfacial kinetics. Rationally designed electrolytes may promote dynamic SEI evolution, enhance ion accessibility to electronically isolated regions, and enable reversible stripping from previously inactive lithium domains. Achieving this goal requires deeper mechanistic understanding of dead lithium formation and reactivation. Advanced operando characterization, combined with theoretical modeling and data-driven approaches, is expected to provide key insights into interfacial evolution processes, while AI-assisted molecular discovery may accelerate the development of functional electrolyte components. Integrating scalability, synthetic simplicity, and cost considerations at the early design stage will be equally important for bridging fundamental research and practical implementation in AFLMBs.

Matthew T. McDowell: More research focus is needed to understand the final stages of the stripping process of lithium in anode-free batteries. How do the last remaining portions of lithium at the interface evolve, and how does the SEI that has grown until that point influence the availability of the remaining lithium? It is likely that nanoscale chemo-mechanical interactions between the remaining lithium and local SEI will influence the stripping process, and these interactions need to be controlled to enable the targeted 100% Coulombic efficiency of anode-free cells. Additionally, the general paradigm in anode-free batteries is to use a stiff current collector (such as Cu or Ni) to force lithium to grow as a uniform film. My group has recently shown that low-yield-strength inclusions and current collectors can enhance stripping of lithium in solid-state batteries by deforming to accommodate lithium morphology changes.[408,409] It would thus be interesting to understand how the mechanical properties of both the current collector and the SEI layers influence the final stages of lithium stripping when using liquid electrolytes.

Jeffrey Lopez: The limited lithium inventory and increased demands placed on SEI performance in AFLMBs necessitate precise control over the SEI composition and morphology. This required level of control can only be achieved through a robust understanding of mechanisms and kinetics of reactions

https://doi.org/10.1021/acsnano.6c06180
ACS Nano XXXX, XXX, XXX−XXX

responsible for interphase formation. SEI formation reactions inherently consume lithium, anions, and solvent from the electrolyte, and in many high-performance electrolytes the SEI is continually repaired and reformed. Furthermore, while SEI repair is critical to cell longevity, efforts must be directed toward developing more static SEIs that can be synthesized during formation cycling and then remain chemically and structurally stable to the large volume changes during plating and stripping. Realizing this improved, static SEI is a significant challenge that demands a deep understanding of the requirements for SEI composition and morphology at nanometer and angstrom length scales. To achieve this level of insight, efforts should continue toward the development of advanced characterization approaches capable of resolving interphase structure and chemistry with increasing spatial and chemical resolution and toward careful fundamental studies of SEI formation processes and their dynamic behavior during cell operation. These efforts will establish the foundation necessary to rationally design electrolytes and formation protocols that will contribute to enabling AFLMBs.

Yijin Liu: The development of lithium metal batteries has been driven largely by laboratory-scale advances enabled by in situ and operando characterization techniques. Methods such as synchrotron X-ray imaging, spectroscopy, and electron microscopy have provided unprecedented insight into lithium plating/stripping behavior, dendrite formation, solid−electrolyte interphase (SEI) evolution, and interfacial instability. These tools allow researchers to probe complex electrochemical and chemo-mechanical processes under well-controlled conditions, revealing mechanistic pathways that guide materials design and electrolyte engineering. However, the experimental environments used in laboratory studies are often limited to small-format cells, slow data acquisition, and carefully controlled cycling protocols that are often not representative of those used in field deployments.[410] This clearly differ substantially from the dynamic conditions encountered in manufacturing or large-format battery operation. As a result, phenomena observed in the lab do not always translate directly to industrially relevant conditions such as high-rate formation, large electrode areas, or tightly constrained manufacturing tolerances. Bridging this gap requires a shift from in situ experimentation toward in-line metrology that can operate within battery manufacturing environments.[411] Unlike laboratory diagnostics that prioritize resolution and mechanistic insight, in-line metrology must deliver rapid, nondestructive, and statistically robust measurements compatible with gigafactory throughput. For lithium metal batteries, this includes detecting early stage defects such as uneven lithium deposition, void formation, and interfacial degradation during electrode fabrication, electrolyte filling, or formation cycling. The central challenge lies in translating the mechanistic understanding gained from high-resolution laboratory tools into simplified sensing modalities and data-driven analytics that can monitor quality and predict failure at scale. Achieving this transition will require tight integration of operando diagnostics, machine learning−based image and signal interpretation, and manufacturing-aware sensor design, ultimately enabling feedback-controlled production lines capable of ensuring reliability for next-generation lithium metal batteries.

Ping Liu: In the near term, AFLMB is a terrific research platform where the lithium inventory is clearly defined by the cathode material. In the long term, AFLMB can become a low-cost technology. Given the limited lithium inventory, minimizing its loss will always be the #1 priority. These batteries will also be expected to be stable after extended period of cycling and storage (including at different states of charge when there is a lithium metal anode). Consequently, the reactivity towards the electrolyte eventually determines the life of the battery. What would be the electrolyte chemistry that offers minimal reactivity? Currently, ether solvents with C−O−C bonds are the most promising although the neighboring C−H bond can become labile. Is it possible to have another heteroatom to replace O while maintaining the ability of the solvent to dissolve salt? Reactivity of the salt also needs to be minimized. While LiFSI has been the choice due to its ability to produce LiF-rich SEI layers, there is evidence for its continuous consumption. How to manage and reduce this loss is crucial for long-term stability.

Yuzhang Li: The performance and longevity of next-generation batteries are increasingly limited by processes occurring at highly reactive electrified interfaces. In systems employing alkali metal anodes, electrolyte molecules experience strong thermodynamic driving forces for reduction at the electrode surface, leading to the spontaneous formation of complex interphases. While extensive effort has been devoted to stabilizing these interfaces during electrochemical cycling, comparatively less attention has been paid to their evolution under open-circuit or resting conditions. In practical batteries, however, devices spend a significant fraction of their lifetime at rest, where parasitic interfacial reactions can continue to consume electrolyte and active lithium. This behavior suggests that calendar aging, rather than cycling alone, may represent a dominant but underappreciated degradation pathway in highly reactive battery chemistries. Understanding degradation under these conditions requires reframing the electrode−electrolyte boundary as a chemically active interface rather than a static passivating layer. The solid electrolyte interphase (SEI), traditionally described as a protective film that suppresses further electrolyte decomposition, is more accurately viewed as a dynamic and heterogeneous medium that mediates ionic transport, chemical reactions, and mechanical evolution at the electrode surface. From this perspective, the SEI functions as a nanoscale interfacial electrolyte whose properties emerge from the coupled processes of electrolyte reduction, species transport, and interphase restructuring. Designing stable metal anodes therefore requires not only controlling electrolyte decomposition pathways but also understanding how these reactions generate functional interfacial architectures capable of sustaining long-term operation and storage. A major barrier to progress in this area has been the difficulty of directly observing electrified interfaces in their native state. Many interphase phases are chemically fragile and structurally heterogeneous, making them challenging to characterize using conventional analytical approaches. Recent advances in cryogenic electron microscopy have begun to address this limitation by enabling the preservation and visualization of sensitive interfacial structures formed during battery operation. More recently, emerging approaches that combine electrochemical control with cryogenic preservation offer the possibility of capturing electrified interfaces at defined states of reaction, providing unprecedented insight into the relationship between electrolyte chemistry, interphase formation, and degradation processes. Continued development of such techniques may play a critical role in establishing mechanistic

https://doi.org/10.1021/acsnano.6c06180
ACS Nano XXXX, XXX, XXX−XXX

links between electrolyte reactions, interfacial structure, and long-term battery stability.

Ju Li: The use of artificial intelligence and self-driving laboratories in developing new liquid electrolyte formulations will be a key trend. Historically, the up to a few weight-percentage additives approach has been prevalent in the industry. But new electrolyte solvents, salts and their combinations at tens of percent level open up big space for exploration, and new knowledge are constantly being generated in laboratories worldwide. Large language model can help aggregate data and knowledge and recommend new experiments to perform, and assist the development of AFLMBs.

Hochun Lee: In my view, cathode prelithiation agents (sacrificial cathodes) are the most practical and promising route to extend the lifetime of anode-free batteries. An ideal sacrificial cathode should serve as a high-density, precisely controlled lithium reservoir, activated under realistic formation conditions without disrupting cathode chemistry or electrolyte stability. It should deliver high Li capacity with low polarization and an appropriate release potential to suppress parasitic reactions. Importantly, the delithiated residue must remain inert, insoluble, and nonblocking to limit impedance growth, gas evolution, and contamination. Finally, manufacturability is critical: the material should be air-stable, slurry-processable, scalable, and cost-effective while maintaining safety and energy density.

Seongjae Ko: Achieving truly reversible lithium plating/stripping with near-unity Coulombic efficiency remains one of the central challenges. A key message emerging from this review is that many strategies proposed in the literature, when evaluated independently at the level of individual materials, often obscure the intrinsic trade-offs involved. Further progress will require a holistic full-cell design philosophy in which complementary materials and cell components are engineered in concert, integrating physicochemical, metallurgical, and materials-science perspectives. The absence of unified evaluation protocols, advanced analytical methodologies, and predictive modeling frameworks continues to hinder systematic progress. Critical questions persist regarding plating–stripping asymmetry, the accurate determination of the Li^+ transference number in electrolytes, and the evolution and stability of interphases under varying electrolyte chemistries and operating conditions. Establishing quantitative descriptors or governing relationships that capture electrolyte and interphase dynamics would represent an essential step toward achieving complete lithium utilization. Addressing these challenges must proceed alongside more rigorous evaluation of safety considerations. Comprehensive investigation of the exothermic reactions and potential toxic gas evolution associated with lithium metal under conditions approaching its melting point will be indispensable to the acceleration of practical deployment. Consolidating diverse research directions and identifying key scientific gaps will catalyze collaborative efforts within the research community and guide future investigations toward uncovering the fundamental principles necessary to enable next-generation batteries with high energy density, reliability, and safety.

Sang Cheol Kim: The importance of the liquid electrolyte in AFLMBs is now well-appreciated by the community. In particular, as outlined in this article, tuning the solvation structure has been central to the design of emerging electrolytes and has led to tremendous improvements in cycling stability. However, our understanding of the solvation structure still lags behind, primarily due to limitations in our ability to experimentally characterize it. Most studies rely on techniques such as Raman, Fourier transform infrared (FT-IR) and NMR spectroscopy. While these techniques reveal features such as Li^+-binding moieties and the electron density around Li^+, they capture only part of the overall solvation structure, and we are far from a holistic understanding of solvation. Development of novel techniques as well as correlative studies to elucidate the solvation structure will be crucial to deepening our understanding and designing high-performance electrolytes. Novel electrolyte design strategies will be a critical path forward for practical AFLMBs. Emerging electrolytes such as HCE, LHCEs and fluorinated electrolytes have led to breakthroughs in improving interfacial stability and cycle life, enabling more than 100 cycles in AFLMBs. However, a common feature shared by these electrolytes is compromised ion transport. While high-entropy electrolytes offer some improvement, ion transport remains insufficient and this bottleneck limits fast-charging, deployment of thick electrodes and even cycling stability. Electrolytes that can satisfy both high interfacial stability as well as facile ion transport will be crucial for achieving practical AFLMBs.

Patrick Joohyun Kim: From my perspective, the separator and interfacial environment represent one of the most critical yet underappreciated factors in anode-free lithium metal batteries. While significant efforts have focused on current collector modification and electrolyte optimization, the separator fundamentally governs the spatial distribution of Li^+-ion flux across the electrode area. In systems with a strictly limited lithium inventory, even minor nonuniformities in ion transport can trigger localized plating, incomplete stripping, and the accumulation of dead lithium. Lithium deposition and stripping are not determined by a single component but by the integrated structural environment defined by separator properties, current collector architecture, electrode design, and cycling conditions. When this environment fails to ensure uniform reactions, irreversible lithium loss becomes unavoidable. Accordingly, lithium loss should be considered a system-level outcome, and mitigation strategies must be evaluated based on long-term retention of active lithium rather than short-term performance gains. Advanced multifunctional separators engineered to regulate Li^+-ion flux, stabilize interfacial contact, and accommodate volume changes offer a practical pathway toward more reliable AFLMBs. A more systematic coupling of separator design with electrolyte chemistry and recovery-oriented strategies will be essential for achieving durable and practically viable AFLMB systems.

Mun Sek Kim: To realize practical LMBs, both in anode-free and lean N/P ratio configurations, we must treat the lithium SEI as a dynamic, evolving component rather than a static passivation layer. SEI formation on lithium is thermodynamically unavoidable; what matters over extended cycling is the residual SEI that remains and accumulates after each cycle. This legacy SEI increasingly acts as a quasi-host, a scaffold that guides subsequent lithium deposition/stripping, meaning that lithium–metal anodes are not truly "host-free" in practice. As the residual SEI builds up, it governs anode thickness growth, localized plating/stripping pathways, interfacial impedance, and the continuous consumption of lithium and electrolyte, all of which ultimately dictate Coulombic efficiency and cycle life. This perspective shifts the design target beyond achieving uniform deposition/stripping during

https://doi.org/10.1021/acsnano.6c06180
ACS Nano XXXX, XXX, XXX–XXX

early cycles. The key scientific challenge lies in controlling exactly where lithium plates and how completely it strips in the presence of an SEI that has been continuously layered and remodeled since the very first charge. In other words, the goal is reliable lithium deposition/stripping beneath a persistent, functional residual SEI, instead of repeatedly rupturing and rebuilding the lithium interphase. In my view, progress will accelerate when we define a new SEI descriptor that captures both the kinetic and thermodynamic aspects established by the physicochemical properties of electrolytes, essentially quantifying SEI reuse versus SEI turnover. A practical way to conceptualize this is SEI recyclability: assessing how well the residual SEI spatiotemporally remains ionically conductive, electronically insulating, and mechanically resilient while supporting repeated lithium transport. By engineering electrolytes and interphases to maximize a reusable residual SEI and minimize continual reconstruction, we can reduce active lithium loss while sustaining uniform, fully reversible plating/stripping dynamics. Controlling this delicate balance is a necessary prerequisite for enabling highly durable AFLMBs.

Min-Ho Kim: For lithium metal batteries (LMBs) to transition from laboratory-scale demonstrations to practical industrial deployment, a new physical paradigm is required to transcend fragmented material innovations and isolated conclusions. All natural phenomena are governed by universal physical laws, and the electrochemical processes occurring inside batteries are no exception. Any newly identified variables must therefore be consistently interpreted within a coherent physical framework grounded in these principles. Conventional electrochemistry has evolved on the basis of homogeneous electron transfer models and one-dimensional ion transport assumptions. However, as battery systems have advanced toward thick porous electrodes and lithium metal plating/stripping mechanisms, these simplified descriptions are no longer sufficient to capture the true system behavior. Achieving meaningful progress in next-generation battery physics therefore requires extending beyond these classical models to account for the intrinsic complexity of lithium metal systems. Lithium metal electrodes represent a high-dimensional complex system in which multiple coupled phenomena coexist, including nonuniform ion concentration distributions in the electrolyte, substrate-dependent heterogeneous charge transfer, continuous evolution of electrode geometry during deposition, and the dynamic formation and reconstruction of the solid electrolyte interphase (SEI). Such complexity inherently limits approaches based on isolated material properties or single performance metrics. Accordingly, the field must move beyond the prevailing paradigm of function-driven material optimization and establish a unified physical framework capable of integrating these coupled phenomena into a coherent understanding of lithium metal behavior. This shift represents a transition from incremental performance improvements to a Big Science approach aimed at uncovering the fundamental causal relationships that govern system behavior. For instance, rather than treating SEI mechanical strength and ionic conductivity separately, a unified descriptor should capture how charge transfer, ion transport, and interfacial mechanics together determine the reversibility and morphological stability of lithium deposition. While establishing such a comprehensive framework remains challenging, it represents a necessary direction for the field. Ultimately, the realization of lithium metal systems will depend not on improving a single performance metric, but on moving toward a quantitative, universal model capable of explaining and predicting these coupled phenomena. This transition—from empirical optimization to predictive, design-driven battery science—will require sustained effort and a fundamental shift in approach.

Hee-Tak Kim: Most studies on AFLMBs have focused on controlling lithium metal deposition, with significant progress achieved in regulating nucleation behavior, morphology, and areal uniformity. In contrast, the factors governing the uniformity of lithium stripping and strategies to control it remain relatively underexplored, despite their critical importance to long-term cycling stability. Unlike dense lithium metal foils, the lithium formed during the first charge of an AFLMB typically adopts a porous structure that allows electrolyte infiltration. Although advances in deposition control can enhance the packing density of lithium deposits, achieving a completely void-free lithium layer remains highly challenging. These intrinsic structural defects facilitate lithium-ion transport deep into the lithium metal electrode, causing stripping to deviate from the ideal top-down stripping (i.e., stripping initiating uniformly from the electrode surface). Instead, lithium dissolution can preferentially occur within the electrode interior or near the current collector, leading to the formation of increasingly porous lithium deposits with enlarged exposed surface area. Addressing this issue therefore requires consideration not only of the lithium deposition process itself, but also of the temporal stability and spatial uniformity of the SEI formed during deposition. When the SEI provides insufficient passivation and continues to evolve with time, pronounced heterogeneity in SEI resistance can emerge along the thickness of the lithium electrode. Under such conditions—particularly in systems exhibiting bottom-up lithium growth—the relatively lower SEI resistance near the electrode interior or in close proximity to the current collector can preferentially induce localized lithium stripping near the current collector surface, rather than at the top lithium surface. This nonideal stripping pathway enlarges the interfacial contact between the electrolyte and the current collector, thereby initiating and progressively accelerating galvanic corrosion. In this context, a deeper mechanistic understanding of the factors governing spatially nonuniform stripping, together with systematic strategies to regulate SEI evolution and resistance gradients, will be critical for advancing the reversibility, durability, and practical viability of AFLMBs.

Ji-Won Jung: In anode-free lithium metal batteries, I regard the current collector not as passive metallic support, but as a structural and electrochemical backbone that must accommodate inherently conflicting requirements. It needs to remain lightweight to avoid compromising energy density, while at the same time maintaining sufficient mechanical stability to withstand repeated lithium plating and stripping without progressive loss of interfacial contact. This trade-off becomes particularly pronounced in three-dimensional current collectors, where porosity and scaffold thickness cannot be selected independently. Although higher pore volumes are effective in accommodating lithium and lowering local current density, these advantages can be quickly offset if the framework lacks mechanical resilience. At present, clear and practical guidelines that connect porosity, mechanical robustness, and target energy density are still largely absent. I also see the absence of standardized evaluation protocols as a growing bottleneck for meaningful progress in this field. Differences in cycling procedures, electrolyte formulations, and cell configurations often obscure direct comparison between studies. Beyond

https://doi.org/10.1021/acsnano.6c06180
ACS Nano XXXX, XXX, XXX−XXX

these factors, mechanical pressure—whether applied in coin cells, pouch cells, or other formats—plays a decisive yet frequently underreported role in governing lithium deposition behavior. At a minimum, pressure conditions should be explicitly defined, and ideally standardized, to ensure consistency across experiments. Such shared protocols, combined with systematically curated datasets, would significantly improve reproducibility and provide a reliable foundation for data-driven and AI-assisted design strategies. Finally, the electrical properties of current collectors warrant renewed consideration. Lithium formed during the initial stages of nucleation is not static, but highly reactive and dynamically redistributed along the surface and through the electronic network of the collector. While surface chemistry has received considerable attention, variations in bulk electrical conductivity and ohmic resistance can be strongly coupled with ionic transport to amplify local instabilities during cycling. A more rigorous experimental and theoretical reassessment of how surface and bulk electrical properties jointly influence lithium behavior will be critical for the rational design of durable anode-free battery systems.

Kelsey B. Hatzell: Advancing toward anode-free battery geometries presents several important scientific and engineering challenges that must be addressed to enable reliable and safe implementation. Key frontier questions remain regarding optimal operating conditions, effective conditioning protocols, cell geometry considerations, and safety management. In particular, a deeper understanding of how temperature, applied pressure, and cell architecture such as pouch cell configurations influence electrochemical behavior is essential. These parameters strongly affect interfacial stability, lithium plating and stripping efficiency, and the onset of parasitic side reactions. Future research should focus on clarifying how these factors interact to drive degradation mechanisms including gas evolution and interfacial instability, which directly impact both performance and safety. Systematic studies that couple controlled operating conditions with advanced diagnostic tools will be critical for identifying strategies that mitigate side reactions and improve cycling stability. Addressing these challenges will guide the development of optimized conditioning protocols and cell architectures, ultimately enabling safer and more robust anode-free battery systems suitable for practical deployment.

Betar M. Gallant: SEI composition is crucially important in AFLMBs, but equally important —yet often overlooked—are the formation dynamics upon the initial several plating steps, i.e., the mechanical establishment of the initial SEI. Ideally, the SEI forms only once in an atom-efficient manner, then acts as a reusable scaffold in subsequent cycles, and some limited evidence for the existence of such scaffolds has been presented previously.[412,413] Yet, it is unclear what factors support the formation of such reusable SEI; how variables such as plating capacity, rate, cell pressure, and temperature can support or hinder such structures; how they evolve and degrade during cycling; and the properties of a deeply cycled anode in which there is an equivalent or higher amount of inactive SEI and dead Li material compared to cyclable Li. These knowledge gaps illustrate the lack of consensus on what the formation step on Cu is actually aiming to achieve from a compositional, morphological, and conceptual point of view, and the ample opportunities to improve AFLMB by better understanding the targeted end state of the ideally formed Cu surface.

Nam-Soon Choi: AFLMBs offer an unparalleled pathway toward ultrahigh energy density; however, their practical deployment remains hindered by unstable SEIs and irreversible lithium plating/stripping on lithiophobic Cu current collectors. Spatially nonuniform current distribution across the SEI further aggravates dendritic lithium growth by preferentially directing Li^+ flux through regions of lower ionic resistance, thereby amplifying localized lithium plating and accelerating interphase degradation. Although electrolyte additives can modulate SEI chemistry, their development remains largely empirical, with limited mechanistic design principles—particularly regarding concentration-dependent reactivity and the sequential formation of multilayer interphases. Consequently, the reproducible construction of robust, hierarchically structured SEIs remains challenging. Importantly, while lithiophilic SEI components facilitate lithium plating, they do not inherently ensure efficient stripping of the deposited lithium. The SEI must therefore accommodate the dynamically evolving electrochemical environment and enable adaptive charge redistribution during cycling. In this regard, an orbital-engineered interfacial strategy that imparts switchable polarity to the SEI through conjugated cyclic molecules, enabling controlled electron density redistribution and facilitating rapid Li^+ transport during lithium plating and stripping. Coupled with hierarchical interfacial structuring—including a Li^+ distributor, lithiophilic nucleation layer, and mechanically resilient scaffold—this design strategy promotes dense, dendrite-free lithium plating and mitigates continuous SEI reconstruction. This molecular-to-macroscopic interfacial engineering paradigm establishes programmable SEI chemistry and provides a general framework for stabilizing lithium metal under fast-cycling conditions.

Jang Wook Choi: Many strategies that are effective in lab-scale small-area cells often fail to translate to large-area ones used in EVs and energy-storage applications, mainly because they are sensitive to spatial uniformities and lose their effectiveness as the cell area increases.

Zheng Chen: As AFLMBs advance toward future practical deployment, the safety of end-of-life recycling will become a defining challenge for their sustainable adoption. After extended cycling, residual lithium metal often persists in chemically reactive and morphologically unstable forms, including electrically isolated and highly porous deposits. These features introduce significant fire and explosion risks during disassembly and render conventional LIB recycling workflows inadequate. Safe recycling of LMBs will therefore require dedicated preprocessing steps that fully deactivate residual lithium prior to mechanical or chemical treatment. Possible future recycling frameworks are expected to rely on controlled discharge and lithium stabilization under inert or regulated environments, enabling subsequent material recovery without thermal runaway or hazardous reactions. Following stabilization, low-temperature, chemistry-driven recycling pathways (e.g., hydrometallurgical approaches), are likely to play a central role in recycling Li-based products (e.g., Li_2CO_3), as they can accommodate the complex electrode and electrolyte degradation products that accumulate during long-term cycling. Besides harvesting degraded or deactivated Li, integrating direct recycling methods to more efficiently regenerate spent cathode materials will provide shorter pathway for complete recycling of those battery active materials, offering the maximum value with minimal requirement for chemicals and energy input. Looking ahead, recycling

https://doi.org/10.1021/acsnano.6c06180
ACS Nano XXXX, XXX, XXX−XXX

safety should be addressed not only at the end of a battery's life but also at the design stage. The incorporation of lithium passivation strategies, nonflammable electrolytes, and architectures that enable safe discharge and disassembly could substantially reduce recycling risk and cost. Integrating recyclability and safety considerations into AFLMB design will be essential to ensuring that gains in energy density are not offset by environmental or safety liabilities, positioning recycling as a core enabler for the commercialization of AFLMB technologies.

Peng Bai: Modern rechargeable batteries are typically engineered to avoid operating at the limiting current, thereby preventing macroscopic transport limitations. Given the relatively thin separators (20−30 μm) and still moderately thin cathodes (80−120 μm) used in most practical cells, the current densities under normal operating conditions are below the system-specific limiting current, i.e., within the underlimiting regime. In principle, this means that complete ion depletion at the electrode surface should not occur; instead, the electrolyte concentration near the interface should reach a steady state with a finite, nonzero value. However, the electrolyte phase adjacent to the current collector is inherently heterogeneous due to the microporous structure of the inert separator, and conventional mathematical homogenization approaches oversimplify this complex microstructure. As a result, although the average current density may remain underlimiting, the true local current density can easily exceed the system-specific limiting current, producing localized overlimiting conditions. Such localized transport limitation can trigger severe ion depletion and the formation of tip-growing dendrites, which may readily propagate through the pores of the separator, whereas the majority of reaction-limited, root-growing whiskers remain mechanically constrained by the separator. Despite the substantial experimental and theoretical challenges associated with probing the real interface between the inert porous separator and the copper current collector, future research should prioritize this buried interface and systematically investigate the nucleation dynamics occurring under confinement within the electrolyte-filled pores of the separator. In particular, understanding how local ion transport, electric field focusing, and interfacial reaction kinetics interact within these confined geometries will be essential for clarifying and resolving the onset of localized dendritic growth in practical battery architectures.

AUTHOR INFORMATION

Corresponding Authors

Il-Doo Kim − *Department of Materials Science and Engineering, KAIST, Daejeon 34141, Republic of Korea; Department of Business Incubation Center, KAIST, Daejeon 34051, Republic of Korea;* orcid.org/0000-0002-9970-2218; Email: idkim@kaist.ac.kr

Hongkyung Lee − *Department of Materials Science and Engineering, Yonsei University, Seoul 03722, Republic of Korea; Department of Energy Science and Engineering, Daegu Gyeongbuk Institute of Science and Technology (DGIST), Daegu 42988, Republic of Korea; Department of Battery Engineering, Yonsei University, Seoul 03722, Republic of Korea;* orcid.org/0000-0002-7732-2089; Email: hongkyung.lee@yonsei.ac.kr

Hyun-Wook Lee − *School of Energy and Chemical Engineering, Ulsan National Institute of Science and Technology (UNIST), Ulsan 44919, Republic of Korea;* orcid.org/0000-0001-9074-1619; Email: hyunwooklee@unist.ac.kr

Authors

Seungwoo Choi − *School of Energy and Chemical Engineering, Ulsan National Institute of Science and Technology (UNIST), Ulsan 44919, Republic of Korea*

Juyoung Kim − *School of Energy and Chemical Engineering, Ulsan National Institute of Science and Technology (UNIST), Ulsan 44919, Republic of Korea*

Jiyeon Seo − *Department of Materials Science and Engineering, Yonsei University, Seoul 03722, Republic of Korea; Department of Energy Science and Engineering, Daegu Gyeongbuk Institute of Science and Technology (DGIST), Daegu 42988, Republic of Korea*

Khalil Amine − *Chemical Sciences and Engineering Division, Argonne National Laboratory, Lemont, Illinois 60439, United States; Pritzker School of Molecular Engineering, University of Chicago, Chicago, Illinois 60637, United States;* orcid.org/0000-0001-9206-3719

Peng Bai − *Department of Energy, Environmental and Chemical Engineering, Washington University in St. Louis, St. Louis, Missouri 63130, United States; Institute of Materials Science and Engineering, Washington University in St. Louis, St. Louis, Missouri 63130, United States;* orcid.org/0000-0002-2419-3498

Dae-Kwon Boo − *Department of Materials Science and Engineering, Konkuk University, Seoul 05029, Republic of Korea; Advanced Materials Program, Department of Materials Science and Engineering, Konkuk University, Seoul 05028, Republic of Korea*

Zheng Chen − *Aiiso Yufeng Li Family Department of Chemical and Nano Engineering, University of California San Diego, La Jolla, California 92093, United States; Sustainable Power and Energy Center and Program of Materials Science and Engineering, University of California San Diego, La Jolla, California 92093, United States;* orcid.org/0000-0002-9186-4298

Yujang Cho − *Department of Materials Science and Engineering, KAIST, Daejeon 34141, Republic of Korea*

Jang Wook Choi − *School of Chemical and Biological Engineering and Institute of Chemical Processes, Seoul National University, Seoul 08826, Republic of Korea; Hyundai Motor Group-Seoul National University (HMG-SNU) Joint Battery Research Center (JBRC), Seoul National University, Seoul 08826, Republic of Korea;* orcid.org/0000-0001-8783-0901

Nam-Soon Choi − *Department of Chemical and Biomolecular Engineering, Korea Advanced Institute of Science and Technology (KAIST), Daejeon 34141, Republic of Korea;* orcid.org/0000-0003-1183-5735

Tae Young Choi − *School of Energy and Chemical Engineering, Ulsan National Institute of Science and Technology (UNIST), Ulsan 44919, Republic of Korea*

Wootaek Choi − *School of Semiconductor Convergence Engineering, Kyungpook National University, Daegu 41566, Republic of Korea*

Yi Cui − *Department of Materials Science and Engineering, Stanford University, Stanford, California 94305, United States; Department of Energy Science and Engineering, Stanford University, Stanford, California 94305, United States; Stanford Institute for Materials and Energy Sciences,*

SLAC National Accelerator Laboratory, Menlo Park, California 94025, United States; orcid.org/0000-0002-6103-6352

Betar M. Gallant − *Department of Mechanical Engineering, Massachusetts Institute of Technology, Cambridge, Massachusetts 02139, United States;* orcid.org/0000-0002-4586-2769

Shiyu Ge − *Department of Chemical and Biological Engineering, Northwestern University, Evanston, Illinois 60208, United States*

Kelsey B. Hatzell − *Andlinger Center for Energy and Environment, Princeton University, Princeton, New Jersey 08540, United States; Department of Mechanical and Aerospace Engineering Department, Princeton University, Princeton, New Jersey 08540, United States;* orcid.org/0000-0002-5222-7288

Yushin Jang − *Department of Battery Engineering, Yonsei University, Seoul 03722, Republic of Korea*

Zhengyu Ju − *Materials Science and Engineering Program, The University of Texas at Austin, Austin, Texas 78712, United States; Walker Department of Mechanical Engineering, The University of Texas at Austin, Austin, Texas 78712, United States;* orcid.org/0000-0002-6994-5286

Ji-Won Jung − *Department of Materials Science and Engineering, Konkuk University, Seoul 05029, Republic of Korea; Advanced Materials Program, Department of Materials Science and Engineering, Konkuk University, Seoul 05028, Republic of Korea;* orcid.org/0000-0001-7044-4764

Hee-Tak Kim − *Department of Chemical and Biomolecular Engineering, Korea Advanced Institute of Science and Technology (KAIST), Daejeon 34141, Republic of Korea;* orcid.org/0000-0003-4578-5422

Ilgyu Kim − *Department of Materials Science and Engineering, Konkuk University, Seoul 05029, Republic of Korea; Advanced Materials Program, Department of Materials Science and Engineering, Konkuk University, Seoul 05028, Republic of Korea*

Min-Ho Kim − *Department of Energy Engineering, Korea Institute of Energy Technology (KENTECH), Naju-si 58217, Republic of Korea*

Mun Sek Kim − *School of Mechanical and Aerospace Engineering, Nanyang Technological University, Singapore 639798, Singapore*

Patrick Joohyun Kim − *School of Chemical Engineering and Applied Chemistry, Kyungpook National University, Daegu 41566, Republic of Korea*

Sang Cheol Kim − *Department of Chemical and Biomolecular Engineering, National University of Singapore, Singapore 117585, Singapore*

Yaejin Kim − *Department of Energy Science and Engineering, Daegu Gyeongbuk Institute of Science and Technology (DGIST), Daegu 42988, Republic of Korea*

Seongjae Ko − *Department of Chemical System Engineering, School of Engineering, The University of Tokyo, Tokyo 113-8656, Japan*

Hyegang Koo − *Department of Battery Engineering, Yonsei University, Seoul 03722, Republic of Korea*

Hochun Lee − *Department of Energy Science and Engineering, Daegu Gyeongbuk Institute of Science and Technology (DGIST), Daegu 42988, Republic of Korea; Energy Science and Engineering Research Center, DGIST, Daegu 42988, Republic of Korea;* orcid.org/0000-0001-9907-5915

Jiyoung Lee − *Department of Chemical Engineering, Ajou University, Gyeonggi-do 16499, Republic of Korea;* orcid.org/0000-0002-8207-9255

Ju Li − *Department of Nuclear Science and Engineering and Department of Materials Science and Engineering, Massachusetts Institute of Technology, Cambridge, Massachusetts 02139, United States;* orcid.org/0000-0002-7841-8058

Yuzhang Li − *Department of Chemical and Biomolecular Engineering and California NanoSystems Institute (CNSI), University of California, Los Angeles, California 90095, United States*

Ping Liu − *Aiiso Yufeng Li Family Department of Chemical and Nano Engineering, University of California San Diego, La Jolla, California 92093, United States; Sustainable Power and Energy Center and Program of Materials Science and Engineering, University of California San Diego, La Jolla, California 92093, United States;* orcid.org/0000-0002-1488-1668

Yijin Liu − *Materials Science and Engineering Program, The University of Texas at Austin, Austin, Texas 78712, United States; Walker Department of Mechanical Engineering, The University of Texas at Austin, Austin, Texas 78712, United States*

Jeffrey Lopez − *Department of Chemical and Biological Engineering, Northwestern University, Evanston, Illinois 60208, United States;* orcid.org/0000-0002-6425-5550

Matthew T. McDowell − *G. W. Woodruff School of Mechanical Engineering, Georgia Institute of Technology, Atlanta, Georgia 30332, United States; School of Materials Science and Engineering, Georgia Institute of Technology, Atlanta, Georgia 30332, United States;* orcid.org/0000-0001-5552-3456

Thanh Nguyen − *Department of Chemical and Biological Engineering, Northwestern University, Evanston, Illinois 60208, United States*

Solomon T. Oyakhire − *School of Chemical and Biomolecular Engineering, Georgia Institute of Technology, Atlanta, Georgia 30332, United States*

Sapna L. Ramesh − *Department of Chemical and Biological Engineering, Northwestern University, Evanston, Illinois 60208, United States*

Mingyu Sagong − *Department of Materials Science and Engineering, KAIST, Daejeon 34141, Republic of Korea*

Nanyang Wang − *School of Mechanical and Aerospace Engineering, Nanyang Technological University, Singapore 639798, Singapore*

Jamie H. Warner − *Materials Science and Engineering Program, The University of Texas at Austin, Austin, Texas 78712, United States; Walker Department of Mechanical Engineering, The University of Texas at Austin, Austin, Texas 78712, United States;* orcid.org/0000-0002-1271-2019

Sujeong Woo − *School of Chemical Engineering and Applied Chemistry, Kyungpook National University, Daegu 41566, Republic of Korea*

Gui-Liang Xu − *Chemical Sciences and Engineering Division, Argonne National Laboratory, Lemont, Illinois 60439, United States;* orcid.org/0000-0001-9969-883X

Kang Xu − *SES AI, Woburn, Massachusetts 01801, United States; Department of Mechanical and Aerospace Engineering,Columbus, OH 43210, United States, The Ohio State University, Columbus, OH 43210, United States;* orcid.org/0000-0002-6946-8635

Yan Yao − *Materials Science and Engineering Program and Texas Center for Superconductivity at the University of Houston, University of Houston, Houston, Texas 77204, United States;* orcid.org/0000-0002-8785-5030

Guihua Yu − *Materials Science and Engineering Program, The University of Texas at Austin, Austin, Texas 78712, United States; Walker Department of Mechanical Engineering, The University of Texas at Austin, Austin, Texas 78712, United States;* orcid.org/0000-0002-3253-0749

Ji-Guang Zhang − *Energy and Environmental Directorate, Pacific Northwest National Laboratory, Richland, Washington 99354, United States;* orcid.org/0000-0001-7343-4609

Complete contact information is available at: https://pubs.acs.org/10.1021/acsnano.6c06180

Author Contributions

†S.C., J.K., and J.S. contributed equally to this work.

Notes

The authors declare no competing financial interest.

■ ACKNOWLEDGMENTS

This work was supported by the 2026 Research Fund (1.260004.01) of UNIST and the National Research Foundation of Korea (NRF) (RS-2024-00428511 for the Korea-USA International Cooperation Project, RS-2025-25441256 for the LEA Core Technology Research Center, and RS-2024-00435493 for the KAIST-MIT Future Energy Initiative Research Center). Mun Sek Kim acknowledges support from the NTU Support Grant for Research (Award No. 025661-00005). Research at the Argonne National Laboratory was funded by the US Department of Energy, Transportation Technologies Office under contract no. DE-AC02-06CH11357.

■ VOCABULARY

Anode- free lithium metal battery; an ultrahigh-energy- density cell configuration assembled without an active material on the negative electrode, where all cyclable lithium is supplied entirely by the cathode during the initial charging process; Lithium inventory- the finite, total amount of chemically and electrochemically cyclable lithium available within a closed battery system required to sustain cell capacity over extended cycling; Dead lithium- isolated metallic lithium fragments detached from the electrical conducting network, combined with chemically degraded lithium species within the solid electrolyte interphase, that can no longer participate in electrochemical reactions; Near-perfect stripping- an ideal electrochemical dissolution process where electrodeposited lithium is nearly 100% extracted back into the electrolyte, minimizing morphological residues and dead lithium formation on the current collector; Lithium compensation strategy- active or passive material and engineering interventions, such as using sacrificial cathode additives or prelithiation techniques, designed to systematically replenish lost lithium and offset capacity decay; Self-recovering closed loop- an advanced electrochemical framework where dynamic interfacial engineering and smart operating protocols allow compromised or isolated lithium to be continuously recaptured and returned to the cyclable inventory

■ REFERENCES

(1) Lin, D.; Liu, Y.; Cui, Y. Reviving the lithium metal anode for high-energy batteries. *Nat. Nanotechnol.* **2017**, *12* (3), 194−206.
(2) Liu, J.; Bao, Z.; Cui, Y.; Dufek, E. J.; Goodenough, J. B.; Khalifah, P.; Li, Q.; Liaw, B. Y.; Liu, P.; Manthiram, A.; et al. Pathways for practical high-energy long-cycling lithium metal batteries. *Nat. Energy* **2019**, *4* (3), 180−186.
(3) Wang, D.; Qiu, J.; Inui, N.; Hagiwara, R.; Hwang, J.; Matsumoto, K. Between Promise and Practice: A Comparative Look at the Energy Density of Li Metal-Free Batteries and Li Metal Batteries. *ACS Energy Lett.* **2023**, *8* (12), 5248−5252.
(4) Brandt, K. Historical development of secondary lithium batteries. *Solid State Ionics* **1994**, *69* (3−4), 173−183.
(5) Xu, K. *Electrolytes, Interfaces and Interphases: Fundamentals and Applications in Batteries*; The Royal Society of Chemistry, 2023.
(6) Zhang, S.; Li, R.; Hu, N.; Deng, T.; Weng, S.; Wu, Z.; Lu, D.; Zhang, H.; Zhang, J.; Wang, X.; et al. Tackling realistic Li^+ flux for high-energy lithium metal batteries. *Nat. Commun.* **2022**, *13* (1), No. 5431.
(7) Li, M.; Zhang, Y.; Zhou, H.; Xin, F.; Whittingham, M. S.; Liaw, B. Lithium inventory tracking as a non-destructive battery evaluation and monitoring method. *Nat. Energy* **2024**, *9* (5), 612−621.
(8) Yang, L.; Hagh, N. M.; Roy, J.; Macciomei, E.; Klein, J. R.; Janakiraman, U.; Fortier, M. E. Review—Challenges and Opportunities in Lithium Metal Battery Technology. *J. Electrochem. Soc.* **2024**, *171* (6), No. 060504.
(9) Zheng, J.; Kim, M. S.; Tu, Z.; Choudhury, S.; Tang, T.; Archer, L. A. Regulating electrodeposition morphology of lithium: towards commercially relevant secondary Li metal batteries. *Chem. Soc. Rev.* **2020**, *49* (9), 2701−2750.
(10) Xu, W.; Wang, J.; Ding, F.; Chen, X.; Nasybulin, E.; Zhang, Y.; Zhang, J.-G. Lithium metal anodes for rechargeable batteries. *Energy Environ. Sci.* **2014**, *7* (2), 513−537.
(11) Yao, W.; Zou, P.; Wang, M.; Zhan, H.; Kang, F.; Yang, C. Design Principle, Optimization Strategies, and Future Perspectives of Anode-Free Configurations for High-Energy Rechargeable Metal Batteries. *Electrochem. Energy Rev.* **2021**, *4* (3), 601−631.
(12) Whittingham, M. S. Electrical energy storage and intercalation chemistry. *Science* **1976**, *192* (4244), 1126−1127.
(13) Huang, W. Z.; Zhao, C. Z.; Wu, P.; Yuan, H.; Feng, W. E.; Liu, Z. Y.; Lu, Y.; Sun, S.; Fu, Z. H.; Hu, J. K.; et al. Anode-Free Solid-State Lithium Batteries: A Review. *Adv. Energy Mater.* **2022**, *12* (26), No. 2201044.
(14) Qian, J.; Adams, B. D.; Zheng, J.; Xu, W.; Henderson, W. A.; Wang, J.; Bowden, M. E.; Xu, S.; Hu, J.; Zhang, J. G. Anode-Free Rechargeable Lithium Metal Batteries. *Adv. Funct. Mater.* **2016**, *26* (39), 7094−7102.
(15) Dong, L.; Zhong, S.; Zhang, S.; Yuan, B.; Liu, J.; Xie, H.; Zhang, C.; Liu, Y.; Yang, C.; Han, J.; He, W. Toward practical anode-free lithium pouch batteries. *Energy Environ. Sci.* **2023**, *16* (12), 5605−5632.
(16) Tian, Y.; An, Y.; Wei, C.; Jiang, H.; Xiong, S.; Feng, J.; Qian, Y. Recently advances and perspectives of anode-free rechargeable batteries. *Nano Energy* **2020**, *78*, No. 105344.
(17) Zhang, J.-G. Anode-less. *Nat. Energy* **2019**, *4* (8), 637−638.
(18) Lee, N.; Oh, J.; Choi, J. W. Anode-less all-solid-state batteries: recent advances and future outlook. *Mater. Fut.* **2023**, *2* (1), No. 013502.
(19) Jiao, X.; Wang, Y.; Kapitanova, O. O.; Xu, X.; Volkov, V. S.; Liu, Y.; Song, Z.; Matic, A.; Xiong, S. Morphology evolution of electrodeposited lithium on metal substrates. *Energy Storage Mater.* **2023**, *61*, No. 102916.
(20) Meng, Q.; Deng, B.; Zhang, H.; Wang, B.; Zhang, W.; Wen, Y.; Ming, H.; Zhu, X.; Guan, Y.; Xiang, Y.; et al. Heterogeneous nucleation and growth of electrodeposited lithium metal on the basal plane of single-layer graphene. *Energy Storage Mater.* **2019**, *16*, 419−425.

(21) Tan, J.; Yao, W.; Ye, M.; Shen, J. Atomistic insights into the morphology of deposited Li. *J. Mater. Chem. A* **2022**, *10* (36), 18577−18591.
(22) Jung, U.; Kim, J.; Seo, J.; Jin, S.; Kim, M.-H.; Lee, H.-W. How operando analysis enables quantitative understanding of dense lithium metal deposition. *Electrochim. Acta* **2025**, *537*, No. 146902.
(23) Kang, J.; Kwon, O.; Choi, S.; Choi, S.; Jang, S.; Eom, H.; Shin, J.; Park, J.; Kim, J. H.; Seol, M.-L.; et al. Reevaluating carbonization: The untapped potential of pristine ZIFs for lithium metal batteries. *Chem. Eng. J.* **2025**, *522*, No. 166980.
(24) Chen, Y.; Ma, Z.; Wang, Y.; Kumar, P.; Zhao, F.; Cai, T.; Cao, Z.; Cavallo, L.; Cheng, H.; Li, Q.; Ming, J. Trace ethylene carbonate-mediated low-concentration ether-based electrolytes for high-voltage lithium metal batteries. *Energy Environ. Sci.* **2024**, *17* (15), 5613−5626.
(25) Ko, S.; Obukata, T.; Shimada, T.; Takenaka, N.; Nakayama, M.; Yamada, A.; Yamada, Y. Electrode potential influences the reversibility of lithium-metal anodes. *Nat. Energy* **2022**, *7* (12), 1217−1224.
(26) Tan, J.; Ye, M.; Shen, J. Tailoring uniform and ordered grain boundaries in the solid electrolyte interphase for dendrite-free lithium metal batteries. *Mater. Today Energy* **2021**, *22*, No. 100858.
(27) Tan, Y. H.; Liu, Z.; Zheng, J. H.; Ju, Z. J.; He, X. Y.; Hao, W.; Wu, Y. C.; Xu, W. S.; Zhang, H. J.; Li, G. Q.; et al. Inorganic Composition Modulation of Solid Electrolyte Interphase for Fast Charging Lithium Metal Batteries. *Adv. Mater.* **2024**, *36* (30), No. e2404815.
(28) Li, Q.; Zhu, S.; Lu, Y. 3D porous Cu current collector/Li-metal composite anode for stable lithium-metal batteries. *Adv. Funct. Mater.* **2017**, *27* (18), No. 1606422.
(29) Chen, X. R.; Yao, Y. X.; Yan, C.; Zhang, R.; Cheng, X. B.; Zhang, Q. A diffusion–reaction competition mechanism to tailor lithium deposition for lithium-metal batteries. *Angew. Chem., Int. Ed.* **2020**, *59* (20), 7743−7747.
(30) Li, T.; Zhang, X.-Q.; Shi, P.; Zhang, Q. Fluorinated solid-electrolyte interphase in high-voltage lithium metal batteries. *Joule* **2019**, *3* (11), 2647−2661.
(31) Jiao, S.; Ren, X.; Cao, R.; Engelhard, M. H.; Liu, Y.; Hu, D.; Mei, D.; Zheng, J.; Zhao, W.; Li, Q.; et al. Stable cycling of high-voltage lithium metal batteries in ether electrolytes. *Nat. Energy* **2018**, *3* (9), 739−746.
(32) Zhang, X. Q.; Chen, X.; Cheng, X. B.; Li, B. Q.; Shen, X.; Yan, C.; Huang, J. Q.; Zhang, Q. Highly stable lithium metal batteries enabled by regulating the solvation of lithium ions in nonaqueous electrolytes. *Angew. Chem., Int. Ed.* **2018**, *57* (19), 5301−5305.
(33) Pei, A.; Zheng, G.; Shi, F.; Li, Y.; Cui, Y. Nanoscale nucleation and growth of electrodeposited lithium metal. *Nano Lett.* **2017**, *17* (2), 1132−1139.
(34) Wood, K. N.; Kazyak, E.; Chadwick, A. F.; Chen, K.-H.; Zhang, J.-G.; Thornton, K.; Dasgupta, N. P. Dendrites and pits: untangling the complex behavior of lithium metal anodes through operando video microscopy. *ACS Cent. Sci.* **2016**, *2* (11), 790−801.
(35) Chen, K.-H.; Wood, K. N.; Kazyak, E.; LePage, W. S.; Davis, A. L.; Sanchez, A. J.; Dasgupta, N. P. Dead lithium: mass transport effects on voltage, capacity, and failure of lithium metal anodes. *J. Mater. Chem. A* **2017**, *5* (23), 11671−11681.
(36) Sanchez, A. J.; Kazyak, E.; Chen, Y.; Chen, K.-H.; Pattison, E. R.; Dasgupta, N. P. Plan-view operando video microscopy of Li metal anodes: identifying the coupled relationships among nucleation, morphology, and reversibility. *ACS Energy Lett.* **2020**, *5* (3), 994−1004.
(37) Li, G.-X.; Koverga, V.; Nguyen, A.; Kou, R.; Ncube, M.; Jiang, H.; Wang, K.; Liao, M.; Guo, H.; Chen, J.; et al. Enhancing lithium-metal battery longevity through minimized coordinating diluent. *Nat. Energy* **2024**, *9* (7), 817−827.
(38) Piao, N.; Ji, X.; Xu, H.; Fan, X.; Chen, L.; Liu, S.; Garaga, M. N.; Greenbaum, S. G.; Wang, L.; Wang, C.; He, X. Countersolvent electrolytes for lithium-metal batteries. *Adv. Energy Mater.* **2020**, *10* (10), No. 1903568.
(39) Fang, C.; Lu, B.; Pawar, G.; Zhang, M.; Cheng, D.; Chen, S.; Ceja, M.; Doux, J.-M.; Musrock, H.; Cai, M.; et al. Pressure-tailored lithium deposition and dissolution in lithium metal batteries. *Nat. Energy* **2021**, *6* (10), 987−994.
(40) Tang, W.; Yin, X.; Kang, S.; Chen, Z.; Tian, B.; Teo, S. L.; Wang, X.; Chi, X.; Loh, K. P.; Lee, H. W.; Zheng, G. W. Lithium silicide surface enrichment: a solution to lithium metal battery. *Adv. Mater.* **2018**, *30* (34), No. 1801745.
(41) Jin, C.; Sheng, O.; Luo, J.; Yuan, H.; Fang, C.; Zhang, W.; Huang, H.; Gan, Y.; Xia, Y.; Liang, C.; et al. 3D lithium metal embedded within lithiophilic porous matrix for stable lithium metal batteries. *Nano Energy* **2017**, *37*, 177−186.
(42) Nguyen, M. H.; Kim, D.; Kim, B. K.; Park, S. Harnessing Liquid Metals with In Situ Polymerized Electrolyte for Anode-Free Lithium Metal Batteries. *Adv. Funct. Mater.* **2024**, *34* (44), No. 2407179.
(43) Peng, G.; Wang, G.; Akbar, A. R.; Zheng, D.; Wang, W.; Huang, L.; Chen, C.; Luo, G.; Feng, S.-P.; Liu, F. Roll-to-roll fabrication of lithium metal anodes with hierarchical lithiophilic structures and controlled deposition for enhanced stability. *Energy Storage Mater.* **2024**, *66*, No. 103205.
(44) Huang, B.; Cai, Z.; Peng, T.; Tan, Y.; Zhang, N.; Liu, W.; Zhong, H.; Mai, Y. Bottom-up deposition of lithium on 3D lithiophobic−lithiophilic host for long-life lithium metal anodes. *J. Mater. Chem. A* **2024**, *12* (23), 13733−13741.
(45) Zheng, J.; Deng, Y.; Yin, J.; Tang, T.; Garcia-Mendez, R.; Zhao, Q.; Archer, L. A. Textured Electrodes: Manipulating Built-In Crystallographic Heterogeneity of Metal Electrodes via Severe Plastic Deformation. *Adv. Mater.* **2022**, *34* (1), No. e2106867.
(46) Wang, B.; Doan, H. A.; Son, S.-B.; Abraham, D. P.; Trask, S. E.; Jansen, A.; Xu, K.; Liao, C. Data-driven design of electrolyte additives supporting high-performance 5 V $LiNi_{0.5}Mn_{1.5}O_4$ positive electrodes. *Nat. Commun.* **2025**, *16* (1), No. 3413.
(47) Kim, S. C.; Oyakhire, S. T.; Athanitis, C.; Wang, J.; Zhang, Z.; Zhang, W.; Boyle, D. T.; Kim, M. S.; Yu, Z.; Gao, X.; et al. Data-driven electrolyte design for lithium metal anodes. *Proc. Natl. Acad. Sci. U.S.A.* **2023**, *120* (10), No. e2214357120.
(48) Krauss, F. T.; Pantenburg, I.; Lehmann, V.; Stich, M.; Weiershauser, J. O.; Bund, A.; Roling, B. Elucidating the Transport of Electrons and Molecules in a Solid Electrolyte Interphase Close to Battery Operation Potentials Using a Four-Electrode-Based Generator-Collector Setup. *J. Am. Chem. Soc.* **2024**, *146* (28), 19009−19018.
(49) Sand, H. J. S. III. On the concentration at the electrodes in a solution, with special reference to the liberation of hydrogen by electrolysis of a mixture of copper sulphate and sulphuric acid. *London, Edinburgh, Dublin Philos. Magazine and J. Sci.* **1901**, *1* (1), 45−79.
(50) Marcus, R. A. On the theory of oxidation-reduction reactions involving electron transfer. I. *J. Chem. Phys.* **1956**, *24* (5), 966−978.
(51) Marcus, R. A. Electrostatic free energy and other properties of states having nonequilibrium polarization. I. *J. Chem. Phys.* **1956**, *24* (5), 979−989.
(52) Dickinson, E. J.; Wain, A. J. The Butler-Volmer equation in electrochemical theory: Origins, value, and practical application. *J. Electroanal. Chem.* **2020**, *872*, No. 114145.
(53) Butler, J. A. V. Studies in heterogeneous equilibria. Part II.—The kinetic interpretation of the nernst theory of electromotive force. *Trans. Faraday Soc.* **1924**, *19* (March), 729−733.
(54) Newman, J.; Tiedemann, W. Porous-electrode theory with battery applications. *AIChE J.* **1975**, *21* (1), 25−41.
(55) Das, S.; Attia, P. M.; Chueh, W. C.; Bazant, M. Z. Electrochemical Kinetics of SEI Growth on Carbon Black: Part II. Modeling. *J. Electrochem. Soc.* **2019**, *166* (4), E107−E118.
(56) Werres, M.; Xu, Y.; Jia, H.; Wang, C.; Xu, W.; Latz, A.; Horstmann, B. Origin of Heterogeneous Stripping of Lithium in Liquid Electrolytes. *ACS Nano* **2023**, *17* (11), 10218−10228.
(57) Chen, Z.; Danilov, D. L.; Eichel, R. A.; Notten, P. H. L. Porous Electrode Modeling and its Applications to Li-Ion Batteries. *Adv. Energy Mater.* **2022**, *12* (32), No. 2201506.

https://doi.org/10.1021/acsnano.6c06180
ACS Nano XXXX, XXX, XXX−XXX

(58) Shi, F.; Pei, A.; Boyle, D. T.; Xie, J.; Yu, X.; Zhang, X.; Cui, Y. Lithium metal stripping beneath the solid electrolyte interphase. *Proc. Natl. Acad. Sci. U.S.A.* **2018**, *115* (34), 8529−8534.
(59) Jo, S.; Song, J.; Kwak, S. J.; Park, K.; Kim, S.; Jo, S.; Lee, S.; Song, G.; Park, A.; Lee, W. B.; Lee, K. T. The Heterogeneous Charge Transfer Mechanism in Lithium Metal Batteries: Revealing Abnormal Lithiophilicity through the Marcus Theory. *J. Am. Chem. Soc.* **2026**, *148* (3), 2930−2941.
(60) Boyle, D. T.; Kong, X.; Pei, A.; Rudnicki, P. E.; Shi, F.; Huang, W.; Bao, Z.; Qin, J.; Cui, Y. Transient Voltammetry with Ultramicroelectrodes Reveals the Electron Transfer Kinetics of Lithium Metal Anodes. *ACS Energy Lett.* **2020**, *5* (3), 701−709.
(61) Sandoval, S. E.; Haslam, C. G.; Vishnugopi, B. S.; Liao, D. W.; Yoon, J. S.; Park, S. H.; Wang, Y.; Mitlin, D.; Hatzell, K. B.; Siegel, D. J.; et al. Electro-chemo-mechanics of anode-free solid-state batteries. *Nat. Mater.* **2025**, *24* (5), 673−681.
(62) Sandoval, S. E.; Lewis, J. A.; Vishnugopi, B. S.; Nelson, D. L.; Schneider, M. M.; Cortes, F. J. Q.; Matthews, C. M.; Watt, J.; Tian, M.; Shevchenko, P.; et al. Structural and electrochemical evolution of alloy interfacial layers in anode-free solid-state batteries. *Joule* **2023**, *7* (9), 2054−2073.
(63) Jung, S.-J.; Lee, C.; Park, C.; Ryu, S.; Lee, J.; Kang, M.-G.; Kim, E.; Kim, J. Y.; Bae, K. Y.; Son, S.; Lee, H. W. Lithiation Diagnostics by Measuring Electrochemodynamics in Solid-State Batteries. *ACS Energy Lett.* **2025**, *10* (7), 3112−3121.
(64) Thorpe, M. A.; Zhang, M.; Liao, D. W.; Sandoval, S. E.; Kim, Y.; McDowell, M. T.; Thouless, M. D.; Dasgupta, N. P. Controlling stack pressure inhomogeneity in anode-free solid-state batteries using elastomeric interlayers. *Matter* **2025**, *8* (3), No. 101955.
(65) Lewis, J. A.; Sandoval, S. E.; Liu, Y.; Nelson, D. L.; Yoon, S. G.; Wang, R.; Zhao, Y.; Tian, M.; Shevchenko, P.; Martínez-Pañeda, E.; Martínez-Pañeda, E. Accelerated Short Circuiting in Anode-Free Solid-State Batteries Driven by Local Lithium Depletion. *Adv. Energy Mater.* **2023**, *13* (12), No. 2204186.
(66) Meldrum, F. C.; O'Shaughnessy, C. Crystallization in Confinement. *Adv. Mater.* **2020**, *32* (31), No. e2001068.
(67) Cooper, E. R.; Li, M.; Gentle, I.; Xia, Q.; Knibbe, R. A Deeper Understanding of Metal Nucleation and Growth in Rechargeable Metal Batteries Through Theory and Experiment. *Angew. Chem., Int. Ed.* **2023**, *62* (51), No. e202309247.
(68) Sangiovanni, D. G.; Mei, A. B.; Edström, D.; Hultman, L.; Chirita, V.; Petrov, I.; Greene, J. E. Effects of surface vibrations on interlayer mass transport: Ab initio molecular dynamics investigation of Ti adatom descent pathways and rates from TiN/TiN(001) islands. *Phys. Rev. B* **2018**, *97* (3), No. 035406.
(69) Vishnugopi, B. S.; Hao, F.; Verma, A.; Mukherjee, P. P. Surface diffusion manifestation in electrodeposition of metal anodes. *Phys. Chem. Chem. Phys.* **2020**, *22* (20), 11286−11295.
(70) Li, Y.; Kim, M. H.; Xie, Z.; Min, J.; Li, Y. Microelectrodes for Battery Materials. *ACS Nano* **2024**, *18* (52), 35119−35129.
(71) Kim, M.-H.; Kim, D. Y.; Li, Y.; Kim, J.; Kim, M. H.; Seo, J.; Cunning, B. V.; Kim, T.; Park, S.-W.; Ruoff, R. S.; et al. Horizontal lithium growth driven by surface dynamics on single crystal Cu(111) foil. *Energy Environ. Sci.* **2024**, *17* (18), 6521−6532.
(72) Yuan, X.; Liu, B.; Mecklenburg, M.; Li, Y. Ultrafast deposition of faceted lithium polyhedra by outpacing SEI formation. *Nature* **2023**, *620* (7972), 86−91.
(73) Jagger, B.; Pasta, M. Solid electrolyte interphases in lithium metal batteries. *Joule* **2023**, *7* (10), 2228−2244.
(74) Newman, J. Engineering Design of Electrochemical Systems. *Ind. Eng. Chem.* **1968**, *60* (4), 12−27.
(75) Newman, J.; Thomas-Alyea, K. E. *Electrochemical Systems*; John Wiley & Sons, 2004.
(76) Barai, P.; Higa, K.; Srinivasan, V. Lithium dendrite growth mechanisms in polymer electrolytes and prevention strategies. *Phys. Chem. Chem. Phys.* **2017**, *19* (31), 20493−20505.
(77) Yuan, S.; Weng, S.; Wang, F.; Dong, X.; Wang, Y.; Wang, Z.; Shen, C.; Bao, J. L.; Wang, X.; Xia, Y. Revisiting the designing criteria of advanced solid electrolyte interphase on lithium metal anode under practical condition. *Nano Energy* **2021**, *83*, No. 105847.
(78) Zheng, J.; Ju, Z.; Zhang, B.; Nai, J.; Liu, T.; Liu, Y.; Xie, Q.; Zhang, W.; Wang, Y.; Tao, X. Lithium ion diffusion mechanism on the inorganic components of the solid−electrolyte interphase. *J. Mater. Chem. A* **2021**, *9* (16), 10251−10259.
(79) Chazalviel, J.-N. Electrochemical aspects of the generation of ramified metallic electrodeposits. *Phys. Rev. A* **1990**, *42* (12), 7355−7367.
(80) Bai, P.; Li, J.; Brushett, F. R.; Bazant, M. Z. Transition of lithium growth mechanisms in liquid electrolytes. *Energy Environ. Sci.* **2016**, *9* (10), 3221−3229.
(81) Xiao, J. How lithium dendrites form in liquid batteries. *Science* **2019**, *366* (6464), 426−427.
(82) Ma, Y.; Selvasundarasekar, S. S.; Sinclair, N.; Zhang, Y.; Xu, S.; Bracey, J.; Akolkar, R. A Modified Sand's Time Incorporating Li-Ion Transport Across the SEI: Basis for Understanding Li Dendrite Formation and Li-Metal Battery Electrolyte Selection. *J. Electrochem. Soc.* **2025**, *172* (3), No. 030506.
(83) Akolkar, R. Modeling dendrite growth during lithium electrodeposition at sub-ambient temperature. *J. Power Sources* **2014**, *246*, 84−89.
(84) Liu, W.; Liu, P.; Mitlin, D. Review of Emerging Concepts in SEI Analysis and Artificial SEI Membranes for Lithium, Sodium, and Potassium Metal Battery Anodes. *Adv. Energy Mater.* **2020**, *10* (43), No. 2002297.
(85) Men, L.; Wu, H.; Zhang, X.; Jin, G.; Liu, Y.; Xu, R. Mechanical integrity of the solid-electrolyte interphase and its role in regulating lithium deposition morphology. *J. Mech. Phys. Solids* **2026**, *211*, No. 106563.
(86) Pokharel, J.; Cresce, A.; Pant, B.; Yang, M. Y.; Gurung, A.; He, W.; Baniya, A.; Lamsal, B. S.; Yang, Z.; Gent, S.; et al. Manipulating the diffusion energy barrier at the lithium metal electrolyte interface for dendrite-free long-life batteries. *Nat. Commun.* **2024**, *15* (1), No. 3085.
(87) Jiang, F. N.; Yang, S. J.; Liu, H.; Cheng, X. B.; Liu, L.; Xiang, R.; Zhang, Q.; Kaskel, S.; Huang, J. Q. Mechanism understanding for stripping electrochemistry of Li metal anode. *SusMat* **2021**, *1* (4), 506−536.
(88) Liu, F.; Xu, R.; Wu, Y.; Boyle, D. T.; Yang, A.; Xu, J.; Zhu, Y.; Ye, Y.; Yu, Z.; Zhang, Z.; et al. Dynamic spatial progression of isolated lithium during battery operations. *Nature* **2021**, *600* (7890), 659−663.
(89) Shin, W.; Manthiram, A. A Facile Potential Hold Method for Fostering an Inorganic Solid-Electrolyte Interphase for Anode-Free Lithium-Metal Batteries. *Angew. Chem., Int. Ed.* **2022**, *61* (13), No. e202115909.
(90) Pande, V.; Viswanathan, V. Computational Screening of Current Collectors for Enabling Anode-Free Lithium Metal Batteries. *ACS Energy Lett.* **2019**, *4* (12), 2952−2959.
(91) Gunnarsdóttir, A. B.; Amanchukwu, C. V.; Menkin, S.; Grey, C. P. Noninvasive In Situ NMR Study of "Dead Lithium" Formation and Lithium Corrosion in Full-Cell Lithium Metal Batteries. *J. Am. Chem. Soc.* **2020**, *142* (49), 20814−20827.
(92) Hsieh, Y.-C.; Leißing, M.; Nowak, S.; Hwang, B.-J.; Winter, M.; Brunklaus, G. Quantification of Dead Lithium via In Situ Nuclear Magnetic Resonance Spectroscopy. *Cell Rep. Phys. Sci.* **2020**, *1* (8), No. 100139.
(93) McShane, E. J.; Colclasure, A. M.; Brown, D. E.; Konz, Z. M.; Smith, K.; McCloskey, B. D. Quantification of Inactive Lithium and Solid−Electrolyte Interphase Species on Graphite Electrodes after Fast Charging. *ACS Energy Lett.* **2020**, *5* (6), 2045−2051.
(94) Tao, M.; Xiang, Y.; Zhao, D.; Shan, P.; Yang, Y. Protocol for quantifying inactive lithium in anode-free lithium batteries by mass spectrometry titration. *Commun. Mater.* **2022**, *3* (1), No. 50.
(95) Li, Y.; Huang, W.; Li, Y.; Pei, A.; Boyle, D. T.; Cui, Y. Correlating Structure and Function of Battery Interphases at Atomic Resolution Using Cryoelectron Microscopy. *Joule* **2018**, *2* (10), 2167−2177.

(96) Fang, C.; Li, J.; Zhang, M.; Zhang, Y.; Yang, F.; Lee, J. Z.; Lee, M.-H.; Alvarado, J.; Schroeder, M. A.; Yang, Y.; et al. Quantifying inactive lithium in lithium metal batteries. *Nature* **2019**, *572* (7770), 511−515.
(97) Dachraoui, W.; Kühnel, R.-S.; Battaglia, C.; Erni, R. Nucleation, growth and dissolution of Li metal dendrites and the formation of dead Li in Li-ion batteries investigated by operando electrochemical liquid cell scanning transmission electron microscopy. *Nano Energy* **2024**, *130*, No. 110086.
(98) Steinberg, K.; Gallant, B. M. Revealing the Role of Lithium Carbonate at Lithium Metal Anodes Through Study of Gas-Reacted Interphases. *J. Electrochem. Soc.* **2024**, *171* (8), No. 080530.
(99) Jiang, Y.; Ye, F. Dead Lithium in Lithium Metal Batteries: Formation, Characterization and Strategies. *Chem.—Eur. J.* **2024**, *30* (43), No. e202400424.
(100) Wei, Z.; Wang, X.; Zhou, M.; Papovic, S.; Zheng, K.; Swierczek, K.; Wu, J.; Xin, X. Revitalizing Lithium Metal Batteries: Strategies for Tackling Dead Lithium Formation and Reactivation. *Small* **2024**, *20* (51), No. e2407395.
(101) Park, J.; Zhao, H.; Kang, S. D.; Lim, K.; Chen, C.-C.; Yu, Y.-S.; Braatz, R. D.; Shapiro, D. A.; Hong, J.; Toney, M. F.; et al. Fictitious phase separation in Li layered oxides driven by electro-autocatalysis. *Nat. Mater.* **2021**, *20* (7), 991−999.
(102) Kang, S. D.; Chueh, W. C. Probing the depths of battery heterogeneity. *Nat. Nanotechnol.* **2023**, *18* (10), 1130.
(103) Kim, M.-H.; Kim, J.; Choi, S.-H.; Wi, T.-U.; Choi, A.; Seo, J.; Lim, C. H.; Park, C.; Lee, H.-W. Mitigating electrode-level heterogeneity using phosphorus nanolayers on graphite for fast-charging batteries. *ACS Energy Lett.* **2023**, *8* (9), 3962−3970.
(104) Kim, J.; Kim, M.-H.; Kim, Y.; Kim, M. S.; Choi, A.; Jeong, K.-M.; Lee, H.-W. Unveiling the role of electrode-level heterogeneity alleviated in a silicon-graphite electrode under operando microscopy. *Energy Storage Mater.* **2023**, *57*, 269−276.
(105) Liu, Y.; Zhu, Y.; Cui, Y. Challenges and opportunities towards fast-charging battery materials. *Nat. Energy* **2019**, *4* (7), 540−550.
(106) Kim, J.-H.; Kim, N.-Y.; Ju, Z.; Hong, Y.-K.; Kang, K.-D.; Pang, J.-H.; Lee, S.-J.; Chae, S.-S.; Park, M.-S.; Kim, J.-Y.; et al. Upscaling high-areal-capacity battery electrodes. *Nat. Energy* **2025**, *10* (3), 295−307.
(107) Arnot, D. J.; Mayilvahanan, K. S.; Hui, Z.; Takeuchi, K. J.; Marschilok, A. C.; Bock, D. C.; Wang, L.; West, A. C.; Takeuchi, E. S. Thick Electrode Design for Facile Electron and Ion Transport: Architectures, Advanced Characterization, and Modeling. *Acc. Mater. Res.* **2022**, *3* (4), 472−483.
(108) Du, Z.; Wood, D. L.; Daniel, C.; Kalnaus, S.; Li, J. Understanding limiting factors in thick electrode performance as applied to high energy density Li-ion batteries. *J. Appl. Electrochem.* **2017**, *47* (3), 405−415.
(109) Guo, Y.; Li, X.; Guo, H.; Qin, Q.; Wang, Z.; Wang, J.; Yan, G. Visualization of concentration polarization in thick electrodes. *Energy Storage Mater.* **2022**, *51*, 476−485.
(110) Park, K.-Y.; Park, J.-W.; Seong, W. M.; Yoon, K.; Hwang, T.-H.; Ko, K.-H.; Han, J.-H.; Jaedong, Y.; Kang, K. Understanding capacity fading mechanism of thick electrodes for lithium-ion rechargeable batteries. *J. Power Sources* **2020**, *468*, No. 228369.
(111) Bai, P.; Guo, J.; Wang, M.; Kushima, A.; Su, L.; Li, J.; Brushett, F. R.; Bazant, M. Z. Interactions between lithium growths and nanoporous ceramic separators. *Joule* **2018**, *2* (11), 2434−2449.
(112) Liu, Y.; Lin, D.; Yuen, P. Y.; Liu, K.; Xie, J.; Dauskardt, R. H.; Cui, Y. An artificial solid electrolyte interphase with high Li-ion conductivity, mechanical strength, and flexibility for stable lithium metal anodes. *Adv. Mater.* **2016**, *29* (10), No. 1605531.
(113) Sun, X.; Yang, S.; Zhang, T.; Shi, Y.; Dong, L.; Ai, G.; Li, D.; Mao, W. Regulating Li-ion flux with a high-dielectric hybrid artificial SEI for stable Li metal anodes. *Nanoscale* **2022**, *14* (13), 5033−5043.
(114) Yu, T.; Zhao, T.; Zhang, N.; Xue, T.; Chen, Y.; Ye, Y.; Wu, F.; Chen, R. Spatially confined LiF nanoparticles in an aligned polymer matrix as the artificial SEI layer for lithium metal anodes. *Nano Lett.* **2023**, *23* (1), 276−282.
(115) Chen, C.; Liang, Q.; Wang, G.; Liu, D.; Xiong, X. Grain-boundary-rich artificial SEI layer for high-rate lithium metal anodes. *Adv. Funct. Mater.* **2022**, *32* (4), No. 2107249.
(116) Kim, S. C.; Wang, J.; Xu, R.; Zhang, P.; Chen, Y.; Huang, Z.; Yang, Y.; Yu, Z.; Oyakhire, S. T.; Zhang, W.; et al. High-entropy electrolytes for practical lithium metal batteries. *Nat. Energy* **2023**, *8* (8), 814−826.
(117) Kim, M. S.; Zhang, Z.; Rudnicki, P. E.; Yu, Z.; Wang, J.; Wang, H.; Oyakhire, S. T.; Chen, Y.; Kim, S. C.; Zhang, W.; et al. Suspension electrolyte with modified Li^+ solvation environment for lithium metal batteries. *Nat. Mater.* **2022**, *21* (4), 445−454.
(118) Yu, Z.; Rudnicki, P. E.; Zhang, Z.; Huang, Z.; Celik, H.; Oyakhire, S. T.; Chen, Y.; Kong, X.; Kim, S. C.; Xiao, X.; et al. Rational solvent molecule tuning for high-performance lithium metal battery electrolytes. *Nat. Energy* **2022**, *7* (1), 94−106.
(119) Wang, H.; Yu, Z.; Kong, X.; Kim, S. C.; Boyle, D. T.; Qin, J.; Bao, Z.; Cui, Y. Liquid electrolyte: The nexus of practical lithium metal batteries. *Joule* **2022**, *6* (3), 588−616.
(120) Li, Z.; Wang, L.; Huang, X.; He, X. Lithium Bis-(Trifluoromethanesulfonyl)Imide (LiTFSI): A Prominent Lithium Salt in Lithium-Ion Battery Electrolytes − Fundamentals, Progress, and Future Perspectives. *Adv. Funct. Mater.* **2024**, *34* (48), No. 2408319.
(121) Li, P. C.; Zhang, Z. Q.; Zhao, Z. W.; Li, J. Q.; Xu, Z. X.; Zhang, H.; Li, G. Dipole Moment Influences the Reversibility and Corrosion of Lithium Metal Anodes. *Adv. Mater.* **2024**, *36* (31), No. e2406359.
(122) Qin, M.; Zeng, Z.; Ma, F.; Gu, C.; Chen, X.; Cheng, S.; Xie, J. Doping in Solvation Structure: Enabling Fluorinated Carbonate Electrolyte for High-Voltage and High-Safety Lithium-Ion Batteries. *ACS Energy Lett.* **2024**, *9* (6), 2536−2544.
(123) Wang, Q.; Zhao, C.; Wang, J.; Yao, Z.; Wang, S.; Kumar, S. G. H.; Ganapathy, S.; Eustace, S.; Bai, X.; Li, B.; Wagemaker, M. High entropy liquid electrolytes for lithium batteries. *Nat. Commun.* **2023**, *14* (1), No. 440.
(124) Wang, Q.; Wang, J.; Heringa, J. R.; Bai, X.; Wagemaker, M. High-Entropy Electrolytes for Lithium-Ion Batteries. *ACS Energy Lett.* **2024**, *9* (8), 3796−3806.
(125) Fang, S.; Bai, T.; Liao, J.; Zhang, S.; Wang, J.; Mo, F.; Zhai, W.; Hu, Z.; Lu, J.; Hui, K. N.; et al. Lithiophilic Cu-Ag Architectures with Li-Si Alloys for Stable Lithium Metal Batteries. *Energy Storage Mater.* **2025**, *81*, No. 104541.
(126) Seo, J.; Lim, J.; Chang, H.; Lee, J.; Woo, J.; Jung, I.; Kim, Y.; Kim, B.; Moon, J.; Lee, H. Sustaining Surface Lithiophilicity of Ultrathin Li-Alloy Coating Layers on Current Collector for Zero-Excess Li-Metal Batteries. *Small* **2024**, *20* (47), No. 2402988.
(127) Li, G.; Han, Z.; Tan, Y.; Wei, Q.; Mao, E.; Du, J.; Fu, L. In-situ construction of lithium-tin alloy skeleton as a lithiophilic host for lithium metal anode. *Electrochim. Acta* **2024**, *473*, No. 143504.
(128) Park, J. B.; Choi, C.; Yu, S.; Chung, K. Y.; Kim, D. W. Porous lithiophilic Li−Si alloy-type interfacial framework via self-discharge mechanism for stable lithium metal anode with superior rate. *Adv. Energy Mater.* **2021**, *11* (37), No. 2101544.
(129) Ye, Y.; Liu, Y.; Wu, J.; Yang, Y. Lithiophilic Li-Zn alloy modified 3D Cu foam for dendrite-free lithium metal anode. *J. Power Sources* **2020**, *472*, No. 228520.
(130) Fu, A.; Wang, C.; Peng, J.; Su, M.; Pei, F.; Cui, J.; Fang, X.; Li, J. F.; Zheng, N. Lithiophilic and antioxidative copper current collectors for highly stable lithium metal batteries. *Adv. Funct. Mater.* **2021**, *31* (15), No. 2009805.
(131) Wang, Z.; Xu, H.; Liu, K.; Dong, N.; Jia, N.; Liu, B.; Lin, D.; Zhao, Z.; Tian, G.; Qi, S.; Wu, D. Separator Engineering Regulating Reversible Li Electrodeposition Enabled by Lithiophilic Polyimide@Ag Coating Layer for Dendrite-Free Lithium Metal Batteries. *Small* **2025**, *21*, No. 2504870.
(132) Tao, J.; Zhang, C.; Li, X.; Chen, X.; Ji, C.; Wan, W.; Wang, C. Advancing anode-less lithium metal batteries: ZnF_2 modification and in situ structural regulation for enhanced performance. *J. Mater. Chem. A* **2024**, *12* (29), 18127−18136.

https://doi.org/10.1021/acsnano.6c06180
ACS Nano XXXX, XXX, XXX−XXX

(133) Sun, F.; Yang, C.; Manke, I.; Chen, L.; Dong, S. Li-based anode: Is dendrite-free sufficient? *Mater. Today* **2020**, *38*, 7−9.
(134) Hatzell, K. B. Anode-Less or Anode-Free? *ACS Energy Lett.* **2023**, *8* (11), 4775−4776.
(135) Jin, H.; Pyo, S.; Seo, H.; Cho, J.; Han, J.; Han, J.; Yun, H.; Kim, H.; Lee, J.; Min, B.; et al. LiF-Rich Solid Electrolyte Interphase Formation by Establishing Sacrificial Layer on the Separator. *Small* **2024**, *20* (36), No. e2401928.
(136) Kim, S.; Byun, Y.; Lee, C.; Lee, Y.; Lee, E.; Eom, K. In-situ constructing LiF-rich lithiophilic interface by unifying additive approach and electrochemical treatment for AFLMBs. *Chem. Eng. J.* **2025**, *507*, No. 160406.
(137) Zhang, J.; Du, Z.; Wang, Y.; Chen, H.; Ai, Q.; Chen, Q.; Hou, G.; Tang, Y. Magnetic Field-Driven Ion Selectivity Boosts LiF-Rich SEI Formation for Enhanced Lithium Metal Battery Performance Across Temperatures. *ACS Appl. Mater. Interfaces* **2025**, *17* (12), 18329−18338.
(138) Zhuang, H.; Xiao, H.; Zhang, T.; Zhang, F.; Han, P.; Xu, M.; Dai, W.; Jiao, J.; Jiang, L.; Gao, Q. LiF-Rich Alloy-Doped SEI Enabling Ultra-Stable and High-Rate Li Metal Anode. *Angew. Chem., Int. Ed.* **2024**, *63* (33), No. e202407315.
(139) Li, X.; Tian, Y.; Shen, L.; Qu, Z.; Ma, T.; Sun, F.; Liu, X.; Zhang, C.; Shen, J.; Li, X.; et al. Electrolyte Interphase Built from Anionic Covalent Organic Frameworks for Lithium Dendrite Suppression. *Adv. Funct. Mater.* **2021**, *31* (22), No. 2009718.
(140) Louli, A. J.; Eldesoky, A.; Weber, R.; Genovese, M.; Coon, M.; deGooyer, J.; Deng, Z.; White, R. T.; Lee, J.; Rodgers, T.; et al. Diagnosing and correcting anode-free cell failure via electrolyte and morphological analysis. *Nat. Energy* **2020**, *5* (9), 693−702.
(141) Yu, L.; Tian, X.; Zheng, M.; Zhang, W.; Sun, C.; Qian, S.; Liu, T.; Li, Z.; Lu, J. The Latent Culprit of Anode-Free Lithium Metal Batteries Degradation. *Adv. Funct. Mater.* **2025**, No. e24486.
(142) Jin, C.; Huang, Y.; Li, L.; Wei, G.; Li, H.; Shang, Q.; Ju, Z.; Lu, G.; Zheng, J.; Sheng, O.; Tao, X. A corrosion inhibiting layer to tackle the irreversible lithium loss in lithium metal batteries. *Nat. Commun.* **2023**, *14* (1), No. 8269.
(143) Zhao, Q.; Stalin, S.; Archer, L. A. Stabilizing metal battery anodes through the design of solid electrolyte interphases. *Joule* **2021**, *5* (5), 1119−1142.
(144) Zhang, Z.; Li, Y.; Xu, R.; Zhou, W.; Li, Y.; Oyakhire, S. T.; Wu, Y.; Xu, J.; Wang, H.; Yu, Z.; et al. Capturing the swelling of solid-electrolyte interphase in lithium metal batteries. *Science* **2022**, *375* (6576), 66−70.
(145) Sayavong, P.; Zhang, W.; Oyakhire, S. T.; Boyle, D. T.; Chen, Y.; Kim, S. C.; Vilá, R. A.; Holmes, S. E.; Kim, M. S.; Bent, S. F.; et al. Dissolution of the Solid Electrolyte Interphase and Its Effects on Lithium Metal Anode Cyclability. *J. Am. Chem. Soc.* **2023**, *145* (22), 12342−12350.
(146) Wang, J.; Luo, J.; Wu, H.; Yu, X.; Wu, X.; Li, Z.; Luo, H.; Zhang, H.; Hong, Y.; Zou, Y.; et al. Visualizing and Regulating Dynamic Evolution of Interfacial Electrolyte Configuration during De-solvation Process on Lithium-Metal Anode. *Angew. Chem., Int. Ed.* **2024**, *63* (17), No. e202400254.
(147) Sun, S.-Y.; Zhang, X.-Q.; Wang, Y.-N.; Li, J.-L.; Zheng, Z.; Huang, J.-Q. Understanding the transport mechanism of lithium ions in solid-electrolyte interphase in lithium metal batteries with liquid electrolytes. *Mater. Today* **2024**, *77*, 39−65.
(148) Chen, X.-R.; Yan, C.; Ding, J.-F.; Peng, H.-J.; Zhang, Q. New insights into "dead lithium" during stripping in lithium metal batteries. *J. Energy Chem.* **2021**, *62*, 289−294.
(149) Jin, C.; Sheng, O.; Wei, G.; Li, H.; Han, Q.; Zhang, Q.; Tao, X. Inhibiting and rejuvenating dead lithium in battery materials. *Nat. Rev. Chem.* **2025**, *9* (8), 553−568.
(150) Hawari, N. H.; Xie, H.; Prayogi, A.; Sumboja, A.; Ding, N. Understanding SEI evolution during the cycling test of anode-free lithium-metal batteries with LiDFOB salt. *RSC Adv.* **2023**, *13* (36), 25673−25680.
(151) Perez-Beltran, S.; Kuai, D.; Balbuena, P. B. SEI Formation and Lithium-Ion Electrodeposition Dynamics in Lithium Metal Batteries via First-Principles Kinetic Monte Carlo Modeling. *ACS Energy Lett.* **2024**, *9* (11), 5268−5278.
(152) An, Y.; Zeng, Y.; Luan, D.; Lou, X. W. Materials design for high-energy-density anode-free batteries. *Matter* **2024**, *7* (4), 1466−1502.
(153) Park, S. K.; Copic, D.; Zhao, T. Z.; Rutkowska, A.; Wen, B.; Sanders, K.; He, R.; Kim, H. K.; De Volder, M. 3D Porous Cu-Composites for Stable Li-Metal Battery Anodes. *ACS Nano* **2023**, *17* (15), 14658−14666.
(154) Tian, M.; Qiao, R.; Cen, G.; Tian, L.; Ben, L.; Yu, H.; De Volder, M.; Zhao, C.; Wang, Q.; Huang, X. Dual-gradient metal layer for practicalizing high-energy lithium batteries. *Nat. Commun.* **2025**, *16* (1), No. 6864.
(155) Li, N.; Ye, Q.; Zhang, K.; Yan, H.; Shen, C.; Wei, B.; Xie, K. Normalized Lithium Growth from the Nucleation Stage for Dendrite-Free Lithium Metal Anodes. *Angew. Chem., Int. Ed.* **2019**, *58* (50), 18246−18251.
(156) He, Y.; Xu, H.; Shi, J.; Liu, P.; Tian, Z.; Dong, N.; Luo, K.; Zhou, X.; Liu, Z. Polydopamine Coating Layer Modified Current Collector for Dendrite-Free Li Metal Anode. *Energy Storage Mater.* **2019**, *23*, 418−426.
(157) Tamwattana, O.; Park, H.; Kim, J.; Hwang, I.; Yoon, G.; Hwang, T.-h.; Kang, Y.-S.; Park, J.; Meethong, N.; Kang, K. High-Dielectric Polymer Coating for Uniform Lithium Deposition in Anode-Free Lithium Batteries. *ACS Energy Lett.* **2021**, *6* (12), 4416−4425.
(158) Jin, S.; Chen, P.; Hong, S.; Shu, H.; Gao, X.; Gao, Z.; Baffour, S.; Fang, M.; Joo, Y. L.; Yang, R.; Archer, L. A. Conformal zwitterionic polymer nanofilms and lithium batteries. *Sci. Adv.* **2025**, *11* (41), No. eady4460.
(159) Oyakhire, S. T.; Huang, W.; Wang, H.; Boyle, D. T.; Schneider, J. R.; de Paula, C.; Wu, Y.; Cui, Y.; Bent, S. F. Revealing and Elucidating ALD-Derived Control of Lithium Plating Microstructure. *Adv. Energy Mater.* **2020**, *10* (44), No. 2002736.
(160) Kim, J.; Lee, G. R.; Chung, R. B. K.; Kim, P. J.; Choi, J. Homogeneous Li deposition guided by ultra-thin lithiophilic layer for highly stable anode-free batteries. *Energy Storage Mater.* **2023**, *61*, No. 102899.
(161) Deng, Y.; Gao, J.; Wang, M.; Deng, J.; Zhou, Y.; Sun, W. Refining grains and optimizing grain boundaries by Al_2Yb to enable a dendrite-free lithium anode. *Energy Environ. Sci.* **2024**, *17* (16), 5901−5910.
(162) Hu, X.; Gao, Y.; Sun, Y.; Hou, Z.; Luo, Y.; Wang, D.; Wang, J.; Zhang, B.; Zheng, Z.; Li, Q. Preserving the Li {110} Texture to Achieve Long Cycle Life in Li Metal Electrode at High Rates. *Adv. Funct. Mater.* **2023**, *34* (11), No. 2307404.
(163) Zheng, J.; Archer, L. A. Crystallographically Textured Electrodes for Rechargeable Batteries: Symmetry, Fabrication, and Characterization. *Chem. Rev.* **2022**, *122* (18), 14440−14470.
(164) Tan, J.; Ma, L.; Yi, P.; Wang, Y.; Li, Z.; Fang, Z.; Li, X.; He, S.; Wang, X.; Ye, M.; Shen, J. Scalable Customization of Crystallographic Plane Controllable Lithium Metal Anodes for Ultralong-Lasting Lithium Metal Batteries. *Adv. Mater.* **2024**, *36* (30), No. e2403570.
(165) Wang, W.; Li, Z.; Chen, S.; Wang, Y.; He, Y.-S.; Ma, Z.-F.; Li, L. The Overlooked Role of Copper Surface Texture in Electrodeposition of Lithium Revealed by Electron Backscatter Diffraction. *ACS Energy Lett.* **2024**, *9* (1), 168−175.
(166) Jin, S.; Huang, M.; Kwon, Y.; Zhang, L.; Li, B.-W.; Oh, S.; Dong, J.; Luo, D.; Biswal, M.; Cunning, B. V.; et al. Colossal grain growth yields single-crystal metal foils by contact-free annealing. *Science* **2018**, *362* (6418), 1021−1025.
(167) Li, S.; Chen, J.; Liu, G.; Wu, H.; Chen, H.; Li, M.; Shi, L.; Wang, Y.; Ma, Y.; Zhao, J. Ultralight Porous Cu Nanowire Aerogels as Stable Hosts for High Li-Content Metal Anodes. *ACS Appl. Mater. Interfaces* **2022**, *14* (51), 56697−56706.
(168) Zhang, S.; Ma, Y.; Zhao, Y.; Qian, Y.; Suo, L.; Wang, X.; Huang, J.; Li, W.; Zhang, B. Lightweight and Flexible 3D ERGO@Cu/PA Mesh Current Collector of Li Metal Battery for Dendrite Suppression. *ACS Appl. Polym. Mater.* **2023**, *5* (5), 3289−3297.

(169) Nahm, Y. W.; Lee, J. S.; Choi, J. H.; Cho, J. S.; Kang, Y. C. 3D Lithiophilic Freestanding Hosts with $SiO_{(x)}$-Embedded Hierarchical Porous N-Doped Carbon Nanofibers for Dendrite-Free Lithium Metal Batteries. *Small* **2025**, *21* (30), No. e2504223.
(170) Wang, X.; Chen, Z.; Jiang, K.; Chen, M.; Passerini, S. 3D Host Design Strategies Guiding "Bottom−Up" Lithium Deposition: A Review. *Adv. Energy Mater.* **2024**, *14* (19), No. 2304229.
(171) Zhang, C.; Lyu, R.; Lv, W.; Li, H.; Jiang, W.; Li, J.; Gu, S.; Zhou, G.; Huang, Z.; Zhang, Y.; et al. A Lightweight 3D Cu Nanowire Network with Phosphidation Gradient as Current Collector for High-Density Nucleation and Stable Deposition of Lithium. *Adv. Mater.* **2019**, *31* (48), No. e1904991.
(172) Gong, M.; Yu, R.; Zhou, C.; Yu, Y.; Pan, Q.; Dong, C.; Shen, C.; Guan, Y.; Sun, C.; Mai, L.; Xu, X. Mechanically Robust Current Collector with Gradient Lithiophilicity Induced by Spontaneous Lithium Ion Diffusion for Stable Lean-Lithium Metal Batteries. *ACS Nano* **2024**, *18*, 20648−20658, DOI: 10.1021/acsnano.4c06111.
(173) Matula, R. A. Electrical resistivity of copper, gold, palladium, and silver. *J. Phys. Chem. Ref. Data* **1979**, *8* (4), 1147−1298.
(174) Choudhury, R.; Wild, J.; Yang, Y. Engineering current collectors for batteries with high specific energy. *Joule* **2021**, *5* (6), 1301−1305.
(175) Barbir, F. *PEM fuel cells: theory and practice*; Academic Press, 2012.
(176) Zhu, P.; Gastol, D.; Marshall, J.; Sommerville, R.; Goodship, V.; Kendrick, E. A review of current collectors for lithium-ion batteries. *J. Power Sources* **2021**, *485*, No. 229321.
(177) Subrenat, A.; Baléo, J.; Le Cloirec, P.; Blanc, P. Electrical behaviour of activated carbon cloth heated by the joule effect: desorption application. *Carbon* **2001**, *39* (5), 707−716.
(178) Yuan, J.; Zhang, Y.; Chen, F.; Gu, Z. An overview of Joule heating in energy storage materials and applications. *J. Mater. Chem. C* **2024**, *12* (37), 14729−14753.
(179) Guo, Q.; Wang, S.; Li, Y.; Wang, J.; Wu, Y.; Yu, Y.; Xia, S.; Hu, D.; Hu, B.; Ye, Z.; et al. Weldable and electrochemically stable composite of graphene and polyvinylidene fluoride as a current collector for promoting reversible lithium plating/stripping. *J. Power Sources* **2023**, *580*, No. 233401.
(180) Lee, S.; Yang, S.; Lee, K.; Jung, Y.; Choi, J.; Kim, T.; Kim, P. J. Dendrite-suppressed Li deposition enabled by surface-tailored carbon-based current collectors for high-rate and stable Li-metal batteries. *Carbon* **2024**, *221*, No. 118941.
(181) Ma, X. X.; Chen, X.; Bai, Y. K.; Shen, X.; Zhang, R.; Zhang, Q. The Defect Chemistry of Carbon Frameworks for Regulating the Lithium Nucleation and Growth Behaviors in Lithium Metal Anodes. *Small* **2021**, *17* (48), No. e2007142.
(182) Cao, X.; Xu, Y.; Zou, L.; Bao, J.; Chen, Y.; Matthews, B. E.; Hu, J.; He, X.; Engelhard, M. H.; Niu, C.; et al. Stability of solid electrolyte interphases and calendar life of lithium metal batteries. *Energy Environ. Sci.* **2023**, *16* (4), 1548−1559.
(183) Kim, S.; Barnes, P.; Zhang, H.; Efaw, C.; Wang, Y.; Park, B.; Li, B.; Chen, B.-R.; Evans, M. C.; Liaw, B.; et al. Calendar life of lithium metal batteries: Accelerated aging and failure analysis. *Energy Storage Mater.* **2024**, *65*, No. 103147.
(184) Lin, D.; Liu, Y.; Li, Y.; Li, Y.; Pei, A.; Xie, J.; Huang, W.; Cui, Y. Fast galvanic lithium corrosion involving a Kirkendall-type mechanism. *Nat. Chem.* **2019**, *11* (4), 382−389.
(185) Kwon, H.; Kim, H.; Hwang, J.; Oh, W.; Roh, Y.; Shin, D.; Kim, H.-T. Borate−pyran lean electrolyte-based Li-metal batteries with minimal Li corrosion. *Nat. Energy* **2024**, *9* (1), 57−69.
(186) Boyle, D. T.; Huang, W.; Wang, H.; Li, Y.; Chen, H.; Yu, Z.; Zhang, W.; Bao, Z.; Cui, Y. Corrosion of lithium metal anodes during calendar ageing and its microscopic origins. *Nat. Energy* **2021**, *6* (5), 487−494.
(187) Yuan, X.; Cheng, D.; Liu, B.; Liang, K.; Liang, K.; Yu, J.; Mecklenburg, M.; Sautet, P.; Li, Y. Engineering battery corrosion films by tuning electrical double layer composition. *Joule* **2024**, *8* (11), 3038−3053.
(188) Ding, J. F.; Xu, R.; Xiao, Y.; Zhang, S.; Song, T. L.; Yan, C.; Huang, J. Q. Dynamic Galvanic Corrosion of Working Lithium Metal Anode Under Practical Conditions. *Adv. Energy Mater.* **2023**, *13* (21), No. 2204305.
(189) Zhen, C.; Yang, X.; Wei, X.; Zhu, Y.; Han, S.; Shi, X.; Deng, L.; Gu, M. D. Revealing Lithium Nitrate-Mediated Solid-Electrolyte Interphase of Lithium Metal Anode via Cryogenic Transmission Electron Microscopy. *Nano Lett.* **2024**, *24* (22), 6714−6721.
(190) Du, H.; Wang, Y.; Kang, Y.; Zhao, Y.; Tian, Y.; Wang, X.; Tan, Y.; Liang, Z.; Wozny, J.; Li, T.; et al. Side Reactions/Changes in Lithium-Ion Batteries: Mechanisms and Strategies for Creating Safer and Better Batteries. *Adv. Mater.* **2024**, *36* (29), No. e2401482.
(191) Louli, A. J.; Eldesoky, A.; deGooyer, J.; Coon, M.; Aiken, C. P.; Simunovic, Z.; Metzger, M.; Dahn, J. R. Different Positive Electrodes for Anode-Free Lithium Metal Cells. *J. Electrochem. Soc.* **2022**, *169* (4), No. 040517.
(192) Betz, J.; Brinkmann, J. P.; Nölle, R.; Lürenbaum, C.; Kolek, M.; Stan, M. C.; Winter, M.; Placke, T. Cross Talk between Transition Metal Cathode and Li Metal Anode: Unraveling Its Influence on the Deposition/Dissolution Behavior and Morphology of Lithium. *Adv. Energy Mater.* **2019**, *9* (21), No. 1900574.
(193) Gervillié-Mouravieff, C.; Ah, L.; Liu, A.; Huang, C.-J.; Meng, Y. S. Deciphering the Impact of the Active Lithium Reservoir in Anode-Free Pouch Cells. *ACS Energy Lett.* **2024**, *9* (4), 1693−1700.
(194) Fraggedakis, D.; Nadkarni, N.; Gao, T.; Zhou, T.; Zhang, Y.; Han, Y.; Stephens, R. M.; Shao-Horn, Y.; Bazant, M. Z. A scaling law to determine phase morphologies during ion intercalation. *Energy Environ. Sci.* **2020**, *13* (7), 2142−2152.
(195) Koo, J. K.; Ran, W. T. A.; Yun, Y.; Seo, J. K.; Kim, M.; Lee, J.; Lee, S.; Kim, J.; Hwang, S. M.; Kim, Y.-J. Probing intraparticle heterogeneity in Ni-rich layered cathodes with different carbon black contents using scanning probe microscopy. *J. Energy Storage* **2022**, *51*, No. 104395.
(196) Kim, M.-H.; Jang, H.; Lee, E.; Seo, J.; Park, J.; Choi, A.; Kim, T.; Choi, M.; Kim, E.; Jung, Y. H.; et al. Metal-to-metal charge transfer for stabilizing high-voltage redox in lithium-rich layered oxide cathodes. *Sci. Adv.* **2025**, *11* (8), No. eadt0232.
(197) Lin, F.; Zhao, K.; Liu, Y. Heterogeneous Reaction Activities and Statistical Characteristics of Particle Cracking in Battery Electrodes. *ACS Energy Lett.* **2021**, *6* (11), 4065−4070.
(198) Li, S.; Zhang, H.; Liu, Y.; Wang, L.; He, X. Comprehensive Understanding of Structure Transition in $LiMn_yFe_{1-y}PO_4$ during Delithiation/Lithiation. *Adv. Funct. Mater.* **2023**, *34* (4), No. 2310057.
(199) Hou, L. P.; Li, Z.; Yao, N.; Bi, C. X.; Li, B. Q.; Chen, X.; Zhang, X. Q.; Zhang, Q. Weakening the Solvating Power of Solvents to Encapsulate Lithium Polysulfides Enables Long-Cycling Lithium-Sulfur Batteries. *Adv. Mater.* **2022**, *34* (45), No. e2205284.
(200) Li, X. Y.; Li, B. Q.; Feng, S.; Li, Z.; Shen, L.; Sun, S. Y.; Chen, Z. X.; Jin, T.; Chen, X.; Zhao, M.; et al. Two-Stage Solvation of Lithium Polysulfides in Working Lithium-Sulfur Batteries. *J. Am. Chem. Soc.* **2025**, *147* (18), 15435−15447.
(201) Li, Z.; Li, B. Q.; Chen, L. L.; Gao, Y. C.; Bi, C. X.; Zhao, M.; Chen, X.; Li, X. Y.; Zhang, Q. Regulating Lithium Bond to Reduce Polysulfide Parasitic Reactivity for High-Stability Lithium Metal Anode. *Angew. Chem., Int. Ed.* **2026**, *65* (10), No. e22034.
(202) Zhu, Y. J.; Bi, C. X.; Zhao, M.; Li, Z.; Feng, W. J.; Sun, F.; Zhang, X. Q.; Li, B. Q.; Huang, J. Q. Deciphering the Species-Dependent Polysulfide Corrosion on Lithium Anode Toward Durable Lithium-Sulfur Batteries. *Adv. Mater.* **2025**, *37* (37), No. e2506132.
(203) Peng, H. J.; Hou, T. Z.; Zhang, Q.; Huang, J. Q.; Cheng, X. B.; Guo, M. Q.; Yuan, Z.; He, L. Y.; Wei, F. Strongly Coupled Interfaces between a Heterogeneous Carbon Host and a Sulfur-Containing Guest for Highly Stable Lithium-Sulfur Batteries: Mechanistic Insight into Capacity Degradation. *Adv. Mater. Interfaces* **2014**, *1* (7), No. 1400227.
(204) Zhou, G.; Paek, E.; Hwang, G. S.; Manthiram, A. Long-life Li/polysulphide batteries with high sulphur loading enabled by

lightweight three-dimensional nitrogen/sulphur-codoped graphene sponge. *Nat. Commun.* **2015**, *6*, No. 7760.
(205) Chen, J.-J.; Yuan, R.-M.; Feng, J.-M.; Zhang, Q.; Huang, J.-X.; Fu, G.; Zheng, M.-S.; Ren, B.; Dong, Q.-F. Conductive Lewis Base Matrix to Recover the Missing Link of Li_0S_8 during the Sulfur Redox Cycle in Li−S Battery. *Chem. Mater.* **2015**, *27* (6), 2048−2055.
(206) He, J.; Manthiram, A. A review on the status and challenges of electrocatalysts in lithium-sulfur batteries. *Energy Storage Mater.* **2019**, *20*, 55−70.
(207) Wang, P.; Xi, B.; Huang, M.; Chen, W.; Feng, J.; Xiong, S. Emerging Catalysts to Promote Kinetics of Lithium−Sulfur Batteries. *Adv. Energy Mater.* **2021**, *11* (7), No. 2002893.
(208) Bi, C.-X.; Zhu, Y.-J.; Li, X.-Y.; Ma, J.; Zhang, X.-Q.; Zhao, M.; Li, B.-Q.; Huang, J.-Q. Galvanic Corrosion of Lithium Metal Anodes in Lithium−Sulfur Batteries. *J. Am. Chem. Soc.* **2025**, *147* (38), 34632−34640.
(209) Bi, C. X.; Zhu, Y. J.; Li, Z.; Zhao, M.; Zhang, X. Q.; Li, B. Q.; Huang, J. Q. Evolution of Lithium Metal Anode Along Cycling in Working Lithium−Sulfur Batteries. *Adv. Energy Mater.* **2024**, *14* (39), No. 2402609.
(210) Zhao, S.; Yan, K.; Zhang, J.; Sun, B.; Wang, G. Reaction Mechanisms of Layered Lithium-Rich Cathode Materials for High-Energy Lithium-Ion Batteries. *Angew. Chem., Int. Ed.* **2021**, *60* (5), 2208−2220.
(211) Hua, W.; Wang, S.; Knapp, M.; Leake, S. J.; Senyshyn, A.; Richter, C.; Yavuz, M.; Binder, J. R.; Grey, C. P.; Ehrenberg, H.; et al. Structural insights into the formation and voltage degradation of lithium- and manganese-rich layered oxides. *Nat. Commun.* **2019**, *10* (1), No. 5365.
(212) Chen, H.; Sun, C. Recent advances in lithium-rich manganese-based cathodes for high energy density lithium-ion batteries. *Chem. Commun.* **2023**, *59* (59), 9029−9055.
(213) Zheng, X.; Xue, Z.; Hao, H.; Cho, Y.; Li, Y.; Kim, C.; Czaja, P.; Lee, S. S.; Bone, S.; Spielman-Sun, E.; et al. Unravelling electro-chemo-mechanical interplay in layered oxide cathode degradation in solid-state batteries. *Sci. Adv.* **2025**, *11* (41), No. eady7189.
(214) Weng, C.; Qiu, M.; Wang, B.; Yang, J.; Mai, W.; Pan, L.; Huang, S.; Li, J. Organic Cathode Electrolyte Interphase Achieving 4.8 V $LiCoO_2$. *Angew. Chem., Int. Ed.* **2025**, *64* (7), No. e202419539.
(215) Sun, Y.; Lee, H.-W.; Seh, Z. W.; Liu, N.; Sun, J.; Li, Y.; Cui, Y. High-capacity battery cathode prelithiation to offset initial lithium loss. *Nat. Energy* **2016**, *1* (1), No. 15008.
(216) Huang, C. J.; Hsu, Y. C.; Shitaw, K. N.; Siao, Y. J.; Wu, S. H.; Wang, C. H.; Su, W. N.; Hwang, B. J. Lithium Oxalate as a Lifespan Extender for Anode-Free Lithium Metal Batteries. *ACS Appl. Mater. Interfaces* **2022**, *14* (23), 26724−26732.
(217) Wang, D.; Zhang, Z.; Hong, B.; Lai, Y. Self-sacrificial organic lithium salt enhanced initial Coulombic efficiency for safer and greener lithium-ion batteries. *Chem. Commun.* **2019**, *55* (72), 10737−10739.
(218) Lee, D.; Kim, J.; Sun, S.; Kim, J.; Paik, U.; Song, T. Sacrificial cathode additives for enhanced cycle performance for liquid and all−solid−state anode−free lithium secondary batteries. *J. Alloys Compd.* **2023**, *950*, No. 169910.
(219) Ding, R.; Tian, S.; Zhang, K.; Cao, J.; Zheng, Y.; Tian, W.; Wang, X.; Wen, L.; Wang, L.; Liang, G. Recent advances in cathode prelithiation additives and their use in lithium−ion batteries. *J. Electroanal. Chem.* **2021**, *893*, No. 115325.
(220) Wang, F.; Wang, B.; Li, J.; Wang, B.; Zhou, Y.; Wang, D.; Liu, H.; Dou, S. Prelithiation: A Crucial Strategy for Boosting the Practical Application of Next-Generation Lithium Ion Battery. *ACS Nano* **2021**, *15* (2), 2197−2218.
(221) Lee, W.; Byeon, Y. S.; Lee, S.; Kong, S.; Park, M. S.; Yoon, W. S. Over- and Hyper-Lithiated Oxides as Sacrificial Cathodes for Lithium-Ion Batteries. *Adv. Energy Mater.* **2024**, *15* (2), No. 2304533.
(222) Wu, Y.; Zhang, W.; Li, S.; Wen, N.; Zheng, J.; Zhang, L.; Zhang, Z.; Lai, Y. $Li_2Cu_{0.1}Ni_{0.9}O_2$ with Copper Substitution: A New Cathode Prelithiation Additive for Lithium-Ion Batteries. *ACS Sustainable Chem. Eng.* **2023**, *11* (3), 1044−1053.
(223) Xiao, R.; Kang, C.; Ren, Y.; Jian, J.; Cui, B.; Yin, G.; Ma, Y.; Zuo, P.; Han, G.; Du, C. Electrolyte-assisted low-voltage decomposition of $Li_2C_2O_4$ for efficient cathode pre-lithiation in lithium-ion batteries. *Chem. Commun.* **2023**, *59* (94), 13982−13985.
(224) Wang, X.; Liu, C.; Zhang, S.; Wang, H.; Wang, R.; Li, Y.; Sun, J. Dual-Functional Cathodic Prelithiation Reagent of Li_3P in Lithium-Ion Battery for Compensating Initial Capacity Loss and Enhancing Safety. *ACS Appl. Energy Mater.* **2021**, *4* (5), 5246−5254.
(225) Zhu, Y.; Chen, Y.; Chen, J.; Yin, J.; Sun, Z.; Zeng, G.; Wu, X.; Chen, L.; Yu, X.; Luo, H.; et al. Lattice Engineering on Li_2CO_3-Based Sacrificial Cathode Prelithiation Agent for Improving the Energy Density of Li-Ion Battery Full-Cell. *Adv. Mater.* **2024**, *36* (13), No. e2312159.
(226) Park, K.; Yu, B. C.; Goodenough, J. B. Li3N as a Cathode Additive for High-Energy-Density Lithium-Ion Batteries. *Adv. Energy Mater.* **2016**, *6* (10), No. 1502534.
(227) Kim, H.; Jun, K.; Szymanski, N.; Sai Avvaru, V.; Cai, Z.; Crafton, M.; Lee, G. H.; Trask, S. E.; Babbe, F.; Byeon, Y. W.; et al. Screening and Development of Sacrificial Cathode Additives for Lithium-Ion Batteries. *Adv. Energy Mater.* **2025**, *15* (21), No. 2403946.
(228) Sun, Y.; Li, Y.; Sun, J.; Li, Y.; Pei, A.; Cui, Y. Stabilized Li3N for efficient battery cathode prelithiation. *Energy Storage Mater.* **2017**, *6*, 119−124.
(229) Zheng, L.; Li, G.; Zhang, J. Grain boundaries boost the prelithiation capability of the Li_2CO_3 cathode additives for high-energy-density lithium-ion batteries. *Chem. Eng. J.* **2023**, *475*, No. 146285.
(230) Zhang, H.; Bai, T.; Cheng, J.; Ji, F.; Zeng, Z.; Li, Y.; Zhang, C.; Wang, J.; Xia, W.; Ci, N.; et al. Unlocking the decomposition limitations of the $Li_2C_2O_4$ for highly efficient cathode preliathiations. *Adv. Powder Mater.* **2024**, *3* (5), No. 100215.
(231) Xia, B.; Zhang, G.; Tao, F.; Huang, M. Promising Pre-Lithiation Agent $Li_2C_2O_4$@KB for High-Performance NCM622 Cell. *Materials* **2025**, *18* (19), 4467.
(232) Lee, W.; Byeon, Y. S.; Jeong, S. H.; Kim, J.-U.; Lee, S.; Park, S.; Park, M.-S.; Yoon, W.-S. Advances and Challenges in Li-Excess Cathode Additives for Next-Generation Li Rechargeable Batteries. *ACS Energy Lett.* **2025**, *10* (7), 3151−3177.
(233) Chen, S.; Wu, G.; Jiang, H.; Wang, J.; Chen, T.; Han, C.; Wang, W.; Yang, R.; Zhao, J.; Tang, Z.; et al. External Li supply reshapes Li deficiency and lifetime limit of batteries. *Nature* **2025**, *638* (8051), 676−683.
(234) Peljo, P.; Girault, H. H. Electrochemical potential window of battery electrolytes: the HOMO−LUMO misconception. *Energy Environ. Sci.* **2018**, *11* (9), 2306−2309.
(235) Goodenough, J. B.; Park, K. S. The Li-ion rechargeable battery: a perspective. *J. Am. Chem. Soc.* **2013**, *135* (4), 1167−1176.
(236) Wan, H.; Xu, J.; Wang, C. Designing electrolytes and interphases for high-energy lithium batteries. *Nat. Rev. Chem.* **2024**, *8* (1), 30−44.
(237) Lim, M.; Lee, J.; Lee, S.; Park, S.; Lee, H. Modulation of Li^+ microenvironment in liquid electrolyte for interface design of Li-metal anodes. *Bull. Korean Chem. Soc.* **2024**, *45* (8), 648−663.
(238) Jeong, S.-K.; Seo, H.-Y.; Kim, D.-H.; Han, H.-K.; Kim, J.-G.; Lee, Y. B.; Iriyama, Y.; Abe, T.; Ogumi, Z. Suppression of dendritic lithium formation by using concentrated electrolyte solutions. *Electrochem. Commun.* **2008**, *10* (4), 635−638.
(239) Qiao, R.; Zhao, Y.; Zhou, S.; Zhang, H.; Liu, F.; Zhou, T.; Sun, B.; Fan, H.; Li, C.; Zhang, Y.; et al. Non-fluorinated electrolytes with micelle-like solvation for ultra-high-energy-density lithium metal batteries. *Chem* **2025**, *11* (2), No. 102306.
(240) Chang, C.; Yao, Y.; Li, R.; Cong, Z.; Li, L.; Guo, Z. H.; Hu, W.; Pu, X. Stable lithium metal batteries enabled by localized high-concentration electrolytes with sevoflurane as a diluent. *J. Mater. Chem. A* **2022**, *10* (16), 9001−9009.
(241) Zheng, Y.; Soto, F. A.; Ponce, V.; Seminario, J. M.; Cao, X.; Zhang, J.-G.; Balbuena, P. B. Localized high concentration electrolyte

behavior near a lithium−metal anode surface. *J. Mater. Chem. A* **2019**, *7* (43), 25047−25055.
(242) Perez Beltran, S.; Cao, X.; Zhang, J.-G.; Balbuena, P. B. Localized High Concentration Electrolytes for High Voltage Lithium−Metal Batteries: Correlation between the Electrolyte Composition and Its Reductive/Oxidative Stability. *Chem. Mater.* **2020**, *32* (14), 5973−5984.
(243) Yu, L.; Chen, S.; Lee, H.; Zhang, L.; Engelhard, M. H.; Li, Q.; Jiao, S.; Liu, J.; Xu, W.; Zhang, J.-G. A Localized High-Concentration Electrolyte with Optimized Solvents and Lithium Difluoro(oxalate)-borate Additive for Stable Lithium Metal Batteries. *ACS Energy Lett.* **2018**, *3* (9), 2059−2067.
(244) Chen, Y.; Yu, Z.; Gong, H.; Zhang, W.; Rudnicki, P. E.; Huang, Z.; Yu, W.; Kim, S. C.; Boyle, D. T.; Sayavong, P.; et al. Failure Process During Fast Charging of Lithium Metal Batteries with Weakly Solvating Fluoroether Electrolytes. *J. Phys. Chem. C* **2024**, *128* (28), 11487−11497.
(245) Kim, S. C.; Gao, X.; Liao, S. L.; Su, H.; Chen, Y.; Zhang, W.; Greenburg, L. C.; Pan, J. A.; Zheng, X.; Ye, Y.; et al. Solvation-property relationship of lithium-sulphur battery electrolytes. *Nat. Commun.* **2024**, *15* (1), No. 1268.
(246) Chen, Y.; Liao, S. L.; Gong, H.; Zhang, Z.; Huang, Z.; Kim, S. C.; Zhang, E.; Lyu, H.; Yu, W.; Lin, Y.; et al. Hyperconjugation-controlled molecular conformation weakens lithium-ion solvation and stabilizes lithium metal anodes. *Chem. Sci.* **2024**, *15* (47), 19805−19819.
(247) Zhang, J.; Li, Q.; Zeng, Y.; Tang, Z.; Sun, D.; Huang, D.; Tang, Y.; Wang, H. Weakly Solvating Cyclic Ether Electrolyte for High-Voltage Lithium Metal Batteries. *ACS Energy Lett.* **2023**, *8* (4), 1752−1761.
(248) Liao, Y.; Lin, W.; Zhang, Y.; Yang, J.; Li, Z.; Ren, Y.; Wang, D.; Huang, Y.; Yuan, L. A Weakly Solvating Ether Electrolyte Enables Fast-Charging and Wide-Temperature Lithium-Ion Pouch Cells. *ACS Nano* **2024**, *18*, 20762−20771.
(249) Karbak, M.; Yim, K.; Meng, Y. S.; Shao, Y.; Xu, W. Weakly solvating electrolytes: a solvation-centric paradigm for rechargeable metal batteries. *Chem. Sci.* **2025**, *16* (44), 20694−20717.
(250) Xu, J. High-entropy electrolytes in boosting battery performance. *Mater. Fut.* **2023**, *2* (4), No. 047501.
(251) Zhao, X.; Fu, Z.; Zhang, X.; Wang, X.; Li, B.; Zhou, D.; Kang, F. More is better: high-entropy electrolyte design in rechargeable batteries. *Energy Environ. Sci.* **2024**, *17* (7), 2406−2430.
(252) Wang, M.; Zheng, M.; Lu, J.; You, Y. High-entropy electrolyte toward battery working under extreme conditions. *Joule* **2024**, *8* (9), 2467−2482.
(253) Ren, K.-F.; Liu, H.; Guo, J.-X.; Sun, X.; Jiang, F.; Guo, C.; Bao, W.; Yu, F.; Kalimuldina, G.; Kong, L.; et al. Working Principles of High-Entropy Electrolytes in Rechargeable Batteries. *ACS Energy Lett.* **2024**, *9* (6), 2960−2980.
(254) Zhang, X. Q.; Cheng, X. B.; Chen, X.; Yan, C.; Zhang, Q. Fluoroethylene Carbonate Additives to Render Uniform Li Deposits in Lithium Metal Batteries. *Adv. Funct. Mater.* **2017**, *27* (10), No. 1605989.
(255) Zhao, Q.; Utomo, N. W.; Kocen, A. L.; Jin, S.; Deng, Y.; Zhu, V. X.; Moganty, S.; Coates, G. W.; Archer, L. A. Upgrading Carbonate Electrolytes for Ultra-stable Practical Lithium Metal Batteries. *Angew. Chem., Int. Ed.* **2022**, *61* (9), No. e202116214.
(256) Ota, H.; Shima, K.; Ue, M.; Yamaki, J.-i. Effect of vinylene carbonate as additive to electrolyte for lithium metal anode. *Electrochim. Acta* **2004**, *49* (4), 565−572.
(257) Yang, Y.; Xiong, J.; Lai, S.; Zhou, R.; Zhao, M.; Geng, H.; Zhang, Y.; Fang, Y.; Li, C.; Zhao, J. Vinyl Ethylene Carbonate as an Effective SEI-Forming Additive in Carbonate-Based Electrolyte for Lithium-Metal Anodes. *ACS Appl. Mater. Interfaces* **2019**, *11* (6), 6118−6125.
(258) Ma, Y.; Zhou, Z.; Li, C.; Wang, L.; Wang, Y.; Cheng, X.; Zuo, P.; Du, C.; Huo, H.; Gao, Y.; et al. Enabling reliable lithium metal batteries by a bifunctional anionic electrolyte additive. *Energy Storage Mater.* **2018**, *11*, 197−204.
(259) Dai, L.; Cai, M.; Zhou, X.; Liang, W.; Zhao, Z.; Xia, Z.; Huang, F.; Jiang, J.; Jiang, W.; Zhang, B.; Ma, Z. Catalysis of a LiF-rich SEI by aromatic structure modified porous polyamine for stable all-solid-state lithium metal batteries. *Chem. Sci.* **2025**, *16* (5), 2453−2464.
(260) Liu, Y.; Tao, X.; Wang, Y.; Jiang, C.; Ma, C.; Sheng, O.; Lu, G.; Lou, X. W. Self-assembled monolayers direct a LiF-rich interphase toward long-life lithium metal batteries. *Science* **2022**, *375* (6582), 739−745.
(261) Wu, Z.; Wang, C.; Hui, Z.; Liu, H.; Wang, S.; Yu, S.; Xing, X.; Holoubek, J.; Miao, Q.; Xin, H. L.; Liu, P. Growing single-crystalline seeds on lithiophobic substrates to enable fast-charging lithium-metal batteries. *Nat. Energy* **2023**, *8*, 340−350.
(262) Dong, P.; Xie, Z.; Li, F.; Hou, S.; Zhang, D.; Gao, W.; Lei, Y.; Yang, B.; Liang, F. Li_3N/Li_2O-rich artificial SEI formed by in-situ dielectric barrier discharge plasma for lithium metal batteries. *Chem. Eng. J.* **2026**, *529*, No. 173130.
(263) Zeng, H.; Yu, K.; Li, J.; Yuan, M.; Wang, J.; Wang, Q.; Lai, A.; Jiang, Y.; Yan, X.; Zhang, G.; et al. Beyond LiF: Tailoring Li_2O-Dominated Solid Electrolyte Interphase for Stable Lithium Metal Batteries. *ACS Nano* **2024**, *18* (3), 1969−1981.
(264) Guo, R.; Gallant, B. M. Li_2O Solid Electrolyte Interphase: Probing Transport Properties at the Chemical Potential of Lithium. *Chem. Mater.* **2020**, *32* (13), 5525−5533.
(265) Hobold, G. M.; Wang, C.; Steinberg, K.; Li, Y.; Gallant, B. M. High lithium oxide prevalence in the lithium solid−electrolyte interphase for high Coulombic efficiency. *Nat. Energy* **2024**, *9* (5), 580−591.
(266) Gao, Y.-C.; Yao, N.; Chen, X.; Yu, L.; Zhang, R.; Zhang, Q. Data-Driven Insight into the Reductive Stability of Ion−Solvent Complexes in Lithium Battery Electrolytes. *J. Am. Chem. Soc.* **2023**, *145* (43), 23764−23770.
(267) Ma, P.; Kumar, R.; Wang, K. H.; Amanchukwu, C. V. Active learning accelerates electrolyte solvent screening for anode-free lithium metal batteries. *Nat. Commun.* **2025**, *16* (1), No. 8396.
(268) Kumar, R.; Vu, M. C.; Ma, P.; Amanchukwu, C. V. Electrolytomics: A Unified Big Data Approach for Electrolyte Design and Discovery. *Chem. Mater.* **2025**, *37* (8), 2720−2734.
(269) Kwon, H.; Kim, S.; Hyun, J.; Lee, H. E.; Kim, S. S.; Kim, Y.; Kim, I. J.; Shin, K.; Kim, S.; Park, C.; et al. Covariance of interphasic properties and fast chargeability of energy-dense lithium metal batteries. *Nat. Energy* **2025**, *10* (9), 1132−1145.
(270) Jang, J.; Wang, C.; Kang, G.; Han, C.; Han, J.; Shin, J.-S.; Ko, S.; Kim, G.; Baek, J.; Kim, H.-T.; et al. Miniature Li^+ solvation by symmetric molecular design for practical and safe Li-metal batteries. *Nat. Energy* **2025**, *10* (4), 502−512.
(271) Ding, J. F.; Xu, R.; Ma, X. X.; Xiao, Y.; Yao, Y. X.; Yan, C.; Huang, J. Q. Quantification of the Dynamic Interface Evolution in High-Efficiency Working Li-Metal Batteries. *Angew. Chem., Int. Ed.* **2022**, *61* (13), No. e202115602.
(272) Wang, D.; Katayama, Y.; von Holtum, B.; Svirinovsky-Arbeli, A.; Smith, M.; Inoue, K.-i.; Hestenes, J. C.; Ah, L.; Iriawan, H.; Ceribelli, N.; et al. Revealing the lithium solid electrolyte interphase in liquid electrolytes via in situ Fourier transform infrared spectroscopy. *Cell Press Blue* **2026**, *1*, No. 100002.
(273) Lee, S.-Y.; Shangguan, J.; Betzler, S.; Harris, S. J.; Doeff, M. M.; Zheng, H. Lithium metal stripping mechanisms revealed through electrochemical liquid cell electron microscopy. *Nano Energy* **2022**, *102*, No. 107641.
(274) Lorger, S.; Narita, K.; Usiskin, R.; Maier, J. Enhanced ion transport in Li_2O and Li_2S films. *Chem. Commun.* **2021**, *57* (53), 6503−6506.
(275) Chen, J.; Buhrmester, C.; Dahn, J. R. Chemical Overcharge and Overdischarge Protection for Lithium-Ion Batteries. *Electrochem. Solid-State Lett.* **2005**, *8* (1), No. A59.
(276) Chen, Y.; Freunberger, S. A.; Peng, Z.; Fontaine, O.; Bruce, P. G. Charging a Li-O_2 battery using a redox mediator. *Nat. Chem.* **2013**, *5* (6), 489−494.

(277) Jin, C.; Liu, T.; Sheng, O.; Li, M.; Liu, T.; Yuan, Y.; Nai, J.; Ju, Z.; Zhang, W.; Liu, Y.; et al. Rejuvenating dead lithium supply in lithium metal anodes by iodine redox. *Nat. Energy* **2021**, *6* (4), 378−387.
(278) Zhang, Y.; Liu, J.; Li, Y.; Zhao, D.; Huang, W.; Zheng, Y.; Zhou, J.; Zhu, C.; Deng, C.; Sun, Y.; et al. Reactivating the Dead Lithium by Redox Shuttle to Promote the Efficient Utilization of Lithium for Anode Free Lithium Metal Batteries. *Adv. Funct. Mater.* **2023**, *33* (40), No. 2301332.
(279) Chen, J.; He, B.; Cheng, Z.; Rao, Z.; He, D.; Liu, D.; Li, X.; Yuan, L.; Huang, Y.; Li, Z. Reactivating Dead Li by Shuttle Effect for High-Performance Anode-Free Li Metal Batteries. *J. Electrochem. Soc.* **2021**, *168* (12), No. 120535.
(280) Jin, C. B.; Zhang, X. Q.; Sheng, O. W.; Sun, S. Y.; Hou, L. P.; Shi, P.; Li, B. Q.; Huang, J. Q.; Tao, X. Y.; Zhang, Q. Reclaiming Inactive Lithium with a Triiodide/Iodide Redox Couple for Practical Lithium Metal Batteries. *Angew. Chem., Int. Ed.* **2021**, *60* (42), 22990−22995.
(281) Li, Y.; Feng, X.; Ren, D.; Ouyang, M.; Lu, L.; Han, X. Thermal Runaway Triggered by Plated Lithium on the Anode after Fast Charging. *ACS Appl. Mater. Interfaces* **2019**, *11* (50), 46839−46850.
(282) Liu, D.; Ren, Z.; Kang, Z.; Dang, Z.; Da, Q.; Zhang, Y.; Yang, P. A periodic reactivation strategy with redox mediator towards dead Lithium-free Lithium metal batteries. *Electrochem. Commun.* **2026**, *182*, No. 108099.
(283) Timke, B.; Winter, M.; Niehoff, P. Impact of Different Amounts of Lithium Plating on the Thermal Safety of Lithium Ion Cells. *J. Electrochem. Soc.* **2024**, *171* (7), No. 070538.
(284) Lu, B.; Li, W.; Cheng, D.; Bhamwala, B.; Ceja, M.; Bao, W.; Fang, C.; Meng, Y. S. Suppressing Chemical Corrosions of Lithium Metal Anodes. *Adv. Energy Mater.* **2022**, *12* (48), No. 2202012.
(285) Xiang, Y.; Tao, M.; Zhong, G.; Liang, Z.; Zheng, G.; Huang, X.; Liu, X.; Jin, Y.; Xu, N.; Armand, M.; et al. Quantitatively analyzing the failure processes of rechargeable Li metal batteries. *Sci. Adv.* **2021**, *7* (46), No. eabj3423.
(286) Cameron, J. M.; Holc, C.; Kibler, A. J.; Peake, C. L.; Walsh, D. A.; Newton, G. N.; Johnson, L. R. Molecular redox species for next-generation batteries. *Chem. Soc. Rev.* **2021**, *50* (10), 5863−5883.
(287) Chen, J.; Cheng, Z.; Liao, Y.; Yuan, L.; Li, Z.; Huang, Y. Selection of Redox Mediators for Reactivating Dead Li in Lithium Metal Batteries. *Adv. Energy Mater.* **2022**, *12* (40), No. 2201800.
(288) Tsao, Y.; Lee, M.; Miller, E. C.; Gao, G.; Park, J.; Chen, S.; Katsumata, T.; Tran, H.; Wang, L.-W.; Toney, M. F.; et al. Designing a Quinone-Based Redox Mediator to Facilitate Li2S Oxidation in Li-S Batteries. *Joule* **2019**, *3* (3), 872−884.
(289) Yang, R.; Wang, F.; Cui, W.-e.; Chen, W.; Lei, T.; Chen, D.; Chen, D.; Xia, L.; Zhang, C.; Cheng, K.; et al. Regenerative redox mediator for the suppression of dead lithium for lithium sulfur pouch cell. *Energy Storage Mater.* **2025**, *75*, No. 104030.
(290) Deng, W.; Yin, X.; Bao, W.; Zhou, X.; Hu, Z.; He, B.; Qiu, B.; Meng, Y. S.; Liu, Z. Quantification of reversible and irreversible lithium in practical lithium-metal batteries. *Nat. Energy* **2022**, *7* (11), 1031−1041.
(291) Jin, W.; Song, G.; Yoo, J. K.; Jung, S. K.; Kim, T. H.; Kim, J. Advancements in Dry Electrode Technologies: Towards Sustainable and Efficient Battery Manufacturing. *ChemElectroChem* **2024**, *11* (17), No. e202400288.
(292) Lu, Y.; Zhao, C.-Z.; Yuan, H.; Hu, J.-K.; Huang, J.-Q.; Zhang, Q. Dry electrode technology, the rising star in solid-state battery industrialization. *Matter* **2022**, *5* (3), 876−898.
(293) Kwon, K.; Kim, J.; Han, S.; Lee, J.; Lee, H.; Kwon, J.; Lee, J.; Seo, J.; Kim, P. J.; Song, T.; Choi, J. Low-Resistance $LiFePO_4$ Thick Film Electrode Processed with Dry Electrode Technology for High-Energy-Density Lithium-Ion Batteries. *Small Sci.* **2024**, *4* (5), No. 2300302.
(294) Chouchane, M.; Yao, W.; Cronk, A.; Zhang, M.; Meng, Y. S. Improved Rate Capability for Dry Thick Electrodes through Finite Elements Method and Machine Learning Coupling. *ACS Energy Lett.* **2024**, *9* (4), 1480−1486.
(295) Kumberg, J.; Müller, M.; Diehm, R.; Spiegel, S.; Wachsmann, C.; Bauer, W.; Scharfer, P.; Schabel, W. Drying of Lithium-Ion Battery Anodes for Use in High-Energy Cells: Influence of Electrode Thickness on Drying Time, Adhesion, and Crack Formation. *Energy Technol.* **2019**, *7* (11), No. 1900722.
(296) Park, D.; Kim, S.; Ha, S.; Hwa, Y.; Kim, J.; Park, J.; Son, Y. Pitch-based quasi-dry thick electrode fabrication process of NCM cathode for lithium-ion batteries. *J. Power Sources* **2024**, *614*, No. 235037.
(297) Ryu, M.; Hong, Y. K.; Lee, S. Y.; Park, J. H. Ultrahigh loading dry-process for solvent-free lithium-ion battery electrode fabrication. *Nat. Commun.* **2023**, *14* (1), No. 1316.
(298) Oh, H.; Kim, G.-S.; Bang, J.; Kim, S.; Jeong, K.-M. Dry-processed thick electrode design with a porous conductive agent enabling 20 mAh cm^{-2} for high-energy-density lithium-ion batteries. *Energy Environ. Sci.* **2025**, *18* (2), 645−658.
(299) Checko, S.; Ju, Z.; Zhang, B.; Zheng, T.; Takeuchi, E. S.; Marschilok, A. C.; Takeuchi, K. J.; Yu, G. Fast-charging, binder-free lithium battery cathodes enabled via multidimensional conductive networks. *Nano Lett.* **2024**, *24* (5), 1695−1702.
(300) Horst, M.; Burmeister, J. K.; Abdollahifar, M.; Pillitteri, S.; Kwade, A. A binder-free dry coating process for high sulfur loading cathodes of Li−S batteries: A proof-of-concept. *J. Power Sources* **2023**, *587*, No. 233675.
(301) Wei, Z.; Kong, D.; Quan, L.; He, J.; Liu, J.; Tang, Z.; Chen, S.; Cai, Q.; Zhang, R.; Liu, H.; et al. Removing electrochemical constraints on polytetrafluoroethylene as dry-process binder for high-loading graphite anodes. *Joule* **2024**, *8* (5), 1350−1363.
(302) Han, S.; Noh, E.-H.; Chae, S.; Kwon, K.; Lee, J.; Woo, J.-S.; Park, S.; Lee, J. W.; Kim, P. J.; Song, T.; et al. Mitigating PTFE decomposition in ultra thick dry-processed anodes for high energy density lithium-ion batteries. *J. Energy Storage* **2024**, *96*, No. 112693.
(303) Tao, R.; Tan, S.; Meyer Iii, H. M.; Sun, X. G.; Steinhoff, B.; Sardo, K.; Bishtawi, A.; Gibbs, T.; Li, J. Insights into the Chemistry of the Cathodic Electrolyte Interphase for PTFE-Based Dry-Processed Cathodes. *ACS Appl. Mater. Interfaces* **2023**, *15* (34), 40488−40495.
(304) Lee, D.; Manthiram, A. Stable Cycling with Intimate Contacts Enabled by Crystallinity-Controlled PTFE-Based Solvent-Free Cathodes in All-Solid-State Batteries. *Small Methods* **2023**, *7* (7), No. e2201680.
(305) Choi, H.; Moon, D.; Sheem, J.; Koo, J. K.; Hong, S.; Oh, S.-M.; Kim, Y.-J. A Solvent-Free Process Enabled by Polytetrafluoroethlyene/Carbon Black Composites for Fabricating Electrodes for Lithium-Ion Batteries with a High Volumetric Energy. *J. Electrochem. Soc.* **2023**, *170* (9), No. 090511.
(306) Ji, Y.; Yang, C.; Han, J.; He, W. Functional Separators for Modulating Li-Ion Flux Toward Uniform Li Deposition: A Review. *Adv. Energy Mater.* **2024**, *14* (38), No. 2402329.
(307) Wang, C.; Wang, A.; Ren, L.; Guan, X.; Wang, D.; Dong, A.; Zhang, C.; Li, G.; Luo, J. Controlling Li ion flux through materials innovation for dendrite-free lithium metal anodes. *Adv. Funct. Mater.* **2019**, *29* (49), No. 1905940.
(308) Ren, W.; Zhu, K.; Zhang, W.; Liang, H.; Xu, L.; Wang, L.; Yang, C.; Yang, Y.; Zhang, P.; Wang, F.; et al. Dendrite-free lithium metal battery enabled by dendritic mesoporous silica coated separator. *Adv. Funct. Mater.* **2023**, *33* (34), No. 2301586.
(309) Liu, X.; Tang, F.; Hu, H.; Huang, H.; Ji, X.; Chen, L.; Liu, Z. Regulation of Li^+ Diffusion via an Engineered Separator to Realize a Homogeneous Lithium Microstructure in Advanced Li-Metal Batteries. *ACS Appl. Mater. Interfaces* **2023**, *15* (10), 13761−13771.
(310) Lei, Q.-K.; Zhang, Q.; Wu, X.-Y.; Wei, X.; Zhang, J.; Wang, K.-X.; Chen, J.-S. Towards ultra-stable lithium metal batteries: Interfacial ionic flux regulated through LiAl LDH-modified polypropylene separator. *Chem. Eng. J.* **2020**, *395*, No. 125187.
(311) Choi, W.; Park, M.; Woo, S.; Kim, H.; Kang, M. S.; Choi, J.; Cho, S. B.; Kim, T.; Kim, P. J. Towards ultra-stable and dendrite-suppressed Li-metal batteries: Ion-regulating graphene-modified separators. *Carbon* **2024**, *230*, No. 119576.

(312) Xu, S. M.; Zhu, Q. C.; Long, J.; Wang, H. H.; Xie, X. F.; Wang, K. X.; Chen, J. S. Low-Overpotential Li−O_2 Batteries Based on TFSI Intercalated Co−Ti Layered Double Oxides. *Adv. Funct. Mater.* **2016**, *26* (9), 1365−1374.
(313) Xiong, P.; Zhang, F.; Zhang, X.; Liu, Y.; Wu, Y.; Wang, S.; Safaei, J.; Sun, B.; Ma, R.; Liu, Z.; et al. Atomic-scale regulation of anionic and cationic migration in alkali metal batteries. *Nat. Commun.* **2021**, *12* (1), No. 4184.
(314) Han, D.-H.; Zhang, M.; Lu, P.-X.; Wan, Y.-L.; Chen, Q.-L.; Niu, H.-Y.; Yu, Z.-W. A multifunctional separator with $Mg(OH)_2$ nanoflake coatings for safe lithium-metal batteries. *J. Energy Chem.* **2021**, *52*, 75−83.
(315) Wang, C.; Li, W.; Jin, Y.; Liu, J.; Wang, H.; Zhang, Q. Functional separator enabled by covalent organic frameworks for high-performance Li metal batteries. *Small* **2023**, *19* (28), No. 2300023.
(316) Li, J.; Chen, L.; Wang, F.; Qin, Z.; Zhang, Y.; Zhang, N.; Liu, X.; Chen, G. Anionic metal-organic framework modified separator boosting efficient Li-ion transport. *Chem. Eng. J.* **2023**, *451*, No. 138536.
(317) Zhang, Z.; Wang, J.; Qin, H.; Zhang, B.; Lin, H.; Zheng, W.; Wang, D.; Ji, X.; Ou, X. Constructing an Anion-Braking Separator to Regulate Local Li^+ Solvation Structure for Stabilizing Lithium Metal Batteries. *ACS Nano* **2024**, *18* (3), 2250−2260.
(318) Shen, K.; Wang, Z.; Bi, X.; Ying, Y.; Zhang, D.; Jin, C.; Hou, G.; Cao, H.; Wu, L.; Zheng, G.; et al. Magnetic Field−Suppressed Lithium Dendrite Growth for Stable Lithium-Metal Batteries. *Adv. Energy Mater.* **2019**, *9* (20), No. 1900260.
(319) Ju, Z.; Zheng, T.; Zhang, B.; Dolocan, A.; Marschilok, A. C.; Takeuchi, E. S.; Takeuchi, K. J.; Yu, G. Magnetically oriented nanosheet interlayer for dynamic regeneration in lithium metal batteries. *Proc. Natl. Acad. Sci. U.S.A.* **2024**, *121* (44), No. e2413739121.
(320) Lim, H.-S.; Nguyen, D. T.; Lochala, J. A.; Cao, X.; Zhang, J.-G. Improving Cycling Performance of Anode-Free Lithium Batteries by Pressure and Voltage Control. *ACS Energy Lett.* **2024**, *9* (1), 126−135.
(321) Liu, W.; Luo, Y.; Hu, Y.; Chen, Z.; Wang, Q.; Chen, Y.; Iqbal, N.; Mitlin, D. Interrelation Between External Pressure, SEI Structure, and Electrodeposit Morphology in an Anode-Free Lithium Metal Battery. *Adv. Energy Mater.* **2023**, *14* (5), No. 2302261.
(322) Zhou, M.; Feng, C.; Xiong, R.; Li, L.; Huang, T.; Li, M.; Zhang, Y.; Zhou, H. Molecular Insights into the Structure and Property Variation of the Pressure-Induced Solid Electrolyte Interphase on a Lithium Metal Anode. *ACS Appl. Mater. Interfaces* **2022**, *14* (21), 24875−24885.
(323) Seongsoo, P.; Rashma, C.; Sang A, H.; Hamzeh, Q.; Janghyuk, M.; Min-Sik, P.; Jung Ho, K. Ionic conductivity and mechanical properties of the solid electrolyte interphase in lithium metal batteries. *Energy Materials* **2023**, *3* (1), No. 300005.
(324) Chang, W.; Xu, T.; Steingart, D. Chemo-Mechanical Effects of Stack Pressure and Temperature on Anode-Free Lithium Metal Batteries. *J. Electrochem. Soc.* **2022**, *169* (9), No. 090530.
(325) Zhang, Y.; Li, K.; Li, Y.; Shen, W.; Qu, X.; Huang, J.; Lin, Y. Decoupling pressure effects in plating and stripping of lithium metal anodes. *J. Energy Storage* **2023**, *74*, No. 109422.
(326) Sim, S.-J.; Jin, B.-S.; Park, J.-H.; Kim, H.-S. A Study on Long-Term Cycling Performance by External Pressure Change for Pouch-Type Lithium Metal Batteries. *J. Electrochem. Sci. Technol.* **2024**, *15* (2), 314−320.
(327) Liu, D.; Wu, B.; Xu, Y.; Ellis, J.; Baranovskiy, A.; Lu, D.; Lochala, J.; Anderson, C.; Baar, K.; Qu, D.; et al. Controlled large-area lithium deposition to reduce swelling of high-energy lithium metal pouch cells in liquid electrolytes. *Nat. Energy* **2024**, *9* (5), 559−569.
(328) Zhang, X.; Wang, Q. J.; Harrison, K. L.; Jungjohann, K.; Boyce, B. L.; Roberts, S. A.; Attia, P. M.; Harris, S. J. Rethinking How External Pressure Can Suppress Dendrites in Lithium Metal Batteries. *J. Electrochem. Soc.* **2019**, *166* (15), A3639−A3652.
(329) Li, L.; Basu, S.; Wang, Y.; Chen, Z.; Hundekar, P.; Wang, B.; Shi, J.; Shi, Y.; Narayanan, S.; Koratkar, N. Self-heating−induced healing of lithium dendrites. *Science* **2018**, *359* (6383), 1513−1516.
(330) Fang, M.; Yue, X.; Dong, Y.; Chen, Y.; Liang, Z. A temperature-dependent solvating electrolyte for wide-temperature and fast-charging lithium metal batteries. *Joule* **2024**, *8* (1), 91−103.
(331) Genovese, M.; Louli, A. J.; Weber, R.; Martin, C.; Taskovic, T.; Dahn, J. R. Hot Formation for Improved Low Temperature Cycling of Anode-Free Lithium Metal Batteries. *J. Electrochem. Soc.* **2019**, *166* (14), A3342−A3347.
(332) Zhang, H.; Zhang, X.; Shen, Z.; Peng, X.; Wang, F.; Xu, F.; Zhao, X. Ultrasound overcomes dendrite puncture in Li metal batteries. *J. Energy Storage* **2024**, *85*, No. 110976.
(333) Huang, A.; Liu, H.; Manor, O.; Liu, P.; Friend, J. Enabling Rapid Charging Lithium Metal Batteries via Surface Acoustic Wave-Driven Electrolyte Flow. *Adv. Mater.* **2020**, *32* (14), No. 1907516.
(334) Zhang, Q.; Bo, L.; Li, H.; Li, J.; Li, T.; Tian, Z.; Qiao, R. Enhancing performance of lithium metal batteries through acoustic field application. *J. Mater. Chem. A* **2025**, *13* (3), 2047−2055.
(335) Ai, Q.; Zhang, B.; Liu, X.; Shin, B.; Guo, W.; Gao, G.; Zhao, L.; Weng, X.; Fang, Q.; Zhai, T.; et al. Strong and brittle lithium dendrites. *Science* **2026**, *391* (6790), 1125−1129.
(336) Kim, B.; Jung, J.; Baek, S.; Lee, B. Degradation of lithium metal batteries due to dead lithium accumulation under ultrasound. *Ultrason. Sonochem.* **2025**, *117*, No. 107334.
(337) Xu, P.; Huang, F.; Sun, Y.; Lei, Y.; Cao, X.; Liang, S.; Fang, G. Anode-Free Alkali Metal Batteries: From Laboratory to Practicability. *Adv. Funct. Mater.* **2024**, *34* (44), No. 2406080.
(338) Cosby, M. R.; Carignan, G. M.; Li, Z.; Efaw, C. M.; Dickerson, C. C.; Yin, L.; Ren, Y.; Li, B.; Dufek, E. J.; Khalifah, P. G. *Operando* Synchrotron Studies of Inhomogeneity during Anode-Free Plating of Li Metal in Pouch Cell Batteries. *J. Electrochem. Soc.* **2022**, *169* (2), No. 020571.
(339) Qiao, D.; Wei, X.; Zhu, J.; Wang, X.; Jiang, B.; Fan, W.; Wei, G.; Han, G.; Lai, X.; Zheng, Y.; Dai, H. Unraveling the mechanism of non-uniform lithium deposition in liquid electrolytes. *Cell Rep. Phys. Sci.* **2024**, *5* (5), No. 101961.
(340) Kwon, H.; Baek, J.; Kim, H.-T. Building lithium metal batteries under lean electrolyte conditions: Challenges and progress. *Energy Storage Mater.* **2023**, *55*, 708−726.
(341) Louli, A. J.; Coon, M.; Genovese, M.; deGooyer, J.; Eldesoky, A.; Dahn, J. R. Optimizing Cycling Conditions for Anode-Free Lithium Metal Cells. *J. Electrochem. Soc.* **2021**, *168* (2), No. 020515.
(342) Zhang, Y.; Bao, W.; Jeffs, E.; Liu, B.; Han, B.; Mai, W.; Li, X.; Li, W.; Xu, Y.; Bhamwala, B.; et al. Unveiling the Impacts of Charge/Discharge Rate on the Cycling Performance of Li-Metal Batteries. *ACS Energy Lett.* **2025**, *10* (2), 872−880.
(343) Zheng, J.; Yan, P.; Mei, D.; Engelhard, M. H.; Cartmell, S. S.; Polzin, B. J.; Wang, C.; Zhang, J. G.; Xu, W. Highly Stable Operation of Lithium Metal Batteries Enabled by the Formation of a Transient High-Concentration Electrolyte Layer. *Adv. Energy Mater.* **2016**, *6* (8), No. 1502151.
(344) Adams, B. D.; Zheng, J.; Ren, X.; Xu, W.; Zhang, J. G. Accurate Determination of Coulombic Efficiency for Lithium Metal Anodes and Lithium Metal Batteries. *Adv. Energy Mater.* **2017**, *8* (7), No. 1702097.
(345) Aurbach, D. Review of selected electrode−solution interactions which determine the performance of Li and Li ion batteries. *J. Power Sources* **2000**, *89* (2), 206−218.
(346) Aurbach, D.; Youngman, O.; Gofer, Y.; Meitav, A. The electrochemical behaviour of 1,3-dioxolane—$LiClO_4$ solutions—I. Uncontaminated solutions. *Electrochim. Acta* **1990**, *35* (3), 625−638.
(347) Li, J.; Arbizzani, C.; Kjelstrup, S.; Xiao, J.; Xia, Y.-y.; Yu, Y.; Yang, Y.; Belharouak, I.; Zawodzinski, T.; Myung, S.-T.; et al. Good practice guide for papers on batteries for the Journal of Power Sources. *J. Power Sources* **2020**, *452*, No. 227824.
(348) Stephan, A. K. Standardized Battery Reporting Guidelines. *Joule* **2021**, *5* (1), 1−2.

(349) Weng, S.; Zhang, X.; Yang, G.; Zhang, S.; Ma, B.; Liu, Q.; Liu, Y.; Peng, C.; Chen, H.; Yu, H.; et al. Temperature-dependent interphase formation and Li^+ transport in lithium metal batteries. *Nat. Commun.* **2023**, *14* (1), No. 4474.
(350) Kim, M.; An, J.; Shin, S.-J.; Hwang, I.; Lee, J.; Park, Y.; Kim, J.; Park, E.; Kim, J.; Park, G.; et al. Anti-corrosive electrolyte design for extending the calendar life of lithium metal batteries. *Energy Environ. Sci.* **2024**, *17* (16), 6079−6090.
(351) Zhang, W.; Koverga, V.; Liu, S.; Zhou, J.; Wang, J.; Bai, P.; Tan, S.; Dandu, N. K.; Wang, Z.; Chen, F.; et al. Single-phase local-high-concentration solid polymer electrolytes for lithium-metal batteries. *Nat. Energy* **2024**, *9* (4), 386−400.
(352) Drvarič Talian, S.; Moškon, J.; Dominko, R.; Gaberšček, M. Reactivity and diffusivity of Li polysulfides: a fundamental study using impedance spectroscopy. *ACS Appl. Mater. Interfaces* **2017**, *9* (35), 29760−29770.
(353) Drvarič Talian, S.; Moškon, J.; Dominko, R.; Gaberšček, M. Impedance response of porous carbon cathodes in polysulfide redox system. *Electrochim. Acta* **2019**, *302*, 169−179.
(354) Moškon, J.; Žuntar, J.; Talian, S. D.; Dominko, R.; Gaberšček, M. A powerful transmission line model for analysis of impedance of insertion battery cells: a case study on the NMC-Li system. *J. Electrochem. Soc.* **2020**, *167* (14), No. 140539.
(355) Drvarič Talian, S.; Bobnar, J.; Sinigoj, A. R.; Humar, I.; Gaberšček, M. Transmission Line Model for Description of the Impedance Response of Li Electrodes with Dendritic Growth. *J. Phys. Chem. C* **2019**, *123* (46), 27997−28007.
(356) Drvarič Talian, S.; Kapun, G.; Moškon, J.; Dominko, R.; Gaberšček, M. Operando impedance spectroscopy with combined dynamic measurements and overvoltage analysis in lithium metal batteries. *Nat. Commun.* **2025**, *16* (1), No. 2030.
(357) Florian, J.; Lyu, H.; Choi, I. R.; Mondonico, L.; Lam, S.; Zhao, Y.; Kim, M. J.; Westover, A.; Cui, Y.; Sacci, R. L.; Bao, Z. Revealing Solvent-Assisted Li^+ Transport in the Solid Electrolyte Interphase operando. *J. Am. Chem. Soc.* **2025**, *147* (46), 42701−42710.
(358) Lu, Y.; Zhao, C.-Z.; Huang, J.-Q.; Zhang, Q. The timescale identification decoupling complicated kinetic processes in lithium batteries. *Joule* **2022**, *6* (6), 1172−1198.
(359) Shao, A.; Wang, H.; Zhang, M.; Liu, J.; Cheng, L.; Li, Y.; Guo, Y.; Wang, Z.; Jia, Q.; Wang, X.; et al. Multiscale interfacial stabilization via prelithiation separator engineering for Ah-level anode-free lithium batteries. *Nat. Commun.* **2025**, *16* (1), No. 4145.
(360) Zhao, Y.; Kumtepeli, V.; Ludwig, S.; Jossen, A. Investigation of the distribution of relaxation times of a porous electrode using a physics-based impedance model. *J. Power Sources* **2022**, *530*, No. 231250.
(361) Zhao, Y.; Kücher, S.; Jossen, A. Investigation of the diffusion phenomena in lithium-ion batteries with distribution of relaxation times. *Electrochim. Acta* **2022**, *432*, No. 141174.
(362) Kim, S.; Didwal, P. N.; Fiates, J.; Dawson, J. A.; Weatherup, R. S.; De Volder, M. Effect of the Formation Rate on the Stability of Anode-Free Lithium Metal Batteries. *ACS Energy Lett.* **2024**, *9* (10), 4753−4760.
(363) Song, J.; Bazant, M. Z. Electrochemical Impedance Imaging via the Distribution of Diffusion Times. *Phys. Rev. Lett.* **2018**, *120* (11), No. 116001.
(364) Li, Y.; Li, Y.; Pei, A.; Yan, K.; Sun, Y.; Wu, C.-L.; Joubert, L.-M.; Chin, R.; Koh, A. L.; Yu, Y.; et al. Atomic structure of sensitive battery materials and interfaces revealed by cryo−electron microscopy. *Science* **2017**, *358* (6362), 506−510.
(365) Zhang, W.; Sayavong, P.; Xiao, X.; Oyakhire, S. T.; Shuchi, S. B.; Vila, R. A.; Boyle, D. T.; Kim, S. C.; Kim, M. S.; Holmes, S. E.; et al. Recovery of isolated lithium through discharged state calendar ageing. *Nature* **2024**, *626* (7998), 306−312.
(366) Zachman, M. J.; Tu, Z.; Choudhury, S.; Archer, L. A.; Kourkoutis, L. F. Cryo-STEM mapping of solid-liquid interfaces and dendrites in lithium-metal batteries. *Nature* **2018**, *560* (7718), 345−349.
(367) Li, Y.; Huang, W.; Li, Y.; Chiu, W.; Cui, Y. Opportunities for Cryogenic Electron Microscopy in Materials Science and Nanoscience. *ACS Nano* **2020**, *14* (8), 9263−9276.
(368) Wang, J.; Huang, W.; Pei, A.; Li, Y.; Shi, F.; Yu, X.; Cui, Y. Improving cyclability of Li metal batteries at elevated temperatures and its origin revealed by cryo-electron microscopy. *Nat. Energy* **2019**, *4* (8), 664−670.
(369) Vilá, R. A.; Boyle, D. T.; Dai, A.; Zhang, W.; Sayavong, P.; Ye, Y.; Yang, Y.; Dionne, J. A.; Cui, Y. LiH formation and its impact on Li batteries revealed by cryogenic electron microscopy. *Sci. Adv.* **2023**, *9* (12), No. eadf3609.
(370) Ma, C.; Xu, F.; Song, T. Dual-Layered Interfacial Evolution of Lithium Metal Anode: SEI Analysis via TOF-SIMS Technology. *ACS Appl. Mater. Interfaces* **2022**, *14* (17), 20197−20207.
(371) Wi, T.-U.; Park, S. O.; Yeom, S. J.; Kim, M.-H.; Kristanto, I.; Wang, H.; Kwak, S. K.; Lee, H.-W. Revealing the Dual-Layered Solid Electrolyte Interphase on Lithium Metal Anodes via Cryogenic Electron Microscopy. *ACS Energy Lett.* **2023**, *8* (5), 2193−2200.
(372) Shuchi, S. B.; D'Acunto, G.; Sayavong, P.; Oyakhire, S. T.; Sanroman Gutierrez, K. M.; Risner-Jamtgaard, J.; Choi, I. R.; Cui, Y.; Bent, S. F. Cryogenic X-ray photoelectron spectroscopy for battery interfaces. *Nature* **2025**, *646* (8086), 850−855.
(373) Oyakhire, S. T.; Gong, H.; Cui, Y.; Bao, Z.; Bent, S. F. An X-ray Photoelectron Spectroscopy Primer for Solid Electrolyte Interphase Characterization in Lithium Metal Anodes. *ACS Energy Lett.* **2022**, *7* (8), 2540−2546.
(374) Peled, E. The Electrochemical Behavior of Alkali and Alkaline Earth Metals in Nonaqueous Battery Systems—The Solid Electrolyte Interphase Model. *J. Electrochem. Soc.* **1979**, *126* (12), 2047.
(375) Aurbach, D.; Daroux, M. L.; Faguy, P. W.; Yeager, E. Identification of Surface Films Formed on Lithium in Propylene Carbonate Solutions. *J. Electrochem. Soc.* **1987**, *134* (7), 1611.
(376) Dey, A. N. Lithium anode film and organic and inorganic electrolyte batteries. *Thin Solid Films* **1977**, *43* (1), 131−171.
(377) Kok, M. D. R.; Robinson, J. B.; Weaving, J. S.; Jnawali, A.; Pham, M.; Iacoviello, F.; Brett, D. J. L.; Shearing, P. R. Virtual unrolling of spirally-wound lithium-ion cells for correlative degradation studies and predictive fault detection. *Sustainable Energy Fuels* **2019**, *3* (11), 2972−2976.
(378) Lu, X.; Zhang, X.; Tan, C.; Heenan, T. M. M.; Lagnoni, M.; O'Regan, K.; Daemi, S.; Bertei, A.; Jones, H. G.; Hinds, G.; et al. Multi-length scale microstructural design of lithium-ion battery electrodes for improved discharge rate performance. *Energy Environ. Sci.* **2021**, *14* (11), 5929−5946.
(379) Lim, J.; Li, Y.; Alsem, D. H.; So, H.; Lee, S. C.; Bai, P.; Cogswell, D. A.; Liu, X.; Jin, N.; Yu, Y.-s.; et al. Origin and hysteresis of lithium compositional spatiodynamics within battery primary particles. *Science* **2016**, *353* (6299), 566−571.
(380) Zhang, F.; Lou, S.; Li, S.; Yu, Z.; Liu, Q.; Dai, A.; Cao, C.; Toney, M. F.; Ge, M.; Xiao, X.; et al. Surface regulation enables high stability of single-crystal lithium-ion cathodes at high voltage. *Nat. Commun.* **2020**, *11* (1), No. 3050.
(381) Kim, S.; Lee, J.-A.; Lee, T. K.; Baek, K.; Kim, J.; Kim, B.; Byun, J. H.; Lee, H.-W.; Kang, S. J.; Choi, J.-A.; et al. Wide-temperature-range operation of lithium-metal batteries using partially and weakly solvating liquid electrolytes. *Energy Environ. Sci.* **2023**, *16* (11), 5108−5122.
(382) Merryweather, A. J.; Schnedermann, C.; Jacquet, Q.; Grey, C. P.; Rao, A. Operando optical tracking of single-particle ion dynamics in batteries. *Nature* **2021**, *594* (7864), 522−528.
(383) Park, K.; Lee, M.; Song, J.; Ha, A. R.; Ha, S.; Jo, S.; Song, J.; Choi, S. H.; Kim, W.; Ryu, K.; et al. Operando Spatial Pressure Mapping Analysis for Prototype Lithium Metal Pouch Cells Under Practical Conditions. *Adv. Sci.* **2023**, *10* (33), No. e2304979.
(384) Yang, H.; Liu, X.; Zheng, J.; Yao, W.; Fang, K.; Lai, X.; Zhai, G.; Wu, M.; Li, G.; Luo, W. Mitigating Overcharge in Ampere-Hour-Level Anode-Free Pouch Cells by Improving Pressure Uniformity. *ACS Energy Lett.* **2024**, *9* (9), 4331−4338.

(385) Lu, X.; Lagnoni, M.; Bertei, A.; Das, S.; Owen, R. E.; Li, Q.; O'Regan, K.; Wade, A.; Finegan, D. P.; Kendrick, E.; et al. Multiscale dynamics of charging and plating in graphite electrodes coupling operando microscopy and phase-field modelling. *Nat. Commun.* **2023**, *14* (1), No. 5127.
(386) Jeon, B.-J.; Lee, Y.-H.; Jeong, K.-M. Unveiling the impact of electrode curvature on N/P ratio variations in cylindrical lithium-ion batteries. *Energy Storage Mater.* **2025**, *76*, No. 104117.
(387) Xu, C.; Merryweather, A. J.; Pandurangi, S. S.; Lun, Z.; Hall, D. S.; Deshpande, V. S.; Fleck, N. A.; Schnedermann, C.; Rao, A.; Grey, C. P. Operando visualization of kinetically induced lithium heterogeneities in single-particle layered Ni-rich cathodes. *Joule* **2022**, *6* (11), 2535−2546.
(388) Zhang, M.; Chouchane, M.; Shojaee, S. A.; Winiarski, B.; Liu, Z.; Li, L.; Pelapur, R.; Shodiev, A.; Yao, W.; Doux, J.-M.; et al. Coupling of multiscale imaging analysis and computational modeling for understanding thick cathode degradation mechanisms. *Joule* **2023**, *7* (1), 201−220.
(389) Kim, D.-H.; Lee, M.-H.; Kim, B. G.; Lee, S.-M.; Choi, J.-H. Porosity controlled carbon-based 3D anode for lithium metal batteries by a slurry based process. *Chem. Commun.* **2020**, *56* (85), 13040−13043.
(390) Liu, L.; Yin, Y. X.; Li, J. Y.; Wang, S. H.; Guo, Y. G.; Wan, L. J. Uniform lithium nucleation/growth induced by lightweight nitrogen-doped graphitic carbon foams for high-performance lithium metal anodes. *Adv. Mater.* **2018**, *30* (10), No. 1706216.
(391) Jiang, G.; Jiang, N.; Zheng, N.; Chen, X.; Mao, J.; Ding, G.; Li, Y.; Sun, F.; Li, Y. MOF-derived porous Co_3O_4-NC nanoflake arrays on carbon fiber cloth as stable hosts for dendrite-free Li metal anodes. *Energy Storage Mater.* **2019**, *23*, 181−189.
(392) Chen, J.; Wang, Y.; Li, S.; Chen, H.; Qiao, X.; Zhao, J.; Ma, Y.; Alshareef, H. N. Porous metal current collectors for alkali metal batteries. *Adv. Sci.* **2023**, *10* (1), No. 2205695.
(393) Chen, H.; Pei, A.; Wan, J.; Lin, D.; Vilá, R.; Wang, H.; Mackanic, D.; Steinrück, H.-G.; Huang, W.; Li, Y.; et al. Tortuosity effects in lithium-metal host anodes. *Joule* **2020**, *4* (4), 938−952.
(394) Chen, J.; Liu, G.; Han, X.; Wu, H.; Hu, T.; Huang, Y.; Zhang, S.; Wang, Y.; Shi, Z.; Zhang, Y.; et al. Engineering high-performance Li metal batteries through dual-gradient porous Cu-CuZn host. *ACS Nano* **2024**, *18* (21), 13662−13674.
(395) Chen, Y.; Chen, K.-H.; Sanchez, A. J.; Kazyak, E.; Goel, V.; Gorlin, Y.; Christensen, J.; Thornton, K.; Dasgupta, N. P. Operando video microscopy of Li plating and re-intercalation on graphite anodes during fast charging. *J. Mater. Chem. A* **2021**, *9* (41), 23522−23536.
(396) Zhao, Q.; Deng, Y.; Utomo, N. W.; Zheng, J.; Biswal, P.; Yin, J.; Archer, L. A. On the crystallography and reversibility of lithium electrodeposits at ultrahigh capacity. *Nat. Commun.* **2021**, *12* (1), No. 6034.
(397) Rathod, D.; Ghosh, N.; Panigrahi, B. K.; Garg, A.; Kumari, P. Thermal modelling of cylindrical Lithium-Ion batteries to study the impact of structural components. *Energy Storage* **2022**, *4* (6), No. e374.
(398) Jones, C. M.; Sudarshan, M.; Garcia, R. E.; Tomar, V. Direct measurement of internal temperatures of commercially-available 18650 lithium-ion batteries. *Sci. Rep.* **2023**, *13* (1), No. 14421.
(399) Ferreira, P.; Tang, S. X. Investigating thermal dynamics in cylindrical Li-ion batteries across varied temperatures based on electrochemical principles. *Sci. Rep.* **2025**, *15* (1), No. 30830.
(400) Senyshyn, A.; Muhlbauer, M. J.; Dolotko, O.; Hofmann, M.; Ehrenberg, H. Homogeneity of lithium distribution in cylinder-type Li-ion batteries. *Sci. Rep.* **2016**, *5*, No. 18380.
(401) Mühlbauer, M.; Petz, D.; Baran, V.; Dolotko, O.; Hofmann, M.; Kostecki, R.; Senyshyn, A. Inhomogeneous distribution of lithium and electrolyte in aged Li-ion cylindrical cells. *J. Power Sources* **2020**, *475*, No. 228690.
(402) Solchenbach, S.; Tacconis, C.; Gomez Martin, A.; Peters, V.; Wallisch, L.; Stanke, A.; Hofer, J.; Renz, D.; Lewerich, B.; Bauer, G.; et al. Electrolyte motion induced salt inhomogeneity − a novel aging mechanism in large-format lithium-ion cells. *Energy Environ. Sci.* **2024**, *17* (19), 7294−7317.
(403) Yu, H.; Wang, L.; Zhang, Z.; Li, Y.; Yang, S.; He, X. Insight Understanding of External Pressure on Lithium Plating in Commercial Lithium-Ion Batteries. *Adv. Funct. Mater.* **2024**, *34* (42), No. 2406966.
(404) Tardy, E.; Thivel, P.-X.; Druart, F.; Kuntz, P.; Devaux, D.; Bultel, Y. Internal temperature distribution in lithium-ion battery cell and module based on a 3D electrothermal model: An investigation of real geometry, entropy change and thermal process. *J. Energy Storage* **2023**, *64*, No. 107090.
(405) Du, X.; Wu, Q.; Wang, Y.-N.; Pan, T.-S.; Wei, Y.-M.; Chen, H.-S.; Song, W.-L.; Fang, D.-N. Visualizing two-dimensional internal temperature distribution in cylindrical Li-ion cells. *J. Power Sources* **2020**, *446*, No. 227343.
(406) Nikodimos, Y.; Shitaw, K. N.; Hagos, T. M.; Yeh, T. I.; Huang, Y. C.; Hsieh, C. L.; Su, H. H.; Su, W. N.; Hwang, B. J. Anode-Free Batteries: Pioneering Energy Storage Revolution. *Chem. Rev.* **2026**, *126* (4), 2391−2483.
(407) Abdollahifar, M.; Paolella, A. Anode-Free Batteries: The Energy Density Prize and the Stability Paradox. *ACS Energy Lett.* **2026**, *11* (2), 1323−1348.
(408) Yoon, S. G.; Vishnugopi, B. S.; Nelson, D. L.; Yong, A. X. B.; Wang, Y.; Sandoval, S. E.; Thomas, T. A.; Cavallaro, K. A.; Shevchenko, P.; Alsaç, E. P.; et al. Interface morphogenesis with a deformable secondary phase in solid-state lithium batteries. *Science* **2025**, *388* (6751), 1062−1068.
(409) Yoon, S. G.; Nelson, D. L.; Jeong, W. J.; Sandoval, S. E.; Thomas, T. A.; Cavallaro, K. A.; Alsaç, E. P.; Shin, J.; McDowell, M. T. Deformable sodium metal current collectors for lithium solid-state batteries. *Matter* **2025**, *8* (11), No. 102463.
(410) Li, W.; Yanyachi, A.; Xia, J.; Kuppan, S.; Zhou, J.; Wang, Y.; Li, Y.; Pianetta, P.; Zhao, K.; Mitlin, D.; et al. Mechanistic Considerations for Battery Charging Protocol Design. *Adv. Energy Mater.* **2026**, *16* (6), No. e04499.
(411) Qian, G.; Kuppan, S.; Gallo, A.; Zhou, J.; Liu, Z.; Liu, Y. From in-situ experimentation to in-line metrology: Advanced imaging characterization for battery research and manufacturing. *Energy Storage Mater.* **2024**, *73*, No. 103819.
(412) Hobold, G. M.; Kim, K.-H.; Gallant, B. M. Beneficial vs. inhibiting passivation by the native lithium solid electrolyte interphase revealed by electrochemical Li^+ exchange. *Energy Environ. Sci.* **2023**, *16* (5), 2247−2261.
(413) Han, B.; Li, X.; Wang, Q.; Zou, Y.; Xu, G.; Cheng, Y.; Zhang, Z.; Zhao, Y.; Deng, Y.; Li, J.; Gu, M. Cryo-Electron Tomography of Highly Deformable and Adherent Solid-Electrolyte Interphase Exoskeleton in Li-Metal Batteries with Ether-Based Electrolyte. *Adv. Mater.* **2022**, *34* (13), No. e2108252.